MOLECULAR ORBITAL STUDIES OF SOME DRUG-RECEPTOR INTERACTIONS

by

Peter W. Borthwick

Department of Physics, The City University, London

Submitted for the degree of PhD

June, 1977

List of contents

List of Tables

List of Illustrations

Acknowledgements

My sincere thanks go to Dr. E.G. Steward for his helpful criticism, advice, and his continuous encouragement given throughout this work.

I would like to thank my colleagues Dave, Gordon, Don, Richard and Chris for being a pleasure to work with, and I would also like to extend my gratitude to include everyone in the physics department at TCU. I am grateful to the Science Research Council and the Edwards Memorial Trust for their financial support.

Although the factual content of this thesis may be criticised, one fact is above criticism...the typing is beautiful! Thank you Glynis.

Abstract

The researches described here were motivated by a desire to investigate the mechanisms of drug-receptor systems. Three such systems have been explicitly considered (a) the CNS inhibitory system of GABA, (b) the CNS excitatory system of glutamic acid, and (c) the multi-functional prostaglandin system. The GABA transmitter-receptor system is the least complex of the three considered, and has thus been the prime object of study. In seeking a fundamental understanding of drug action at the molecular level the macroscopic physico-chemical parameter approach (Hansch analysis) has been abandoned in favour of the methods of theoretical quantum chemistry.

Various theoretical methods have been considered and compared, with CNDO/2 being chosen as appropriate to the present study. The CNDO/2 method has been used to investigate some aspects of the gas-phase properties of GABA and GLU agonists. These aspects include the variation of atomic charges during conformational changes, the intramoleculer hydrogen-bonding between terminal groups of α,ω amino-carboxydic acids and the intermolecular invariance in electron distribution of functional groups. The use of the electrostatic potential as a means of probing the interaction sites of a drug has also been considered in detail.

Acknowledging that drug-receptor events occur in the biophase (rather than gas-phase), the possibility of allowing for the solvent effect in theoretical conformation studies has been discussed. Three theoretical solvent effect methods have been compared using β-alanine as a test solute. A continuum approximation to the solvent has been found to be appropriate for use with CNDO/2 and GABA-type molecules.

This point represents the end of the preparatory stage, and it is considered that our techniques are sufficiently developed to attempt an elucidation of GABA and GLU transmitter-receptor interactions. It subsequently proved possible to develop working hypotheses concerning the requirements for agonism, antagonism and inactivity.

A feasability study on the use of quantum methods with the prostaglandins concluded that only if a 'molecular fragment' approach was used can conformational problems be contemplated. The 'molecular fragment' idea was outlined and a brief example of its use given.

List of abbreviations, symbols and conventions

Molecules

αAG	α,γ -aminobutyric acid
αFG	α-fluoroγ -aminobutyric acid
αGA	α-quanidinoacetic acid
ATA	4-aminotetrolic acid
ACA	4-aminocrotonic acid
βA	β-alanine
βHG	β-hydroxy-γ-aminobutyric acid
βGP	β-guanidinopropionic acid
BIC	bicuculline
GABA	γ-aminobutyric acid
GLU	glutamic acid
ImA	Imidazoleacetic acid
ITA	Ibotenic acid
MEG	Methyl-ester GABA
MM	Muscimol
PG	Prostaglandin

Quantum chemistry

AO	Atomic Orbital
BI	Bond Index
CI	Configuration Interaction
CNDO	Complete Neglect of Differential Overlap
EHT	Extended Huckel Theory
EPACE	Extended PACE
EP	Electrostatic Potential
GTO	Gaussian Type Orbital
HMO	Huckel Molecular Orbital theory
INDO	Intermediate Neglect of Differential Overlap
LCAO	Linear Combination of Atomic Orbitals
MO	Molecular Orbital
MINDO	Modified-INDO
NDDO	Neglect of Diatomic Differential Overlap
NAP	Net Atomic Population
PACE	Population Analysis using Classical Energies
PCILO	Perturbation of Configuration Interaction using Localised Orbitals
PPP	Pariser-Parr-Pople method
RHF	Roothaan-Hartree-Fock
SO	Spin Orbital

STO	Slater Type Orbital
SCF	Self-Consistent Field
ZDO	Zero Differential Overlap
Σ	Sum of atomic charges of a functional group

Miscellaneous

$\mathcal{B}^{AB}$	Conformational BI space
$\mathcal{C}^{A}$	Conformational NAP space
CD	Circular dichroism
CNS	Central nervous system
$\mathcal{F}$	Folded region of molecular conformation
NMR	Nuclear Magnetic Resonance
ORD	Optical Rotatory Dispersion
PAR	Physico-chemical Activity Relationship
PNS	Peripheral Nervous System
R	Rectus:asymmetric-carbon convention (see Appendix C)
$\mathcal{R}^{+}$	Positive pharmacophore region
$\mathcal{R}^{-}$	Negative pharmacophore region
S	Sinister:asymmetric-carbon convention (see Appendix C)
SAR	Structure Activity Relationship
x_T	Inter-$\mathcal{R}^{+}\mathcal{R}^{-}$ distance

1.1 Introduction

A piece of research starts with a question. The relevant starting question for this research was the time-honoured one "is it sufficient to know that drug A has a curative effect on illness B without an understanding of why?" The short-term answer to this question may well be 'yes!', however, in the long-term this is unsatisfactory. It is only by an understanding of the mode of action of A that drugs of greater efficacy and probable safety can be designed for the treatment of B. Ideally one seeks an understanding at the molecular level, for it is at this level that the fundamental events in drug action occur.

It is now known that many drugs act via a receptor mechanism. A receptor is an entity capable of recognising specific drugs, and binding with them in order to make a predetermined physico-chemical change. The object of this thesis is to study three such drug-receptor systems, at the molecular level, in order to gain some understanding of their mode of action. The receptor systems explicitly studied here are (i) the central nervous system (CNS) inhibitory receptor system of γ-aminobutyric acid (GABA), (ii) the CNS excitatory receptor system of L-glutamic acid (GLU), and (iii) the multi-functional prostaglandin (PG) receptor system.

There are essentially two possible modes in which an elucidation of the receptor can progress:

(i) the receptor itself can be the object of study in a direct approach, or

(ii) the drugs acting at the receptor can be considered. In this case, the complementarily of drug and receptor is appealed to in order to make deductions about the receptor. The general picture has emerged of a receptor (R) and drug (D) interacting according to the scheme

$$R + D \rightarrow (RD) \rightarrow (RD)^* \rightarrow \text{response}$$

where (RD) is the drug-receptor complex which, for antagonists ("blockers") is inactive but for agonists becomes active (RD)* - probably by a conformational modification of the complex. The active complexing of R with D can only occur if electro-spatial requirements of the receptor are closely matched by the drug, and it is this latter complementarity that is crucial to this research. (NB: the 'electro-spatial requirements for receptor activity' are often referred to as "pharmacophore".)

It is the second approach that will be adopted in this thesis.

Chapter 1 is devoted to setting the scene and outlining the research problem. In Chapter 2 the most appropriate basic tool is chosen from a fairly wide variety available. Getting the 'feel' of the tool and finding its capabilities and shortcomings is the subject of Chapter 3. In Chapter 4 the basic tool is fitted with a compatible attachment, which will enable us to use it in water. The final two chapters (5 and 6) deal with the application of previous chapters to the basic research problem.

1.2 Drug design

1.2.1 Introduction

The problem of the medicinal chemist is, for a given drug[f], to find a chemical compound which has the same biological action with minimal side effects, but which is more potent than the parent drug. Originally, a large number of molecules of a similar type to the original drug would be synthesised and tested for effect. In this approach no attempt would be made to correlate the results of the tests, and consequently a large amount of potentially valuable data was wasted.

1.2.2 PAR methods

In order to utilise all the available data, the physico-chemical activity relationship (PAR) scheme was proposed (Hansch & Fujita, 1964). This scheme treats potency as a function of a molecule's steric (E_s), electronic (σ), and lipophilic (P) character. The basic equation of the method is the Hansch equation

$$\log(1/C) = k_1(\log P)^2 + k_2(\log P) + k_3\sigma + k_4 E_s + k_5$$

where C is the concentration required to give a fixed response, (hence 1/C defines "relative potency"), σ is the Hammett constant (Hammett, 1940), E_s is usually Tafts steric parameter (Taft, 1956) and P is the octanol/water partition coefficient. Hence, for n prospective drugs a set of n-equations is generated

$$\alpha^i = \sum_{j=1}^{5} k_j \beta_j^i \qquad i = 1, \ldots, n$$

where the α, β are known and the k_j may be determined by multiple linear regression analysis. The Hansch equation may then be used for a theoretical prediction of potency.

1.2.3 SAR methods

It can sometimes be difficult or impossible to obtain the physicochemical parameters required for a PAR study. In such cases an alternative structure-activity relationship (SAR) scheme is available (Free & Wilson, 1964). In this approach the assumption is that the substituent groups of a parent compound contribute linearly and in an

---

f For our purposes a 'drug' is defined as any endogenous or exogenous molecule which is active in a biological system.

additive sense to the biological activity. Hence, the molecules of interest are represented as

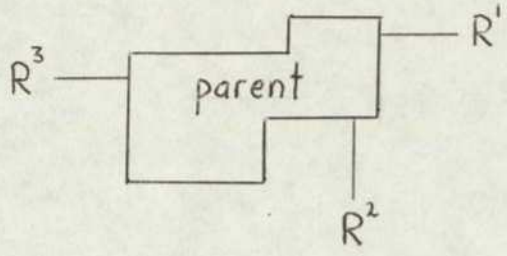

and a set of equations,

$$\log(1/C) = a[R'_i] + b[R^2_i] + c[R^3_i] + d$$

are generated, where R_i^j (j = 1,2,3) are the contributions to activity for the substituent at the R^j position of the i^{th} congener and d is the contribution of the parent compound. The constants a,b,c and d are again determined by multiple regression techniques.

1.2.4 Molecular orbital methods

A third potentially useful tool for the medicinal chemist are the theoretical techniques of quantum chemistry. These techniques may be used as a part of PAR studies, for example the Hammett constant can be replaced by a different measure of electronic character such as the electron density calculated by molecular orbital (MO) methods (Kier, 1971). More significantly MO techniques may be used within the SAR formalism to provide a fundamental understanding of the particular molecular requirements necessary for biological activity (Berges & Peradejordi, 1974).

1.2.5 PAR v SAR

Although the Hansch method is rather crude and the separation of factors is oversimplified, it has been successfully applied for a wide range of molecular systems (Hansch, 1973). It nevertheless remains that PAR is essentially a macroscopic approach which does not progress our knowledge of the actual mechanisms by which drugs work.

Alternatively, the SAR model is useful when physicochemical parameters are not available or when a quantitative measure of the contributions of the various substituent groups is required. In the SAR method the derived constants contain not only information of steric, electronic and lipophilic effects, but also account for effects which may not fall into these categories. However, this advantage of SAR has to be equated with the disadvantage that although one may find that a functional group at a certain position changes potency, one has no idea which attributes of that group are responsible for the change.

It is at this point the MO methods can make an important contribution by offering an explanation at the atomic level of the factors governing potency.

1.2.6 The problem of conformation

Consider the biologically important inhibitory interneuronal transmitter system of GABA. One may represent the molecules as:

$$R_1 - \boxed{-CH_2.CH_2-} - R_2$$

If $R_1 = -NH_3^+$ and $R_2 = -COO^-$ (β-alanine), then the SAR method as defined in 1.2.3 gives

$$\log(1/C_1) = a\left[NH_3^+\right] + b\left[COO^-\right] + c \qquad \text{(i)}$$

If now $R_1 = NH_3^+.CH_2-$ (GABA), then

$$\log(1/C_2) = a\left[NH_3^+.CH_2\right] + b\left[COO^-\right] + c \qquad \text{(ii)}$$

Subtracting (i) from (ii) $\Rightarrow$ $a\left[NH_3^+.CH_2\right] > a\left[NH_3^+\right]$ (iii)

since for inhibition at interneuronal synapses (1.5.2) GABA is considerably more potent than β-alanine (Swagel, Skeda & Roberts, 1973). However,

$$\log(1/C_2) = a\left[NH_3^+\right] + b\left[CH_2.COO^-\right] + c \qquad \text{(iv)}$$

and so $b\left[CH_2.COO^-\right] > b\left[COO^-\right]$ (v)

Equations (ii) and (v) lead to the prediction:

$$\log(1/C_3) = a\left[NH_3^+.CH_2\right] + b\left[CH_2.COO^-\right] + c > \log(1/C_2) \qquad \text{(vi)}$$

ie δ-aminovaleric acid is more potent than GABA. This is a fallacious result (Swagel et al, 1973)!

The reason that the SAR method breaks down is due to the prime importance of the spatial interelation between the R_i that exists in the GABA system. Analytically, one can say that the failing is due to a variable contribution from the 'parent' (ie c not constant) in equations (i), (ii) and (vi), due to conformational differences in the $-CH_2.CH_2$ moiety between the molecules. The PAR method also fails to predict a peak activity for GABA, since the usual parameters increase monotonically with increasing chain length.

In such cases as above it is clear that explicit consideration of conformation is necessary if the SAR method is to be of any utility. Thus, it has become accepted to regard conformation as an SAR parameter (Kier, 1971; Gill, 1965; Steward & Clarke, 1975).

1.3 Determination of conformation

1.3.1 Introduction

In 1.2.6 the importance of conformation within the SAR formalism was demonstrated. There are two ways available for determining conformation: (i) by indirect methods, ie deductions based on measurements of spectra, diffraction patterns, dielectric increments, etc, or (ii) by direct methods, ie direct determination of conformational energy by classical or quantum theoretical calculations. The approaches (i) and (ii) will now be discussed.

1.3.2 The indirect methods

a) X-ray crystal structure determinations are capable of providing a conformation adopted by the molecule in the crystalline state. Often, in X-ray diffraction determinations of crystal structure, the heavy-atom method is used. This procedure can significantly alter the conformation of the parent compound cf GABA and GABA.HCl (Steward, Player and Warner, 1973). Since the crystal structures of parent, parent/heavy atom and hydrated-parent molecules generally show differing conformations, it may be that *in vivo* the parent molecule will display a whole spectrum of conformations depending on the degree of ionisation and hydration. The relevance of crystal structure conformations, determined by X-ray diffraction, to *in vivo* situations must therefore by questioned.

X-ray methods have, of course, been important in many ways, including the understanding of the electronic properties (eg ionic form, hydrogen bonding sites, etc.) of molecules. It is likely that the structure of the receptor will ultimately be elucidated by this method.

b) Nuclear magnetic resonance (NMR) is being increasingly used to determine the conformation of molecules in solution, Though, of course in NMR analysis the spectrum is interpreted by making empirical assumptions concerning the rotomers present in solution. For example, Ham (1974) in a NMR study of GABA and related compounds although not reporting the method of analysis used, stated that NMR "interprets the spectrum in terms of variable populations of staggered rotomers having dihedral angles of 60° and 180°." A separate NMR study on GABA (Parry Jones, Roberts & Ahmed, 1971), in which the results were interpreted in a different way to the previous work, led to a conflicting conclusion. Until a uniform and less arbitrary method of interpreting NMR data can be found, the results of this highly empirical technique must be considered with caution. The state of NMR analysis *now* has been likened to that existing in theoretical quantum chemistry *ten years ago*! (Willcott & Davis, 1975)

c) A study in which the dielectric increments of α-ω amino-carboxylic acids were used to deduce conformation was made by Edwards, Farrell & Job (1973, 1974). They demonstrated that the dipole moments were consistent with fully extended conformations of the molecules. They did not state whether any other deductions were possible from the data.

d) The analysis of microwave spectra is another empirical method by which conformation of a gaseous molecule can be estimated. As with NMR an empirical assumption must be made on which the conformational deductions are made, eg the assumption of a $V_3(1 - \cos 3\theta)$ potential.

e) Two methods for finding conformation that are finding increasing application are Optical Rotatory Dispension (ORD) and Circular Dichroism (CD). ORD is based on the variations in the degree of rotation with wavelength of plane polarised light, and CD is based on the differences in the absorption of left and right circularly polarised light with changing wavelength.

1.3.3 The direct methods

These methods are direct because an inherent attribute of the molecule itself is calculated, ie its conformational energy. The assumption that the conformation in which the total internal energy (B 2.5, equation (xvii)) of the molecule is minimal leads to the concept of preferred conformation. The physical significance of the preferred conformation is defined by the Hellmann-Feynman theorem as the equilibrium conformation of the molecule, in which all repulsive and attractive forces between nuclei and electrons have been balanced (Hellmann, 1937; Feynman, 1939). It is only in the past 25 years that the theoretical approach has become possible due largely to the development of the electronic computer. In 1950 a calculation on a hydrocarbon with ca.12 carbon atoms, at the level of Huckel Molecular Orbital (HMO) theory, would take about a year using a desk calculator. Today the same calculation would not take a second - literally!

The relationships between the direct methods may be summarised by the following outline scheme:

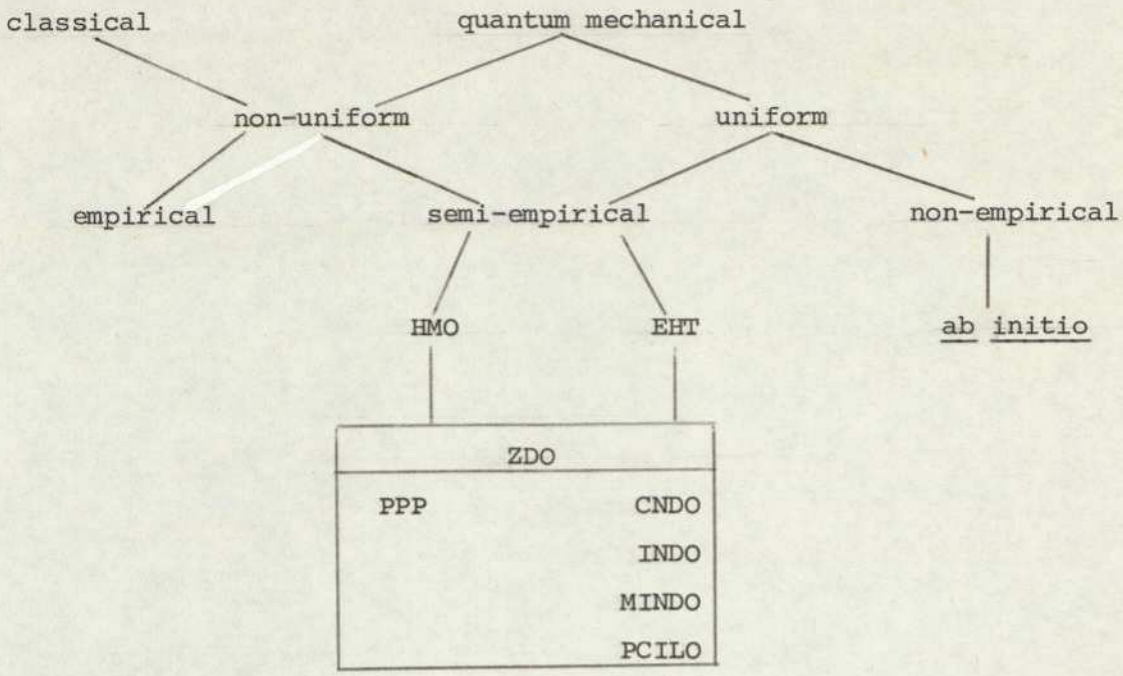

The direct methods are divided into quantum and classical, within both regimes the conformational energy of the conservative molecule can be sought. The classical methods are open to the criticism that no explicit consideration is given to the electron in the treatment of problems of a chemical nature. The quantum methods traditionally developed along two paths (i) molecular orbital (MO) theory (Hund, 1927; Mulliken, 1928, 1929; Hartree, 1928) and (ii) valence bond (VB) theory (Heitler and London, 1927).

The VB theory is based on the chemical concept that atoms exist within molecules, and that the structure of the molecule can be interpreted in terms of its constituent atoms and the bonds between them. In contrast the MO method is more physical, the molecule is considered as an assortment of nuclear fragments held in an electronic 'glue' of varying density. Of the two, VB theory, in its original form, has been discarded in favour of the MO, largely because the latter lends itself more readily to a semi-empirical interpretation. Thus, all quantum methods in the outline scheme are MO methods (although PCILO does contain a degree of VB formalism).

The MO methods have in common that they all attempt a solution of the n-body non-relativistic Schrodinger equation. The solution of this equation must of necessity be approximate, it is how the approximations are made which separates the different MO methods. A detailed discussion of MO formalism and methods is given in Appendix B.

1.3.4 Discussion

The indirect methods have limitations due to their empiricism, they are also relatively lengthy processes. A further limitation is that they are phase-dependent in that microwave analysis requires a gas, NMR requires that the substance is suitably soluble, and X-ray diffraction requires that a crystal can be grown. In contrast, the quantum mechanical MO methods are at worst semi-empirical, and can provide conformational information rapidly. The MO methods give a conformational energy which is relevant to the gas-phase (ie 'conservative' molecule), allowance for a solvent phase can be made and this is the subject of Chapter 4. As a by-product of theoretical conformational analysis the molecular wave-function provides information about the electron distribution of the molecule which can be used in PAR studies.

The potentiality and scope of theoretical calculations is such as to lead us to believe that through them a fundamental understanding of not just drug action, but of chemical processes in general may be attained. The scope of the theoretical methods will now be discussed.

1.4 Scope in the application of the theoretical methods

1.4.1 Introduction

In this section a brief mention is made of some of the more important concepts used in the theoretical analyse. They are (i) the conformation space, (ii) free-energy, (iii) population analysis, (iv) electronic indices, (v) the solvent effect, and (vi) the electrostatic potential field.

1.4.2 The conformation space

Clearly, for every single-bond of the form A_1A_2-A_3A_4 (A_i,i=1...,4 are atoms such that $A_j A_1 A_2$ j = 1 or 4 are not collinear), rotation about that bond generates an infinity of conformations which in the absence of symmetry are all distinct. Hence, for a molecule with n bonds of the type specified, there are ∞^n possible distinct conformations of an n-dimensional conformation space to be considered. As stated earlier, the assumption that the lower the total internal energy associated with a particular conformation the more stable it is, leads to the prediction of the preferred conformers of the molecule.

1.4.3 Free energy

A possible refinement to the basing of conclusions on the results of an internal energy study, is to convert to a (Helmholtz) free-energy picture. A free-energy approach will only be necessary if potential surface entropy or temperature changes are important. This aspect of conformational studies will be discussed in greater detail in 3.6.

1.4.4 Population analysis

Associated with the concept of free energy is the idea of a population analysis. The probability P_ρ of a molecule having the conformation associated with the point ρ in conformation space is given by a Boltzmann distribution function

$$P_\rho = \exp(-E_\rho/RT)$$

where E_ρ is the energy (internal or more correctly free) of the molecule in the conformation at ρ, R is the Universal gas constant and ,T the absolute temperature. E_ρ is usually an energy relative to the energy at the preferred conformation. For convenience the function P_ρ may be normalised by defining $P = \int \cdots \int P_\rho \, d\rho$, and defining $P'_\rho = P_\rho / P$ The replacement of E_ρ by P'_ρ leads to a population analysis rather than energy analysis picture. A less rigorous but often convenient way of looking at conformational maps is to note that according to a Boltzmann

distribution states within 5 kcal mol^{-1} of the global energy minimum contain 99.97% of the entire molecular population. However, this final point will be discussed in more detail in 3.6.3.

1.4.5 The electronic indices: NAP and BI

The theoretical quantum methods provide the medicinal chemist with the means of determining the amount of electron probability distribution which is associated with a particular atomic site, this leads to the concept of 'charge' on an atom. It is also possible to determine the amount of electron probability distribution associated with the region between atoms, this leads to the concept of the 'bond' between atoms. The way in which the total electron distribution should be partitioned into atomic charges is still the subject of much discussion and research (Mulliken, 1955; Roby, 1974; Jug, 1973; Dean & Richards, 1975). In this study the most common definitions of 'charge' and 'bond' have been used this allows the comparison of our results with a maximal subset of other workers. Rigorous definitions of 'charge' and 'bond' (strictly nett atomic population (NAP) and bond index (BI) respectively) are now given.

The LCAO molecular wavefunction (see Appendix B) is

$$\langle i| = \sum_{\mu} c_{\mu i} \langle \mu|$$

and the density matrix (bond-order matrix) is then defined as

$$P_{\mu\nu} = 2 \sum_{i} c_{\mu i} c_{\nu i}$$

the summation being over all occupied orbitals. From this matrix we have that the NAP on atom A,

$$= 2 + \sum_{\mu} P^{A}_{\mu\mu} \quad \text{, for atoms with } Z > 2$$

$$= \sum_{\mu} P^{A}_{\mu\mu} \quad \text{, for atoms with } Z \leq 2$$

where μ refers to atomic orbitals in the (valence) basis set of atom A. We shall adopt the generally accepted convention of using the terms 'NAP' and 'charge' on an atom interchangeably.

The bond-index (BI), for the bonding between atoms A and B is defined as

$$= \tfrac{1}{2} \sum_{\mu,\nu} \left(P^{AB}_{\mu\nu}\right)^2$$

where μ, ν $(\mu \neq \nu)$ refer to atomic orbitals in the basis sets of atoms A and B respectively.

Finally it should be noted that theoretical classical methods do not provide information on the electronic distribution of the molecules.

1.4.6 The solvent effect

As has already been stressed, the conformational calculations discussed so far all refer to a conservative molecule. It has often been the assumption that the results of a conservative-molecule conformational study have immediate relevance to the conformations adopted in the bio-phase (eg the studies by Kier (1971)). In retrospect it has been shown, perhaps not surprisingly, that the conformational modes a molecule populates in solution can be significantly different to those populated by the conservative molecule (Pullman & Berthod, 1975; Warner & Steward, 1975; see also Chapter 4). This aspect of theoretical conformational prediction has recently been receiving much attention, and techniques are now available which allow for the solvent effect to be incorporated into the calculations (Pullman & Pullman, 1975; Beveridge, Radna, Schnuelle & Kelly, 1974; Hopfinger, 1973). These methods will be fully discussed in Chapter 4.

1.4.7 The electrostatic potential

The charge of an atom gives information relevant to the electron distribution at, or in the immediate vicinity of, the atomic nucleus. The electron distribution at extranuclear points is not specified.

An alternative way in which the electronic distribution may be visualised is via electrostatic potential (EP) calculations. In this approach a test unit protonic charge is placed at points within the field of the molecular nuclear-electronic distribution and the resulting electrostatic interaction is calculated. This permits isopotential contours to be drawn in the electrostatic field of the molecule, providing information on likely protonation, alkylation and hydration sites. The EP maps also provide details of the electrostatic and hydrogen bonding sites of a molecule or molecular fragment. The EP field calculations are complementary to the charge distribution in the sense that they provide information of the extra-nuclear electron distribution, but not in the vicinity of the nuclei (since this is highly repulsive to a protonic charge). Electrostatic potentials provide the material for Section 3.7.

1.5 Some limitations of the theoretical methods

1.5.1 Introduction

The theoretical methods are not without their shortcomings, and this section is a consideration of some of the limitations and ways in which they can be minimised. The topics considered are (i) the conformational grid, (ii) independent rotations, and (iii) geometry optimization.

1.5.2 The conformational grid

In 1.4.2 it was stated that for a molecule with n single-bonds (of the type defined in 1.4.2) there are ∞^n possible distinct conformations to be considered. Hence, in order to make conformational problems practicable it is usual to assume that rotation about bonds occurs in increments of m°. In the majority of studies m is taken to be either 20 or 30. A theoretical conformational study then necessitates the computation of the molecular energy at a limited $\left(\frac{360}{m}\right)^n$ conformations of the full n- dimensional conformational continuum.

1.5.3 Independent rotations

Apart from the limitation of calculating conformational energy on a grid of m°-increments about the single bonds, it is often necessary to make approximations which allow us to effectively reduce n. This is usually done by assuming a particular rotation to be independent of the others. A fuller discussion of this point and its validity is made in 3.5. , and only a brief illustration is given here. Consider a molecule with 3 degrees of conformational freedom ($n = 3$), this would normally require 18^3 (=5832) calculations. By assuming that a methyl group, say, adopts a classical staggered conformation with respect to an adjacent tetrahedral carbon, irrespective of the orientation adopted by the rest of the molecule, the number of calculations is reduced to 18^2 (=324).

1.5.4 Geometry optimisation

A further limitation in the theoretical conformational studies is the assumption that the bond lengths and bond angles are conformationally invariant for a given molecule. The validity of this assumption has been the subject of several studies (eg Gordon & Neubauer, 1974; Kohler, Weller & Klopper, 1975). It is a fact that the optimisation of the internal geometry (ie minimising the total energy with respect to all bond lengths and angles) at each conformation can have a profound effect on the shape of the conformational energy surface (Weller, Klopper & Kohler, 1975). The fact that a geometry optimised surface is different from that without

optimisation does not, however, imply that it is necessarily more correct (Weller et al, 1975). It is, for example, possible that (a) the theoretical method does not predict internal co-ordinates accurately, or (b) the theoretical energy predicted is insensitive to changes in internal co-ordinates, then the validity of geometry optimisation must be carefully considered.

We must conclude that in conformational studies it is not practicable, for computational reasons, to optimise geometry at a sufficient number of conformations for the procedure to be generally valid.

1.6 The γ-aminobutyric and glutamic acid neurotransmitter systems

1.6.1 Introduction

Chapter 5 of this thesis will concentrate on the application of theoretical quantum chemistry to the γ-aminobutyric acid (GABA) and L-glutamic acid (GLU) neurotransmitter systems. Molecules active in the GABA system are zwitterions at physiological pH (Wyman, 1936), while those active in the GLU system are mono-anions (Johnson, Curtis, De Groat & Duggan, 1968). The canonical molecules are shown below:

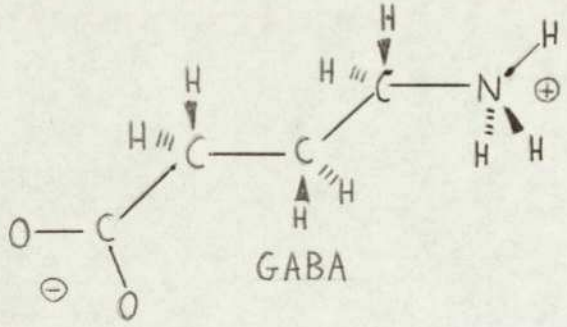

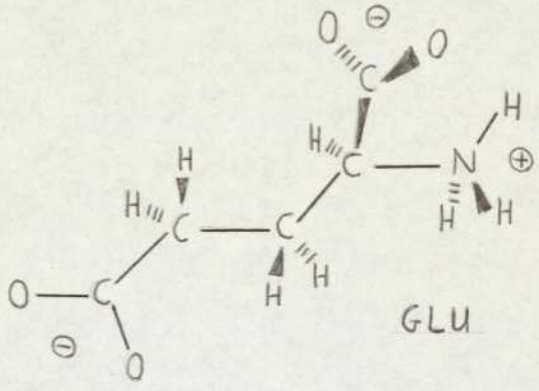

Although these molecules are structurally similar (GLU = γ-carboxy - GABA), as we shall see, their pharmacological actions are very different. This section is devoted to the pharmacology of the GABA and GLU systems.

1.6.2 Nerve impulse transmission

The following is a brief and simplified statement of the sequence of events concerning nerve impulse transmission. This is included for completeness, because it is the broad background of this research.

In the central nervous system (CNS) the transfer of an electrical impulse from one nerve to, eg, another is effected by means of a chemical process. The initial impulse propagating down the axon of nerve cell (neurone) I causes small 'packets' (vesicles) of a chemical substance (transmitter) to move towards the pre-synaptic membrane (see Figure 1.1). On arrival at the pre-synaptic membrane the vesicles release into the synaptic cleft the transmitter, which then traverses the cleft to the post-synaptic membrane - a phospholipid bilayer possessing protein macromolecules

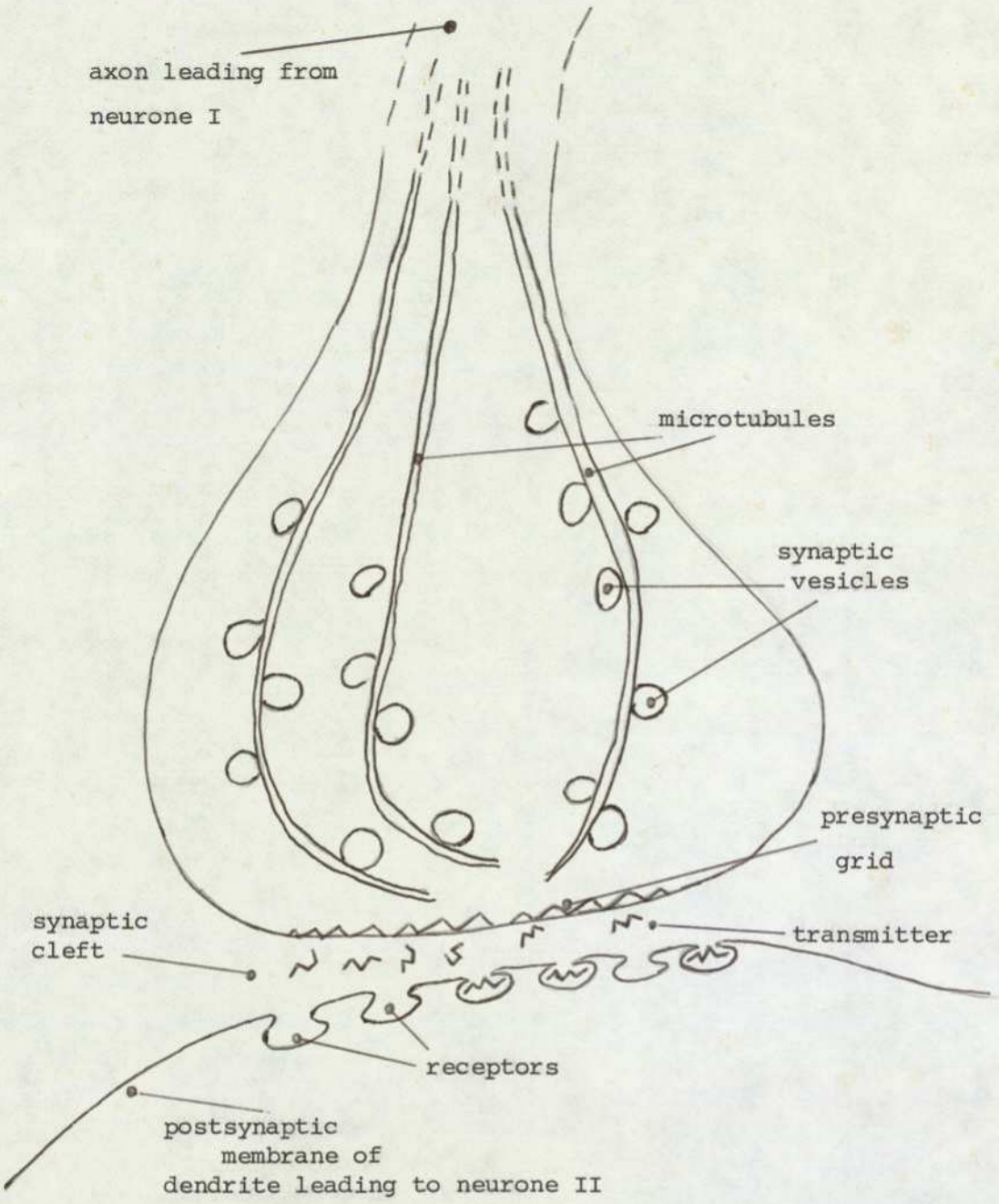

Fig. 1.1 Morphology of a synapse (after Gray, 1975). Vesicles move along microtubules to vesicle attachment sites on the presynaptic grid - a triangular array of protein units. Thence, they release the transmitter substance they contain into the synaptic cleft via pores in the presynaptic grid.

capable of 'recognising' the transmitter (receptors). The arriving transmitter molecule forms a complex with the receptor, this process then leads to a change in the selective permeability of the post-synaptic membrane and the subsequent initiation of an impulse in the dendrite of nerve cell II (NB the axon from nerve cell I need not necessarily synapse on a dendrite, it could also synapse with a neurone or even another axon). Finally, the neurotransmitter actions are terminated in part by uptake processes, and enzymic degradation of the transmitter. Our interest lies in those parts of the nervous system in which GABA and GLU are the naturally occurring transmitters.

The selective change in permeability to ions caused by the forming of the transmitter/receptor complex may be such as to either hyperpolarize or depolarize the resting (normal) membrane potential. If the membrane is hyperpolarized the endogenous transmitter is said to be inhibitory - GABA is an inhibitory transmitter (McIlwain & Bachelard, 1971), ie the firing rate of nerve cell II is reduced if GABA is released at the synapse in Figure 1.1. Similarly, if the membrane is depolarized, the endogenous transmitter is excitatory - GLU is an excitatory transmitter (McIlwain et al, 1971).

Not all drugs which have action at the receptor have the effect of the canonical transmitter (agonists); there are also those which block the action of the transmitter (antagonists). This latter type of drug action is of great importance pharmacologically, eg antihistamines (histamine antagonists).

1.7 The prostaglandins

1.7.1 Introduction

Chapter 6 will concentrate on the application of theoretical quantum chemistry to the class of pharmacologically active molecules collectively known as the prostaglandins (PGs). It should be noted that Chapter 6 is essentially a brief feasibility study of the extension of the techniques more fully applied to GABA and GLU systems on the PGs (ie large molecules). The specific PG of interest in this study is designated PGE_1, and this is shown below:

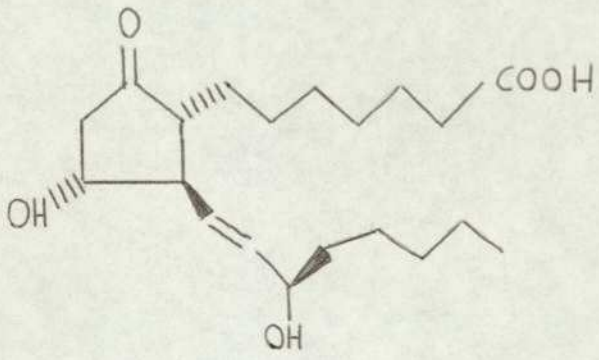

The numbering scheme and general nomenclature of the naturally occurring PGs are given in Appendix A.

1.7.2 Pharmacology of the prostaglandins

Ionically the PGs are neutral and have little structural or chemical similarity to the molecules of the GABA and GLU systems. There is probably no other class of compounds that has so many different actions on cells, tissues and organs. They are known to (i) induce parturition (Karim, Trussell, Patch & Hillier, 1968) and in large doses may induce abortion (Karim & Filshie, 1970), (ii) inhibit gastric acid secretion (Robert, 1968), and so be useful in the treatment of peptic ulcers (Karim, Carter, Bhana & Ganesan, 1973), (iii) be bronchodilators (Cuthbert, 1969), having use in asthma therapy, (iv) inhibit platelet aggregation (Kloeze, 1967), making them important in the possible prevention of thrombosis, (v) have a function in the central nervous system (Horton, 1969) being potentially useful for the treatment of hypertension (Hensby, 1974), (vi) be luteolytic (Pharriss & Wyngarden, 1969), a property already being exploited by animal breeders (Upjohn Veterinary Symposium, 1975).

The PGs are highly potent and show high structure-activity specificity. For example, PGE_1 and PGE_2 (differing only by a double-bond in the 5,6 position) have opposite effects on induced erythrocythe swelling, acting at concentrations as low as $10^{-11}M$ (Andersen & Ramwell, 1974).

Unlike the vesicle storage of GABA, the PGs are synthesised from precursor fatty acids as and when they are required. The PGs can act at receptors, and there is some evidence for the existence of more than one type of prostaglandin receptor. Acting at receptors means that an important development in PG pharmacology would be the discovery of a specific antagonist, and poly(phloretin phosphate) seems a likely candidate.

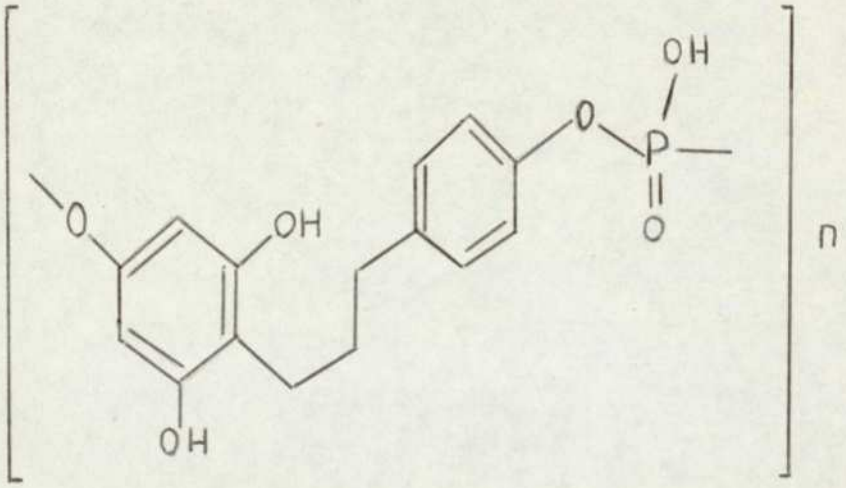

Poly (phloretin phosphate) - PPP

The ubiquity, rapid availability and high potency suggests a position of primary importance in future pharmacological research for the prostaglandins.

2.1 Introduction

Appendix B contains a detailed discussion of the formalisms which lead to the classical and quantum methods for predicting the preferred conformation of molecules. It also contains a description of the many semi-empirical methods that exist within the quantum mechanical formalism.

This chapter begins with a general discussion concerning the relative merits of the different methods described in Appendix B. The available studies on GABA are then compared and contrasted. A comparative study of the GLU agonist ibotenic acid (ITA) is made, using the PCILO, CNDO/2 and EHT MO methods. A further investigation of PCILO and CNDO/2, in relation to resonance, results in the choice of CNDO/2 as the MO method of choice for the study of the GABA and GLU systems. Finally the suitability of CNDO/2 for the PGs is discussed.

2.2 A general discussion of the semi-empirical methods for predicting molecular conformation

2.2.1 Introduction

In this section a discussion and comparison of the many semi-empirical MO methods is made in the light of already published data. As a result of the discussion, guidelines in the form of an artificial key, are provided for arriving at a suitable method for any particular study. It is shown that the key has failings, and that therefore more basic research into the theoretical methods is needed. A philosophy governing the direction that research could take is outlined.

2.2.2 A comparison of the semi-empirical methods

Although the non-uniform HMO and PPP (B 3.2 and B 3.3 respectively) methods are not theoretically strong, they have been used successfully in a number of studies. The opinion has been expressed (Offenhartz, 1970) that the success of these methods is due to the symmetry, and the chemico-electronic simplicity of the molecules to which they have been applied, plus a low criteria for what the authors consider as success. It may be regarded as a failure of the general theory behind HMO and PPP that no one variant of the many parameterization schemes has led to a widely reliable version. However, these methods (HMO in particular) have an important role in the teaching of chemistry. As an introduction to the concepts of MO theory HMO is an invaluable tool.

After the π - electron methods of the previous paragraph, increasing theoretical sophistication yields the all-valence electron EHT method. This method has been widely used, particularly in the field of medicinal chemistry where its computational rapidity made it suitable for large organic drug molecules. The theoretical basis of EHT in comparison to the RHF formalism has been studied (Allen, 1970; Blyholder & Coulson, 1968; Allen & Russell, 1967) and the primary sources of error indicated. The chief source of error

(Allen, 1970) seems due to the variation of $\sum_{\alpha} V_{\alpha}(r)$ in the core Hamiltonian matrix (B 2.4, equation (xiii)) during deformations in the internal co-ordinates and rotations about bonds. Since V_{α} is the potential of the electrostatic field produced by the nuclei and electrons, it follows that the errors will be greatest when there are high excess charges on the atoms. Unfortunately a recognised failing of EHT is that it predicts high excess charges for heteroatoms (Pullman, 1968)! Hence, although EHT may be suitable for hydrocarbons it should be used with caution when heteroatoms are involved (Herndon and Fever, 1968). The EHT prediction that the HOH angle in water is 140° (experimental value is 104.5°) is a striking example of how it may fail when heteroatoms are involved.

The SCF all-valence electron semi-empirical methods represent the next increase in sophistication. CNDO/2 is the most widely used of these methods; because of this its main failings are now known. It is known that CNDO/2 often fails to predict the conformational behaviour of conjugated systems correctly (Gropen & Seip, 1971); it is also apparent that the current parameterization of the method for 2nd row atoms of the periodic table is unsatisfactory (Veillard, 1975). The charges produced by the CNDO/2 method are more realistic than those of the EHT method (see 2.4.2). The INDO method although computationally slower than CNDO/2 does not, in general, differ from the latter in its conformational and charge predictions. It is widely believed that INDO does not offer a significant improvement over CNDO/2 to warrant the extra computing time (Golebiewski & Parczewski, 1974). The NDDO scheme has not been really tested yet, although available results suggest that much work is required on the parameterization. A study (Davidson, Jorgensen & Allen, 1970) using NDDO and CNDO/2 showed that although NDDO predictions of internal geometries were slightly superior to CNDO/2, the latter method was better for isomerization energies, barriers to rotation, dipole moments and force constants! This illustrates the point that when dealing with semi-empirical methods, increasing the theoretical sophistication of the method is no guarantee of improved results, unless the parameterization of the empirical parameters is good.

The PCILO method seems ideally suited to conformational problems relating to large organic molecules since it is computationally very fast (much more so than CNDO). Its predictions are in good agreement with experiments in those conjugated systems where CNDO is known to fail (Perahia & Pullman, 1973). The theoretical problems

concerning the density matrix and the treatment of resonance have been considered in Sections 2.4 and 2.5. PCILO is a relatively recent development (1970) and before it can be critically evaluated, more studies applying the method to small molecules on which experimental comparisons can be made are needed.

The latest of the SCF all-valence electron methods is MINDO/3. The method, not surprisingly, performs very well for molecules similar to those on which the empirical parameters were based. It remains to be seen how useful the method is with molecules significantly different from those on which it was parameterized.

In summing up the semi-empirical methods, it is true to say that they have been the most fruitful in SAR studies (Kier, 1971) and indeed have contributed much to the understanding of chemistry in general (Dewar, 1975).

2.2.3 Some general guidelines for the choice of methods

Based on the discussion of the methods made in 2.2.2 it is possible to formulate a scheme of recommendations which may reduce the possibility of choosing a method ill-suited to the study of a particular molecule. This is presented below in the form of an artificial key.

1. Problem conformational	— 2
Not above	ab initio ≠
2. Complex conformational problem	— 4
Not above	— 3
3. Small molecule	ab initio
Medium or large molecule	— 4
4. Heteroatom system	— 5
Hydrocarbon	— 6
5. 1st row (Periodic table) atoms only	— 7
Molecule contains 2nd row atoms	MINDO or PCILO
6. Rotation within conjugated system (ie )	EHT, MINDO, PCILO
Not above	any method
7. Rotation about Hetero-Hetero atom bond with lone pairs on both atoms	MINDO or PCILO
Not above	— 8
8. Rotation within conjugated system	MINDO or PCILO
Not above	CNDO, MINDO, PCILO

As an illustration on the use of the key, consider the problem of the conformational modes of biphenyl,

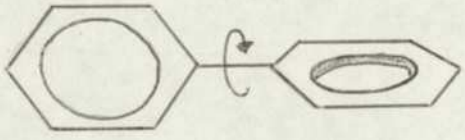

The results of studies made by EHT (Hoffmann, Bissell & Farnum, 1969) and PCILO (Perahia & Pullman, 1973) predict an angle of twist between the rings of c.60° and c.30° respectively. These results are in better agreement with the experimentally determined (Almenningen & Bastiansen, 1958) value of 42° than CNDO, the use of which is contra-

≠ For exceptionally large molecules (eg PGs) even one calculation at ab initio level may be inconvenient, as for example in our work with PGs. In these cases a semi-empirical method must be chosen which is suitable to the needs of the problem under study.

indicated by the key, which gives a value of 90° for the angle (Tinland, 1968). No result is currently available for MINDO.

The key is at present limited by the paucity of selection criteria: most paths lead to several methods. An example of the unsatisfactory nature of present selection criteria is provided by the propionaldehyde molecule:

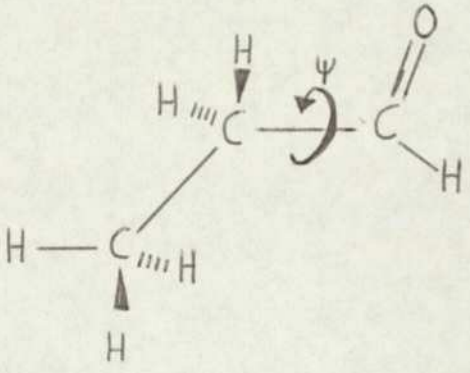

Ψ = 0 shown

Ψ increasing as indicated by direction of arrows

A small molecule has been chosen as an example in order to allow ab initio results to be included. The key recommends either CNDO, PCILO or MINDO for use with this molecule. The results of the various studies on this molecule are:

i) Ab initio ≠(Radom, Latham, Hehre & Pople, 1972) - two minima at $\Psi = \overset{+}{-} sc$, ap (see Appendix C), the latter being the most stable.

ii) Experimental methods - microwave (Butcher & Wilson, 1964) and NMR (Karabatsos & Hsi, 1965), two minima at Ψ = ca.50°, ca.180°, the former being the most stable.

iii) PCILO (Kohler et al, 1975) - two minima at Ψ = c.75°, 180°, the former being the most stable.

iv) CNDO (Herndon et al, 1968) - one minima at Ψ = 90°. A maximum at = 180° (see diagram below).

v) EHT (Kohler, 1971) - two minima at Ψ = 50°, 180°, the latter being the most stable.

The qualitative ab initio picture is endorsed by the empirical experimental results, and two minima are again given by the PCILO method. However, CNDO/2 (which is also recommended) is not even in qualitative agreement with all the other methods, giving only one minimum at a different angle. The best agreement with ab initio is given by the EHT method!

≠ Only qualitative results can be given because the method was used for a very limited number of points in conformation space.

All the above results are those made without geometry optimization (see 1.5.4)

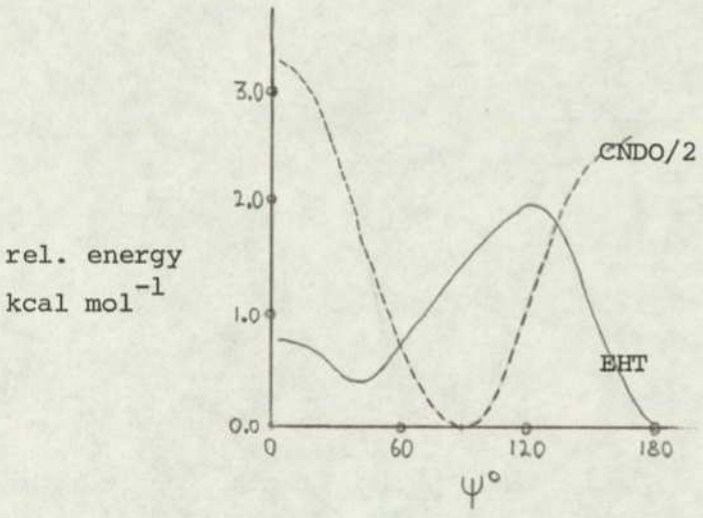

Concerning the newer methods, PCILO and MINDO, much work needs to be done on these because they tend to appear in the key where other methods fail rather than because of their own proven suitability at these particular points.

2.2.4 Philosophy for the future development of the theoretical methods

It is convenient to imagine chemistry as being represented by a 'floor' inlayed on which are then the many chemical compounds. It shall be assumed that the floor is constructed such that around a particular molecule A are its close structural analogues.

A major philosophical question them emerges as to how one can best provide a theoretical covering for the floor. Should one attempt to provide a single ab initio fitted carpet or should one hope to design several different semi-empirical coloured-rugs? If we adopt the latter approach we must concede that rugs of a particular colour are more suited to certain areas of floor than others. Naturally the rugs overlap, for example, over the piece of floor occupied by ethane, rugs of a great many colours overlap, however, over hydrogen peroxide the covering is sparse! The rug approach is very flexible, because as rugs of a new colour are produced (eg PCILO) the distribution of old rugs on the floor can be adjusted to get optimum effect from the new one, perhaps allowing old worn out and fading rugs (eg EHT) to be reduced in size.

The above scenario suggests that several semi-empirical methods together with knowledge concerning their areas of success and failure offer a viable (and perhaps even more desirable) alternative to sophisticated, computationally demanding ab initio methods for the general theoretical description of chemistry. In order to make the 'rug' approach succeed, clearly what is needed is a better knowledge of which types of molecule and in which situations failures (and successes) of a particular method are likely to occur, and if possible why they occur. The artificial key presented in 2.2.2 represents a crude illustration of the type of guidance which could become available to the user (rather than developer) of theoretical methods in the future.

It should be noted that the 'rug' approach allows a semi-empirical method to be of considerable value even though it is less than perfection. In certain circumstances it is even still possible for a method to be of use in an area where it is known to perform badly. For example, SAR is of a comparative nature and usually involves homologous series. It may therefore be possible to obtain meaningful results using EHT charges despite the bad quantitative prediction of this electronic index by EHT MO theory.

Finally, although the classical methods may still have a useful role to play, chemistry is essentially 'the science of the valency electron' and it is difficult to find any philosophical justification

for the use of methods in which no explicit consideration is made of the electron.

2.3 A comparison of previous theoretical MO studies on GABA

2.3.1 Introduction

For the GABA molecule the key (2.2.3) recommends either CNDO, PCILO or MINDO$^{\neq}$. Studies of the GABA molecule have been made using CNDO/2 (Warner & Steward, 1975), PCILO (Pullman & Berthod, 1974) and EHT (Kier & Truitt, 1970). A comparison of these results is now made with a view to choosing the most suitable method with which to study GABA analogues.

2.3.2 The EHT study

Chronologically the first study to be made on GABA was that by Kier et al (1970) using EHT. This was a very unsatisfactory study, no charge data were reported, only energy profiles (see sub-section 3.5. for a fuller discussion of the (in)validity of this approach) were calculated, and the calculations were made at (large) intervals of 60° allowing the possibility of subtleties in energy variation to be missed. The results implied that the preferred conformation of the conservative molecule was 'all-trans' (see Fig. below)

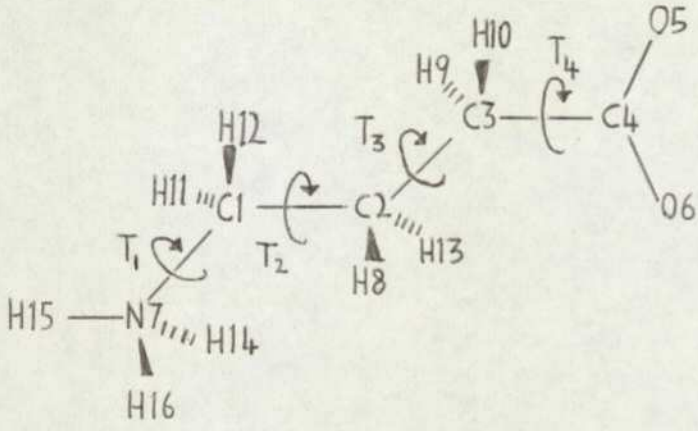

'All trans' conformer

$T_1=T_2=T_3=T_4=180°$

The Klyne-Prelog convention (Appendix C) is used to define the torsion angles, which are $T_1=\{H15.N7-C1.C2\}$, $T_2=\{N7.C1-C2.C3\}$, $T_3=\{C1.C2-C3.C4\}$ and $T_4=\{C2.C3-C4O5\}$. It is evident that the 'Kier conformation' of GABA corresponds to $T_1=T_2=T_3=T_4=180°$.

$^{\neq}$ Computer programmes for MINDO/3 calculations were not generally available at the outset of this work.

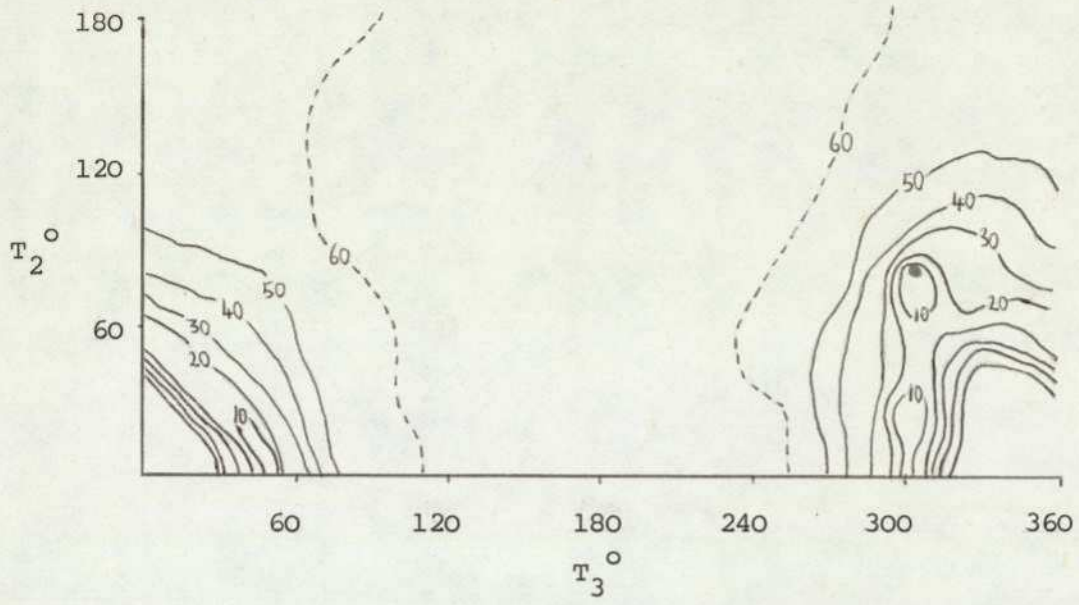

(a) CNDO/2

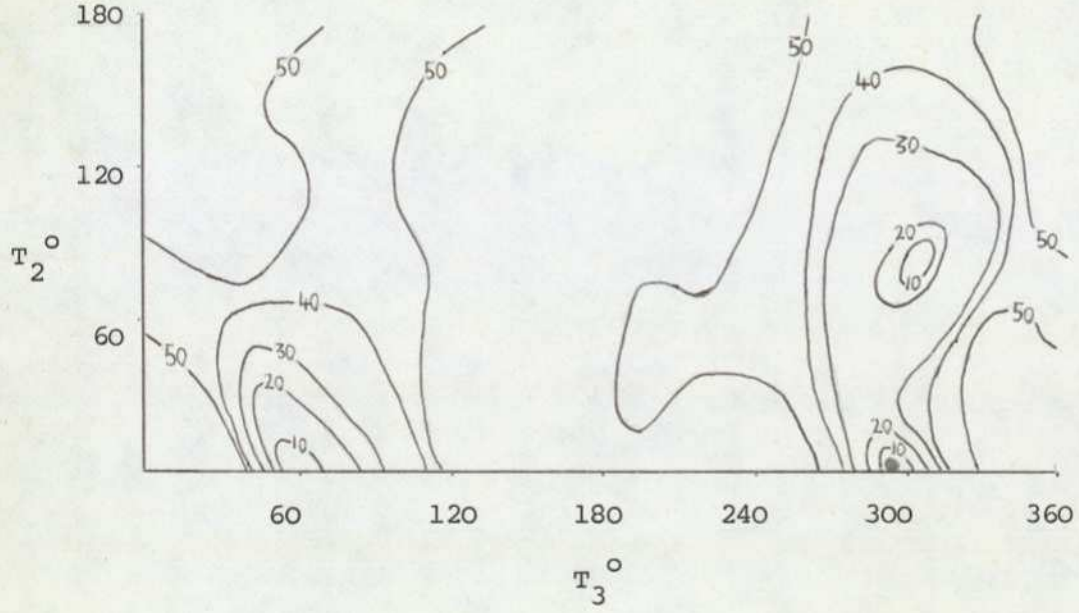

(b) PCILO

Fig. 2.1 T_2-T_3 energy surfaces for GABA. Method of calculation (a) CNDO/2 and (b) PCILO. Global energy minimum marked by ● , contours in kcal mol^{-1} relative to global minimum.

2.3.3 The CNDO/2 study

The CNDO/2 study (Warner et al, 1975), in contrast to the EHT one, took the form of a (T_2, T_3)-conformational energy surface, using a close 20o grid which was refined to 5° (see 3.6.3) around minima. The results show that the global minimum is a relatively folded conformation ($T_1 = 180°$, $T_2 = \mp 80°$, $T_3 = \mp 55°$, $T_4 = 180°$). The 'all-trans' global minimum of the EHT study appears as a shallow local minimum ca.60 kcal mol^{-1} above the global minimum. The CNDO/2 energy surface for the zwitterion is shown in Figure 2.1(a).

At this stage the EHT and CNDO/2 methods offer completely differing scenarios of the preferred conformers of the conservative GABA zwitterion. EHT suggests that methylene staggering forces are dominant, whereas CNDO/2 predicts electrostatic attractive forces to be crucial. The available evidence (and common sense) favours the CNDO/2 result as this method is generally thought to be superior to EHT for polar molecules (Offenhartz, 1970; Kier, 1971), and the presence of heteroatoms does not favour the use of EHT. However, as we have seen, theoretical evidence is not always to be believed (2.2.2, propionaldehyde example). For this reason the PCILO study (Pullman et al, 1974) (which also contained some limited ab initio computations) was particularly relevant.

2.3.4 The PCILO study

The PCILO study was of the (T_2,T_3) energy surface calculated on a 30° grid, this surface is shown in Figure 2.1(b). The surface shows that the preferred conformation is highly-folded ($T_1 = 180°$, $T_2 = 0°$, $T_3 = -60°$, $T_4 = 180°$) and the 'fully-trans' form is ca.55 kcal mol^{-1} above the global minima. The PCILO results are thus in qualitative agreement with CNDO/2 and contradict the EHT study. It is now of interest to make a closer comparison of the CNDO/2, PCILO and limited ab initio results.

2.3.5 A detailed comparison of CNDO/2 and PCILO results

In both PCILO and CNDO studies there are minima at ($T_2 = 0°$, $T_3 = \mp 60°$) and ($T_2 = \mp 90°$, $T_3 = \mp 60°$), the methods appear to differ as to which of these are the global minima. In the CNDO study the ($\mp 90°$, $60°$) minima only become the global ones when a 5° grid is constructed, and hence a similar refinement to the PCILO calculations may bave brought agreement between the methods. Interpreting the CNDO study as having been made on a 30° grid (by interpolation where necessary), apart from inverting the ordering of the

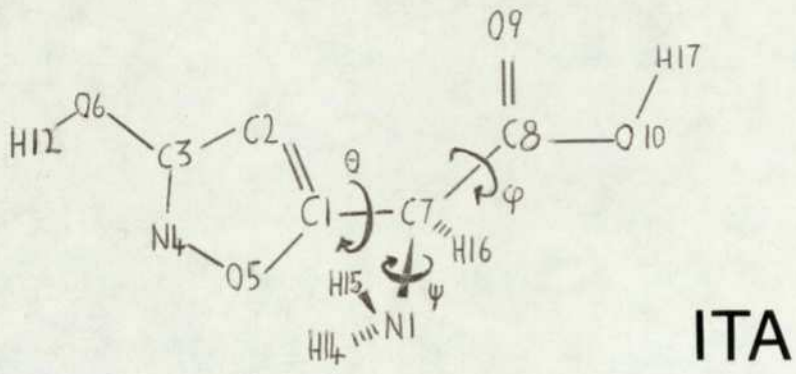

Fig. 2.2. Ibotenic acid molecule. Conformation shown defines $\theta = \psi = \phi = 0^{\circ}$. In this conformation C2.C1.C7.C8.O9 are planar and C1.C7 bond bisects the H14.N1.H15 angle looking down N1.C7.

conformation	T_2°	T_3°	ΔE (kcal mol^{-1})		
			PCILO	ab initio	CNDO/2
Global minimum	0	±60	0	0	0
Secondary minimum	∓90	±60	9	14	26
Crystal structure	180	±60	41	30	46
Fully extended	180	180	54	44	49

Table 2.1 Relative energies of conformations of GABA. Comparison of PCILO, ab initio and CNDO/2. Results are based on a 30° grid study (CNDO values have, where necessary, been interpolated from a 20° grid).

minima, causes a shift in the values of the contours (eg in Fig.2,1(a) the dotted 60 kcal mol^{-1} contour corresponds approximately to the 50kcal mol^{-1} contour of the PCILO map) leading to an energy surface very similar to the PCILO one (Figure 2.1(b)). In Table 2.1 the relative energies of some relevant conformations (viz minima, crystal structure, fully extended) are given for PCILO, CNDO and ab initio (STO-3G basis) MO methods. The three methods appearing in Table 2.1 are consistent in their ordering of conformational energies.

2.3.6 Conclusions

Previously made studies of GABA have been brought together. For the first time a detailed comparison of the conformational scenarios predicted for this molecule by PCILO, CNDO, (limited) ab initio and EHT MO methods has been made. It is concluded that CNDO and PCILO MO methods present a fairly unified picture of the conformational modes of the conservative molecule. This picture is supported by available ab initio calculations and is in conflict with the EHT results.

2.4 An investigation into the description of the conformational and electronic modes of the GLU agonist ITA by CNDO/2, PCILO and EHT MO methods

A conformational study of the glutamate agonist R(ITA) (Figure 2.2) has recently been made using the CNDO/2 scheme (Borthwick and Steward, 1976). This molecule contains the carboxyl and amino groups, which are the most commonly occurring in the type of drugs active at glutamate and GABA receptor sites. It also contains the heterocyclic isoxazolidone structure which for this comparison would seem more interesting than a carbon chain (eg GABA, glycine, etc). It was therefore decided to use this molecule as a model for the comparison of CNDO/2, EHT and PCILO semi-empirical MO methods.

The non-ionic, zwitterionic, and mono-anionic molecules were studied since each contains structural features not present in the other forms. The non-ionic molecule is shown in Fig.2.2, the zwitterion is formed by moving the H17 proton to the $-NH_2$ group, and the anion is formed by removal of the H12 proton from the zwitterion. Standard bond-lengths and angles (Pople & Beveridge, 1970) have been used in this study, with the exception of those of the isoxazolidone ring which were taken from the muscimol crystal structure (Brehm, 1973).

The MO methods to be compared here have been described in detail in Appendix B. The conformational angles used in this investigation are defined in Figure 2.2. For subsections in which a single

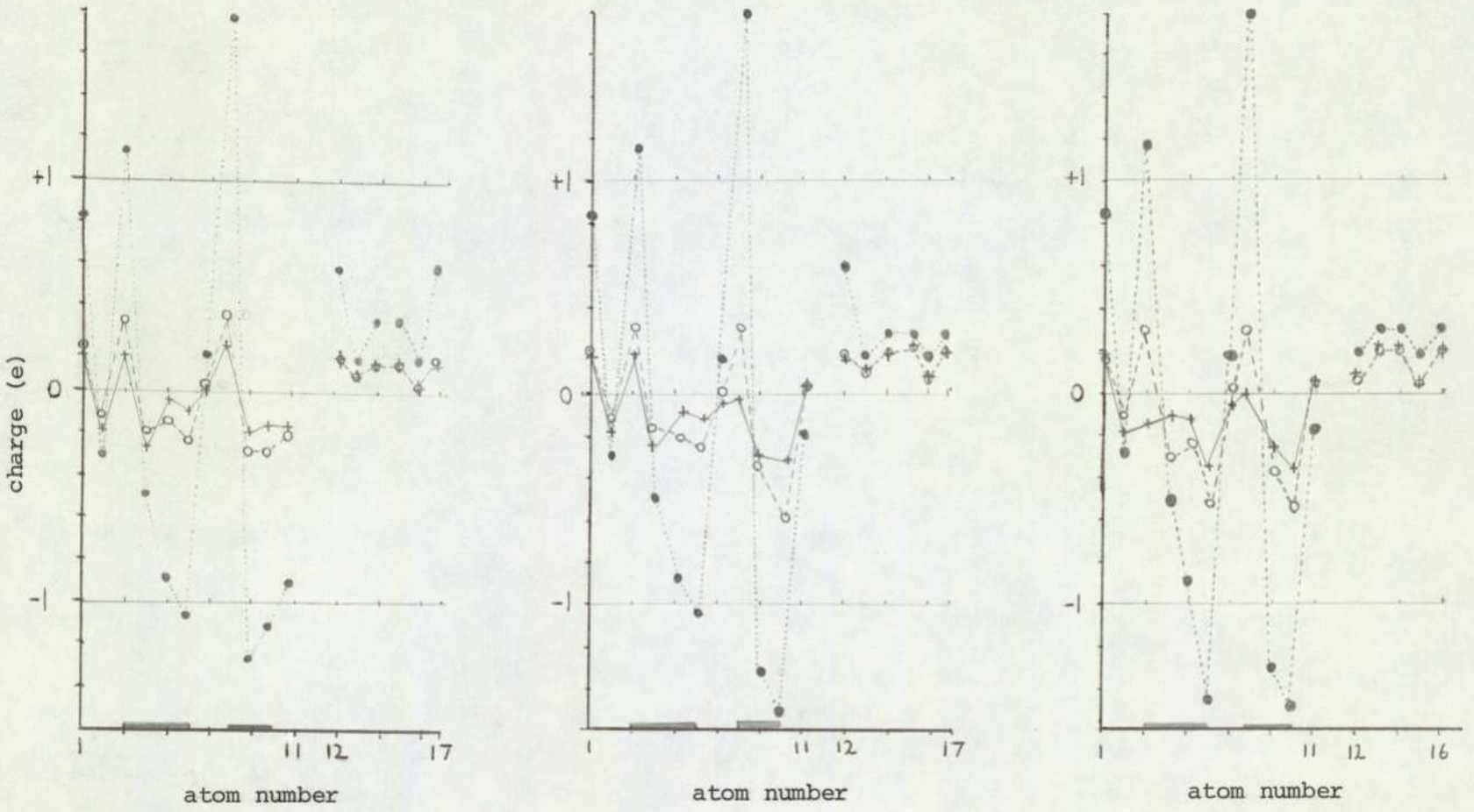

Fig. 2.3. Atomic charges for ITA ionic species. Charges calculated by (i) EHT ..•.. (ii) CNDO/2 -.o.- , and (iii) PCILO -/+- (see Fig. 2.2 for atom numbers).

conformation is being discussed, that conformation is $\theta = \varphi = \psi = 0°$ Where only one angle is being varied the remaining two are fixed at $0°$.

The comparison of the methods will be made for the charges, energy, conformation and barriers to rotation of ITA. Each molecular parameter will be discussed as a separate subsection.

2.4.2 A comparison of charge prediction

The concept of charge has been discussed in 1.4.5, and the definition in that section used here.

It can be seen from Figures 2.3(a-c) that the charges predicted by the CNDO and PCILO methods are, in general, in very good agreement. Exceptions to this statement occur with atoms involved in the resonance of the $-COO^-$ group and $-CON^-$ moiety. Reasons for these differences will be discussed in section 2.5, but it is noted here that in these situations the EHT results (and *ab initio* results for $-COO^-$ group (Ryan & Whitten, 1972)) qualitatively support the CNDO picture. Further, a consistent relative ordering of the N4 and O5 charges is not obtained in any of the three molecular forms. On the basis of these results there seems a small but consistent trend for PCILO to make carbons more and oxygens less negative than CNDO.≠

Attention has previously been drawn to the small positive charge (and sometimes even a slight negative charge) that CNDO predicts on hydrogen atoms in comparison to other methods (Pullman, 1968). This observation is not noted for CNDO in comparison with PCILO, which is seen to reproduce CNDO hydrogen charges closely.

The failure of EHT in that it exaggerates charge separations (sigma -bond polarisation effect) (Pullman, 1968) is again well illustrated here. The C-atom in the $-COO^-$ group has a charge of ca.+1.8e and one of the bonded oxygens a charge of ca.-1.5e! However, there is reasonable qualitative agreement between EHT and PCILO/CNDO charges.

For the $-NH_3^+$ group, CNDO and PCILO predict a small positive charge on the nitrogen, while EHT suggests a negative charge. *Ab initio* calculations (Csizmadia, 1974; Dean *et al*, 1976) tend to support the EHT picture.

≠ I have recently noted this trend in a paper on morphine-like opiate narcotics (Loew, Berkowitz, Weinstein & Srebrenik, 1974), in which both PCILO and INDO methods were used. In this latter reference the trend is remarkably consistent. It would be of interest to see which method gives charges closer to *ab initio* values.

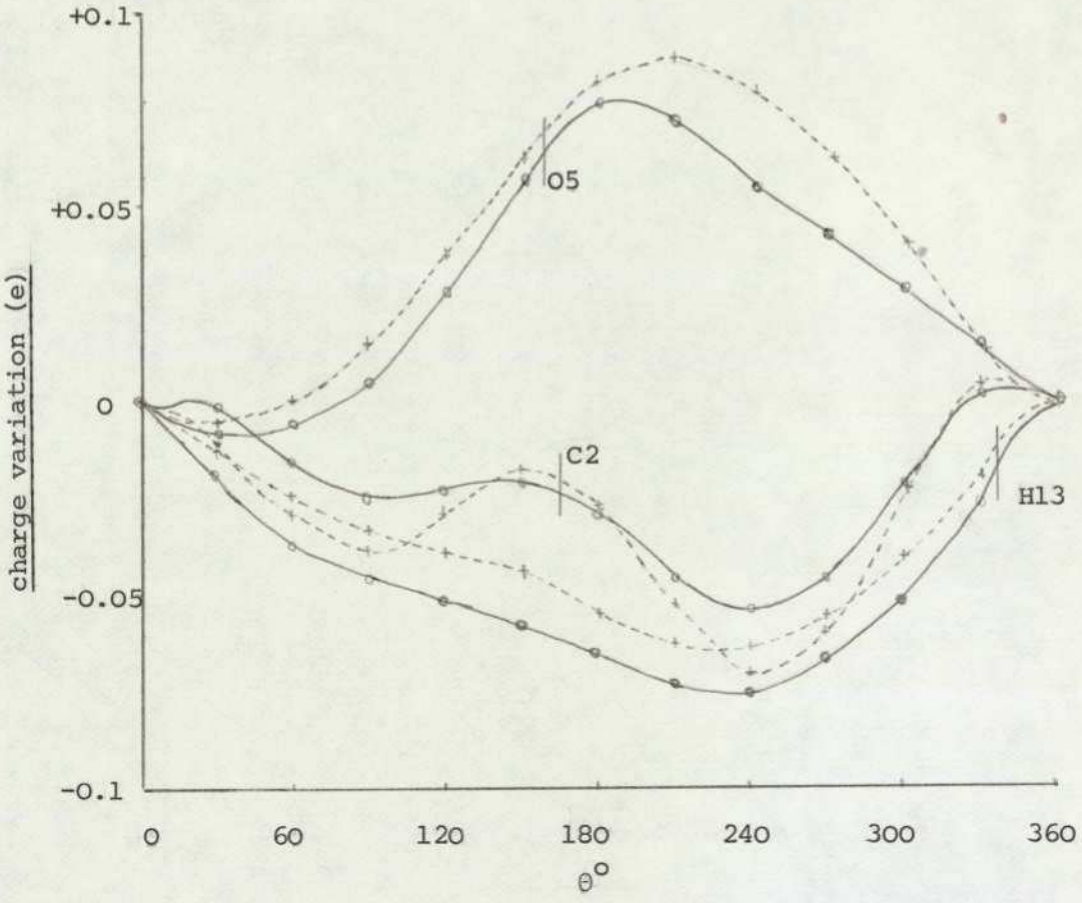

Fig. 2.4 Charge variation on atoms C2, O5, H13 during 360° rotations of θ in the zwitterion. Calculation by CNDO/2 and PCILO all other variations ⩽ 0.05 (n.b. EHT variation ⩽ 0.05 for <u>all</u> atoms).

Species	PCILO	CNDO/2
Non-ionic	2.93	3.01
Zwitterion	10.74	10.65
Mono-anion	15.19	14.00

Table 2.2

Dipole moments (Debyes) for ITA species as calculated by PCILO and CNDO/2.

Species	PCILO	CNDO/2	EHT
Non-ionic	-85889	-85928	-28560
Zwitterion	-85765	-85802	-28606
Mono-anion	-85270	-85304	-28536

Table 2.3

Total internal energies (kcal mol^{-1}) for ITA species as calculated by CNDO,PCILO and EHT.

Rotation	PCILO	CNDO/2	EHT
θ	5.2	10.8	19.0
ϕ	4.2	10.0	29.1
ψ	1.8	1.2	3.0
ΔE_{θ}	3.5	4.0	-0.6
ΔE_{ϕ}	4.0	2.7	0.4

Table 2.4

Maximum barrier to rotation and energy differences between minima (kcal mol^{-1}) for the ITA zwitterion calculated by PCILO,CNDO/2 and EHT.

In 3.3 it will be shown that for most molecules the variation of charge over conformation space is expected to be order of 0.1e. Figure 2.4 shows the variation in PCILO and CNDO charges for atoms C2,O5 and H13 in the zwitterion ($0 \leqslant \theta < 2\pi$): all other atoms have a variation $\leqslant 0.05e$. It can be seen from Fig.2.4 that the two methods give a consistent qualitative picture of the inductive effects on these atoms during a θ-rotation, and that the total variation of charge is $< 0.1e$. With EHT the maximum variation in charge is consistently less than with PCILO and CNDO, and the quality of the variation seems less sensitive to conformational changes also.

PCILO and CNDO dipole moments (table 2.2) are in good agreement.

2.4.3 A comparison of energy predictions

The PCILO and CNDO energies are in remarkable agreement (Table 2.3), better than 0.1% in all cases. EHT gives energies ca.3 times larger than the PCILO/CNDO ones, and the relative energy differences between molecular species are not even qualitatively reproduced. Exaggerated energies (as with charges) have previously been noted as a feature of EHT (see eg. Dashevski, 1973). For example, PCILO/CNDO give ca.-12000 kcal mol^{-1} for ethane compared to -6000 kcal mol^{-1} with EHT. The bad reproduction of the relative zwitterion/mono-anion energy difference may well be due to interaction between two non-bonded fragments of the molecule causing increased stabilisation in the mono-anion. Such stabilisation has been noted (Hoffman & Olofson, 1966) with EHT in the case of anions of allylic systems.

2.4.4 A comparison of conformational predictions

Figures 2.5(a-c) show the relative energies of the zwitterion calculated by the different methods plotted aginst conformational angles θ, Φ and Ψ respectively. The $-COO^-$ group has been kept as

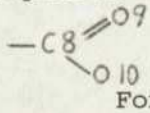

for all methods in this comparative study.

For the θ-rotation CNDO predicts $\theta = 60^\circ$ (NH_3^+ nitrogen (N11) lying in plane of ring adjacent to cyclic oxygen (O5)) as the global minimum, with $\theta = 270^\circ$ as a secondary local minimum. PCILO also predicts this secondary minimum, but moves the global minimum to $\theta = 30^\circ$≠

≠ Along the PCILO energy curve the CNDO minimum energy position ($\theta = 60^\circ$) is only ca.0.2 kcal mol^{-1} from the PCILO position ($\theta = 30^\circ$). Hence, in the sense that $\theta = 60^\circ$ is energetically easily accessible to the molecule in the PCILO picture, we may say that the PCILO minima are compatable with those of the CNDO method.

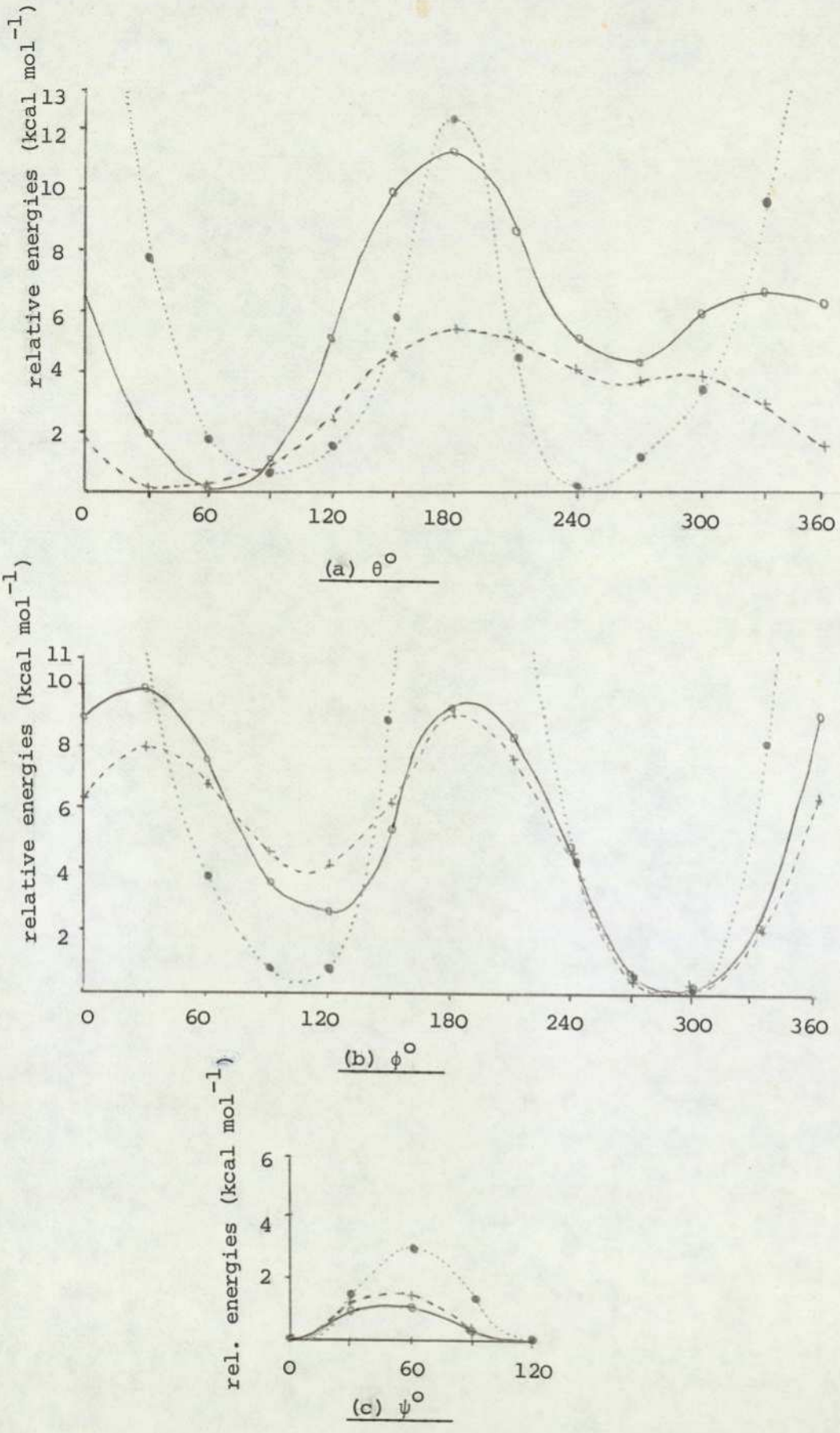

Fig. 2.5. Energy profiles for ITA zwitterion. Absolute minimum at (+sc, -sc, sp) according to CNDO( ) and PCILO ( ), and at (-ac, -sc, sp) according to EHT( ).

(calculations on a 10^{o} grid show this value to be $\theta = 40^{o}$). EHT gives minima at $\theta = 90^{o}$, 240^{o}, with an inversion of global and secondary minima compared with the PCILO/CNDO picture (global and secondary maxima are likewise inverted).

For the φ-rotation all three methods agree on $\varphi = 120^{o}, 300^{o}$ as secondary and global minima respectively. These conformations correspond to a planar arrangement of atoms N11, C7, C8, O9 and O10. This conformation is largely determined by electrostatic attraction of N11 and O10 atoms, $\varphi = 300^{o}$ being preferred over $\varphi = 120^{o}$, since in the former conformation the more negative O10 atom is adjacent to N11.

For the ψ-rotation again all methods agree on a unique minimum at $\psi = 0^{o}$ (staggering of $-NH_3^+$ protons with atoms of the adjacent carbon) and a maximum at $\psi = 60^{o}$ (eclipsed conformation).

2.4.5 A comparison of barriers to rotation

The maximum barriers to rotation and ΔE values between minima are given in Table 2.4. EHT consistently predicts greater barriers to rotation and smaller ΔE values than CNDO and PCILO. It is an established failing of EHT that barriers to rotation are exaggerated in comparison to experimental values (see eg. Dashevski, 1973).

2.4.6 Conclusions

The tendency previously reported in the literature for EHT to exaggerate, relative to other MO methods, charges and energies has again been noted here. A tendency for PCILO to predict carbon atoms more negative, and oxygen atoms less negative than CNDO is now also suggested. Another interesting phenomenon which does not appear to have been noted before is related to the variation of charge with changing conformation. Although EHT exaggerates the magnitude of the charge, the variation with conformation is less than with PCILO or CNDO in both amplitude and sensitivity. This may in part explain the failure of EHT to predict stabilised conformers for the folded GABA molecule.

The results of this study suggest a combined PCILO/CNDO picture of the conformational and electronic modes of ITA as distinct from the EHT description. The same division (viz PCILO/CNDO v EHT) was obtained from the discussion of GABA conformational studies in Section 2.3.

Comparisons such as are presented here serve two purposes: (i) they clearly aid a decision to be made on the suitability of MO methods for the chosen problem; but perhaps more significantly,

(ii) they provide a way in which the different MO methods can be calibrated against each other.

2.5 A study of resonance within the PCILO and CNDO formalisms

2.5.1 Introduction

From the comparison of studies on GABA made in 2.3 it is established that CNDO and PCILO MO methods present a fairly unified picture of the conformational modes of the molecule. This picture is supported by the limited ab initio calculations and is in conflict with the EHT results. In a study of EHT, CNDO and PCILO on ITA, the calculated charges and energies again suggest that EHT performs badly in comparison with both CNDO and PCILO. It is at this stage EHT is rejected as a possible MO method with which to study the GABA and GLU systems. The question of whether PCILO or CNDO is more suitable remained to be answered.

We have seen that the conformational spaces of GABA (GABA system) as predicted by PCILO and CNDO are in accord. Similarly, the conformational scenarios of ITA (GLU system) are consistent in both PCILO and CNDO methods. Thus it is not possible to decide, using conformation as a criterion, the relative suitability of CNDO or PCILO for calculations on the GABA and GLU systems.

Therefore, it is noted that the PCILO method does not lead to as satisfactory a theoretical description of resonance as CNDO (see Appendix B). There now follows a hitherto unreported study of resonance within the PCILO and CNDO formalisms, the aim of which is to elucidate how the theoretical shortcomings of PCILO manifest themselves.

2.5.2 Resonance within the CNDO formalism

In every MO method with the exception of PCILO the Slater determinent is constructed from delocalised orbitals. Thus the delocalisation occurring when resonance is involved normally presents no theoretical difficulties within the Hartree-Fock formalism. For example, the $-COO^-$ group is represented as

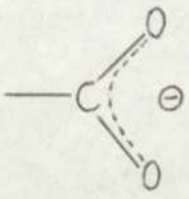

the CO-bond lengths being about midway between those for single- and double-bonds, the bond-index (1.4.5) is then also approximately the average of single- and double-bond values. It would, of course, be possible to localise the position of the double-bond (by adjusting the CO-bond lengths) and perform calculations on

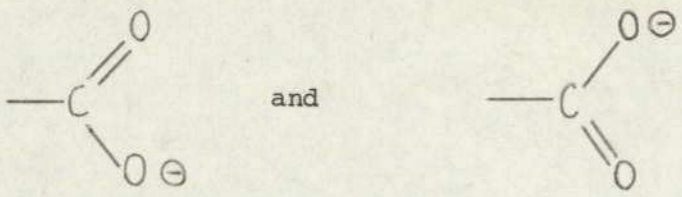

This results in the following charges (calculations made on a conformer of ibotenic acid),

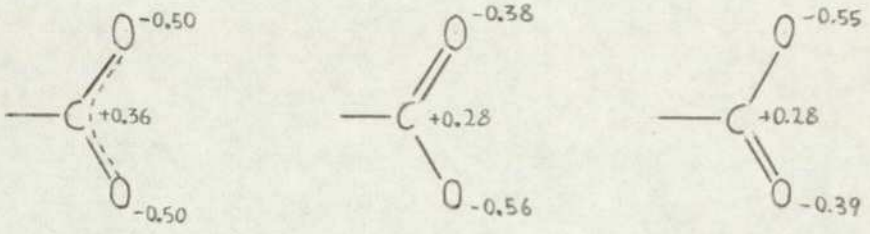

I II III

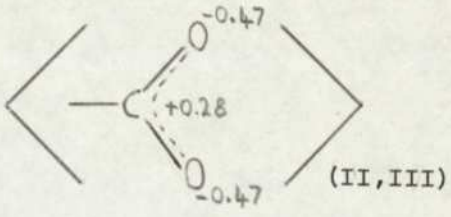

IV

In constructing a pseudo-resonance (IV) as the average of the two possible localised forms II and III, it is noted that the changes on the oxygens reproduce those of form I well, whereas the carbon atoms charge is not so well represented. The energies of forms II and III are greater than that of form I, the extra stabilisation of the latter form is ca. 40 kcal mol^{-1}. This energy is the 'resonance energy' - a quantity which CNDO/2 predicts quite well (Dewar, 1969).

2.5.3 Resonance within the PCILO formalism

However, with the PCILO method, in contrast to CNDO/2, the Slater determinant is constructed via localised orbitals. The PCILO method in its present formulation thus contains internal weaknesses which make it unsuitable theoretically in the study of resonating systems (the resolution of this difficulty requires a formulation using a totally symmetric zeroth order wavefunction). Since only localised bonds are possible a resonance structure of type I is not possible and an average of the two localised forms must be made. We will now consider ways in which, by averaging localised forms, a pseudo-resonance (eg form IV) can be set up in the PCILO formalism.

2.5.4 Comparison of resonance descriptions

The problem will be discussed, for the moment, in the context of an arbitrary conformer of the (R) ITA mono-anion (shown below). The $-CON^-$

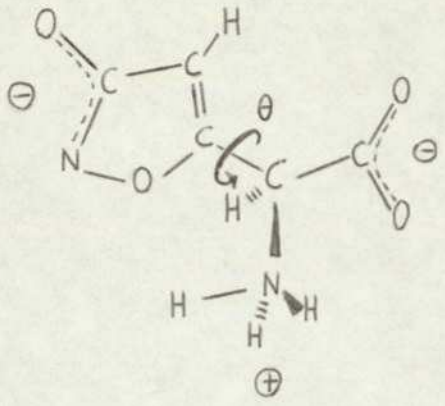

ITA

moiety of the isoxazolidone ring has been chosen because it lacks the symmetry of the $-COO^-$ group, therefore providing extra points of comparison.

The CNDO results are shown below

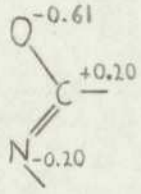

V

-85020

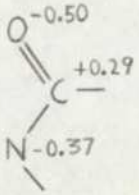

VI

-85063

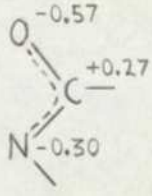

VII

-85085

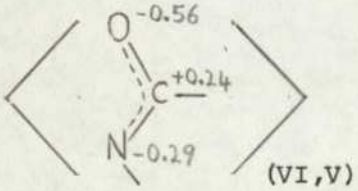

VIII

-85042

it is noted here as with the $-COO^-$ group that in the averaged structure VIII the delocalisation of charge from the central C-atom is smaller compared with the actual resonance (VII). Before considering PCILO as a final remark we note a 'resonance energy' of 22 kcal mol^{-1} and a preference for form VI over V by 43 kcal mol^{-1}, in the conformation considered (both resonance energy and relative stabilisations of hybrids are actually θ-dependent).

The PCILO method leads to the following charges

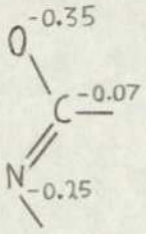

IX

-84957

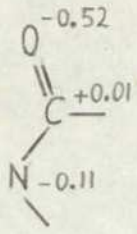

X

-85016

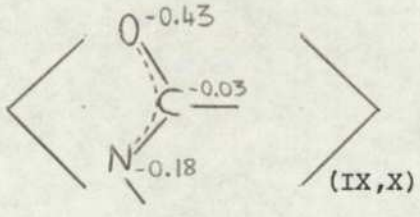

XI

-84987

The results may be summarised:

(i) PCILO and CNDO/2 are in agreement that the localised double bond on the oxygen rather than the nitrogen leads to the more stable resonance form.

(ii) As expected there is less delocalisation of charge from the C-atom with the PCILO method. The relative ordering of charge is reproduced, however, there is qualitative disagreement in the case of the C-atom. The overall charge on the $-CON^-$ moiety is -0.61 and -0.65 for CNDO and PCILO respectively.

(iii) Since the PCILO hybrid resonance structure is defined as the average of the two localised forms, this definition does not lead to a meaningful concept of resonance energy.

2.5.5 A study of the relation between resonance and conformation

Finally, it is of interest to calculate the conformational behaviour differences in the θ-rotation caused by the two localised $-CON^-$ structures in ITA. The variation of energy with θ (the conformation in which $\theta = 0^\circ$ and the direction of rotation is shown in diagram) is shown in Figure 2.6 for the two resonance hybrids. Clearly the different resonance forms give rise to different energy profiles. The only practical solution is that in a conformation study the average of the two profiles should be taken. This does not account for the fact that one resonance hybrid is preferred to the other.

With reference to Figure 2.6 it is noted that in an averaged conformational energy profile the depth of energy barriers and overall

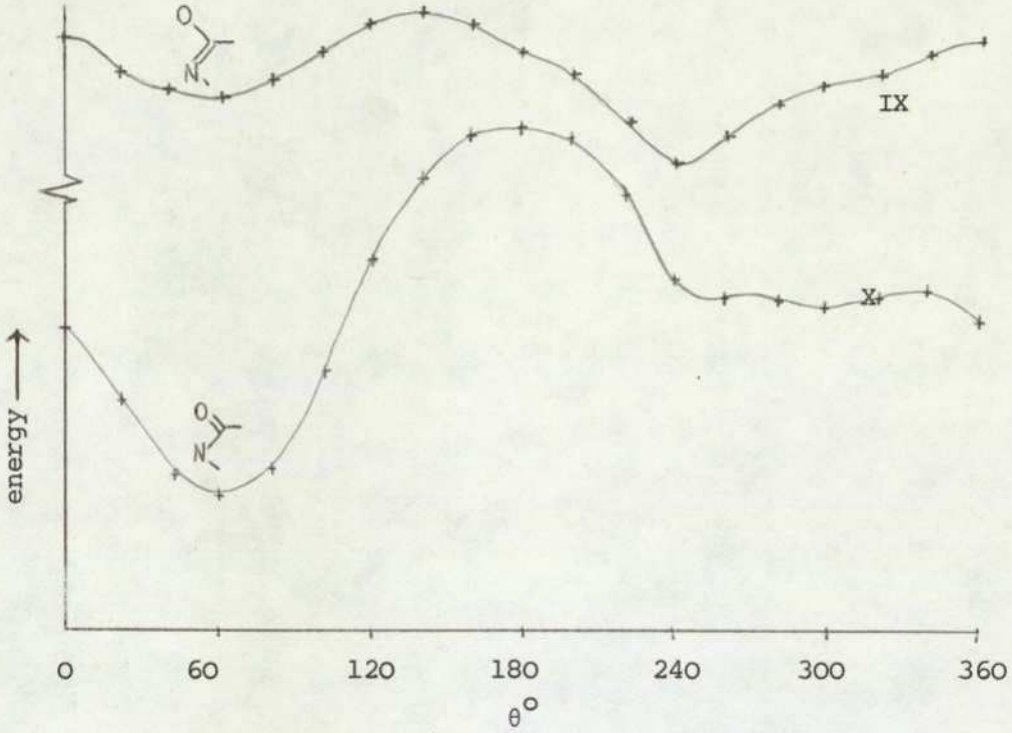

Fig. 2.6. Comparison of PCILO θ-energy profiles for localized $-CON^-$ structures of the ITA mono-anion.

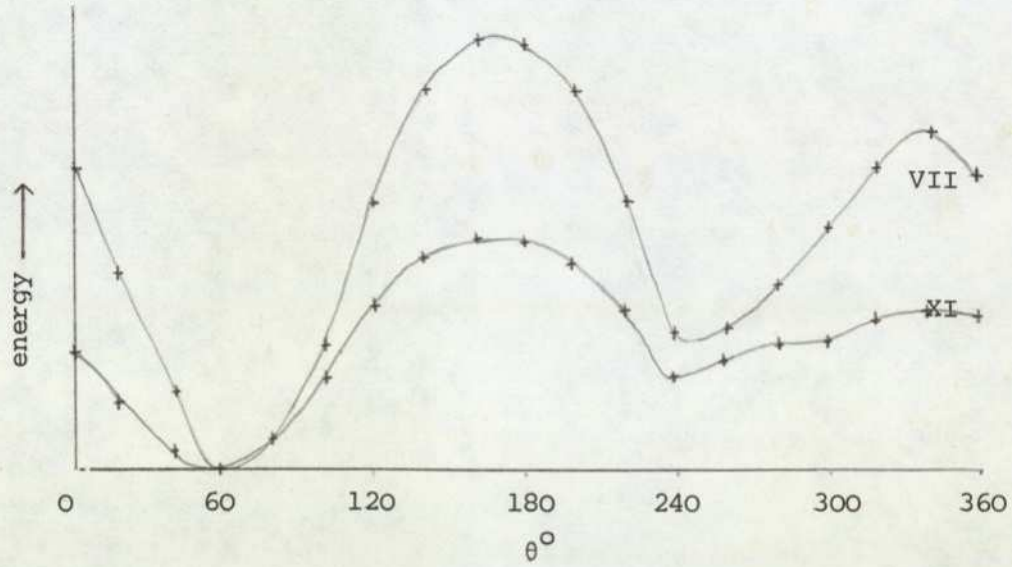

Fig. 2.7. Comparison of θ-energy profiles of the ITA mono-anion. Profiles calculated by CNDO (form VII, see text) and PCILO (form XI).

shape is largely determined by the dominant =O resonance. The comparison of an averaged energy profile for the PCILO method with the CNDO profile is shown in Figure 2.7 for the mono-anion (the zwitterion is dealt with in subsection 2.4.4).

Figure 2.7 shows that the conformational features of the PCILO and CNDO curves are in agreement, the position and relative ordering of the minima are similarly predicted.

2.5.6 Conclusions

Since the two localised forms of a resonance may lead to different conformational behaviour of a molecule, the PCILO GABA study should have been made as the average of 2 energy surfaces - one for each of

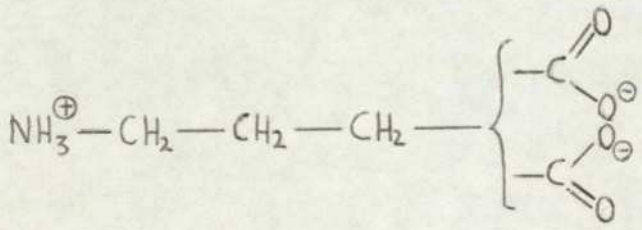

although apparently this was not done (Pullman, private communication). In fact even this is inadequate since it assumes both resonance hybrids contribute equally in all conformations. It is, however, obvious that every PCILO study should require twice the calculations of the corresponding CNDO study, if there is a resonance involved (this is almost always the case in the GABA and GLU systems). Although the problem with resonance is specifically mentioned in the documentation of the PCILO computer programme (Daudey, 1973) no published paper using the programme has, to my present knowledge, acknowledged the problem.

2.6 The choice of theoretical MO method for GABA, GLU and PG systems

2.6.1 Choice between CNDO and PCILO for the GABA and GLU systems

It has been stated (Golebiewski et al, 1974): "All things considered, the safest approach is to study a conformational problem simultaneously with two or even more methods". Generalising this statement by removing the word 'conformational', it is felt that such a multi-method treatment of problems by semi-empirical methods is desirable, PCILO and CNDO providing two suitable methods. Accepting that for our studies, the amount of computation makes a multi-method treatment unrealistic for calculations on the molecules of the GABA and GLU systems, a choice between PCILO and CNDO/2 must be made.

The crucial factor is that all GABA agonists comprise of at least one of:-

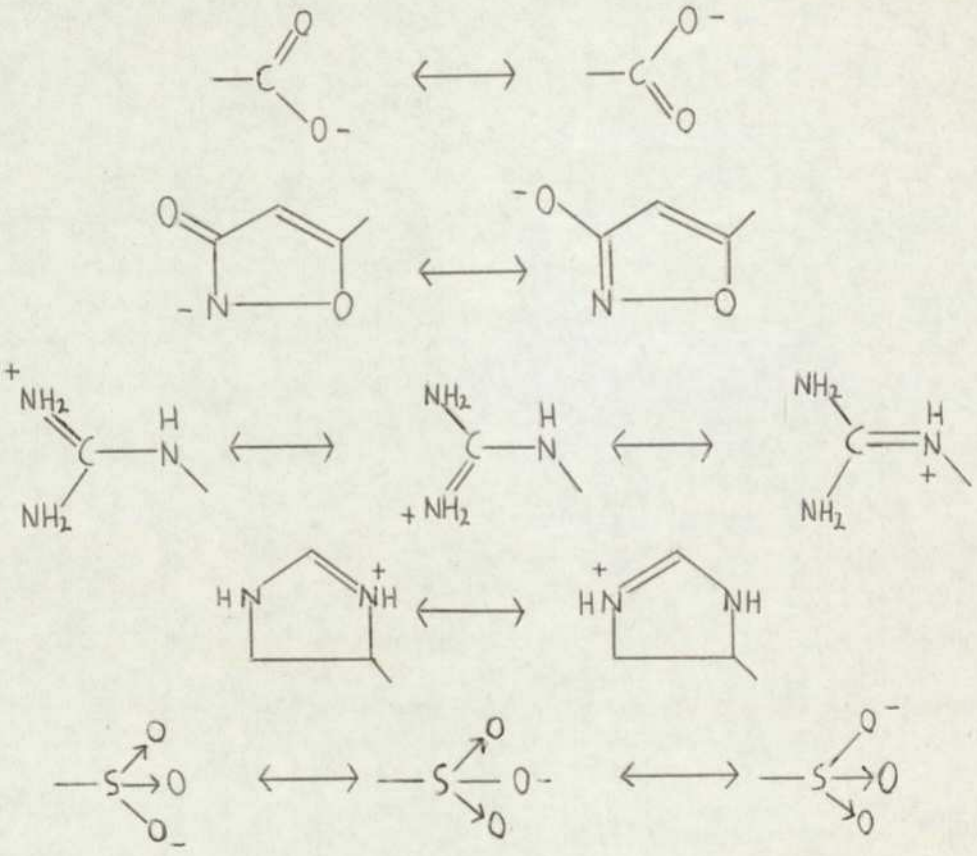

The importance of resonance structures in GABA and GLU agonists, and the inability of PCILO to satisfactorily account for it, are strong recommendations for the use of CNDO. Hence, on the basis of the superiority of CNDO over PCILO for calculations on the electronic (rather than conformational) modes of the small polar molecules exhibiting resonance, the former method is preferred for theoretical MO calculations relating to the GABA and GLU pharmacophores.

2.6.2 The suitability of CNDO for calculations on the PGs

Since the PGs are non-polar molecules with a large number of possible conformational rotations, only the most rapid methods are practicable. It is probably true to say that, at this stage, for any conformational problem on a PG only simple classical energy calculations are feasible.

For the calculations of electronic structure involving just one conformation (eg the crystal structure), CNDO/2 should be theoretically suitable (see artificial key 2.2.2). Further, as the PG studies were the last to be made chronologically, it was possible to say:

(i) At the time of initiating our research on PGs a good deal of expertise had been acquired in interpreting the results of this MO method; and

(ii) in the study of electronic structure CNDO had proved itself to be a reliable method.

CNDO/2 is seen as a suitable method for our requirements in studying the PGs, and we have no reservations in using it for calculations on those molecules.

3.1 Introduction

This chapter deals with CNDO calculations made on GABA and GLU type molecules in the gas phase.

Explicitly considered in Section 3.2 is the computer programming required to obtain results within the CNDO/2 formalism. Subsequent sections of Chapter 3 discuss some features of the results. For example, Section 3.3 shows how the electron distribution is relatively insensitive to conformational changes. Section 3.4 then demonstrates how certain characteristic electron distributions (functional groups) are preserved between different molecules. In Section 3.5 the formation and consequences of intramolecular hydrogen-bonding between terminal charged-functional groups are considered. Free-energy and its relevance form the contents of Section 3.6. In Section 3.7 the $-COO^-$ and $-CON^-$ groups are compared and contrasted via consideration of their electrostatic-potential fields. The effective charge-centres of functional groups and the resulting definition of an intercharge separation (χ_T) parameter are the contents of Section 3.8. Finally, the overall conclusion to Chapter 3 is contained in 3.9.

3.2 Implementation of the CNDO/2 method

3.2.1 Introduction

In all our work using CNDO/2 the basic program used has been one distributed by the Quantum Chemistry Program Exchange (QCPE). It is therefore considered that the program (QCPE 91) was well tried and tested, and performs numerical computations in accord with CNDO/2 theory.

QCPE 91 in its basic form as written by G.A. Segal (1966) and as supplied by QCPE, was not suitable for conformational studies. Hence, some initial modification of the program was made to (a) convert the program to run on a CDC 7600 computer, and (b) add subroutines enabling the input atomic co-ordinates to be modified for conformational rotations. Details of these changes and our subsequent checks that the program still reproduced available reference results can be found in Warner (1975).

At that stage the program was capable of performing CNDO/2 conformational studies on molecules containing lst row atoms of the periodic table.

3.2.2 Two modifications to the CNDO/2 program

(i) Modification to achieve convergence

During a study of the rigid GABA agonist 4-aminotetrolic acid (4-ATA) (Warner, Borthwick & Steward, 1975) a problem arose concerning convergence of the SCF energy. The 4-ATA ($NH_3^+.CH_2.C\vdots C.COO^-$) molecule is shown below

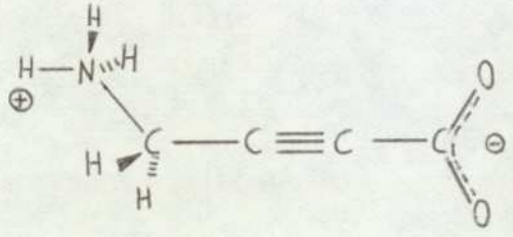

Calculations on the non-ionic molecule revealed that the electronic energy values converged steadily towards the self-consistent solution - the self-consistency criterion for QCPE 91 is 10^{-4} a.u between successive electronic energy values. However, when computations were made on the zwitterion the electronic energy values were found to oscillate (with constant amplitude) and a SCF solution was not being obtained. This problem was overcome by averaging the Fock matrix (B2.3) obtained in each cycle of the iterative scheme with that obtained in the previous cycle.

This procedure was programmed in the more general form of a weighted average,

$$F_{i+1} = kF_i + (1-k)F_{i+1}$$

where $k \leqslant 1$ and $i > 1$. After convergence had been reached using the averaging procedure, a further iteration was made without it to confirm the self-consistency of the solution. The averaging is theoretically valid since the Hermitian nature of the Fock matrix is preserved.

(ii) Modification to speed convergence

The initial set of LCAO coefficients in a CNDO/2 calculation are the eigenvectors of Schrodinger's equation using a simple Huckel theory Hamiltonian. These coefficients are often far from the converged SCF values and hence many iterations of the self-consistent cycle are required. In general the Huckel eigenvectors are the best available initial set. When a conformational study is being performed it is possible that the final eigenvalues of the computation at the previous grid point are a preferable initial set of eigenvectors, to those of the Huckel Hamiltonian. (A similar idea to this has been briefly alluded to in a paper by Singh and Ferro (1974).)

Commonly, the preparation of a conformational energy-surface requires calculating the energy of a molecule as function of two torsion angles: we often use a grid of 20° intervals (1.5.2) necessitating $18^2 = 324$ CNDO computations. Further, a finer grid is normally used in the regions of minimum energy. If SCF MO methods are used, the amount of computation required is considerable and any method of reducing it is welcome.

As stated in the first paragraph, our technique uses the final LCAO coefficients obtained for one conformation as the basis for the calculation at the next grid point. Some examples of CNDO/2 calculations employing this procedure are given in Table 3.1. The values in Table 3.1 refer to a grid of 20° with a self-consistency criterion of 10^{-4} a.u in the electronic energy.

It can be seen from Table 3.1 that considerable economies are sometimes possible. Using a 5° grid the savings can be even greater. For the ibotenic acid mono-anion the saving is 14 sec. per conformation, which over a complete conformation space is a total saving of ca.4500 sec. (1¼ hrs) of CDC 7600 central processor time. It should be stressed that the CDC 7600 is a very fast machine, on The City University ICL 1905E computer this

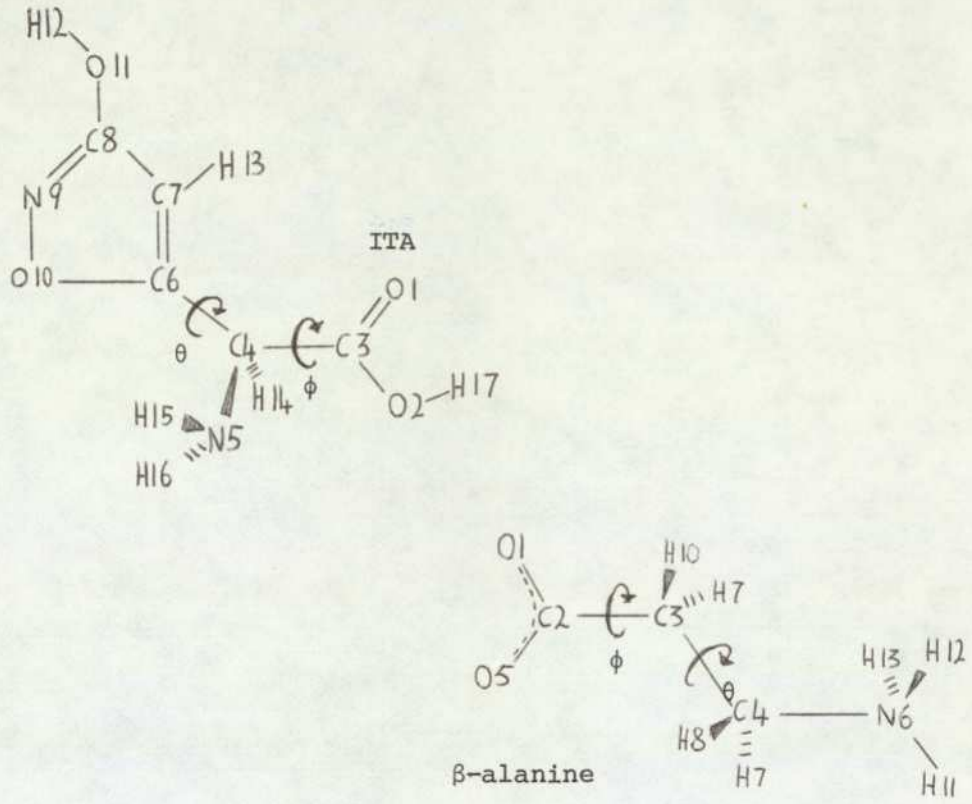

Fig. 3.1 Atomic numbering scheme for ITA and β-alanine.

Molecule	Time/conformation: normal calculation (sec)	Time/conformation: coefficients saved from a previous calculation (sec)
Muscimol	19	9
ITA mono-anion	35	21
γ-aminobutyric acid	9	7
α-fluoro γ-aminobutyric acid	11	11
4-ATA	9	7

Table 3.1

Comparison of CNDO/2 calculations with and without the 'vector saving' routines.

saving of 1¼ hrs would represent a saving of 6 days of computing time!

In addition the saving of eigenvectors can be useful in cases where convergence is difficult to achieve. For example, in the case of ibotenic acid the problem encountered with 4-ATA zwitterion occurs and an averaging of Fock matrices must be made in order to force convergence (see part (i) of this subsection). However, using the saved eigenvectors from a previous conformation leads immediately to convergence without any averaging.

Finally, it should be mentioned that there appears to be no reason why the method should not be employed with more sophisticated SCF procedures such as (M)INDO, NDDO and ab initio. However, in these approaches the calculation of electron repulsion integrals takes up a progressively greater fraction of the total time and savings made in the iterative part of the computation will represent a smaller percentage of the whole. Details of the implementation of the saving of eigenvectors in the QCPE 91 program are to be found in Warner (1975).

3.2.3 Conclusions

At this stage we have a computer program which will produce results within the CNDO/2 formalism in agreement with previous reference calculations (eg ethane). This program is specially suited to conformational studies, being faster than the basic program due to the vector-saving routine described in 3.2.2. Using the vector-averaging routine it is possible to obtain results on molecules that could not be considered using the basic program (QCPE 91).

The remainder of this chapter uses the QCPE 91 program with the modifications described in a study of some concepts relevant to the quantum chemical analysis of drugs.

3.3 Variation of electronic structure with conformation

3.3.1 Introduction

The electronic structure of the isolated molecule is of importance since this must be understood before either the water molecule binding sites (supermolecule), or dipole components (continuum) necessary for theoretical solvent effect calculations can be determined (see 1.4.6). Furthermore, this electronic structure may be of intrinsic value at the transmitter/receptor binding site (Steward, Borthwick, Clarke & Warner, 1975) where the environment may not necessarily be aqueous. It is evident that the electronic structure is a function of the conformation. However, the details of the dependence between electronic parameters and conformation has not, to my knowledge, been reported in any detail. Contained in this section is an investigation of the latter aspects and, in particular, a report of the useful extent to which the electron distribution may be regarded as conformationally invariant.

The results presented in this section are based on the assumption that the conformation space is a function of the torsion angles only. The geometry optimization problem of varying the internal structure parameters (bond lengths and interbond angles) has not been considered. However, the following observations may be indicative of the magnitude of the effect on the NAPs,

(i) the NAP[≠] distribution for the $-COO^-$ group in 4-ATA is

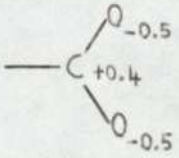

the interbond angles being 120°;

(ii) starting from 120° the carboxyl angles were optimised in a study of glycine (Oegerle & Sabin, 1973), the resulting NAP distribution was found to be

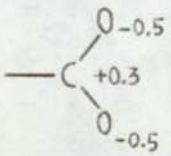

≠ NAPs will hereafter always be quoted as the (NAP-atomic number) of the atom concerned, since if a NAP is given as —O8.3 the '8' is effectively redundant with the atomic symbol 'O'.

(iii) it will be seen later (3.4.3) that the NAP distribution of the $-COO^-$ group is intermolecularly invariant to within our $\pm$0.1e level of invariance. Hence, the implication is that to within the level of approximation recommended here, the NAPs will be invariant with respect to geometry optimisation.

3.3.2 Intramolecular invariance of NAP with conformation

Our MO studies on GABA (Warner & Steward, 1975), 4-ATA (Warner, Borthwick & Steward, 1975) and ITA (Borthwick & Steward, 1976) have shown that between the various minimum energy conformations of each molecule the variation of NAP is small. An investigation has therefore been made to establish whether the variation in the NAP of an atom throughout the complete conformation space of the molecule to which it belongs is small enough to allow a level of approximation such that its NAP may be regarded as invariant yet still permitting meaningful quantitative comparisons between different atoms within that molecule. This invariance, if found, would greatly simplify the comparison of molecules in the study of their drug action at the molecular level.

In the following estimation of the variation of NAP over conformation space only two torsion angles, θ and ϕ will be varied simultaneously and the conformation space is therefore 2-dimensional: the approach applies equally, however, to an n-dimensional conformation space. (It should be pointed out that we are not considering energy minima, and so the suitability of the method for the location of energy minima is not in question here.)

If the NAP of atom A at point (θ, ϕ) is denoted by $\mathcal{L}^A(\theta, \phi)$, then as we are not primarily concerned with absolute NAP, a 'relative $\mathcal{L}^A$-space' may be defined

$$\mathcal{L}'^A(\theta,\phi) = \mathcal{L}^A(\theta,\phi) - \mathcal{L}^A(0,0) \qquad \text{(i)}$$

For θ-rotations only, the maximum variation in NAP may then be written

$$\Delta\mathcal{L}^A_\phi(\theta) = \left|\sup_\theta \{\mathcal{L}'^A_\phi(\theta)\} - \inf_\theta \{\mathcal{L}'^A_\phi(\theta)\}\right| \qquad \text{(ii)}$$

Also a given rotation of $\theta = \alpha$ say, is a rotation from some starting value T_1, to T_2 where $T_2 - T_1 = \alpha$. This point is illustrated in the following diagram.

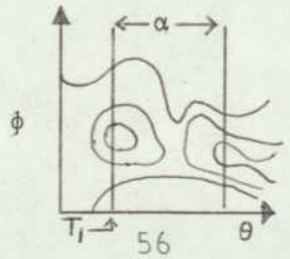

It is now possible to distinguish two types of surface.

(a) type I surfaces

Molecules in this category have $\mathcal{C}^A$-spaces which do not show a large range of variation (eg ITA, 4-ATA). Thus

$$\Delta\mathcal{C}^A_\phi(T_1) \simeq \Delta\mathcal{C}^A_\phi(T_2) \qquad \text{(iii)}$$

An approximation for the maximum variation in NAP for atom A over $\mathcal{C}^A$-space may then be defined as

$$\Delta\mathcal{C}^A \;:=\; \Delta\mathcal{C}^A_\phi(\theta) + \Delta\mathcal{C}^A_\theta(\phi) \qquad \text{(iv)}$$

(b) type II surfaces

Many of the neurotransmitter drugs (eg glycine, β-alanine, GABA and its analogues) can adopt very folded conformations (3.5). This results in surfaces showing quite considerable NAP variation, and (iii) does not hold. This type of expression can be used, however, if it is modified in such a way that the torsion angles (θ, ϕ) are defined uniquely such that their zeros correspond to the fully-folded molecule (ie the conformer in which the bonds defining the 'backbone chain' of the molecule form the maximum number of cis configurations), then $\Delta\mathcal{C}^A$ will have values

$$\Delta\mathcal{C}^A \leqslant \Delta\mathcal{C}^A_o(\theta) + \Delta\mathcal{C}^A_o(\phi) \qquad \text{(iv)}^1$$

Thus, if conformations involving the close approach of atoms of the functional groups are now rejected (- for molecules of the GABA type those groups will be the $-COO^-$ and $-NH_3^+$ terminal groups, and we would wish to exclude conformations such that $|\theta|, |\phi| <$ ca.40° of fully-folded —), then

$$\Delta\mathcal{C}^A < \Delta\mathcal{C}^A_o(\theta) + \Delta\mathcal{C}^A_o(\phi) \qquad \text{(iv)}^2$$

will usually apply, giving an upper limit to the variation of NAP over conformation space. $\Delta\mathcal{C}$ is the variation of NAP over a space excluding the region (defined above) around the origin (see also section 3.5).

As examples of type I and II surfaces Tables 3.2 and 3.3 give values for variation in NAP in ITA (non-ionic) and β-alanine (zwitterion), respectively (angles used are defined in Fig.3.1).

The results suggest that taking 0.1e as a basic NAP unit for molecules exhibiting both type I and type II NAP surfaces will allow useful quantitative comparisons of NAP to be made, whilst giving a maximum variation of $\pm$0.1e over conformation space for most conformations of the molecules under consideration here. The type of 'pathological' conformations, which have been deliberately excluded above, are those where the close approach

ATOM	$\Delta\mathcal{C}_o^A(\theta)+\Delta\mathcal{C}_o^A(\phi)$	ATOM	$\Delta\mathcal{C}_o^A(\theta)+\Delta\mathcal{C}_o^A(\phi)$
O1	0.034	O10	0.027
O2	0.012	O11	0.007
C3	0.028	H12	0.007
C4	0.013	H13	0.071
N5	0.021	H14	0.045
C6	0.022	H15	0.020
C7	0.040	H16	0.018
C8	0.010	H17	0.012
C9	0.019		

Table 3.2

Variation in NAP over conformation space for the ITA non-ionic molecule. Type I surface, $\Delta\mathcal{C}_o^A(\theta)+\Delta\mathcal{C}_o^A(\phi)$ a good approximation to the actual variation of NAP over $\mathcal{C}^A$-space ($\Delta\mathcal{C}^A$).

ATOM	$\Delta\mathcal{C}_o^A(\theta)+\Delta\mathcal{C}_o^A(\phi)$	$\Delta\mathcal{C}^A$	ATOM	$\Delta\mathcal{C}_o^A(\theta)+\Delta\mathcal{C}_o^A(\phi)$	$\Delta\mathcal{C}^A$
O1	0.253	0.087	H8	0.052	
C2	0.040		H9	0.071	
C3	0.018		H10	0.096	
C4	0.040		H11	0.204	0.080
O5	0.230	0.110	H12	0.147	0.027
N6	0.364	0.097	H13	0.169	0.048
H7	0.056				

Table 3.3

Variation in NAP over conformation space for the β-alanine molecule. Type II surface, $\Delta\mathcal{C}_o^A(\theta)+\Delta\mathcal{C}_o^A(\phi)$ an exaggerated upper limit to $\Delta\mathcal{C}^A$ (which has been explicitly found in cases of high $\Delta\mathcal{C}_o^A(\theta)+\Delta\mathcal{C}_o^A(\phi)$ values).

of atoms to distances of the order of the sum of their Van der Waals radii may lead to electron-inductive processes (type II in the region of the ϕ,θ-origin): examples of this are GABA in appreciably folded conformations, and ITA non-ionic molecule.

All the results of this section are strictly valid only for the CNDO method. However, available evidence (2.4.2) suggests that O.le may also be relevant for PCILO and EHT, particularly the latter method.

3.3.3 Intramolecular invariance of BI with conformation

Just as the NAP gives us a way of specifying the electron density associated with the atomic cores, it is possible to define a quantity which describes the electron density associated in the interatomic bonding. Such a quantity is the bond-index (BI), which has been defined in 1.4.5. In this subsection an investigation has been made analogous to that of 3.3.2, this time for BI instead of NAP.

The BI and NAP are both derived from the same (density) matrix and so to minimise computer-time we have made the assumption that they behave sufficiently alike to allow equations analogous to those for intramolecular NAP variation to hold for a $\mathcal{B}^{AB}$-space. BI variations have been calculated (Table 3.4) for some typical bonds in the ITA zwitterion (type I surface) and β-alanine zwitterion (type II surface). For type II surfaces there are some noticeably large values for $\Delta\mathcal{B}^{AB}_{o}(\theta) + \Delta\mathcal{B}^{AB}_{o}(\phi)$ As for NAP this represents, for these surfaces, a rough upper bound for $\Delta\mathcal{B}^{AB}$ which is the actual variation over the surface for conformers ca.40° away from fully-folded. For NAP determination it was possible, for the large values of $\Delta\mathcal{C}^{A}_{o}(\theta) + \Delta\mathcal{C}^{A}_{o}(\phi)$, explicitly to calculate $\Delta\mathcal{C}^{A}$ (eqn.(iv)^2), but the equivalent has not been possible for the BI variation.≠ However, for the NAP variation over the β-alanine surface the following inequality can be applied for these exaggerated values:

$$\Delta\mathcal{C}^{A} < \Delta\mathcal{C}^{A}_{o}(\theta) + \Delta\mathcal{C}^{A}_{o}(\phi) \qquad (v)$$

with the obvious definition of $\Delta\mathcal{C}^{A}_{o}(\theta)$. Values for both sides of (v) are given in Table 3.5, which shows that $\Delta\mathcal{C}^{A}_{o}(\theta) + \Delta\mathcal{C}^{A}_{o}(\phi)$ gives a much closer (lower bound) approximation to $\Delta\mathcal{C}^{A}$ than does $\Delta\mathcal{C}^{A}_{o}(\theta) + \Delta\mathcal{C}^{A}_{o}(\phi)$, and similarly for $\mathcal{B}^{AB}$-space (Table 3.4).

≠ This is because when the ITA and β-alanine studies were made BI values were (unlike NAP) not a standard output option of the program

ITA			β-alanine			
ATOM A	ATOM B	$\Delta B^{AB}_{o}(\theta)+\Delta B^{AB}_{o}(\phi)$	ATOM A	ATOM B	$\Delta B^{AB}_{o}(\theta)+\Delta B^{AB}_{o}(\phi)$	$\Delta B^{AB}_{o}(\theta)+\Delta B^{AB}_{o}(\phi)$
O2	C3	0.048	O1	C2	0.651	0.177
C3	C4	0.042	C2	O5	0.648	0.161
C4	N5	0.022	C2	C3	0.210	0.048
C4	C6	0.026	C3	C4	0.038	
C8	C7	0.010	C4	N6	0.257	0.060
C6	C7	0.051	N6	H11	1.250	0.088
C8	N9	0.028	N6	H12	0.036	
N9	O10	0.027	N6	H13	0.044	
C6	O10	0.050	C4	H10	0.019	
C8	O11	0.014				
O11	H12	0.003				
C6	H13	0.043				
N5	H15	0.023				
C4	H14	0.031				

Table 3.4

Variation in BI over conformation space for the ITA zwitterion (type I surface) and β-alanine zwitterion (type II surface).

ATOM A	$\Delta c^{A}_{o}(\theta)+\Delta c^{A}_{o}(\phi)$	Δc^{A}	$\Delta c^{A}_{o}(\theta)+\Delta c^{A}_{o}(\phi)$
O1	0.253	0.089	0.052
O5	0.230	0.110	0.071
N6	0.364	0.097	0.035
H11	0.204	0.080	0.039
H12	0.147	0.027	0.024
H13	0.169	0.048	0.039

Table 3.5

Variation in NAP for β-alanine zwitterion (type II surface) illustrating inequalities $\Delta c^{A}_{o}(\theta)+\Delta c^{A}_{o}(\phi) \leq \Delta c^{A} < \Delta c^{A}_{o}(\theta)+\Delta c^{A}_{o}(\phi)$.

On the basis of these results, BIs are hereafter quoted to one decimal place as indicating the level of approximation for reasonable BI invariance over conformation space. However, care must be exercised with type II surfaces as it seems that the limit of 40° is sometimes too close to the fully-folded conformer to allow strict BI invariance to this accuracy (see also section 3.5).

3.3.4 Summary

A level of approximation has been found for which the NAP and BI are intramolecular invariants over the conformation space of a molecule (with the possible exception of conformers discussed in section 3.5), and for which useful quantitative comparisons can still be made between different atoms.

There are perhaps additional advantages in quoting NAP (and BI) to a comparatively high degree of approximation. Firstly, it has been observed that in CNDO-type calculations the convergence of the density matrix is slower than that of the SCF energy value (Howland & Flurry, 1972). Most CNDO programs use the energy convergence as the criterion for a 'successful' calculation, and so at 'completion' of the calculation the density matrix may not yet be converged. In a recent study (Burdon & Parsons, 1976) it was shown that the difference between spin densities calculated with energy and density matrix convergence differed by ca 0.05Oe in the case of the particular radical studied. The latter paper notes that this convergence problem is not as great for the NAPs of cations as it is for radicals, however, it may be significant that problems with convergence were encountered in some of our studies on zwitterions (section 3.2.2). The level of approximation used here ensures the invariance of NAP with respect to the above caution on the use of CNDO. It is, however, evident that in the past many authors (ourselves included) have been guilty of overquoting the degree of accuracy of NAP values.

It is further important to realise that in empirical potential energy (PE) calculations an allowance is sometimes made for electrostatic interaction (Steward & Clarke, 1975; Gill, 1959; Warner, 1975). The charges used in such electrostatic potentials are usually theoretical MO values relevant to a single (arbitrary) conformation. The use of these charges throughout the calculation of a PE conformation space represents a tacit assumption of the

results of this section (viz intramolecular invariance of NAP over a conformation space).

It will be seen in subsequent sections of this thesis that the approximations and assumptions proposed here, in 3.3.2 and 3.3.3 are well justified by their usefulness in allowing a great simplification in the reporting and discussion of charge distributions particularly in the context of structure-activity correlations.

3.4 Idealised geometries, structure and interatomic invariance of functional groups

3.4.1 Idealised geometries

In section 3.3 the variation of electronic structure with changing conformation has been considered. To analyse the electronic structure within a single conformation of a molecule, however, and to make comparisons between different molecules, it is desirable as far as possible to rationalise the structural parameters used. Pople and Gordon (1967) have stated, as an example, that 'in the theory of alternation of bond lengths in polyenes, it is better to start with a theory of electronic structure based on equal bond lengths and then discover the 'driving force' causing alternation (alternating bond order), rather than starting with a geometrical model with alternation already built in'. The usefulness of this type of approach, as opposed to employing energy-optimised or crystal-structure coordinates, has been effectively demonstrated by Schroeder, Makino and Tolles (1973) in their studies of five-membered heteroaromatic compounds. Here the utility of the idealised geometry concept has been investigated.

For an idealised ITA non-ionic molecule, standard bond-lengths and angles (Pople & Beveridge, 1970) for all exocyclic atoms and a regular pentagon of side 1.4Å for the ring (even though it is heterogeneous) give an NAP distribution (Fig.3.2(a)) which reproduces that of the crystal structure model to within $\pm$0.1e. This result is relevant since Burdon and Parsons (1976) have also stated that an 'injudicious' choice of geometry may give rise NAPs at variance to those obtained with a more realistic geometry. The level of approximation used here ensures the invariance of NAPs with respect to this comment on the use of CNDO. However, 'injudicious' is a relative term and if a blatantly incorrect geometry is used then the NAP will violate the $\pm$0.1e variation expected. Such violations have in fact been detected in the first calculations of some of our studies, enabling a rapid identification and correction of the error in the input coordinates.

Returning to the idealised ITA non-ionic molecule, the carboxyl group has an implied double-bond (via the input bond-length) a further idealisation involving the use of equal C-O bond-lengths for both single and double bond resulted in the same

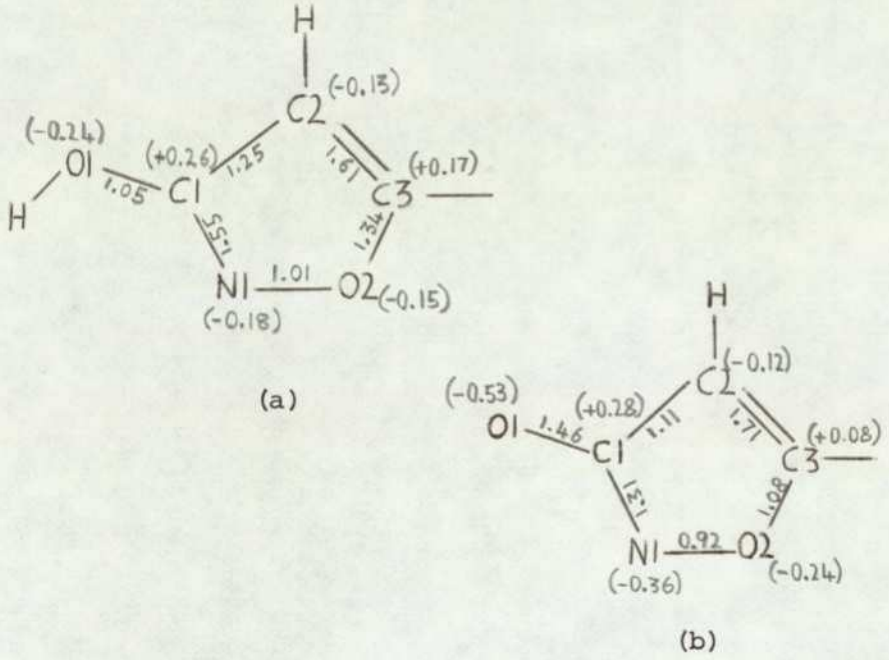

Fig. 3.2 Idealised isoxazolidone rings: electronic indices.

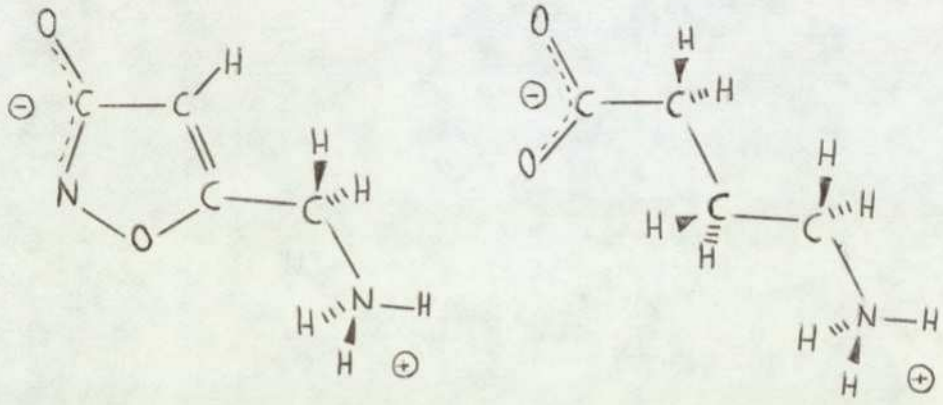

Fig. 3.3 Comparison of muscimol and GABA structures.

NAP distribution at this level of approximation. The charge alternation in the ring is similar to that reported for non-heteroaromatic (Pople & Gordon, 1967; Hehre & Pople, 1970) systems and tetrazole rings (Schroeder et al, 1973): it is likely to contribute to the electrostatic stability of the ring. The BI values for the N1-C1 and C2-C3 bonds indicate, as expected classically, a double-bond character. In a conventional CNDO calculation the double-bonds would be assumed classically or from crystal-structure determination, whereas with an idealised geometry, free from any assumption of bond character, the bonding characteristics of the molecule are obtained. Similarly, by using a uniform bond-length for the C-O bonds in the -COOH and $-COO^-$ groups, it is possible to use their BI to deduce their respective single-, resonating double- and double-bond characters. This is in accord with the greater importance of mutual orientation effects of bonding orbitals than precise interatomic distances (Muller & Pritchard, 1959).

Similar calculations to those above were made on the idealised ITA mono-anion (Fig. 3.2(b)) - it is this form which is predominant at physiological pH (Johnson et al, 1968) and is thus that which is of interest as a powerful agonist of L-glutamic acid in the CNS (Curtis & Watkins, 1965). The NAP distribution again shows alternation and again reproduces that of the calculations (Borthwick & Steward, 1976) using the crystal-structure isoxazolidone ring coordinates (Brehm, 1973) to within $\pm$0.1e. The double-bond character of the C2-C3 bond is also again suggested. There is now, however, a decrease in electron population in the N1-C1 bond and an increase in the C1-O1 bond in going from non-ionic to mono-anionic structures. Already we have 1.6 as the BI value for the cyclic C-N double bond and if it is assumed that the C-N single bond would have a value of 1.0 (as in the $-NH_2$ group, although the hybridizations are not compatible), then a value of 1.3 corresponds to a resonating double-bond (cf a value of 1.5 for a resonating double bond in the $-COO^-$ group (see section 3.4.2). The following structure for the anionic isoxazolidone configuration, based on an idealised geometry is therefore suggested

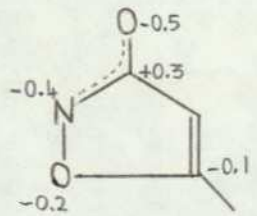

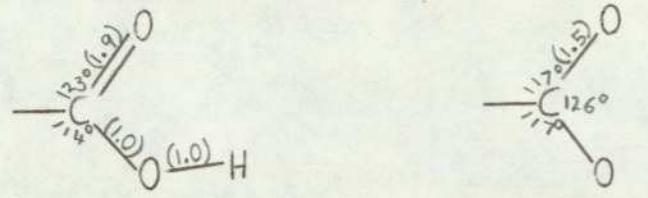

(a)

(b)

Fig. 3.4 The carboxyl and amino groups: experimental interbond angles and calculated typical BI values.

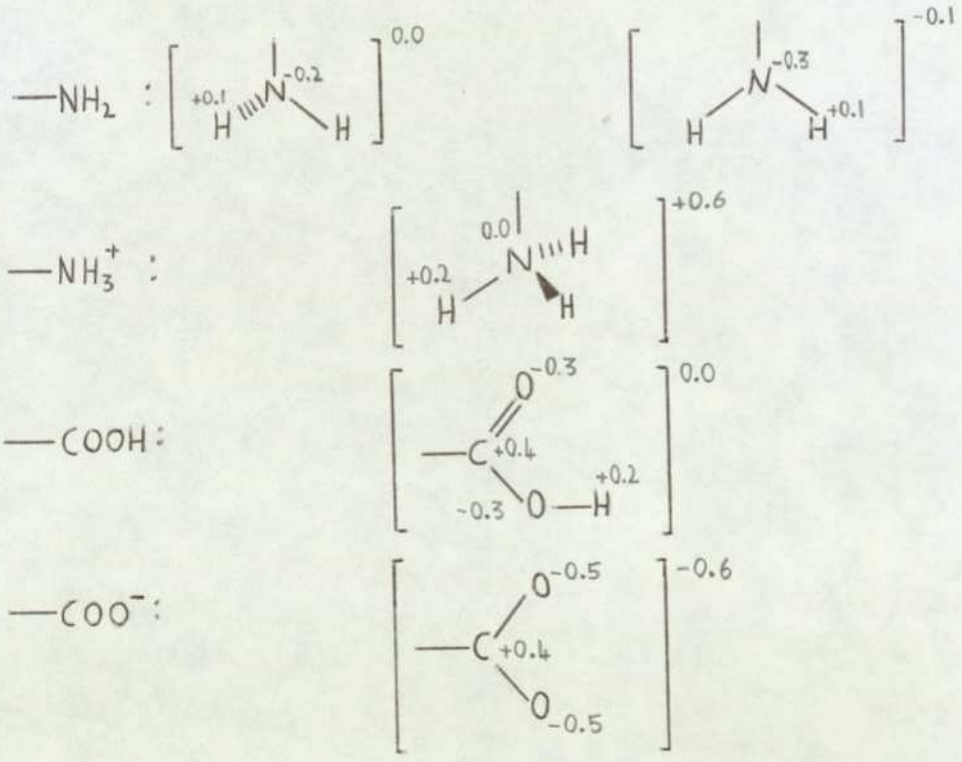

Fig. 3.6 The carboxyl and amino groups: NAP distributions.

the predicted bonding is in agreement with the bonding implied by X-ray crystal structure bond lengths.

It can be seen from the results above that in the muscimol zwitterion (Fig. 3.3), the $-CON^-$ grouping has an analogous charge and bond configuration to the $-COO^-$ group in 4-ATA and GABA - this result is of importance in the understanding of the action of muscimol as an agonist of GABA.

The data are in accord with, and provide further justification for, the comments of Pople and Gordon on idealised geometries. It is concluded that the study of some aspects of molecular construction treated in an idealised manner can be important in the overall study of a molecule or series of homologous molecules (such homologous families are frequently of interest in pharmacological situations).

3.4.2 Structure of some functional groups

Theoretical calculations of the inherent bond characters of the -COOH and $-COO^-$ groups lead to the BI values in Fig.3.4(a) and for the $-NH_2$ and $-NH_3^+$ groups to the BI values in Fig.3.4(b) as being representative. The range of BI for the C-O bonds is in accord with the classical structure of groups with single, resonating double, and double bonds. The resonating bond has a BI approximately midway between that of the single and double bonds. The NAP configuration of $-COO^-$ is also compatible with classical ideas in that each oxygen atom has a charge of ca 0.5e (Fig.3.6). The $-NH_3^+$ group, however, has its positive charge distributed among the protons (Fig.3.6) which is contrary to the position indicated by many authors, who place the formal positive charge on the nitrogen atom (eg Bonner & Castro, 1965).

The interbond angles for the sp^2 carbon in CNDO studies are often assumed to be 120° planar for both the -COOH and $-COO^-$ groups (Oegerle & sabin, 1973; Pople & Beveridge, 1970). A more realistic set of angles would be those of Fig.3.4(a) interatomic repulsion between the more highly charged O^- atoms in the $-COO^-$ group causing the increased angle. The angles of Fig.3.4(a) were found by a study of X-ray crystal structures, as typical structures the reader is referred to (i) for -COOH group, Jones & Pauling (1976), and (ii) for $-COO^-$ group, Jose & Pant (1965). That equal 120° angles are unrealistic is implied from the geometry optimisation performed by Oegerle & Sabin, 1973). The planarity of the group is well established from crystal structure determinations.

For the $-NH_2$ and $-NH_3^+$ groups the bond angles are taken as tetrahedral as found in crystal structures (Karle & Karle, 1964; Steward, Player & Warner, 1973). In the Pople and Beveridge parameterisation the standard geometry for an $-NH_2$ group where the nitrogen has no excess valence is pyramidal rather than planar. Not unexpectedly, this is confirmed by theoretical calculations on ITA: the pyramidal configuration is found to be more stable than the planar by ca.12 kcal mol^{-1}. In a given single conformation it is found that the overall charge on the pyramidal $-NH_2$ group agrees more closely with the classical notion of the group being 'uncharged', than for a planar arrangement (Fig.3.6)

The structure of the $-CON^-$ isoxazolidone moiety has been discussed already (3.4.1).

The molecule β-guanidino-propionic acid (βGP), $(NH_2)_2.C:N^+H.(CH_2)_2.COO^-$, is important as a GABA agonist (Edwards & Kuffler, 1969). The NAP and BI values for the guanidinium ion are shown below

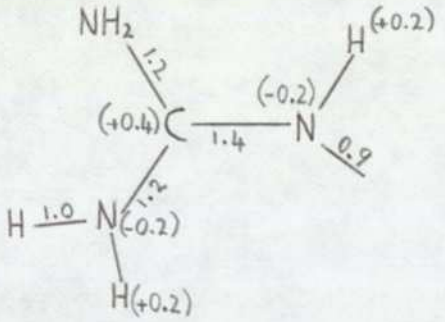

The classical description of the guanidinium ion is (eg Bonner & Castro, 1965)

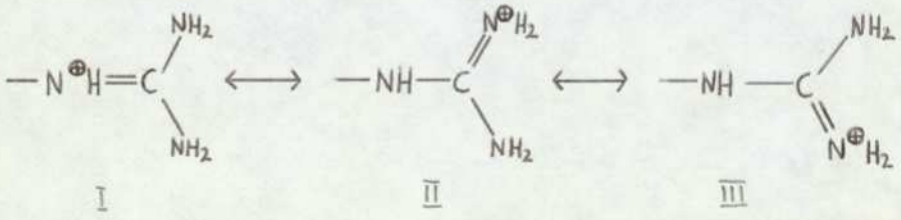

The CNDO calculations made on an idealised geometry model show (i) the formal +ve charge assigned to the nitrogen is delocalised onto the attached protons and the central carbon atom, (ii) that the CN-bond BI are in accord with the value of a resonating CN-bond (ca.1.3) established in Fig.3.2 (b), this resonance agrees with the crystal structure bond lengths (Steward, Warner & Clarke, 1974), (iii) there is a preference for I over either II or III. Owing to the central C atom having

an excess valency of 1, a planar rather than pyramidal geometry is predicted (Pople & Beveridge, 1970), and confirmed by crystal structures of the guanidino group.

Imidazole acetic acid is a potent agonist of GABA (McGeer, McGeer & McLennan, 1961), and calculations carried out on the imidazole cation (idealised structure) are shown below

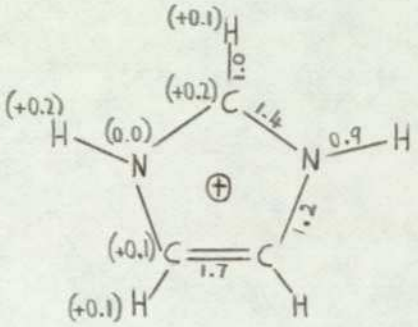

The calculated indices show there to be a resonance between the two equivalent forms, in agreement with crystal structure bond-lengths (Jones & Pauling, 1976). Again the formal positive charge on the nitrogen is delocalised on to the surrounding atoms.

Sulphonic analogues of GABA and β -alanine are also neurotransmitter drugs (Curtis & Watkins, 1960). The NAP distribution of the $-SO_3^-$ group is shown below

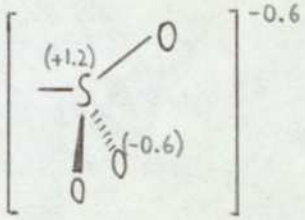

It is of interest that the charges on each O atom are analogues to that on those atoms in the $-COO^-$ group, the overall NAP on the $-SO_3$ group is also that found for the $-COO^-$ group.

3.4.3 Intermolecular invariance of the functional groups

It has been mentioned earlier (3.3.4) that NAP values have been used in PE calculations for electrostatic potential terms, and that the assumption is made in these calculations that the NAP distribution of the charged functional groups is an intramolecular invariant. In eg Steward & Clarke (1975) where the PE results on a series of related molecules are compared, a further tacit assumption of intermolecular invariance of NAP has been made. The validity of this latter assumption is now considered.

Figure 3.5 shows the NAP distributions of several type I and type II neurotransmitter molecules. Within the approximations of 3.3.2 the distributions in Fig.3.5 are representative of the

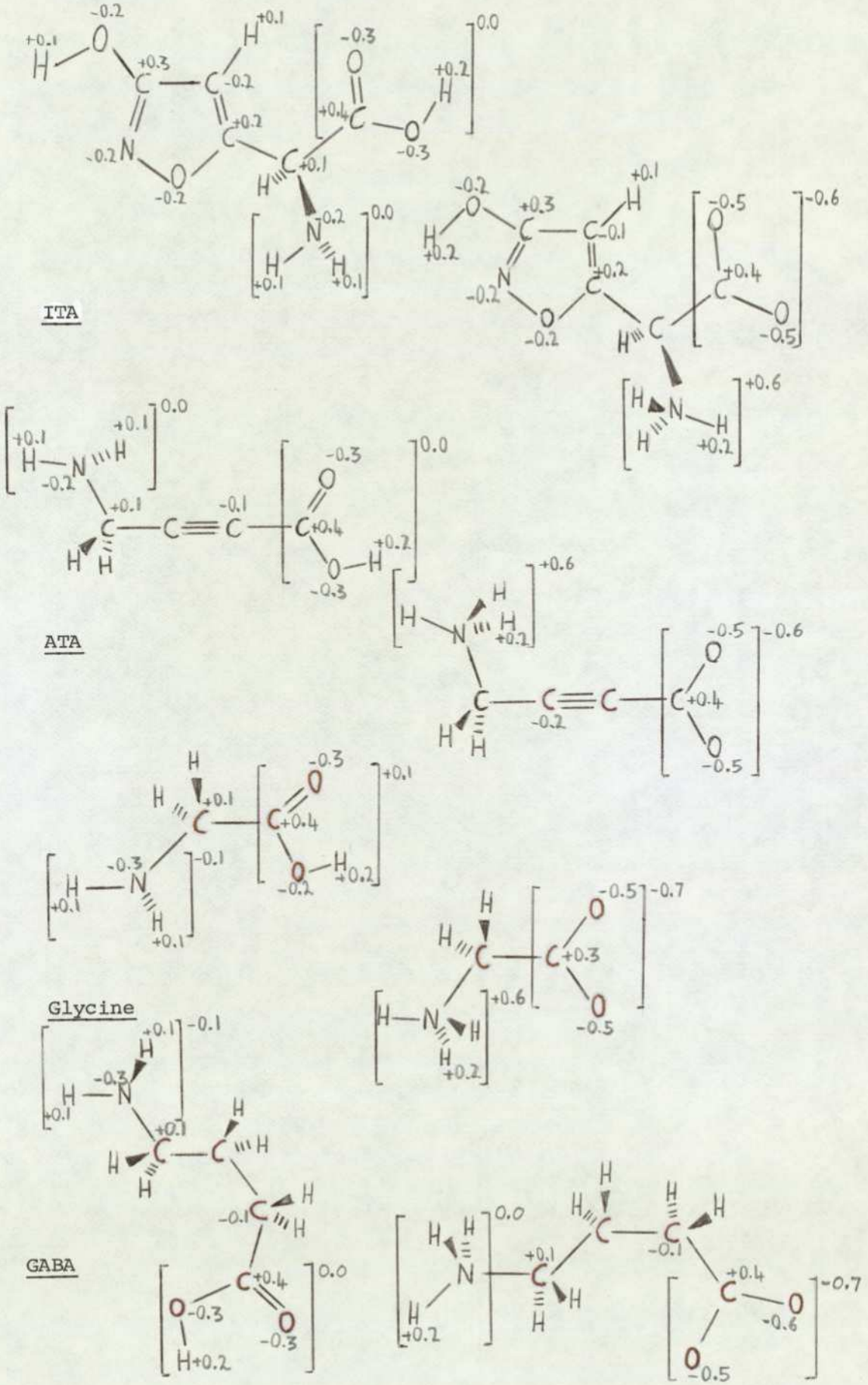

Fig.3.5 NAP distributions for ITA, ATA, glycine and GABA.

molecules for all points in their conformation spaces. The results suggest that the functional groups (NH_2, NH_3^+, COOH, COO^-) are invariant between different molecules of the general type under consideration. The invariant structures are shown in Fig.3.6, and further justification for considering them as invariant has been found by calculations on L-glutamic acid, β-alanine, 4-aminocrotonic acid (4-ACA), α-F-GABA and β-OH-GABA.

The total charge (Σ) of the functional groups has been written as a superscript on the NAP representations. At first appearance it may seem that Σ has a possible error of, eg $-COO^-$ group, ± 3 x 0.1e due to variations in the NAPs of its constituent atoms. In practice this is found not to be the case, and Σ is a conserved quantity of the group in both an intra- and inter-molecular sense to again $\pm$0.1e. This invariance is not unexpected and is discussed in 3.4.4. The observation that the electronic structure of functional groups is intermolecularly invariant is crucial to the 'ab initio by fragments' MO method (Christoffersen, 1972).

The possible invariance of the isoxazolidone group has also been investigated. Calculations for this group in the ITA mono-anion gave the NAP distribution shown below:

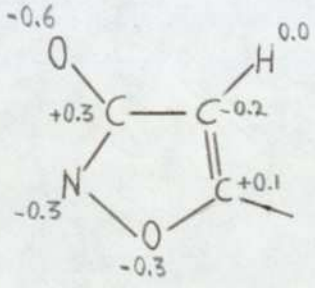

If the group is NAP invariant, then for its occurence in the zwitterionic and non-ionic molecules of muscimol we expect the NAP distribution from above diagram and Fig.3.5, respectively. The calculated NAP distributions agree completely with these predictions for the non-ionic molecule, and for the zwitterion there is a difference of only 0.1e (ie within the limits of the approximation the structure is invariant) in the exocyclic oxygen and central ring carbon.

3.4.4 Summary

The concept of idealised geometries has been investigated and utilised. Thus, a close electronic analogy has been found

between the $-COO^-$ group and the $-CON^-$ isoxazolidone moiety - a result which explains how muscimol can have GABA agonist activity.

In quoting NAP and BI to one decimal place, it is found that the functional groups are intermolecularly invariant with respect to these quantities. This is in a sense to be expected, since if functional groups were not intermolecularly invariant we could not assume just because the -COOH group in H.COOH is responsible for the acidic nature of formic acid, that the molecule CH_3.COOH would be acidic. So basic to chemistry is the idea of functional groups imparting definite chemical properties to the compounds containing them, that any result other than their intermolecular invariance (in a gross sense) would have been intolerable.

The electronic structure of some other functional groups has been calculated, these results will be important in characterising the electronic requirements of the receptors. The electronic structure is also required in order that effective charge centres of the functional groups can be found (see 3.8) for use in structure-activity studies of conformational flexibility.

3.5 Some aspects of the conformational modes of the conservative zwitterion

3.5.1 Terminal-group interactions

In the preceeding discussion 'pathological' conformations in which the $\pm$0.1e invariance of NAP and BI may be violated were referred to. These conformations are those resulting from the close-approach of functional groups, which in the GABA and GLU pharmacophores are often the end groups of α-w amino-acids and their analogues. In these 'pathological' conformations resulting from the close approach of end groups it is recognised that there are opportunities for intramolecular hydrogen bonding to occur. This does occur in crystal structures, for example, between the guanidino and carboxylate groups in β-GP. The folding of some zwitterions is now considered in this context. Fig.3.7(a) shows an energy-contour map for highly-folded conformers of the (R) α-fluoro- γ-amino butyric acid (αFG) zwitterion:rotations T_2 and T_3 are defined with respect to the fully-folded molecule in the sense indicated in Fig.3.7(b). The $-NH_3^+$ protons are held in staggered conformation with respect to those of the adjacent methylene group, and the $-COO^-$ atoms are planar with the two adjacent carbons of the molecules heavy-atom backbone. The region of conformation space (Fig.3.7(a)) may be divided in 3 subregions:
Subregion 1 - Steric repulsion is the dominant factor. This is the non-equilibrium region of 'pathological' conformations.
Subregion 2 - Here the type II surface has the character of a type I surface: steric effects have little or no significance, the dominant forces being those of methylene staggering and electrostatics.
Subregion 3 - There is a balance between the attractive and repulsive forces. There are six areas of enhanced stabilisation for the present example. To investigate these, a 'section' through one was taken along the line ($T_2 = -85^\circ$, $T_3 = 0^\circ - 100^\circ$) shown in Fig.3.7(a) and the corresponding molecular geometry calculated at 10° intervals along the line. The angle δ (Fig.3.7(b)) is defined to be a measure in terms of T_3, of the deviation from N-H-O linearity (ie δ is the angle made by the carboxyl O, the amino N and that amino proton (H^1) which adopts an intermediate spatial position with respect to the O and N). The results (Fig.3.8) show (i) δ as a function of T_3 and (ii) the BI between H^1 and the carboxyl oxygen as a function of T_3.

There is a close reciprocal correlation between the BI

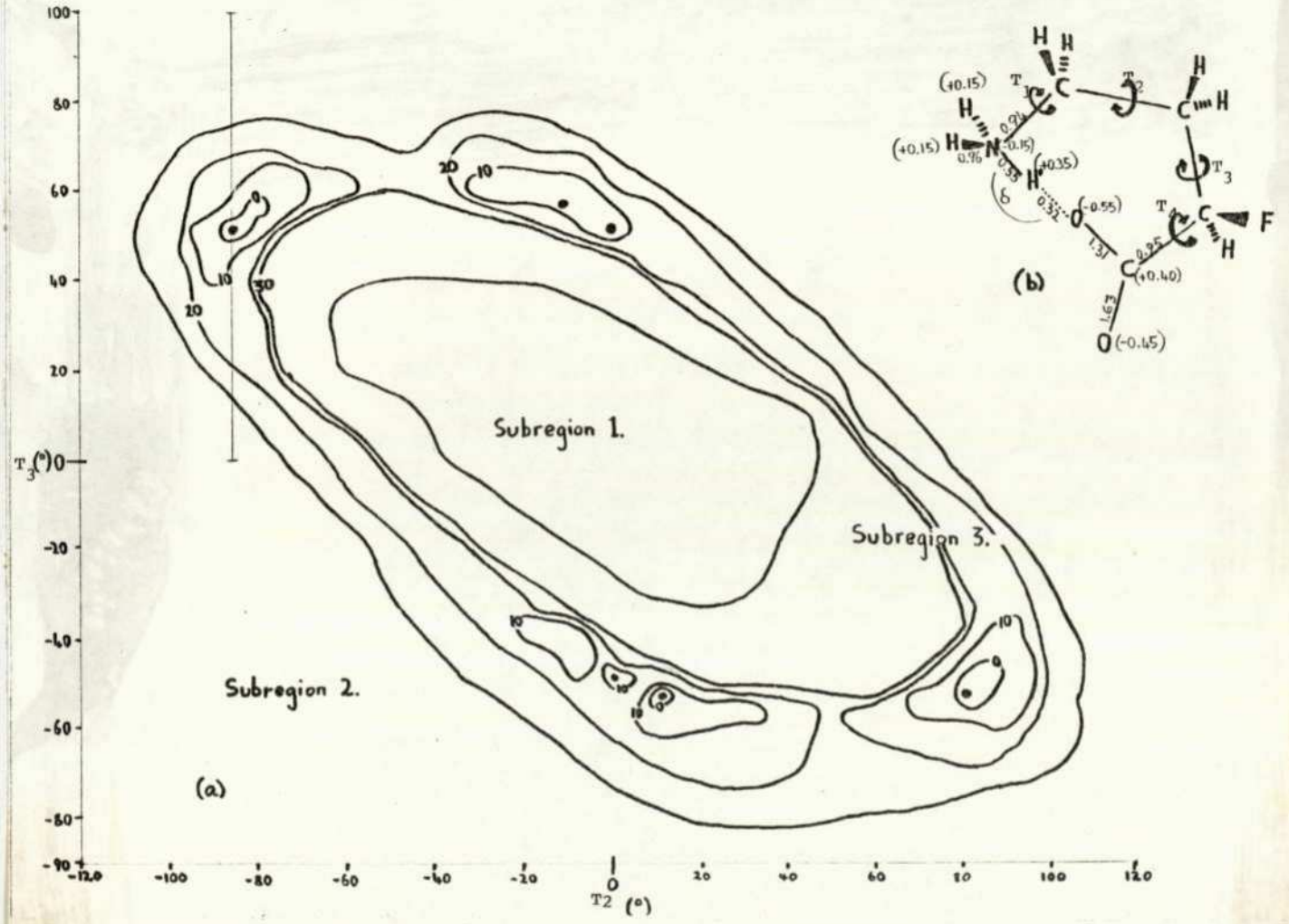

FIG. 3.7 (A) ENERGY CONTOUR MAP FOR αFG. CONTOURS IN KCAL MOL^{-1} WITH RESPECT TO THE GLOBAL MINIMUM. INNERMOST CONTOUR REPRESENTS APPROXIMATE LIMIT OF CONVERGENT SCF ENERGIES. VERTICAL LINE IS THAT ALONG WHICH THE VALUES OF BI AND δ IN FIG. 3.8 WERE CALCULATED. MINIMA ARE REPRESENTED AS •.

(B) THE FULLY-FOLDED αFG ZWITTERION WITH THE SENSE OF TORSIONAL ROTATIONS INDICATED. BI AND CHARGES (IN BRACKETS) RELEVENT TO THE DISCUSSION ARE GIVEN.

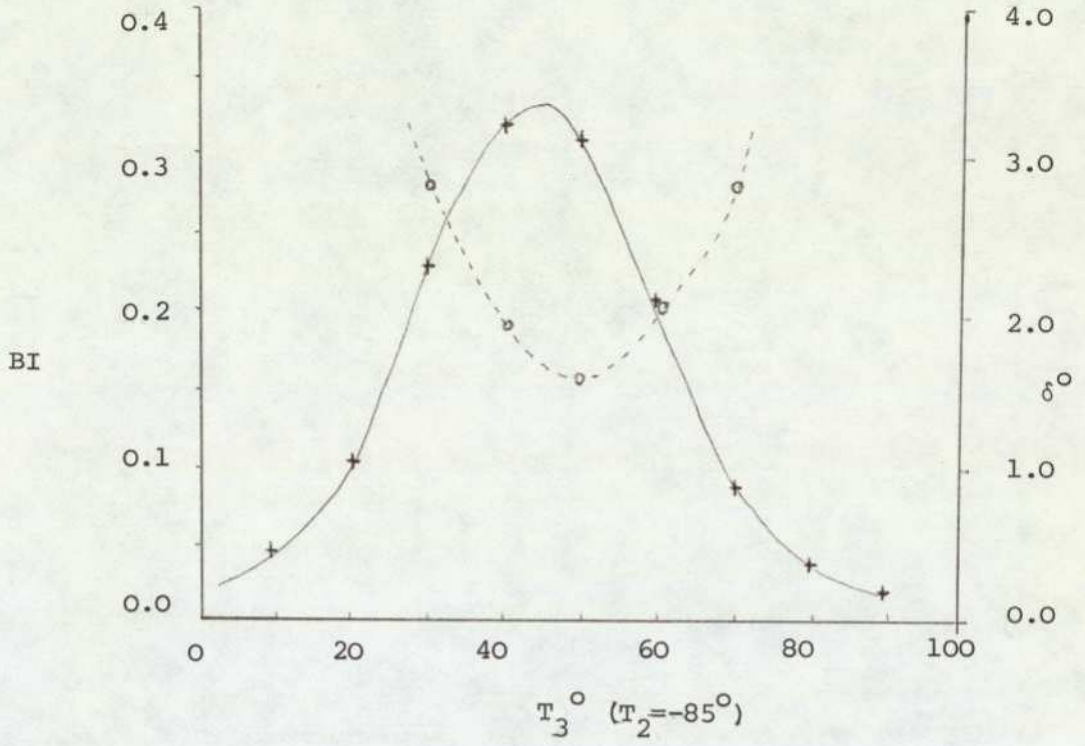

Fig.3.8 Graphs of BI(H'...O) and δ(angle OÑH') against the T_3 rotation (T_2=-85°, see Fig.3.7). Graph of BI .v. T_3 represented by —+— , and of δ .v. T_3 by ..o.. .

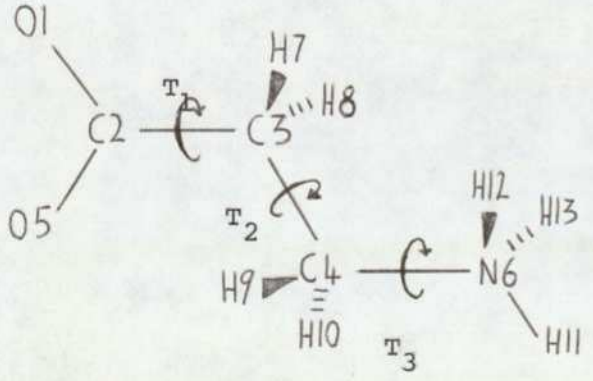

Fig.3.9 The β-alanine zwitterion showing atomic numbering scheme and torsion angles(T_1= 0°, T_2=T_3= 180° as shown).

and δ values. At T_3 = ca.50°, the conformation of minimum energy, BI is nearly at its maximum, and δ is minimum. It thus appears that this region of enhanced stability within region 3 is due to an intramolecular hydrogen-bond between ends of the zwitterion rather than electrostatic bonding. This localised bonding outside region 1 is responsible for the high BI values in Table 3.4. The NH..O bond length is only ca 2.2Å. However, it is an intramolecular hydrogen-bond with its geometry inextricably associated with the constraints of the rest of the molecule, and presumably a short distance here is energetically preferable to a more awkward angular arrangement. At the point (T_2 = -50°, T_3 = 60°) a point of relatively high energy within region 3, the NH...O distance is ca.2.0Å and δ = 57°, which is almost the maximum δ can attain (beyond this stabilisation occurs with respect to a different $-NH_3^+$ hydrogen, H* say, and δ* begins to decrease). A further study of this type of hydrogen bond is made in 3.5.3 for the β-alanine zwitterion.

A consequence of the comments in this section is that within region 3 the conformations of the $-NH_3^+$ and $-COO^-$ groups dictate that the T_2, T_3 angles will be such that hydrogen bonding occurs. Conversely any fixed values of the T_2 and T_3 angles will for similar reasons dictate the $-NH_3^+$ and $-COO^-$ conformations, and hence in these situations a true interdependence of all angles T_1 - T_4 exists. It is due to this total interdependence that the essentially linear-independent approximations of 3.3.2 and 3.3.3 require careful treatment when this type of region is encountered in a conformational space.

3.5.2 Interdependence of rotations in β-alanine

In the previous subsection (3.5.1) it is predicted that within region 3 there will be an interdependence in the torsional freedoms of an α-ω amino acid. Here this prediction is tested for the β-alanine (βA) molecule. βA has been chosen as an example since its zwitterion possesses a high degree of symmetry and only 3 torsion angles, thereby allowing a 'full' conformational study to be made. By a 'full' conformational study is meant a 3-dimensional conformation space on a 20° grid (refined to a smaller 10° grid around the minima).

The βA zwitterion, with the torsion angles indicated is shown in Fig.3.9. The torsion angles are defined as T_1 ={O5.C2-C3.C4}, T_2 ={C2.C3 - C4.N6} and T_3 ={C3.C4-N6.H11}. Bond-lengths and

angles were again not optimised in this study but were assigned standard values (Pople & Beveridge, 1970), with the exception of the $-COO^-$ group (see 3.4.2 for $-COO^-$ group geometry). The symmetry relations of the molecule give, if $E(T_1, T_2, T_3)$ is the energy at the conformation defined by T_1, T_2, T_3,

$$E(T_1,T_2,T_3) = E(T_1 \pm 180^\circ, T_2, T_3 \pm 120^\circ) = E(-T_1,-T_2,-T_3)$$

For any particular value of T_2, the characteristics of the corresponding T_1-T_3 surface indicates the extent to which the rotation of the $-COO^-$ (T_1) and $-NH_3^+$ (T_3) groups may be independent. Thus, if for a value of T_2 the surface is relatively planar, the rotation of these groups has little effect on the internal energy of the molecule and the two end-rotations would be considered as relatively independent. For βA the r.m.s deviation (σ) of the T_1-T_3 surface from planarity has been calculated for each value of T_2 in the range $0^\circ \leqslant T_2 \leqslant 180^\circ$ (Fig.3.10).

σ has a maximum value of ca.115 kcal mol^{-1} at $T_2 = 40^\circ$ and then decreases rapidly to flatten out at T_2 = ca.90°. At $T_2 = 180^\circ$, σ= ca.6 kcal mol^{-1}.

These results have relevance for conformational studies. The βA molecule may be expected to have a minimum in a fully-extended conformation ($T_2 = 180^\circ$) stabilised by methylene staggering interactions. The Fig.3.10 shows that it would be permissible to locate this minimum assuming independence between the torsion angles. However, for minima that may be expected to occur in hydrogen-bonded folded-conformations (at ca.$T_2 = 40^\circ$), clearly a study assuming full interdependence of the torsion angles is required. Hence, with MO studies of zwitterions, such as α-ω amino acids and their derivatives, in which a full conformational study is not possible, the justification for a detailed search for minima in very folded conformations must be questioned: since any initial assumptions (as in the GABA studies discussed in Section 2.3) regarding end-group conformation will predetermine the detailed location of the folded energy-minima in what will generally be an arbitrary way. For the GABA studies the best one can probably do is to acknowledge the existence of minima in conformations lying within a zone analogous to region 3 (Fig.3.7(a)), but not to be (on the evidence of a T_2 - T_3 (GABA torsion angles T) surface) any more precise than that.

Finally, in the light of the results of this section, it is probably fair to say that our study of 4-ATA (Warner et al, 1975) could have been validly made assuming independence of the rotations

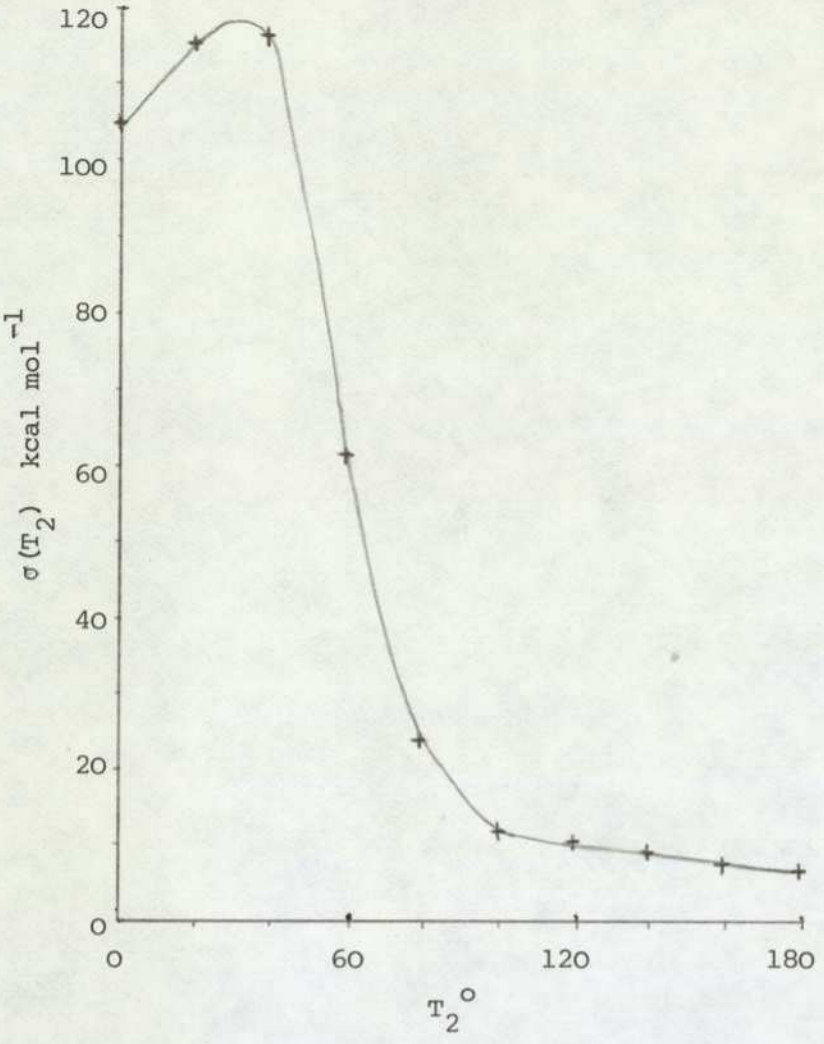

Fig. 3.10 Graph of r.m.s. deviation in energy (σ) over T_1-T_3 surfaces for the βA zwitterion against T_2.

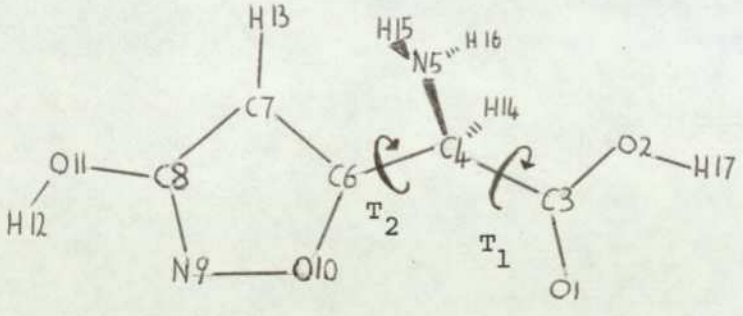

Fig. 3.11 The ITA molecule showing torsion angles. Non-ionic species is shown; zwitterion is formed by the bonding of H17 to N5, mono-anion is then formed by removal of H12 proton.

(see also comment in 3.8.4 noting X_T(ATA) = 5.8Å).

3.5.3 Intramolecular hydrogen-bonding in β-alanine

The numerically large values of σ for the conformations corresponding to a folded molecule (T_2 small) indicate that the relative orientations of $-NH_3^+$ AND $-COO^-$ groups are then energetically important and this can be interpreted in terms of intramolecular bonding (3.5.1). For this reason the global minimum G (ie $T_1 = 140^\circ$, $T_2 = 30^\circ$, $T_3 = 110^\circ$ - the conformational energy map for the βA zwitterion is to be found in section 4.2.1) was considered. Setting $T_1 = 140^\circ$, $T_2 = 30^\circ$, the BI was calculated for $T_3 = -40^\circ$ to $+20^\circ$ in steps of 10°. A maximum BI of 0.37 was at $T_3 = -10^\circ$ (= $-10^\circ + 120^\circ = 110^\circ$) ie at the global minimum G. The hydrogen-bond lengths found for βA are in agreement with those found for αFG, and are thus likely to be typical of those quantities calculated by CNDO/2.

Classically the $-NH_3^+$ group would be expected to adopt a staggered configuration with respect to the adjacent methylene, this is found in the case of 4-ATA. At the minimum G in the βA conformational space the hydrogen bonding results in an eclipsed configuration for the $-NH_3^+$ group and adjacent methylene group.

3.5.4 BI and NAP values for hydrogen-bond stabilised conformers

At the ($T_2 = -85^\circ$, $T_3 = 50^\circ$) minimum in the αFG conformation space (Fig.3.7(a)) the BI and NAP values are:

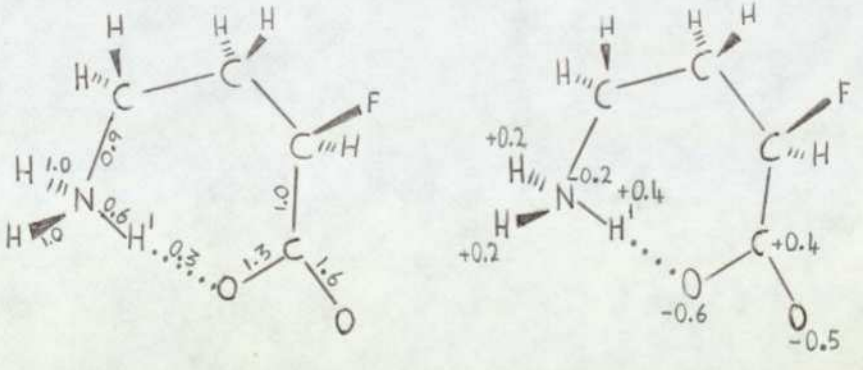

From Fig.3.4(b) it is seen that the usual BI for the onium N-H bond is 0.9, and thus the corresponding value in the hydrogen bonded conformer is ca.two thirds of the usual zwitterion value. Similarly, the carboxyl O-H is only ca.one third of the value found in the usual -COOH group (see Fig.3.4(a)). It is therefore possible to consider the hydrogen-bonded conformer as being a

hybrid zwitterion/non-zwitterion in which the H atom is 'shared' between $-NH_2$ and $-COO^-$ groups. At the minimum ($T_2 = -85^\circ$, $T_3 = 50^\circ$) the hybrid form is 2:1:: zwitterion:non-zwitterion.

The charges on the folded-minima conformers are explicable in terms of electron induction processes, as can be seen on a NAP 'difference diagram' for (folded-minima - extended) conformers:

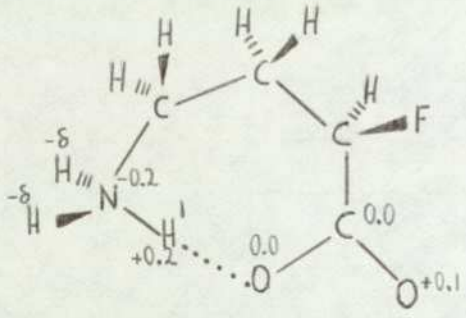

It is seen that the change in NAP distribution of an intramolecular hydrogen bond is greater for the $-NH_3^+$ rather than $-COO^-$ group (see also 4.5.3).

3.6 The relevance of free-energy and related topics

3.6.1 Introduction

In the conformational studies of GABA and 4-ATA the contour maps were constructed on a grid of the internal energies. The most populated conformational mode was then determined as the point of lowest internal energy in the surface. However, the equilibrium position between conformers is more correctly determined by free-energy considerations, as the internal energy approach assumes that changes in entropy are unimportant. Farnell, Richards and Ganellin (1974) have pointed out that the relative population of two minima (conveniently visualised as valleys) is a function not only of their relative depths, but also of their curvatures. The entropy is related to the width of the valley (and thus its curvature), and so a sufficiently wide valley may have a greater population than a narrow one, even though the latter is much deeper, eg

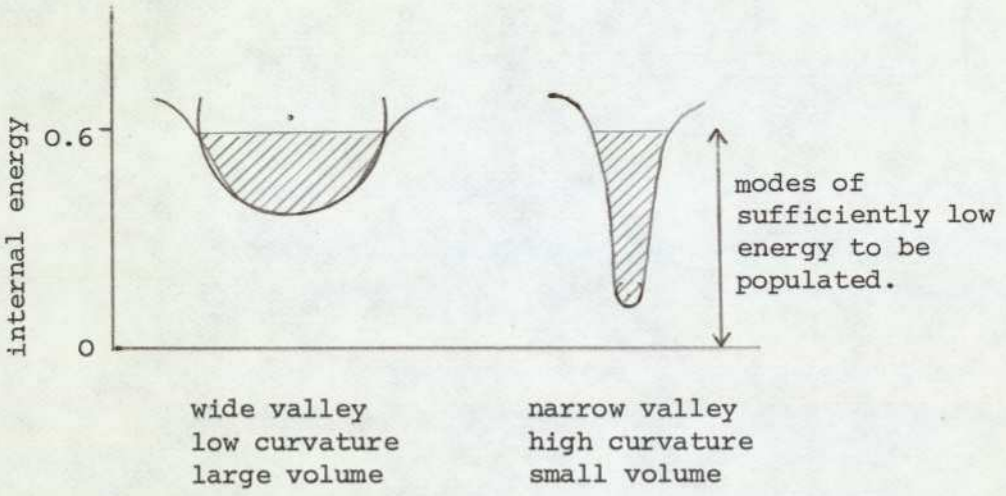

The differences between internal-energy and free-energy approaches to the construction of energy surfaces has been looked at in the context of the ITA mono-anion.

3.6.2 Free-energy aspects of the conformers of the ITA mono-anion

In common with Farnell et al, for determining the relative populations of minima in an energy surface a classical Boltzmann-distribution partition function was used

$$Zp = \sum_{T_1,T_2} \exp(-E(T_1,T_2)/\mathcal{R}T) \qquad \text{(i)}$$

where $\mathcal{R}$ is the universal gas constant, T the absolute temperature ($T = 300^{\circ}K$ in all the calculations) and $E(T_1, T_2)$ the internal energy at a point $P = (T_1, T_2)$ on the energy surface. [The torsion

angles T_1 and T_2 are defined as $T_1 = \{C6.C4 - C3.O1\}$ and $T_2 = \{C7.C6 - C4.C3\}$ (see Fig.3.11), and the resulting internal-energy map is given in the original paper (Borthwick and Steward, 1976). Equation (i) has been used to calculate a Zp for each 20° grid square on the internal-energy surface, the summation being taken over all points (25) that lie within that square on a 5° grid. This allows a contour map to be drawn on which the energy at each point has been corrected for the topology of the surface in the vicinity of that point. This is a map of free-energy relative to the global minimum (ie inf $\{Zp\}$), where the relative free-energy Ap' is defined as

$$Ap' = -\Re T \ln(Zp/\inf_p\{Zp\}) \qquad \text{(ii)}$$

It is now possible to make comparisons with a relative internal-energy (Ep') contour map, where Ep' is defined by

$$Ep' = -(Ep - \inf_p\{Ep\}) \qquad \text{(iii)}$$

calculating the internal energies required for equation (i) involves calculating the entire T_1- T_2energy surface on a 5° grid, and this is clearly not computationally practicable in the CNDO/2 scheme. A 5° grid was therefore produced by interpolating on the 20° grid with a bi-cubic spline surface-fitting routine. The interpolated values were then checked at a number of random points by actual CNDO/2 computations and found to agree to better than 0.1 kcal mol^{-1}. It must be pointed out that the degree of fit produced by the bi-cubic spline is a function of the surface being interpolated, and in general the best fits will be for surfaces of little curvature, and unfortunately it is this type of surface for which free-energy will be least significant. It is likely that the categories of surface defined in 3.2.1 (viz type I and type II) are again relevant as those for which free-energy has (type II) or has not (type I) significance.

However, from the contour maps (Ap map not shown because gross features are essentially same as Ep map) it was noticed that in going from an Ep to Ap approach, there was a decrease in the population of the regions of maxiumum energy, and an increase in the population of the two minimum - a migration to the valleys. The quasi-planar regions show little difference in population, which is to be expected, since as has been stated, free-energy is essentially a correction for surface curvature.

Using $$P_1 = P_o \exp(-E/\Re T) \qquad \text{(iv)}$$

it is possible to calculate from our Ep and Ap 20° grids a conformer population ratio $P(M_1^{12})/P(M_2^{12})$ at the two minima M_1^{12} and M_2^{12} for E = Ep and E = Ap respectively. It is found that

$$(P(M_1^{12})/P(M_2^{12})_{Ep} = 147.5$$

and $$(P(M_1^{12})/P(M_2^{12}))_{Ap} = 221.8$$

showing an increased bias towards M_1^{12} in the free-energy approach.

3.6.3 Importance of free-energy and discussion of results

In conformational studies contours are often drawn in intevals only as far as 5 or 6 kcal mol^{-1} from the global minimum. From equation (iv) it can be seen that the molecules lying inside these contours represent 99.97% and 99.99% of all the molecular population respectively. Since the number of molecules

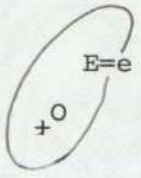

within contour is $n_e = \int_0^e P_1 \, dE$, which by (iv) is

$$P_o \int \exp(-E/\mathcal{R}T) \, dE = P_o \mathcal{R}T(1 - \exp(-e/\mathcal{R}T)) \qquad (v)$$

The normalisation condition for the distribution is given by (v) when $e = \infty$, ie $n_\infty = P_o \mathcal{R}T$, if $n_\infty = 100$ then n_e will be the percentage population and we have $P_o = 100/\mathcal{R}T$. Thus,

$$n_e = 100(1 - \exp(-e/\mathcal{R}T)) \qquad (vi)$$

If e = 5 and 6kcal mol^{-1} respectively (vi) gives$^{\neq}$ $n_5 = 99.97\%$ and $n_6 = 99.99\%$.

In the study of ITA the positions (as distinct from populations) of the respective Ep- and Ap- map minima were found to be different by about 5° in the sense of the rotation studied (T_1). An investigation of the E energy-grid for the region of the global minimum revealed that no two adjacent grid points on the 5° grid had energies differing by amounts significantly greater than $\mathcal{R}T$. It is therefore concluded that for the location of minima (i) the positions of Ep- and Ap- map minima are unlikely to be distinguishable as a result of random thermal vibrations,

---

$\neq$ at $37^{\circ}C$ is 0.615 kcal mol^{-1}

and (ii) the use of a 5^{o} grid is seeking energy differences which again are not significant with respect to thermal energy fluctuation.

From this point the calculation of free-energy maps and 5^{o} grid internal-energy maps have not been made (but see comments on free-energy of solvent effects (4.1.2)). A population analysis is a useful device and 5 kcal contours will frequently be marked on energy maps. This is particularly useful when two (or more) energy surfaces are being compared.

3.7 Electrostatic potential calculations

3.7.1 Theory

The electrostatic potential is a 1st order approximation to the interaction energy between a molecule and a unit protonic point charge. It has been shown to provide useful information about the relative activity of various chemical features. Detailed discussion of various approximations in which the potential may be calculated are to be found elsewhere (Giessner-Prettre and Pullman, 1972).

The approximation to the electrostatic potential (EP) at the point p which will be investigated in this section is

$$V(p) = \sum_{A} (Z_A/R_{pA} - P_{AA}V_{AH}) \qquad (i)$$

where Z_A is the nuclear core charge, R_{pA} is the distance from p to atomic nucleus A, P_{AA} is the NAP as originally defined in 1.4.5 (ie $\sum_{\mu \in A} P_{\mu\mu}$). V_{AH} is the nuclear attraction integral over s-orbitals. This level of approximation is not expected to yield absolute numerical values of significance. However, the comparative depths of EP minima and the general topology of EP contours are likely to parallel the results of more sophisticated calculations (Giessner-Prettre and Pullman, 1972).

It is now intended to investigate the utility of the approximate EP equation (i). The EPs will be calculated using a readily available computer program (program QCPE 249, 1974). All parameters and input data for this program are consistent with the CNDO/2 MO SCF method.

3.7.2 An electrostatic-potential study of the carboxylate group

The $-COO^-$ group is ubiquitous in drugs of the GABA and glutamate neurotransmitter systems. Not only does it represent the negatively charged group ($\mathcal{R}^-$) of the canonical transmitters (as well as in the majority of their agonists), but may also be present as a part of the receptor involved in the transmitter-receptor interaction. Because of its importance it has been used as a test structure on which EP calculations have been made. The $-COO^-$ group (calculations made on GABA in its crystal conformation (Steward, Player & Warner, 1973(a))) has been considered with respect to (i) protonation, and (ii) hydrogen bonding.

(i) Protonation

The EP of the $-COO^-$ group is shown in Fig.3.12, there are two minima (m_1, m_2) of almost equivalent strength ca. -125 kcal mol^{-1}, with m_1 slightly more stable than m_2 (presumably due to asymmetry). A unit protonic charge approaching within the cone Θ_i will be attracted into minimum m_1. The most favourable directions of approach are along the reaction paths labelled p_i and q_i, the former path seems associated with the direction of the $C-O^-$ bond and is the most likely mode of approach. It is therefore expected that the $-COO^-$ group will protonate to -COOH with the proton positioned in the region of m_1 or m_2, eg

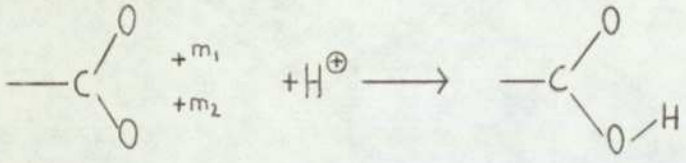

The in-plane interaction is predicted to be greatest. Protonation at this site is theoretically supported by a CNDO/2 study on glycine (Oegerle & Sabin, 1973) in which an optimisation of the internal geometry of the -COOH group placed the proton in a position compatible with the EP minimum found here (ie either m_1 or m_2). Experimental support for protonation at m_1 or m_2 comes from numerous crystal structure determinations, although this support may be regarded as indirect since the -COOH proton is usually involved in hydrogen bonding when in a crystalline environment.

In our study of the 4-ATA non-zwitterion it was noted that a secondary minimum for the ψ rotation occurred at

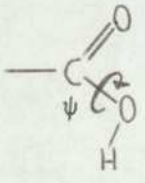

A refinement of our EP calculations subsequently showed the existence of a shallow minimum in the position n_1 (Fig.3.12) lying on the reaction path q_1. No such minimum was observed for the related position with respect to m_2 on path q_2. The existence of the minimum n_1 (or the non-existence of a related minimum n_2) is to be attributed to assymmetry present in the body of the molecule, since the $-COO^-$ group itself is totally symmetric.

Assuming protonation to have occurred (at the favoured site), we can consider the subsequent possibilities by a study of

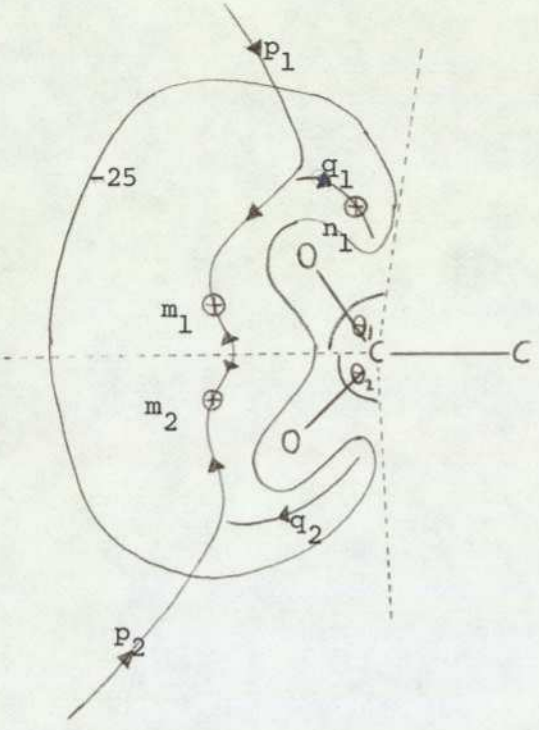

Fig. 3.12 Electrostatic potential map in region of $-COO^-$ group. Trajectories followed by unit protonic charge and a -25 kcal reference contour are shown. Minima are marked ⊕ .

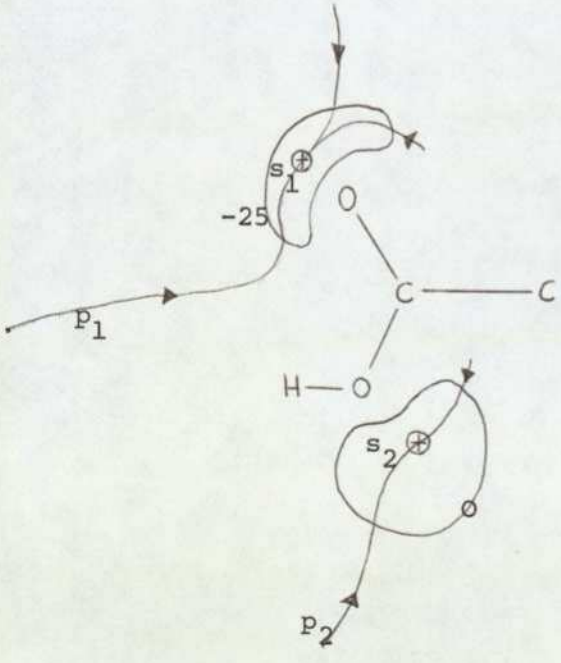

Fig. 3.13 Electrostatic potential map in region of -COOH group. Trajectories followed by unit protonic charge, and either -25 or O kcal reference contour are shown. Minima are marked ⊕ .

the resulting -COOH group. The EP is shown in Fig.3.13 with reaction paths as indicated. At the global minima, s_1, the EP is only ca -40 kcal mol^{-1}, and at s_2 it is further reduced to ca -10 kcal mol^{-1}. Protonation at the most favourable site (in-plane still favoured) would imply that the new COH angle would be close to 180°, which is extremely unlikely! Thus it would seem that a second protonation of the $-COO^-$ group is not favoured, a fact supported by the non-existence of 1,1-glycols except in a very few special circumstances (eg Bonner & Castro, 1965).

(ii) Hydrogen bonding

The minima of the EP are not to be expected to determine hydrogen-bond directions in a crystalline environment, since many other factors (mainly constraints imposed by the hydrogen-bond donor-complex) will extensively modify these directions. It may be, however, that the minima give a good indication of the number of hydrogen bonds the $-COO^-$ group is normally able to form. Thus, the EP suggests that the $-COO^-$ group can act as an acceptor for a maximum of 3 hydrogen bonds:

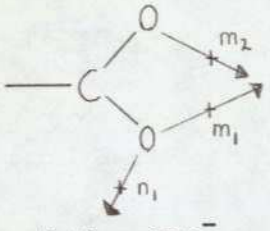

From a survey of the $-COO^-$ groups in a fairly random sample of X-ray crystal structure determinations (GABA (Steward, Player & Warner, 1973 (a));α-amino-n-butyric acid (Akimoto & Iitaka, 1972); β-alanine (Jose & Pant, 1965);L-threonine (Shoemaker, Donohue, Schomaker & Corey, 1950);L-glutamic acid (Hirokawa, 1955); kainic acid monohydrate (Watase, Tomiie & Nitta, 1958); L-mimosine (Mostad, Romming & Rosenquist, 1973);L-histadine (Madden, McGandy, Seeman, Harding & Hoy, 1972);DL-serine(Shoemaker , Barieau, Donohue & Lu, 1953);α-glycine* (Marsh,1958);β-hydroxy -GABA (Tomita, 1971); DL-tyrosine (Mostad & Romming, 1973); methionine sulphoximine (Neidle & Rogers, 1970); β-GP*(Steward, Warner & Clarke, 1974); L-aspartic acid (Derissen, Endeman & Peerdeman (1968); L-arginine dihydrate* (Karle & Karle, 1964)), all but a very few (*) take part in 3 hydrogen bonds. Further of the 4 $-COO^-$ groups not having 3 hydrogen bonds α-glycine (4) and β-hydroxy-GABA (5) are unusual in that a bifurcated hydrogen-bond is involved.

The -COOH group has an EP suggesting a hydrogen bonding scheme:

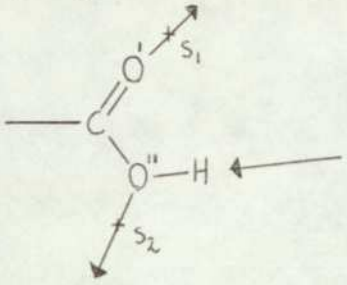

The hydrogen bond associated with m_2 must be considered as questionable since s_2 has an EP of ca -10 kcal mol^{-1}. Again a survey of some -COOH groups was made (L-aspartic acid (Derissen et al,1968); L-glutamic acid (Hirokawa, 1955);γ-guanidinobutyric acid.HCl*(Maeda, Fujiwara & Tomita, 1972); L-cysteic acid (Hendrickson & Karle, 1971); kainic acid monohydrate*(Watase, Tomiie & Nitta, 1958); GABA.HCl* (Steward, Player & Warner, 1973(b)); DL-tryptophan formate (Bye, Mostad & Romming, 1973); glycocyamine .HBr* (Roy, Kajumdar & Saha, 1967); fumaramic acid (Benghiat & Leiserowitz, 1972)). All these structures (except those marked *) have 2 hydrogen bonds in the scheme:

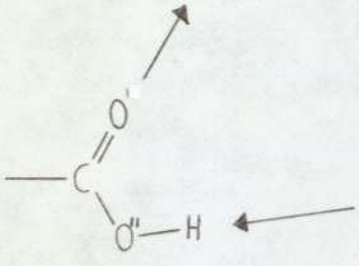

Of the 4 remaining structures (*), 3 are heavy-atom complexes of the form $-\overset{O''}{\overset{\|}{C}}-O'H\cdots\begin{Bmatrix}Cl^-\\Br^-\end{Bmatrix}$. In all 4 cases the extra hydrogen-bond occurs at O' and only in one case does a fourth bond occur with O'' as acceptor. That O' usually accepts only 1 hydrogen bond is supported by a survey (Donohue, 1967) in which 10 out of 12 -C=O groups were acceptors for just 1 hydrogen bond. It therefore seems that the usual hydrogen bonding scheme for the -COOH group is as depicted in the last diagram, and the 10 kcal mol^{-1} minimum is not capable of supporting a hydrogen bond.

3.7.3 Discussion of results on the carboxylate group

Throughout this discussion of EPs the assumption has been made that after a minimum of the EP has been involved in a hydrogen bond type interaction, the electrostatic potential field is not drastically modified. In other words, all interactions are assumed to occur simultaneously. Correlation with observation is encouraging enough to believe that this assumption is not too

unreasonable.

From the theoretical EP and experimental data a typical number of hydrogen bonds made by the $-COO^-$ and -COOH groups has been noticed. In cases where there is an unusual number of hydrogen bonds there is often present one or more 'weak' hydrogen bonds (eg bifurcated, OH... $\{^{Cl^-}_{Br^-}$, hydration hydrogen-bonds). It seems that the groups have a basic 'electron reservoir' which will normally provide for, in the case of $-COO^-$, 3 hydrogen bonds of the type $O^-...H-N^+$, but may provide for more than 3 if 'weaker' hydrogen bonds are involved which make less of a demand on the 'electron reservoir'. The high incidence of molecules marked * comprising a guanidino group then leads one to suspect that the $N_{guan}-H...O^-$ bond is significantly weaker than the $N^+_{onium}-H...O^-$ bond. Comparison of hydrogen-bond lengths in GABA and β-GP are consistent with this proposal (Table 3.6), if it is accepted that the weaker the bond the greater the H...O separation. That there is a difference in the hydrogen bonding properties of the guanidino and onium groups is suggested by the different CNDO/2 NAP values of

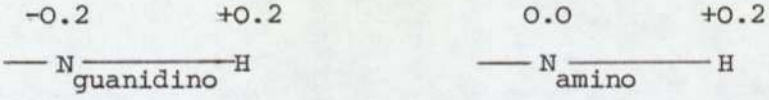

It is possible that the property of the guanidino group to form a weaker hydrogen bond than the onium group is of significance in receptor-transmitter interaction. Specifically the guanidino group would seem more amenable to uptake processes by virtue of its weaker hydrogen bonding to a receptor protein. The question as to whether hydration bonds are comparatively weak has also been looked at, the results are summarised in Table 3.7. The $OH...O^-$ bonds fall into two groups (i) donor-acceptor distance 2.55-2.72 Å, all bonds other than those involving H_2O fall into this group, (ii) donor-acceptor distance 2.73-2.90 Å , all bonds involving H_2O molecules are in this range. The assumption that the longer bonds are 'weaker' implies that hydration bonds fall into the catagory of 'weak' bonds, and thus make less of a demand on the 'electron reservoir' of the $-COO^-$ group.

3.7.4 An electrostatic-potential study of the $-CON^-$ group

It has already been seen that the $-CON^-$ moiety of the isoxazolidone ring has an analogous electronic structure to the $-COO^-$ group from the point of view of NAP and BI distributions (3.4.1). It is now intended to investigate whether the similarities in these structures extends to their EP profiles.

The EP is shown in Fig.3.14. There are three minima, m_1, m_2 and m_3 with potential values of ca. -125, -110 and -75 kcal mol^{-1}, respectively; the reaction paths (p,q) are also shown.

(i) Protonation

A proton approaching within the cone Θ_1, will tend to move towards to the region of m_1, whilst a proton approaching within the cone defined by Θ_2 will move towards m_3. It is expected that the first protonation will occur at m_1 - being the global minimum, ie

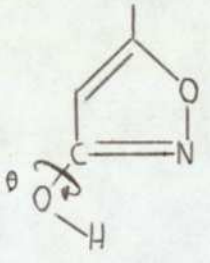

with OH planar-cis to CN. This is consistent with the MO calculations which predict two minima for the θ rotation {H.O - C.N} in planar-cis and planar-trans conformations, the former being most stable.

The EP after the initial protonation is shown in Fig.3.15. There are two minima m_1 (-30 kcal mol^{-1}) and m_2 (-10 kcal mol^{-1}) and second protonation is discounted in this case.

(ii) Hydrogen bonding

The EPs imply hydrogen bonding schemes

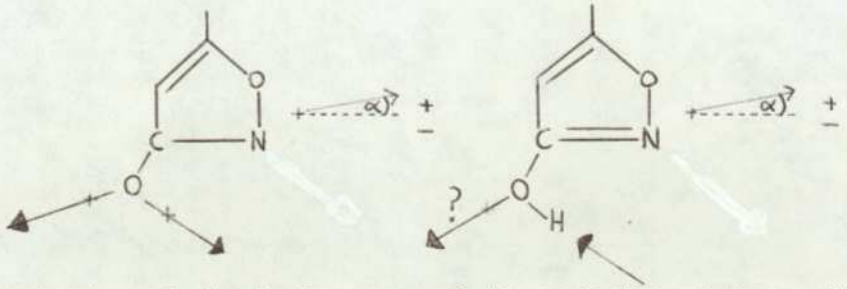

The orientation of the hydrogen bond through the minimum adjacent to the O-N bond is not clear. This bond may be directed toward the oxygen (α -ve) or toward the nitrogen (α +ve), the present calculations do not resolve the problem. Fortunately, it has been noted that there is an exaggeration of oxygen potentials with

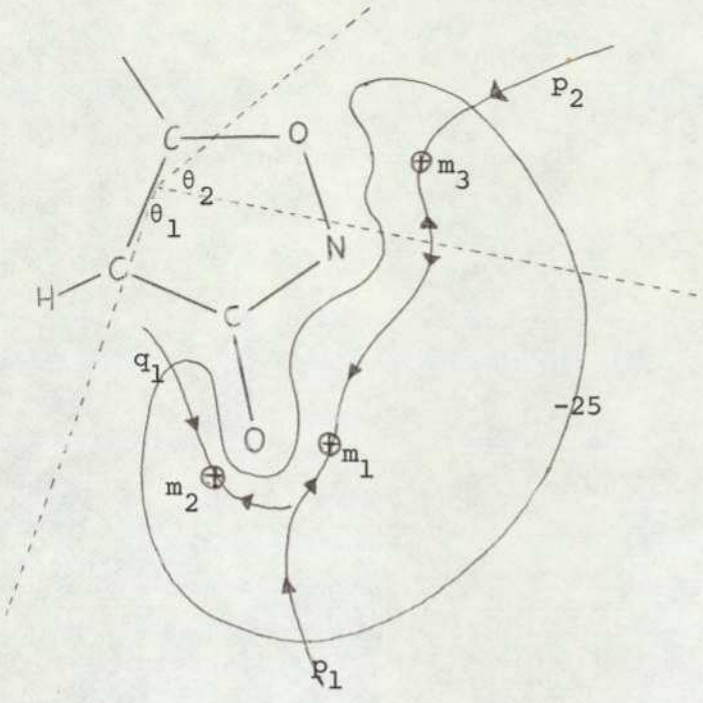

Fig. 3.14 Electrostatic potential map of $-CON^-$ moiety of isoxazolidone ring. Trajectories followed by unit protonic charge and -25 kcal reference contour are shown. Minima are marked ⊕ .

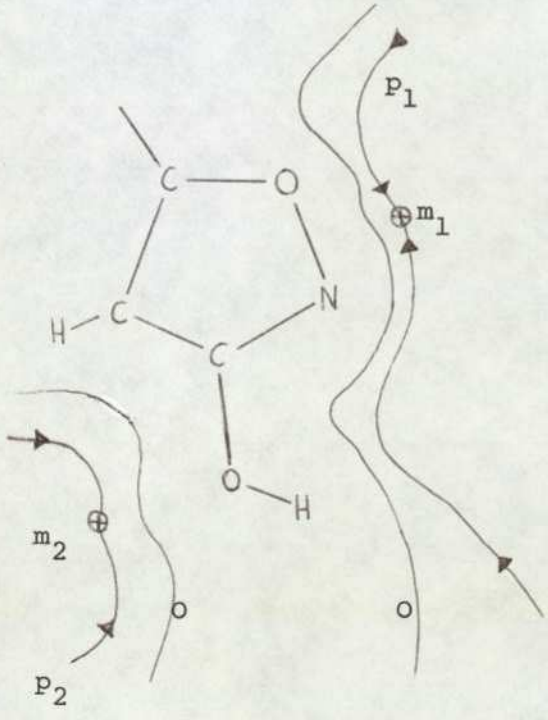

Fig. 3.15 Electrostatic potential map of the -CONH moiety of isoxazolidone ring.

respect to those of nitrogen in CNDO calculated potentials. This suggests that the hydrogen bond at m_3 is intrinsically associated with the nitrogen rather than the cyclic oxygen. In the protonated -CONH- structure, m_2 has the same order of magnitude of EP as m_2 for -COOH (Fig.3.13), and so by analogy it is not expected to be involved in hydrogen bonding. The global minimum (m_1) of the -CONH- group is again by analogy with -COOH expected to be associated with a hydrogen bond. The following scenarios are hence expected for hydrogen bonding,

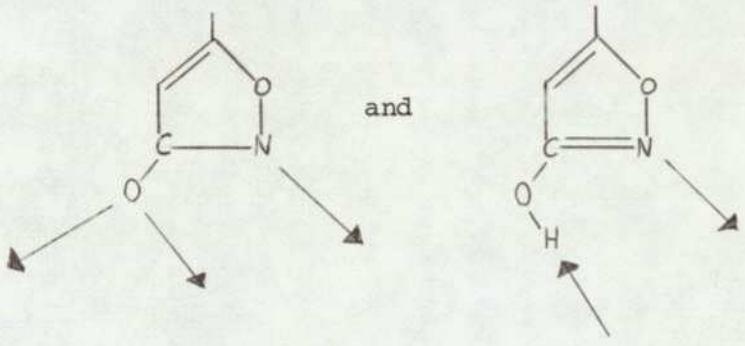

3.7.5 Discussion of results on the $-CON^-$ group

X-ray crystal structure determinations (Brehm, Krogsgaard-Larsen & Hjeds, 1974; Brehm, 1972) made on isoxazolidones (including muscimol on which these theoretical EP calculations were made) show

(i) That the $-CON^-$ moiety is involved in 3 hydrogen bonds as predicted.

(ii) Two of the hydrogen bonds are associated with the exocyclic oxygen and one with the cyclic nitrogen.

Recently two additional crystal structures have been received (L. Brehm, private communication) one of which conforms to the above observations. The second structure (4-Aminomethyl-5-methyl-3-isoxazolol Hemihydrate)

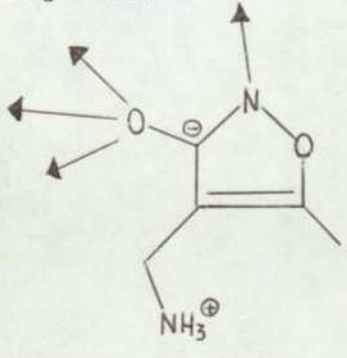

has 4 hydrogen bonds as shown. As might be expected from the remarks made earlier there should be 'weak' hydrogen bonds involved. The separations for the 3 hydrogen-bonds associated with the exocyclic oxygen are given in Table 3.8. Comparison of Tables 3.6

* all lengths in Å

GABA		βGP	
$N^+H...O^-$	$H...O^-$	$N^+H...O^-$	$H...O^-$
2.768	1.63	2.847	1.88
2.726	1.63	2.967	2.18
2.746	1.64	2.837	1.98
		2.810	2.02
		2.826[a]	1.89

a intramolecular bond

Table 3.6

Comparison of $N^+H...O^-$ hydrogen bonds in GABA and βGP.

Molecule	OH source	O source	OH...O
Allokainic acid	carboxyl	carboxylate	2.71
Kainic acid	carboxyl	"	2.71
"	water	"	2.83
"	"	"	2.85
l-cysteic acid	$-SO_3H$	"	2.66
l-arganine dihyd.	water	"	2.74
	"	"	2.89
L-aspartate	carboxyl	"	2.56
DL-serine	hydroxyl	"	2.67

Table 3.7

Some typical $OH...O^-$ hydrogen bonds. Note the comparative weakness of the hydrogen bonds associated with water molecules.

	ATOM A	$H...O^-$	$A-H...O^-$
(1)	N^+	1.73	2.725
(2)	N^+	2.17	2.857
(3)	O_{H_2O}	1.95	2.838

Table 3.8

Hydrogen-bond lengths in the 4-aminomethyl-5-methyl -3-isoxazolol hemihydrate molecule.

and 3.8 shows one N^+-H...O bond (2) to be of similar dimension to those of βGP and one bond (3) to be an hydration bond, these it has been suggested (3.7.3) are 'weak' bonds. That the N^+-H...O bond (2) is 'weak' is supported by the N^+-H...O bond lengths for muscimol (monoclinic) which has 2 hydrogen bonds to the exocyclic oxygen and are therefore expected to represent 'normal' rather than 'weak' bonds. The bond lengths for muscimol are given below, and if these are considered as 'normal', then bond (1) in Table 3.8 is also 'normal', whereas bond (2) by comparison is indeed weaker.

H...O^-	N^+-H...O^-
1.79	2.710
1.83	2.773

3.7.6 Conclusions

Theoretical EP calculations within the framework of CNDO/2 formalism, have led to results compatible with experimental observations on carboxyl groups and the isoxazolidone ring. The $-COO^-$ group has again been found to be analogous to the $-CON^-$ moiety, both having EP contour maps of similar nephroid shape and similar electrostatic properties.

Protonation sites are predicted consistent with CNDO/2 calculated energy profiles for rotation about $\geq C-\overset{*}{C}-OH$ bonds, and with available experimental evidence. The $-COO^-$ and $-CON^-$ groups are theoretically found to be implicated in 3 hydrogen bonds of normal strength, but this figure may be greater if some of the bonds are relatively weak. The sort of 'weak' bonds envisaged are those such as co-ordination, bifurcated and bonds to counter-ions (Br^-, Cl^-, etc) and water molecules. The 'weak' bond may also be a weak form of the ordinary N^+-H...O^- hydrogen bond, where N^+ may be from an onium or guanidino group and O^- from either the $-COO^-$ or $-CON^-$ function. From Tables 3.6 and 3.8 as a rough guide we may summarise as follows

N^+H...O^- bond-type	H...O^-	N^+H...O^-
strong	1.60 - 1.85	2.70 - 2.80
weak	1.85 - 2.20	2.80 - 3.00

It is concluded that EP maps, even in a relatively crude formalism are capable of predicting events relating to

protonation (alkylation) and to hydrogen bonding. Some work has already been done on nucleic acid bases in which their comparative reactivities have been discussed via EP maps (Bonaccorsi, Pullman, Scrocco & Tomasi, 1972). The present study differs in that we have concentrated on comparing EPs of two functional groups rather than the EPs of whole molecules. This has allowed us to discover fundemental similarities in the $-COO^-$ and $-CON^-$ groups which may have been overlooked in a study considering only the gross features of a whole molecule. This study has also shown not only can the fact that hydrogen-bonding occurs at a particular molecular feature be obtained from EP maps, but also the number of such bonds can be implied. It is expected that the electrostatic potential map will find and increasing use in both organic chemistry and in pharmacological studies of SAR on biologically active molecules.

3.8 Intercharge separation measurements in the GABA and GLU pharmacophores

3.8.1 Introduction

In section 1.2.6 it was shown that the mutual separation (x_T) of the terminal groups in the α-w amino carboxylic acids is of great importance in the determination of their relative potencies (ie the conformation as well as composition of a molecule is crucial for GABA agonism). In early work Kier (1970, 1973, 1974) used measurements based on the nitrogen atom (N^+) and an oxygen atom (O^-).

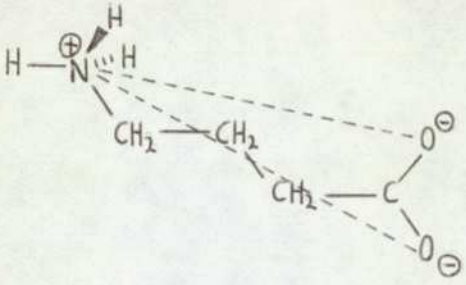

This leads to 2 intercharge separations. Ham (1974) in an NMR study of GABA has used again the nitrogen atom, but in the negative region ($\mathfrak{R}^-$) of the molecule he has used the carboxyl carbon,

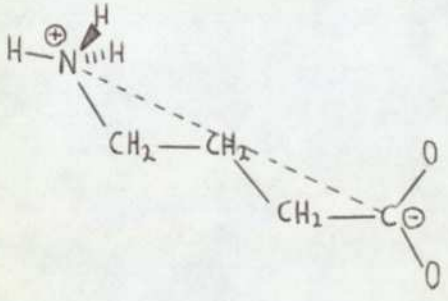

This leads to a unique intercharge separation. It is now intended to discuss these proposed intercharge separations in the light of our data and if necessary to suggest more realistic (from the point of view of the theoretical calculations) charge centres.

3.8.2 The x_T-distance in the GABA pharmacophore

An obvious criticism of both Ham and Kier's suggestions is the use of the (N^+) nitrogen atom as a charge centre. It has been shown (3.4.2) that the charge on the onium group resides not on the nitrogen atom, but is equally distributed amongst the onium protons. It is proposed that for the positively charged region ($\mathfrak{R}^+$) of the GABA pharmacophore, when represented by an onium group, the centroid of the triangle formed by the onium

protons is used to define the $\mathfrak{R}^+$-charge centre.

Since initially the receptor will not distinguish the individual O atoms of the carboxylate group, but will only recognise the resultant EP field of the group, it is felt that Kier's scheme is unnecessarily complex as a first approximation. Ham's choice of the carbon atom, although leading to a simplifying single intercharge measurement, is perhaps unwise as this atom carries a substantial +ve charge. Hence it is proposed here to use the mid-point of the line joining the oxygen atoms as the carboxylate charge centre, this point gives the simplified single intercharge separation. Thus the intercharge centre separation measurement (x_T) proposed is

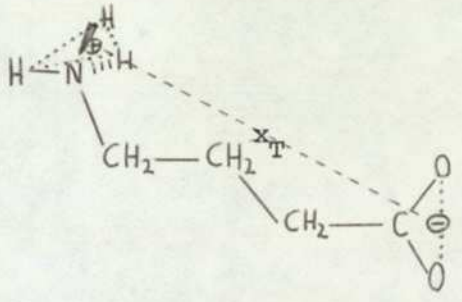

The above definition of x_T has the advantage over previous definitions in being based on theoretical charge-distributions. If our proposed charge-centres are logically defined, there should be a good correlation between $\vec{x}_T$ and $\vec{\mu}$ (the direction of the dipole of the molecule as calculated from CNDO/2 method).

As a model on which to test the correlation between $\vec{x}_T$ and $\vec{\mu}$ the β-alanine (βA) zwitterion has been used. The fully-extended βA zwitterion is shown in Fig.3.16, superimposed on the figure are $\vec{\mu}$, and $\vec{x}_T$ for the various definitions. Figure 3.16 clearly shows that our definition of points defining the x_T distance leads to an x_T whose direction is closest to the direction of μ. This shows that our x_T has a physical interpretation lacking to varying extents in the work published by other authors.

The charge centre of the -CON$^-$ group in muscimol is defined in the obvious way by analogy with the -COO$^-$ group. More problematic is the guanidino group (3.4.2). The charge distribution is

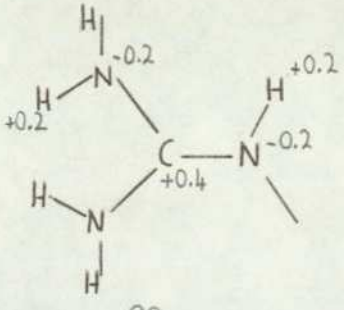

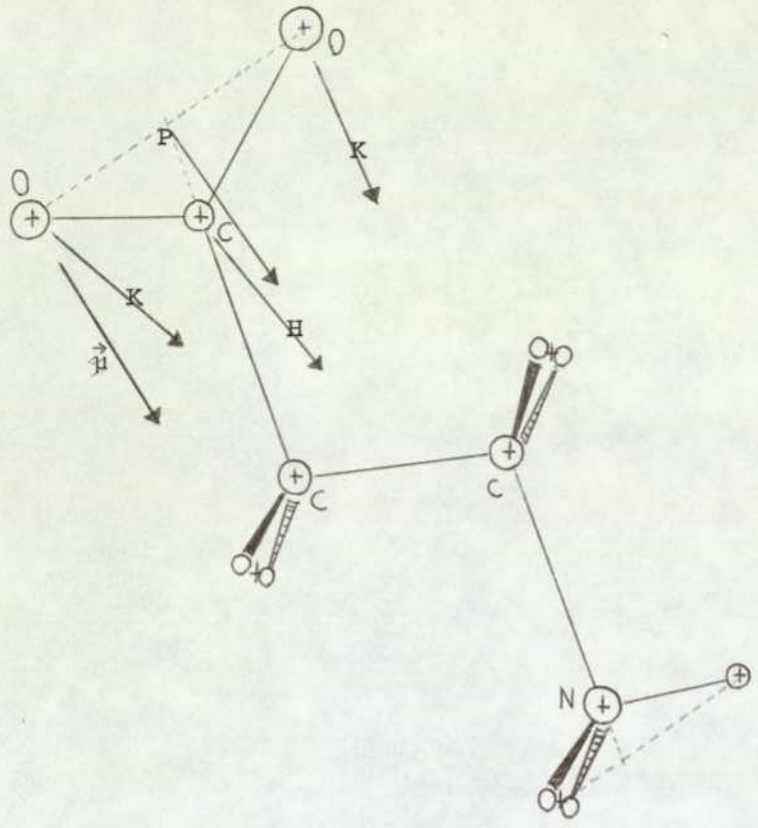

Fig. 3.16 Comparison of $\vec{x}_T$s and CNDO/2 calculated dipole direction ($\vec{\mu}$) for βA. (key: 'H'=Ham, 'K'=Kier, 'P'=present study.)

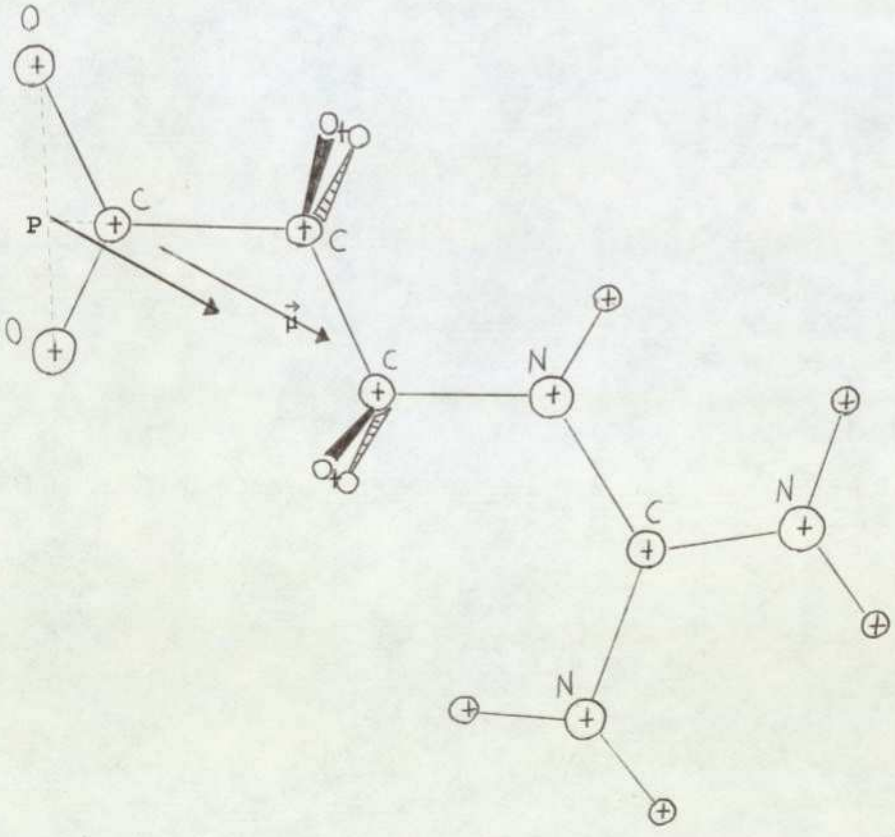

Fig 3.17 Comparison of $\vec{x}_T$ and CNDO/2 calculated $\vec{\mu}$ for βGP. (key: 'P'=present study, '$\vec{\mu}$'=CNDO theoretical dipole direction.)

and a charge centre is suggested by a continual reduction of the protonic +ve charges thus:

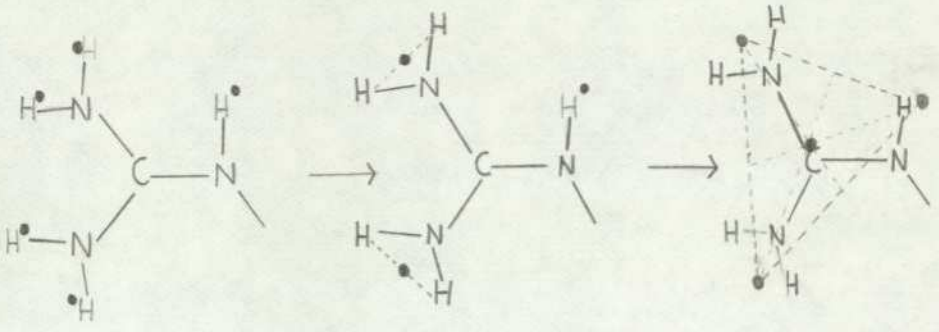

As the centre of +ve protonic charges lies close to the central highly +ve carbon we have no hesitation in suggesting that carbon as the effective unique charge centre of the guanidino group. Figure 3.17 shows the good correlation of $\vec{\mu}$ with $\vec{x}_T$ for βGP justifying the choice of charge centre.

Using x_Ts as defined here, Steward and Clarke have found a good correlation between x_T and relative potency of agonists in the GABA pharmacophore (Steward & Clarke, 1975).

3.8.3 The x_T-distances in the GLU pharmacophore

In the glutamate pharmacophore the problem of charge centres for the functional groups is similar to that for the GABA system, since the same groups are active in both systems. The added complication posed with GLU and its agonists is that there are now two $\mathcal{R}^-$ regions leading to the pharmacophore depicted in fig.3.18. Fortunately, the glycine-like part of glutamate ($\mathcal{R}^+$ and $\mathcal{R}_1^-$), is such that x_{T3} is unaffected by torsional rotations since the charge centres of the $-NH_3^+$ and $-COO^-$ groups lie on their axes of rotation. Since the glycine-like feature is common to all glutamate agonists, the pharmacophore is reduced to two x_T measurements viz. x_{T1} and x_{T2}. A correlation between x_T distributions (calculated as with the GABA study using PE methods) and the relative potencies of glutamate agonists has been made, the results of which are discussed in 5.8.3.

In the GABA pharmacophore our $\vec{x}_T$ was well correlated with $\vec{\mu}$. However, since in the GLU system there are now two x_Ts, it is unclear how these may correlate with $\vec{\mu}$. The ITA mono-anion has been looked at in an attempt to resolve this question. The planar projectionsof ITA mono-anion are shown in Fig.3.19 with $\vec{x}_T$s and $\vec{\mu}$ superimposed. The $-CON^-$ moiety of ITA is as usual treated as an analogue of the $-COO^-$ group and thus the $-CON^-$ charge centre is considered as being the mid-point of the line joining the O^- and N^- atoms.

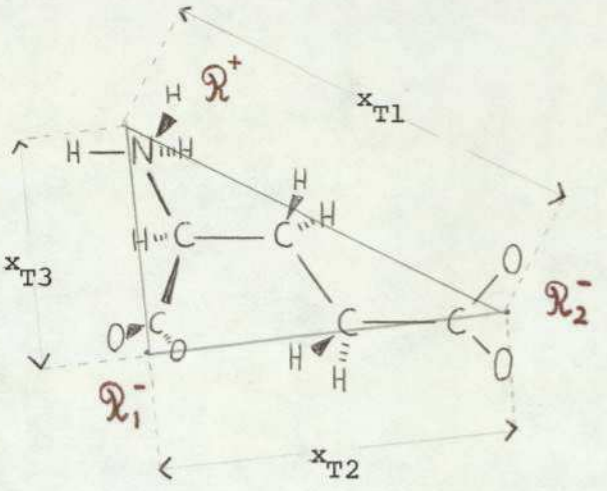

Fig. 3.18 The glutamate pharmacophore.

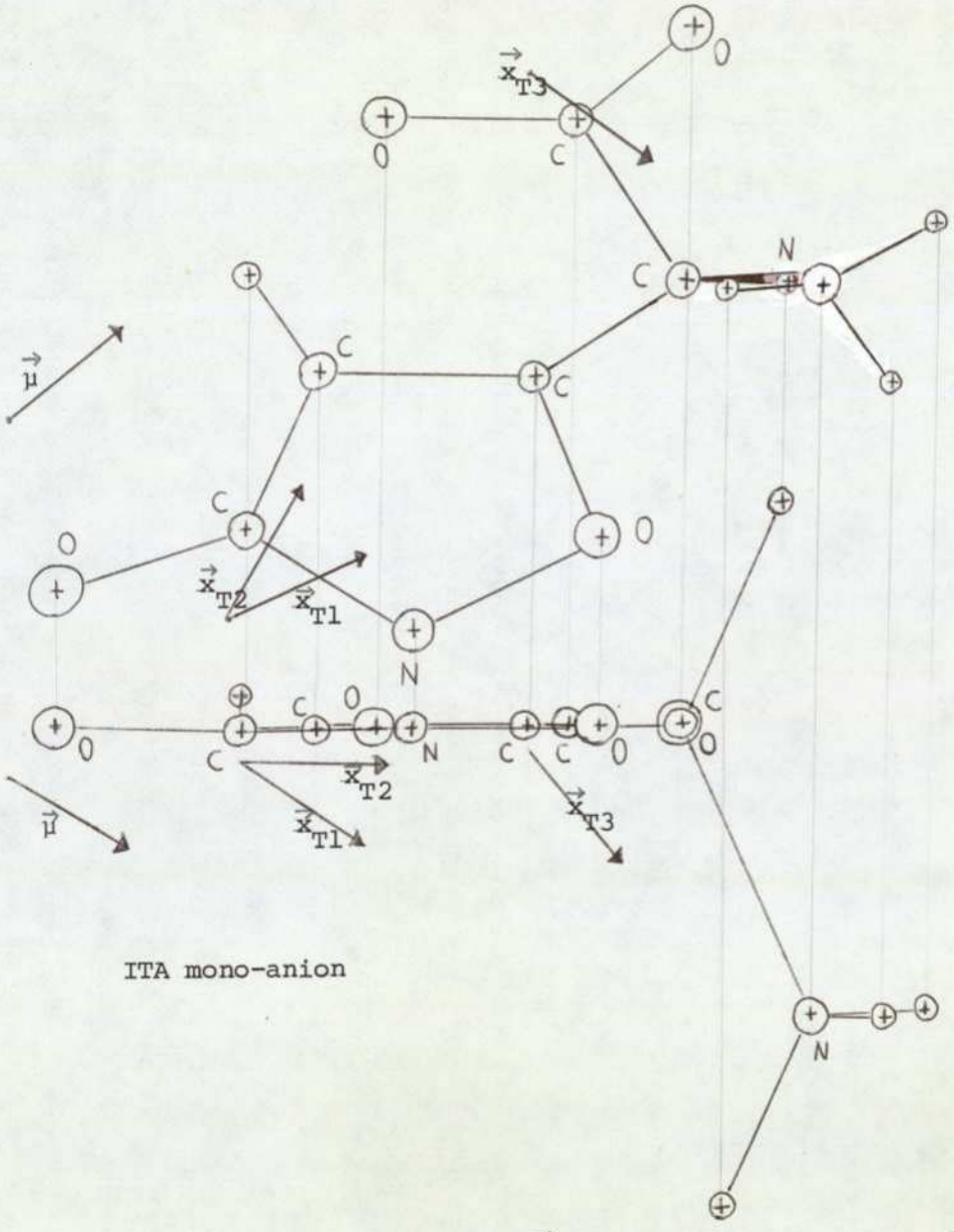

ITA mono-anion

Fig. 3.19 Comparison of $\vec{x}_T$s and CNDO/2 calculated $\vec{\mu}$ for ITA mono-anion. Projections are shown on two mutually orthogonal planes.

The results shown in Fig.3.19 clearly indicate a good correlation of $\vec{\mu}$ with $\vec{x}_{T1}$, suggesting the possibility of a single distance GLU pharmacophore based on x_{T1}. This will also be considered in 5.8.3.

Finally, since in GABA and glutamate pharmacophores the charged $\mathfrak{X}^-$ and $\mathfrak{X}^+$ regions and their separations are important, it is to be expected that the experimental dipole-moment should be a useful parameter in SAR studies of these systems.

3.8.4 Summary

It has been shown that

(i) The definition of charge centres proposed here leads to a better physical interpretation of x_T than has previously been used.

(ii) The three x_Ts of the glutamate pharmacophore may be reduced to two, x_{T3} being a constant feature of the pharmacophore.

(iii) The possibility exists of further reducing the two glutamate x_Ts to just x_{T1}. This suggestion is based on the good correlation between $\vec{x}_{T1}$ and $\vec{\mu}$.

Finally, the parameter x_T may be useful in providing an additional indication as to whether or not in a particular conformation the torsional angles describing α-w group rotations are independent. For example, consider Fig.3.20 which refers to conformations of the βA zwitterion. If the $-NH_3^+$ group is unaffected by electrostatic effects of the $-COO^-$, it should adopt a staggered configuration with respect to the vicinal methylene, and the unshaded area in the figure represents such conformations. The shaded area, within which the $-COO^-$ group has affected the configuration of the $-NH_3^+$ group, occurs for $x_T \lesssim 3.2\text{Å}$. Thus we may use this value of x_T as a guide to deciding in which conformations the $-NH_3^+$ and $-COO^-$ groups of amino carboxylic acids may be treated as independent in their rotational preferences, ie conformations in which $x_T \gtrsim 3.2\text{Å}$.

3.9 Conclusion

3.9.1 Overview

At the end of Chapter 2 a theoretical MO method (viz CNDO/2) was chosen as being suited to our requirements for studying molecules of the GABA and GLU meurotransmitter systems. In the present chapter that method has been used to determine gas-phase conformational and electronic properties characteristic of molecules active in the GABA and GLU systems. The aim has largely been to develop a 'feel' for the behaviour of CNDO/2 in dealing with molecules of the GABA type, and to establish a set of reference data. The latter point is of some relevance, since knowing what the method should predict is necessary before anomalies can be detected, and so often it is the anomaly which provides the vital clue to identifying and solving a problem.

In section 2.2.3 the use of CNDO/2 was not recommended for conformational studies in 3 situations

(i) when system is conjugated, eg

(ii) when system has lone-pair bearing heteroatoms, eg

(iii) when a 2nd row atom is involved, eg

We have been careful to avoid the use of CNDO/2 in the above situations and, fortunately, this has not proved restrictive. Hence with the above proviso, it is felt that the CNDO/2 MO method provides an excellent theoretical method for the study of GABA- and GLU-type molecules. It is now proposed to proceed, with a degree of confidence, to study the GABA, GLU and PG systems using CNDO/2.

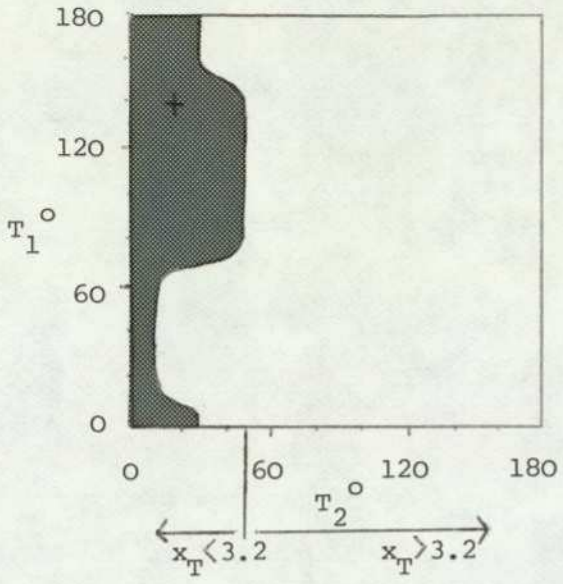

+ --denotes free-space global minimum.

Fig. 3.20 T_1-T_2 conformation space of βA showing regions in which T_3 is 'staggered' or 'eclipsed'. Shaded area denotes those conformations for which T_3 is 'eclipsed'.(βA molecule with torsion angles can be found in Fig. 3.9.)

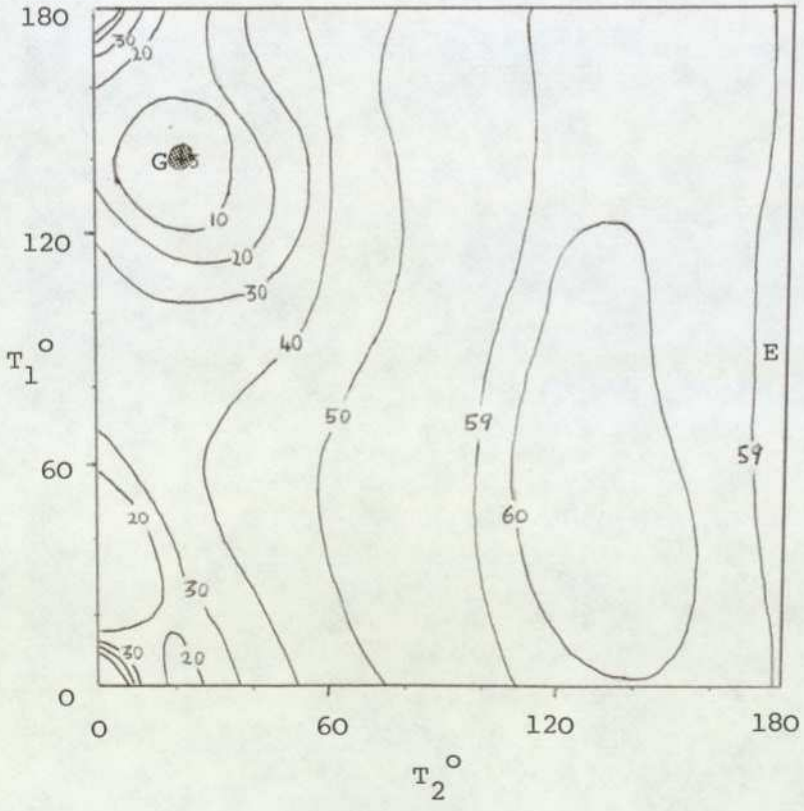

Fig. 4.1 T_1-T_2 free-space energy-surface for the βA zwitterion. Global minimum (G) is marked '+'; a second minimum -energy region (E) occurs for extended conformers.

4.1 Introduction

4.1.1 The need for the inclusion of the solvent

In the first MO studies on GABA by Kier & Truitt (1970), no mention of the types of environment relevant to the interaction of GABA with the receptor were made. In subsequent studies on GABA agonists Kier et al (1973, 1974) have maintained this apparent unawareness as to the relevance of free-space calculations in transmitter/receptor interactions. However, the majority of authors (eg Pullman, Richards, Beveridge & Hopfinger in Proceedings of the 7th Jerusalem symposium on quantum chemistry and biochemistry, 1975) have acknowledged that the biophase is not synonymous with free-space. Having accepted the previous observation the question of exactly what is the phase relevant to transmitter/receptor interactions arises. At some stage in these interactions it is expected that the transmitter is in an aqueous phase. Close to the receptor the phase may well be that of the lipoid neuronal membrane in which case the free-space results may be relevant. The SAR study of Steward and Clarke (1975) in the GABA system using empirical calculations which incorporated an allowance for an aqueous environment yielded good results - this suggests that the aqueous medium allowance (at least) is worthy of detailed consideration for future SAR studies on the GABA and GLU systems.

To produce any meaningful SAR for the GABA system, solvent effects are in a sense forced on us. This is evident since 4-ATA and MM are rigid GABA agonists with invariant x_Ts of ca 5.8Å and 5.1Å, and as MM has a potency comparable with GABA (Johnston, 1968) it is assumed 5.1Å is close to the intercharge separation required by the receptor (x_R). Glycine by contrast has an x_T of 3.2Å and is virtually inactive at GABA receptors. The free-space calculations on GABA show that at the global minimum the x_T is 2.4Å, thus we would be forced to conclude on the basis of free-space calculations that GABA displays an x_T incompatible with activity at GABA receptors! Clearly, then, for the GABA system, and presumably likewise the GLU system, the free-space approach is inadequate for SAR studies.

With the evidence that a simple allowance for an aqueous environment yields good SAR results (Steward & Clarke, 1975), the possible ways of computing the solvent effect are now considered.

4.1.2 Present approaches to the solvent effect

In this subsection the two main methods being used at this time are considered in the context of the general theoretical formalism of solvent effects. The two main methods are known as the supermolecule and continuum, these methods are implimented in different ways by different authors. The way in which the supermolecule and continuum methods arise from the thermodynamic treatment of a particle (solvent and solute) ensemble comprise the remainder of this subsection.

A dilute solution is essentially an ensemble of systems comprising one solute molecule surrounded by many solvent molecules. The thermodynamic properties of such a system are defined by the Boltzmann distribution partition-function

$$Z = \sum_i \exp(-E_i/kT) = \sum_i Z_i \qquad \text{(i)}$$

where E_i are energy states of the system, k is the Boltzmann constant and T the absolute temperature. If the states are sufficiently close to be continuous rather than discrete then, $\sum \rightarrow \int$ and (i) becomes

$$Z = \int \exp(-E(Q)/kT)\, dQ \qquad \text{(ii)}$$

where for an N molecule system $Q = (q_i,\ldots,q_N)$, the q_i being configurational coordinates (q_i), they define its position $(\underline{R}_i)$, orientation $(\underline{\theta}_i)$ and its conformation as defined by bond lengths (r_i), bond angles (θ_i) and its torsion angles (T_i), ie $q=\{\underline{R}_i,\underline{\theta}_i,\underline{r}_i,\underline{\theta}_i,\underline{T}_i\}$
Equation (ii) may be written

$$Z = \int_{q_1}\cdots\int_{q_N} \exp(-E(Q)/kT)\, dq_1\ldots dq_N$$

$$= \int_{\bar{q}_1}\int_{q_2}\int_{T_1}\cdots\int_{q_N} \exp(-E(Q)/kT)\, dT_1 d\bar{q}_1 dq_2\ldots dq_N$$

since $dQ=dq_1\ldots dq_N$ and $dq_i=dR_i d\theta_i dr_i d\theta_i dT_i = dT_i d\bar{q}_i$

Hence,

$$Z = \int_{T_1}\left[\int_{\bar{q}_1}\cdots\int_{q_N} \exp(-E(Q)/kT)\, dq_1\ldots dq_N\right] dT_1$$

and

$$Z=\int_{T_1} Z(T_1)\, dT_1 \qquad \text{(iii)}$$

If molecule 1 is now the solute molecule, equation (iii) defines the reduced partition function $(Z(T_1))$ for the solute molecule. A similar partitioning of equation (ii) in which explicit consideration is now made additionally for a molecule of the solvent (labeled 2) leads to

$$Z=\int_{q_2}\int_{T_1} Z(T_1,q_2)\, dT_1 dq_2 \qquad \text{(iv)}$$

Equations (iii) and (iv) lead to the continuum and supermolecule methods respectively.

(a) The continuum method

In this model the $E(Q)$ appearing in $Z(T_i)$ (equation (iii)) is approximated by

$$E(Q) \simeq E^{eff}(T_i) + E_{solvent} \qquad (v)$$

where E^{eff} is the effective solvent-solute interaction energy and $E_{solvent}$ is the solvent-solvent interaction energy. In the continuum method the solvent-solvent interactions are constant and may be neglected for our purposes. Hence, $E(Q) \simeq E^{eff}(T_i)$ which may be written as

$$E(Q) \simeq E_{solute}(T_i) + E_{solute\text{-}solvent}(T_i) \qquad (vi)$$

$$\simeq E_{solute} + E_{cav} + E_{dis} + E_{es} \qquad (vii)$$

where E_{solute} is the free-space energy of the solute (MO calculated).

E_{cav} is the energy required to form a cavity in the solvent continuum to accommodate the solute molecule.

E_{es} is the electrostatic solute-solvent binding energy

and E_{dis} is the interaction energy due to dispersion forces.

Schematically we have

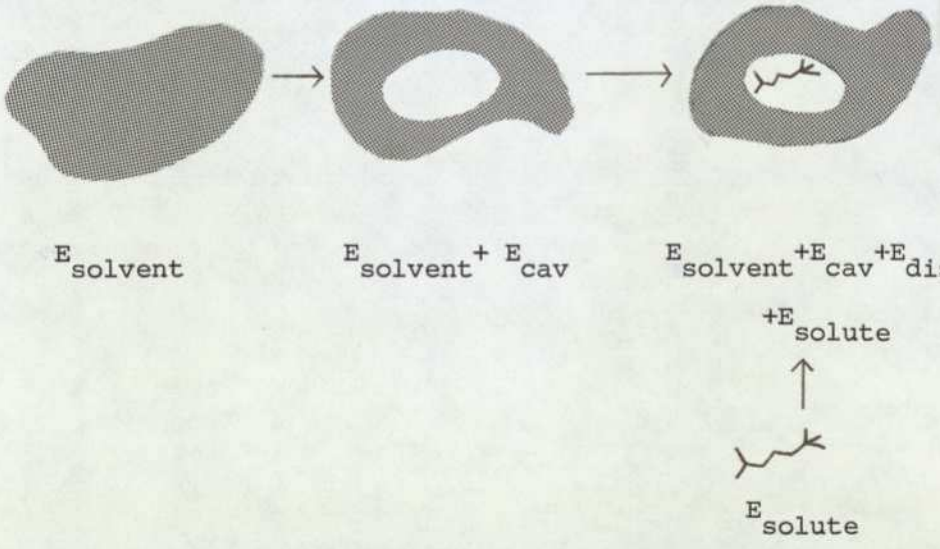

With the continuum model two approaches to the evaluation of (vii) have been made. Beveridge, Radna, Schnuelle & Kelly (1974) have used the work of Onsager (1936) to calculate E_{es}, and E_{solute} was calculated at the INDO level. Alternatively, Clarke (1976) has calculated E_{es} according to Buckingham (1953), and E_{solute} at the CNDO level. This latter approach is expected to be superior for highly polar molecules of the GABA and GLU type.

Finally in this discussion of the theoretical background to the continuum method we show that the continuum conformational energy is approximately a conformational free-energy. In 3.6.2 the configurational free-energy (A) of a system is given by

$$A = -k\,T \ln Z \qquad \text{(viii)}$$

The conformational free-energy is then

$$A_i(T_1) = -kT \ln Z_i(T_1) = -kT \ln(\exp(-E_i^{eff}(T_1)/kT)) \qquad \text{(ix)}$$

(this equation uses $E(Q) \simeq E^{eff}(T_1)$, equation (i) and equation (viii)). Equation (ix) reduces to $A_i(T_1) = E_i^{eff}(T_1) \simeq E(Q)$, ie the conformational energy calculated using the continuum model is approximately a conformational free-energy.

(b) The supermolecule method

In this model the $E(Q)$ appearing in $Z(T_1,q_2)$ (equation (iv) is approximated by

$$E(Q) \simeq E(T_1,q_2) + E_{solvent} \qquad \text{(x)}$$

The method is easily extended to an entire solvation shell of n solvent molecules leading to a reduced partition defined by

$$Z = \int_{T_1}\int_{q_2}\cdots\int_{q_{n+1}} Z(T_1,q_2,\ldots,q_{n+1})\, dT_1 dq_2 \ldots dq_{n+1} \qquad \text{(xi)}$$

with $E(Q) = E(q_1,q_2,\ldots,q_{n+1},\ldots,q_N) \simeq E(T_1,q_2,\ldots,q_{n+1}) + E_{solvent}$

The supermolecule method of Pullman and Pullman (1975) follows by the evaluation of $E(T_1,q_2,\ldots,q_{n+1})$ by the PCILO method, ie PCILO calculations are made on the free-space ensemble (for GABA)

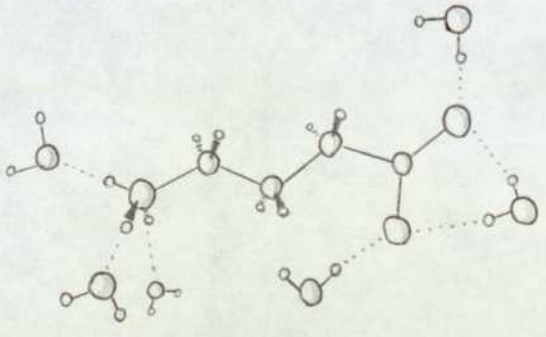

It should be noted that molecules of the 1st hydration shell only are presently considered, thus a possible extension is to explicitly consider hydration shells beyond the 1st. An obvious alternative is to explicitly consider the 1st hydration shell and then use the continuum method to account for subsequent shells in a hybrid continuum-supermolecule scheme.

It is now intended to move from the theory of continuum and supermolecule method to their practical application with molecules of the GABA and GLU systems.

4.2 The continuum method applied to β-alanine

4.2.1 The free-space results for βA

The free-space CNDO/2 calculations for βA have been referred to in 3.5.2 and 3.5.3. The minimum-energy conformation (G) occurs at ($T_1 = 140^\circ$, $T_2 = 30^\circ$, $T_3 = -10^\circ$), with x_T = ca. 3.0Å: this is depicted below. The torsion angles T_{1-3} are defined in 3.5.2, and a typical T_1 - T_2 energy surface is Fig.4.1.

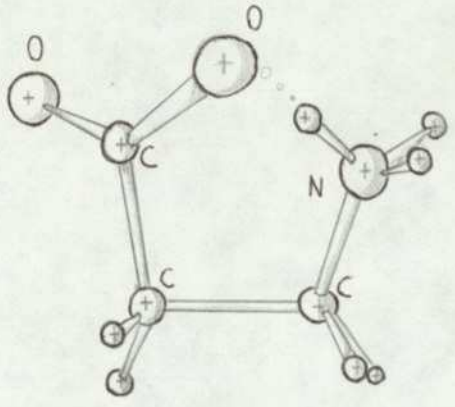

β-alanine at its free-space minimum energy conformation.

Apart from the highly localised global minimum (G), there is a secondary minimum (E) corresponding to a fully-trans conformation. The minimum E is effectively unpopulated being ca. 60 kcal mol^{-1} above G.

The x_T at G is less than that of glycine and therefore incompatible with GABA agonism as noted in 4.1.1.

4.2.2 The continuum solvent results: βA

The continuum method has been applied to the βA zwitterion. Four T_1 - T_2 energy surfaces have been calculated for the solvated molecule using the procedures of both Beveridge and Clarke (as outlined in 4.1.2), for both $T_3 = 0^\circ$ and $T_3 = 60^\circ$. In both approaches the 'best' energy occurs on the $T_3 = 60^\circ$ ($-NH_3^+$ configuration 'staggered') surfaces. The T_1- T_2 surfaces ($T_3 = 60^\circ$) calculated using Onsager theory (Beveridge) are shown in Fig.4.2 and Buckingham theory (Clarke) in Fig.4.3.

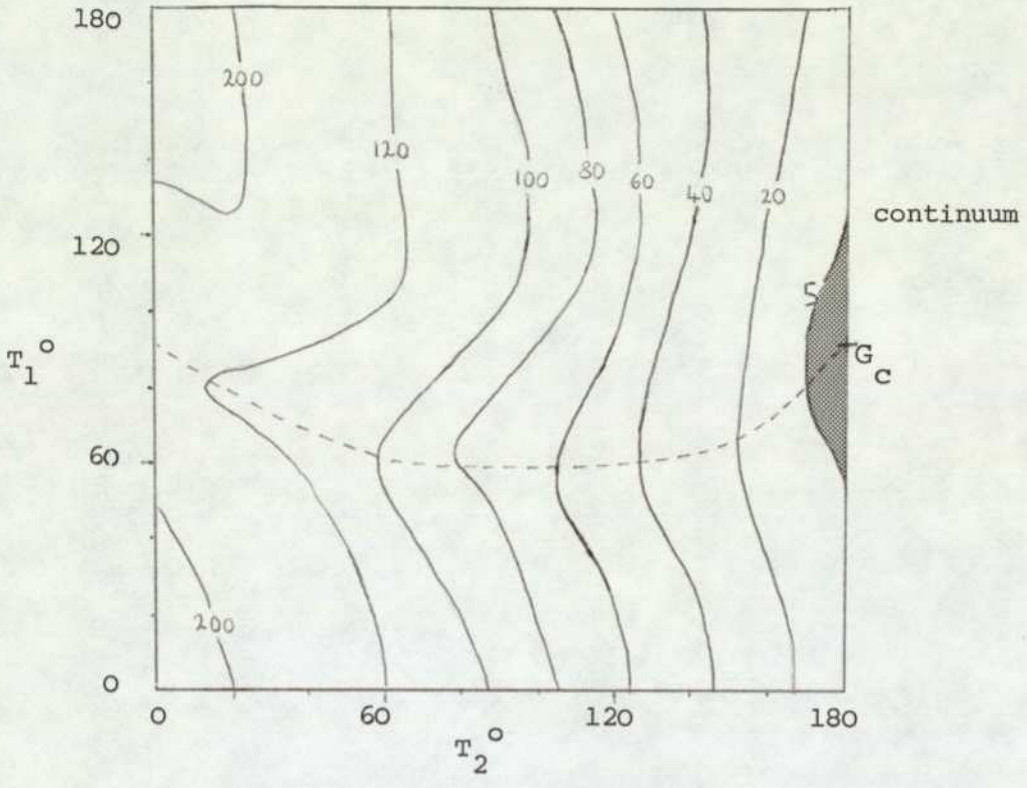

Fig. 4.2 T_1-T_2 energy-surface (T_3=60°) for βA in aqueous solution (according to Beveridge method). Global minimum (G_c) is marked +, dotted line shows path of minimum as a function of T_2. The contours are labeled in kcal mol^{-1} relative to G_c.

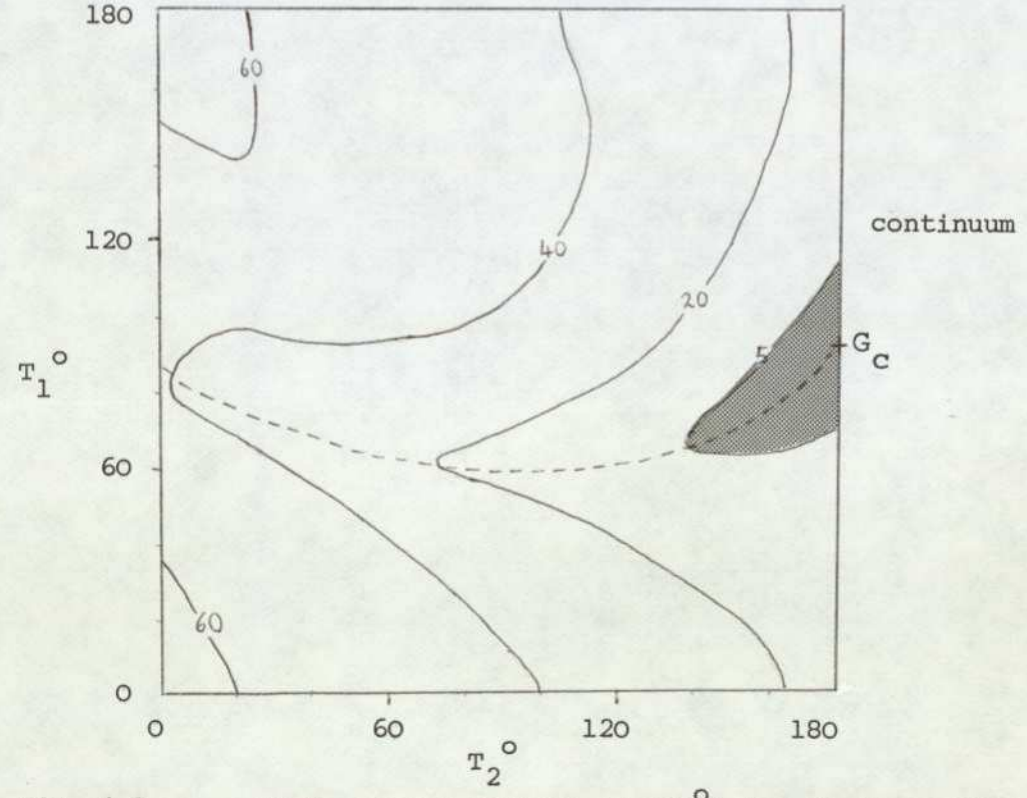

Fig. 4.3 T_1-T_2 energy-surface (T_3=60°) for βA in aqueous solution (according to Clarke method). For other details see caption to Fig. 4.2.

4.2.3 Discussion of results: the 2 continuum models for βA

The results are in good qualitative agreement, in that

(i) The minimum (G_c) is predicted to be at ($T_1 = 90^o$, $T_2 = 180^o$) with $T_3 = 60^o$ (rather than $T_3 = 0^o$), ie at the secondary minimum E of the free-space calculations.

(ii) A greater number of conformational modes are available in solution to the molecule than in free-space - this is evident from a comparison of the 5 kcal mol^{-1} contours.

(iii) The more extended conformations are favoured in solution.

It is noted, however, that the energy gradient as one moves across the energy surfaces from $T_2 = 180^o$ to $T_2 = 0^o$ ($T_3 = 60^o$) is far greater in the case of the Beveridge method (ca. 200 kcal mol^{-1} compared to ca. 60 kcal mol^{-1}). Since the major contributing factor to the solvated-molecule energy is the E_{es} term, and Clarke's method is theoretically more suitable for evaluating E_{es} for polar molecules, it is expected that this method yields the more realistic energy gradient.

The solvent-effect minimum-energy conformation of the βA zwitterion is shown below.

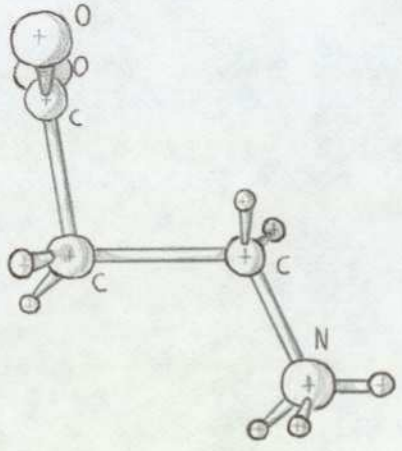

β-alanine in its continuum solvent minimum-energy conformer.

In this conformation x_T = ca. 4.7Å, a distance expected to be compatible with GABA agonism (Steward & Clarke, 1975). Hence, with free-space calculations one would conclude that both GABA and βA have x_T-values too small for the molecules to act at GABA receptors. It is only when a continuum solvent effect is introduced into the calculations that x_T-values leading to the correct deduction is possible viz both molecules can interact with the GABA receptor.

It has been pointed out (Pullman & Pullman, 1975) that a weakness of the continuum methods is their inability to predict conformations which may be stabilised by a bridging water molecule. For example, empirical calculations showed (Lipkind, Arkhipova & Popov, 1970) that a seven-membered ring occurring in dipeptides (called 'C_7-form') was stabilised by an intramolecular hydrogen bond, as predicted by experimental studies in inert solvents (Cung, Marrang & Neel, 1973). When a continuum allowance was made in the empirical calculations for the presence of a polar solvent the C_7-form was no longer a stable conformation. This is, however, contrary to experimental evidence (depolarised Rayleigh scattering and laser Raman spectroscopy)(Avignon, Garrigou-Lagrange & Bothorel, 1973) which shows that water further stabilises the ring structure by a bridging H_2O molecule thus

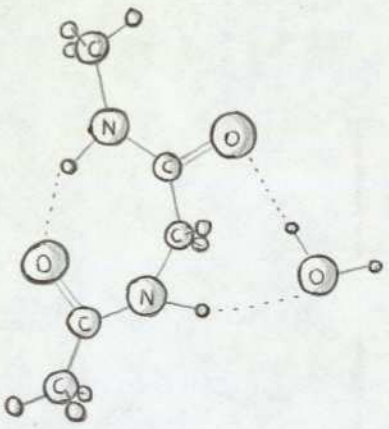

Such a deduction is naturally beyond the scope of the continuum approach. Since we must concede that a situation such as discussed above can occur for βA (eg the conformer (90°, 120°, 60°) may be stabilised by a bridging H_2O molecule), there may be stable conformers other than those predicted by the continuum calculations.

4.3 The supermolecule method applied to βA

4.3.1 The solvation scheme for α-w amino carboxylic acids

In the supermolecule approach, it is necessary to know the sites on the solute molecule at which water molecules will bind. The solvation sites of the $-COO^-$ and $-NH_3^+$ groups is now discussed.

(a) Solvation of the $-COO^-$ group

The solvation of the $-COO^-$ group has been based on an *ab initio* study (Port & Pullman, 1974), in an STO-3G basis, of the formate ion. This study shows a preference for 3 water molecules lying in the plane of the $-COO^-$ group as shown below

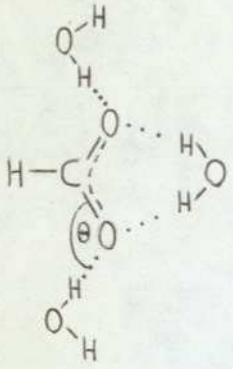

$\theta = 110^\circ$

$O^-...H\text{-}O = 2.65$ Å

This scheme was used for a study of GABA by Pullman & Berthod (1975) in which an optimisation of θ was made. It was found that in the presence of the more sterically bulky methylene instead of the hydrogen caused θ to increase to 150°. We have assumed the solvation scheme used for GABA in our study of βA.

Our EP results for the $-COO^-$ group (3.7.3) predicted minima at (calculation made on asymmetric conformation of GABA)

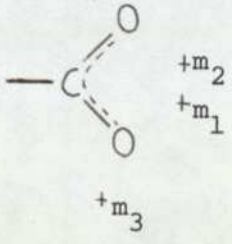

In a symmetric situation (eg formate ion), it is expected that the EP field would have minima

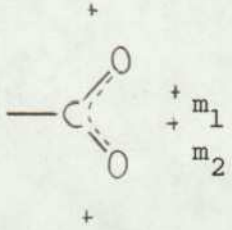

particularly if the hydrogen-bonds associated with the minima are weak (eg hydration bonds). The hydration scheme found by the ab initio study is thus not inconsistent with the character of the electrostatic field. Since the EP minima m_1 and m_2 are global, bridging water molecule should be the preferred one - this is as found by the ab initio calculations (Port & Pullman, 1974). The hydrogen-bond distance of 2.65Å is perhaps rather short compared with hydration bonds found in crystal structures, but such comparisons between crystalline and aqueous phases are not necessarily valid.

(b) Solvation of the $-NH_3^+$ group

This has been based on an ab initio study (Port & Pullman, 1974), in an STO-3G basis, of the ethylammonium ion. This study shows a preference for 3 water molecules lying along the N^+-H bonds, with an N^+-H...O distance of 2.60Å. It was found that tilting the water molecule so as to direct an oxygen lone-pair into the line of the bond does not improve the energy (similar conclusions with respect to lone-pairs have been made for O...O hydrogen bonds (Kroon, Kanters, Van Duijneveldt-Van de Rijdt, Van Duijneveldt & Vliegenthart, 1975)). It was also found that the rotation of the water molecule about the hydrogen-bond axis had no effect on the energy. The formation of 3 hydrogen bonds by ammonium groups is in agreement with the interpretation of their NMR spectra as given by Fraenkel & Kim (1966).

The results of (a) and (b) were used by Pullman and Berthod in their supermolecule study (1975) of GABA, leading to a solvation scheme of 6 water molecules. A fortuitous property of this solvation scheme is that the axial symmetry of the $-COO^-$ and $-NH_3^+$ groups is preserved, thus eg the symmetry of the T_1 rotation of βA is also preserved reducing the number of required conformations.

With reference to the GABA supermolecule study, the solvation scheme was based on ab initio calculations in which the $-COO^-$ group is treated as a true resonance 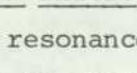 , this is also true of CNDO. However, in the PCILO calculations the $-COO^-$ group must be represented as 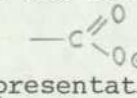 , and so they may be criticised since their $-COO^-$ representation and solvation scheme are not compatible: this is not true of the CNDO/2 calculations.

It is noted that the supermolecule method will predict the situation

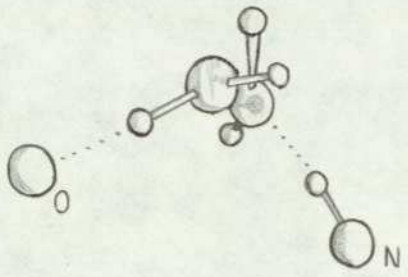

as highly unstable, whereas in solution what may well occur is

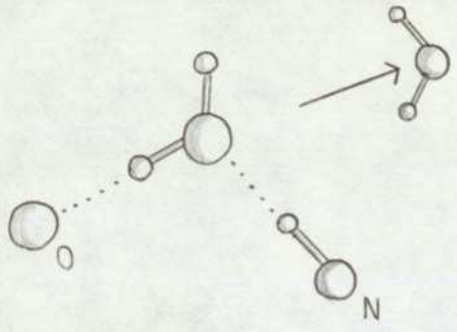

It is possible to stabilise the conformation (90°, 120°, 60°) in this way for βA

producing a stabilised conformation! Hence, it is apparent in the GABA and GLU systems where flexible molecules are involved, positional reorganisation of the water molecules may be expected and the choice of solvation sites is thus a function of solute conformation. However, in the present supermolecule approach the solvation sites and solvent orientations are considered to be conformational invariants. Unfortunately, the supermolecule method is already too demanding with respect to computer time, and an optimisation of the energy with respect to the number and position of solvation sites would not be practicable. It is felt that this is a serious defect in the method as applied to flexible molecules.

4.3.2 The results for βA supermolecule

Free-space MO calculations were carried out on the βA supermolecule as described in 4.3.1. The torsion angles describing the conformer are as for the βA zwitterion (3.5.2). Feasibility studies on the supermolecule indicated that the calculation of only one T_1 - T_2 energy surface was practicable because of the great demand this method places on computer resources. Since both the continuum method for βA (4.2.2) and the supermolecule method applied to GABA (Pullman & Berthod, 1975) implied that the $-NH_3^+$ group adopted

a staggered conformation with respect to the adjacent methylene, a T_1 - T_2 energy surface on a 30° grid for $T_3 = 60^\circ$ has been calculated (Fig.4.4). It has been observed that the solvation scheme employed preserves the molecular symmetry, hence as in previous calculations on βA only a quadrant of the energy surface has been calculated. The symmetry relations for generating the whole surface are given in 3.5.2.

4.3.3 Discussion of results: βA supermolecule

The supermolecule method applied to βA gives an energy surface (Fig.4.4) showing 3 minima. The global minimum (G_s) ($T_1 = 150^\circ$, $T_2 = 30^\circ$) is highly localised, a secondary minimum (S_s) ($T_1 = 90^\circ$, $T_2 = 30^\circ$) is only ca. 3kcal mol^{-1} less stable than G_s. A relatively flat minimum (E_s) also occurs in the fully-extended conformation ($T_1 = 0^\circ$, $T_2 = 180^\circ$), but this is ca. 18 kcal mol^{-1} less stable than G_s.

The global minimum G_s is close to the free-space global minimum G ($T_1 = 140^\circ$, $T_2 = 30^\circ$), and the extended-conformer minimum E_s differs only from the free-space minimum E ($T_1 = 90^\circ$, $T_2 = 180^\circ$) by a rotation of 90° in the carboxylate group. The x_T at G_s is again incompatible with the range of x_T thought necessary (4.1.1) for action at GABA receptors.

It is possible, via the NAPs, to understand how the different supermolecule conformations are stabilised or otherwise. Destabilisations can be traced to steric repulsions between a water molecule bound to the cationic head and one bound to the anionic head. On the other hand the minima G_s,S_s (Fig.4.4) are due to favourable hydrogen bonding orientations of two water molecules. The minima E_s (Fig.4.4) does not coincide with any interactions between water molecules and is presumably due to the same factors that lead to the free-space minimum E. Thus it is concluded that the detail of Fig.4.4 is due primarily to the disposition of solvent molecules, making energy optimisation with respect to elements of the first hydration shell important (see 4.3.1).

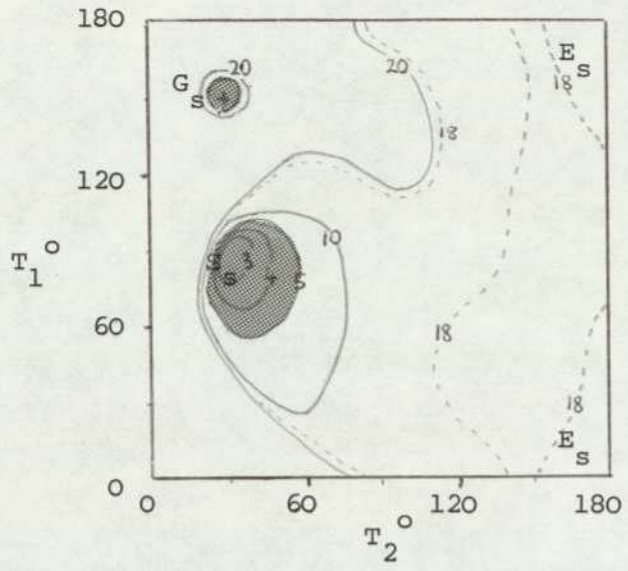

Fig. 4.4. T_1-T_2 energy-surface (T_3=60°) for βA in aqueous solution (calculated according to Pullman scheme). G_s is the global minimum (marked +), S_s is a secondary minimum and E_s is a region of minimum energy occuring for fully extended conformers. Contours in kcal mol^{-1} relative to G_s.

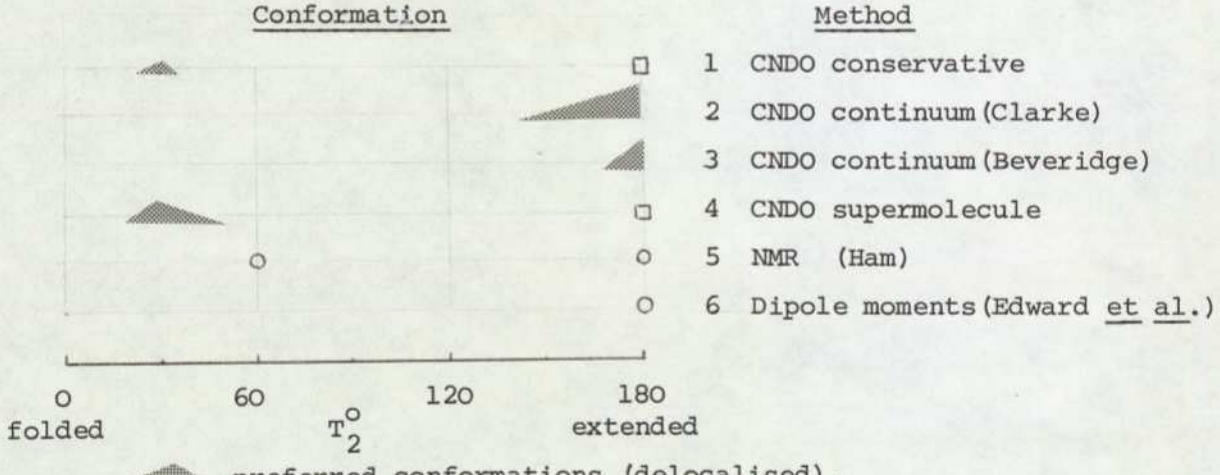

-preferred conformations (delocalised).

o -preferred conformations (localised).

□ -other minimum (>5 kcal mol^{-1} above preferred conformer).

Fig. 4.5 Summary of conformational predictions made for the βA zwitterion by various methods.

4.4 Conclusions on the theoretical solvent approaches

4.4.1 Comparison of results of conformational studies on βA in solution

The conformational predictions of the various studies are summarised in Fig.4.5. The theoretical predictions have been discussed at some length already. The supermolecule results parallel those of the conservative molecule, giving increased weighting to the $T_2 = 30^{\circ}$ conformer. Note that methods 2-4 predict an increased number of conformations accessible to the molecule in solution. All theoretical methods 1-4 suggest that the fully-extended molecule is stabilised at least to some degree.

The NMR measurements are as usual open to criticism on the basis of their interpretation. The only conformers allowed in the analysis were $T_2 = \pm 60^{\circ}$ and $T_1 = 180^{\circ}$, and it is therefore no surprise that these were the conformations found! In method 6, a self-consistency argument was used assuming two cases (i) freely-rotating and (ii) fully-extended molecules. It was found that the best interpretation of the results was for a fully-extended molecule. The empirical methods do not predict a spectrum of conformers in solution, but again they confirm the stabilisation of the fully-extended molecule.

4.4.2 Review of theoretical solvent predictions in relation to GABA receptor activity

On an x_T .v. log (relative potency) plot (Fig.4.6), it is possible to mark the positions of two GABA analogues with fixed x_T viz MM and gly. In addition the x_T ranges of two semi-rigid analogues viz. cis, trans-4-aminocrotonic acids (4-ACA) can be drawn. (The log (rel.potency) values have, where possible, been taken from Steward & Clarke (1975), additionally for cis,trans-4-ACA potencies of ca. 0.25 and 1.0 times GABAs have been used (Beart, 1975).) A straight line joining the points representing MM and gly is consistent with x_T and potency ranges for cis, trans-4-ACA. It must be emphasised that a straight line has been drawn for simplification and is used merely to indicate a trend existing on the diagram.

It is now possible to superimpose on to the plane points representing βA and GABA for x_Ts calculated by (1) CNDO/2 free-space, (2) continuum (Buckingham), (3) continuum (Onsager) and (4) supermolecule methods. It is evident that approaches (1) and

(4) produce x_T .v. log (rel. potency) lines of incorrect slope, whereas lines drawn for (2) and (3) have slopes consistent with that of the deduced trend based on the rigid and semi-rigid analogues of GABA. Additionally it is noted from Fig.4.6 that the continuum (Onsager) method (3) is not entirely consistent with the x_T range of trans-4-ACA.

Hence, of the 4 possible theoretical approaches to constructing conformation-activity relationships (CAR) in the GABA and GLU systems, only the continuum solvent effect methods offer any real hope of success. Of the two continuum methods, on present evidence, the Buckingham theory based variant is preferred for any future CAR studies on molecules of the GABA or GLU type.

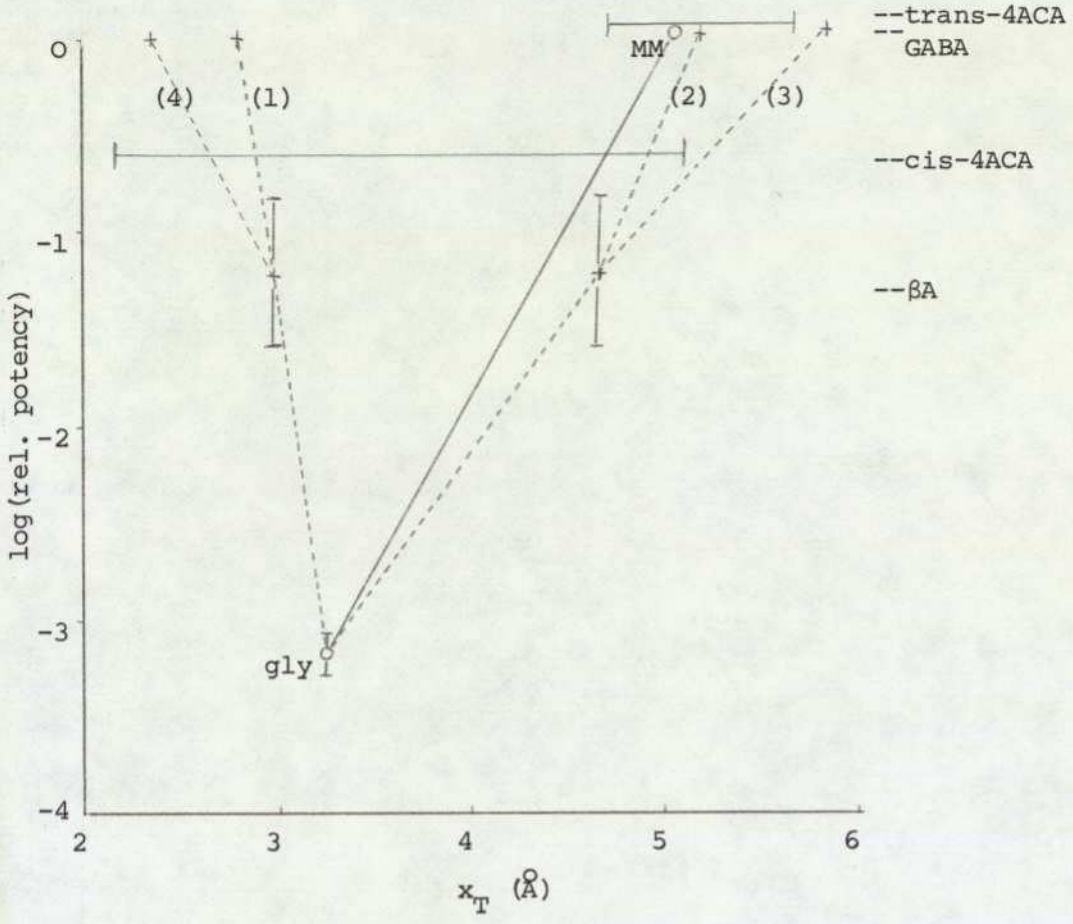

o rigid analogues

⊢—⊣ semi-rigid analogues (range of x_T indicated).

\+ flexible analogues (x_T at preferred conformation).

Fig. 4.6 Log(rel. potency) .v. x_T plots calculated by different theoretical schemes for some GABA agonists. Methods are (1) conservative molecule, (2) continuum (Buckingham), (3) continuum (Onsager) and (4) supermolecule.

molecule	energy (kcal mol^{-1})
supermolecule (E_S)	-121816
βA zwitterion ($E_{\beta A}$)	-46994
water (E_W)	-12458

Table 4.1

CNDO/2 energies of βA supermolecule, βA and water.

4.5 Electronic effects associated with the solvation process

4.5.1 Introduction

The construction of the supermolecule allows a detailed study to be made of the changes in electronic distribution that occur on solvation of the solute molecule. Of particular interest are the effects hydration has in perhaps masking or perhaps repeating the drug molecule features required for recognition by the receptor. Electronic parameters have been calculated for water, βA and the βA-supermolecule, the two latter molecules being considered only in the fully-extended conformation. Thus this study does not involve conformational changes and it is noted that (a) the apparent unsuitability of the supermolecule method to conformational studies of GABA-type zwitterions does not necessarily preclude its use in understanding electronic effects and, (b) the cooperative effects between solvent molecules have been minimised.

The electron distribution of hydrogen bonds has been considered before, eg for (i) dimers of formamide (Pullman & Berthod, 1968), (ii) water, methanol, formic acid dimers and the hydrogen maleate ion (Morita & Nagakura, 1972) and (iii) NH...O bonds in systems including ammonia, ammonium, imidazole, and glycine as proton donors and formic acid, formate ion, and glycine as acceptors (Singh & Ferro, 1974). However, the bonding of water to a zwitterion has not to my knowledge been studied. Pullman in his various supermolecule studies has certainly not attempted discussion of electronic aspects presumably due to shortcomings in the PCILO density matrix (Appendix B .).The previous studies (i)-(iii) were all performed using CNDO/2, which is the method used here. It is probably true to say that CNDO/2 predicts hydrogen bonds which are too short (3.5.3), however when the method is used in conjunction with more realistic bond-lengths (as in this section, ie ab initio calculated ones) the predicted energies are in good agreement with experiment (Pullman & Berthod, 1968).

4.5.2 Water, βA and the βA-supermolecule: NAP and BI values

In order to understand the changes of electronic distribution which occur on solvation of βA to the βA supermolecule it is first necessary to consider the conservative H_2O and βA molecules.

(a) The conservative water molecule

CNDO/2 calculations made (here) on a water molecule using the experimentally determined angle (Dressler & Ramsay, 1959) and a

standard bond-length (Pople & Beveridge, 1970) give a NAP and BI distribution

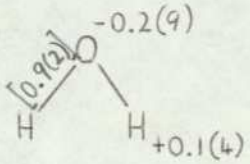

(b) The conservative βA molecule

CNDO/2 calculations made on the βA zwitterion, using standard geometries with the exception of those for the $-COO^-$ group (3.4.2), give a NAP and BI distribution

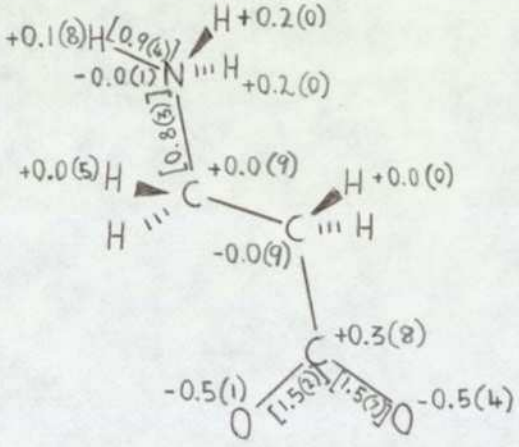

The total charge on the $-COO^-$ group is -0.6(7), and on the $-NH_3^+$ group +0.5(7). The NAP and BI values for βA are as established in Chapter 3.

(c) The solvated βA zwitterion

CNDO/2 calculations on the βA-supermolecule (as described in 4.3.1) gave NAP and BI values

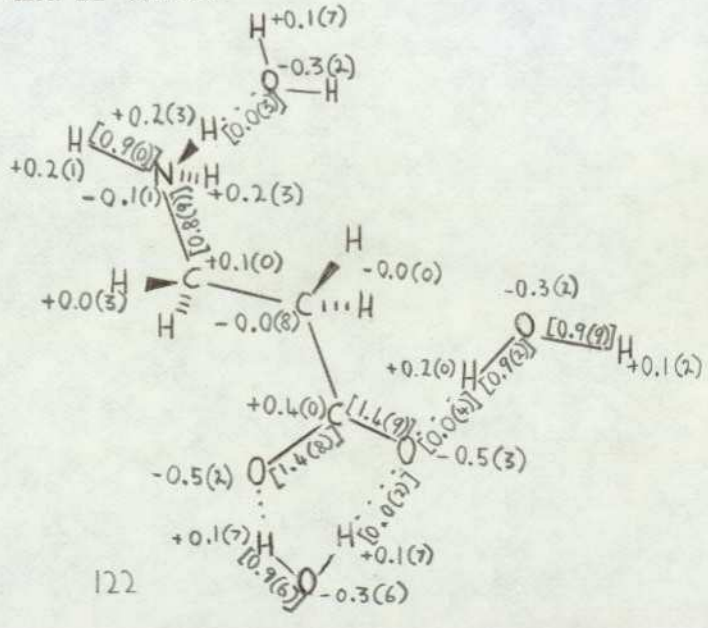

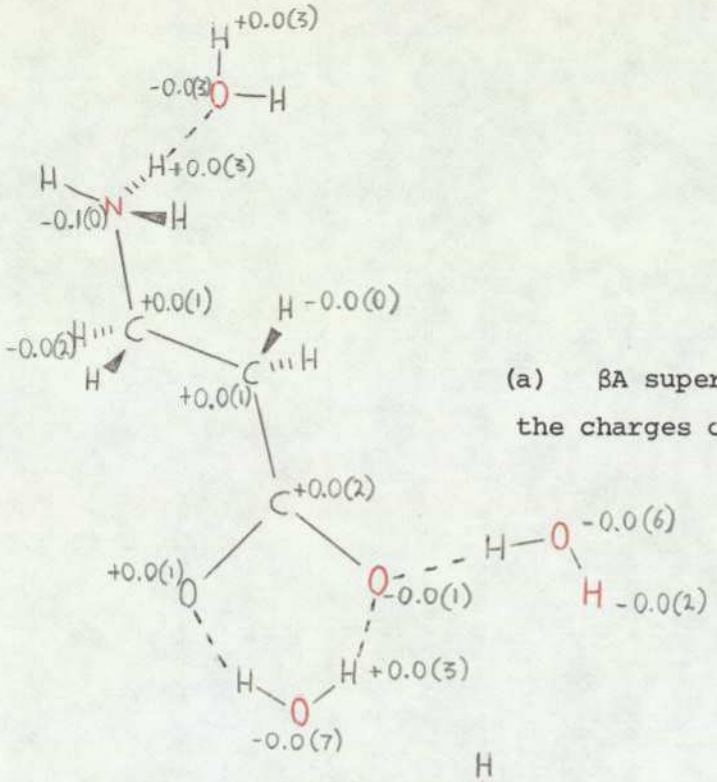

(a) βA supermolecule charges minus the charges of its component molecules.

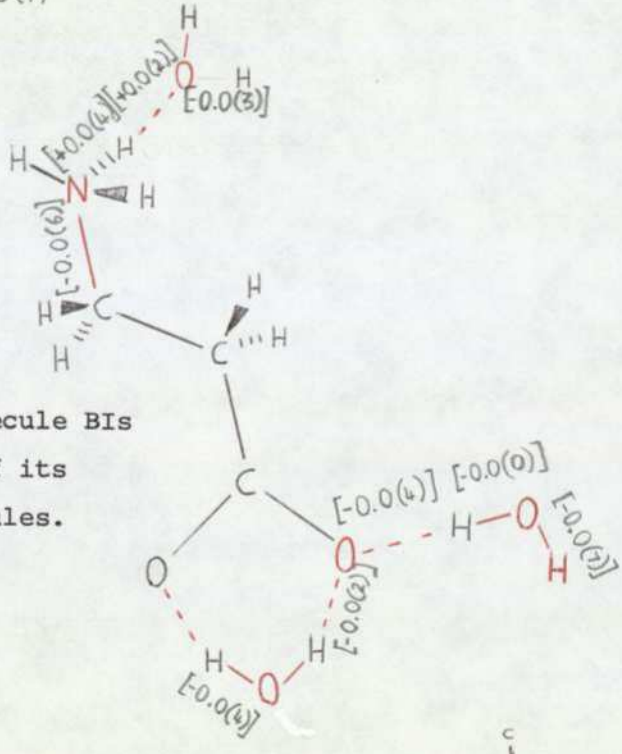

(b) βA supermolecule BIs minus the BIs of its component molecules.

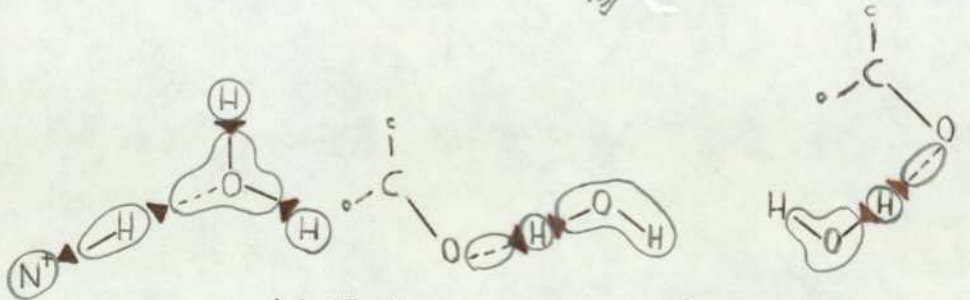

(c) Electron movement in the formation of hydration bonds.

Fig. 4.7 Changes in electron distribution which occur on the solvation of βA zwitterion.

The total charge on the $-COO^-$ group is now -0.6(5), and on the $-NH_3^+$ group is +0.5(6). Hence, the total charge on these groups is therefore conserved on solvation. This is important since it seems to imply that the receptor will be able to identify the molecule electrostatically, even when fully solvated - this point is amplified in 4.5.4.

4.5.3 Solute-solvent hydrogen-bonding

In order to understand the formation of hydration bonds in the βA-supermolecule it is necessary to study the changes in electronic distribution which occur on solvation. Thus diagrams of NAP and BI for (supermolecule- βA molecule-water molecules) are given in Figs.4.7(a) and (b) respectively. Increased electron population is shown in red on these figures. From Figs.4.7 (a), (b) the electron movement involved in forming the hydration bonds is evident: this is shown in Fig.4.7(c) explicitly.

From Fig.4.7(c) it is seen that in hydration bonds II and III the water molecule donates its proton to the bond $O-H...O^-$, which in turn provides the electronic substance for the $H...O^-$ bond. In the case of hydration bond I the onium group donates its proton to the $N^+-H...O$ bond, and although this proton undoubtedly supplies electronic density into the H...O bond, there may again be contributions to this from the water protons. The electron donation provided by the water hydrogen-atoms is in qualitative agreement with calculations made by Morita & Nagakura (1972). The increased positive charge on a hydrogen atom when involved in a hydrogen bond was also noted in Pullman & Berthod (1968).

The (CNDO/2) energies for the βA-supermolecule and its component molecules are given in Table 4.1. The quantity $E_s-(E_{\beta A} + 6E_w)$ is identified with the energy in the hydrogen bonds of the supermolecule, E_{bond} say. From Table 4.1, E_{bond} = 74 kcal mol^{-1} which represents a total of 7 hydrogen bonds. The supermolecule method used with the CNDO/2 formalism thus gives a hydrogen-bond energy of ca. 10 kcal mol^{-1} per bond. If in the continuum method $E_{\beta A}$ is subtracted from the total solvation energy the remaining energy is that due to solvent-solute interactions. If it is assumed (i) that this solvent-solute interaction is primarily due to hydrogen bonding between the solute molecule and the 1st hydration shell, and (ii) the 1st hydration shell has the form used in the supermolecule calculations,

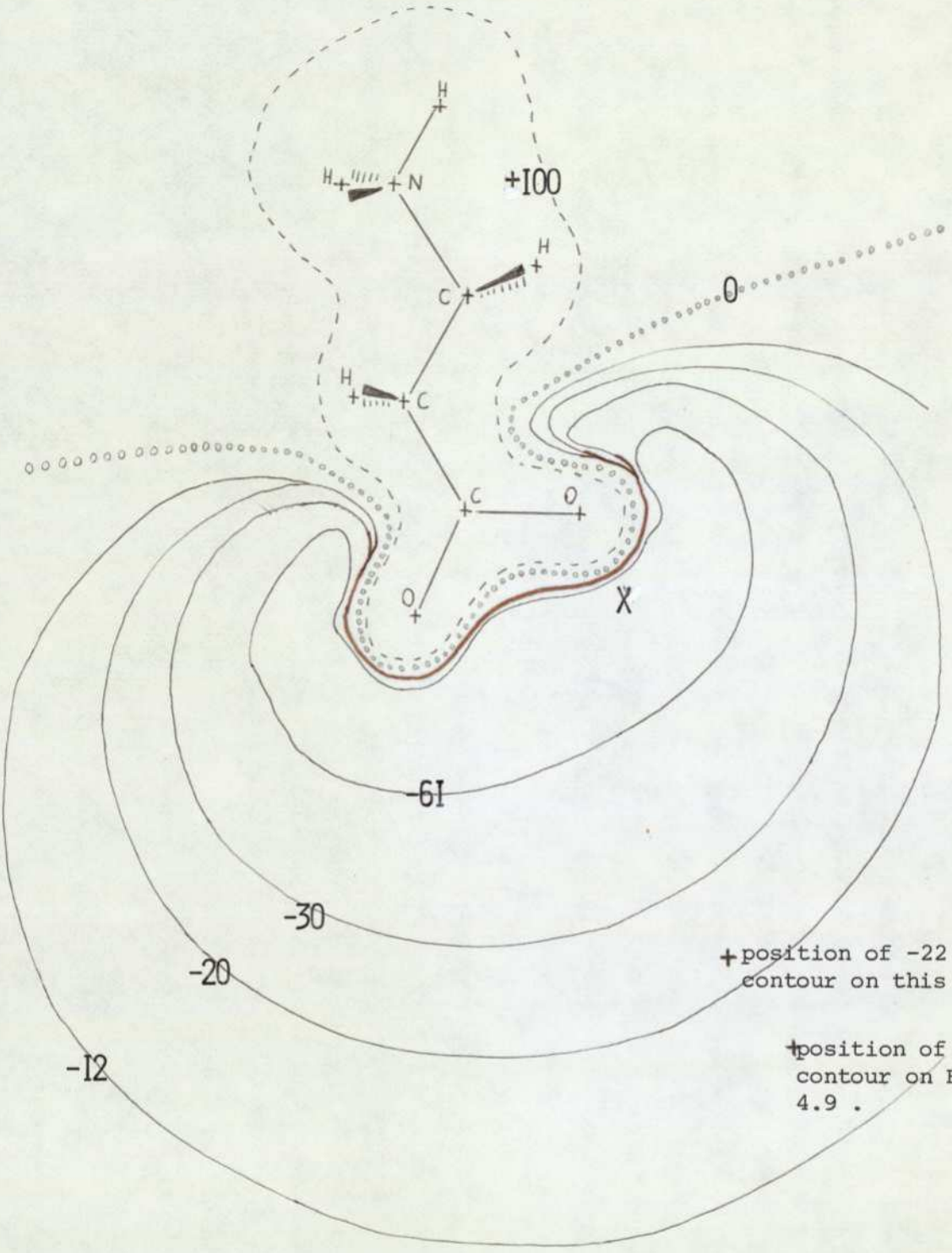

Fig. 4.8 The electrostatic-potential field associated with the βA zwitterion. The field is shown for the fully-extended molecule in the plane of the heavy atoms. The minimum energy of the field is -121 kcal mol^{-1} (X) and the contours are labeled in kcal mol^{-1}.

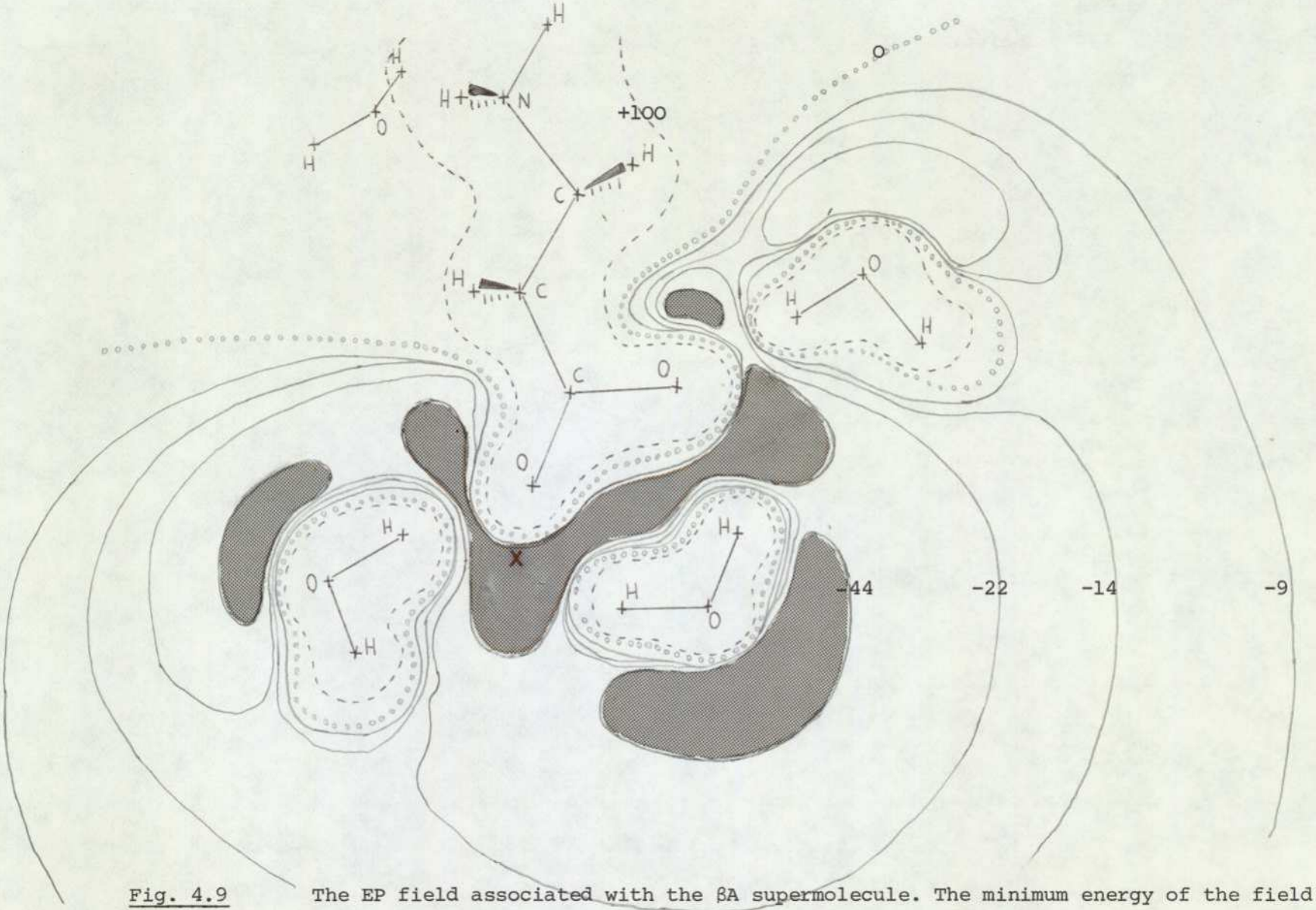

Fig. 4.9 The EP field associated with the βA supermolecule. The minimum energy of the field occurs at X and has the value -87 kcal mol^{-1}. (All other details of this map are as for Fig. 4.8).

then energy values of ca. 4 and ca. 33 kcal mol^{-1} per hydrogen bond are obtained for the Buckingham and Onsager approaches respectively. The value of 4 kcal mol^{-1} obtained from the Buckingham continuum approach is in excellent quantitative agreement with the usually accepted range of 2-5 kcal mol^{-1} per bond (Barker, 1971). This result supports the claim that the Buckingham method is superior to that of Onsager for polar molecules of the GABA type (Clarke 1976).

4.5.4 A comment on dipole moments: βA

In the free-space calculations (3.8.2) it was shown that our definition of charge centres on the functional groups led to an x_T which was correlated with the theoretical dipole-moment direction $\vec{\mu}$. If Pullmans' hydration scheme for αω-amino carboxylic acids is assumed, then as it has been observed that the symmetry of the $-NH_3^+$ and $-COO^-$ groups is preserved, and $\vec{x}_T$ is still correlated with $\vec{\mu}$ in solution (assuming anisotropy introduced by water molecules in the 2, 3, etc. hydration shells is negligible).

The experimental determination of dipole moments is typically made by using measurements of the dielectric increment (Edward, Farrell & Job, 1973). Deductions are then made assuming either free-rotation or full-extension of molecules in solution. Owing to differences in measured values and in the interpretation of those values, a range of dipole moments 14.6 - 22.2 D exists in the literature (Edward et al, 1973, 1974; Buckingham, 1953; Kirkwood, 1939). The CNDO/2 MO values are in the ranges 9.8 - 19.0 D (conservative zwitterion) and 14.1 - 22.1 D (supermolecule). The experimental results are not in mutual accord, and evaluation of theoretical schemes against them is difficult. The theoretical supermolecule results do seem to be more consistent with the experimental results than those of conservative molecule, however.

4.5.5 Charge distribution in the hydration shells

Since the necessary data were readily available, EP maps for the βA zwitterion (Fig.4.8) and the βA supermolecule (Fig.4.9) have been computed as a possible means of furthering understanding of the hydration process. The near equivalence of the -22 and -20 kcal mol^{-1} contours in the solvated and conservative molecule maps respectively, provide a useful reference contour. Hence, it is seen that the 1st solvation shell of the molecule tends to enhance the EP field of the transmitter, enabling more efficient recognition by electrostatic receptor sites. In the remainder of this subsection reasons for this enhancement and the propagation of such effects

beyond the 1st hydration shell are sought. The apparent lack of charge buffering by the 1st hydration shell may explain (and is certainly consistent with) some of the similarities of free-space and supermolecule results for the βA molecule (eg the global minima in Figs. 4.1 and 4.4).

A clue to the mechanism of the enhancement is given by the changes that occur to a water molecule subsequent to its hydrogen bonding, ie

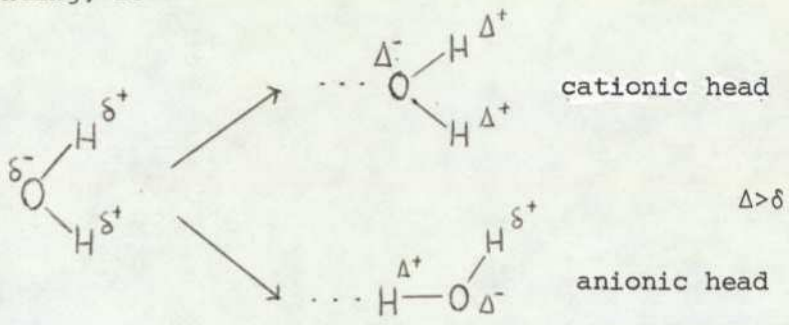

It is this process which provides a 'transmission' of the zwitterion charges by the 1st hydration shell. The processes are explicitly stated below

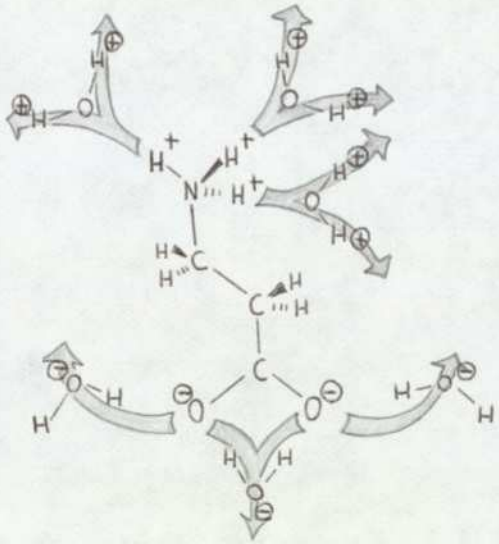

It is now of interest to speculate how the above charge distribution may be affected by subsequent hydration shells. At the cationic head only the following situation is possible

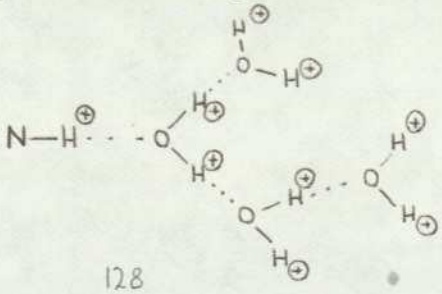

resulting in a positive charge being directed outwards from all points of the water structure periphery. Calculations on dimeric water (Morita & Nagakura, 1972) show that the charge changes (Fig.4.10) which occur in water-water bonding will be such as to tend to amplify the +ve charge from the 1st hydration-shell cationic-head water molecules. Hence, at the cationic head the water structure provides a 'transmission with amplification' effect of the basic $-NH_3^+$ positive charge. Clearly, this effect cannot go on for ever, and a situation is expected in which the water protons are soon so electron deficient that they can no longer supply electronic substance (see Fig.4.7(c)) for the hydrogen bond to the next water molecule, and the water 'structuring' breaks down.

At the anionic head, on the present model, if the charge flow from Fig.4.10 is assumed, the following situation is expected to occur

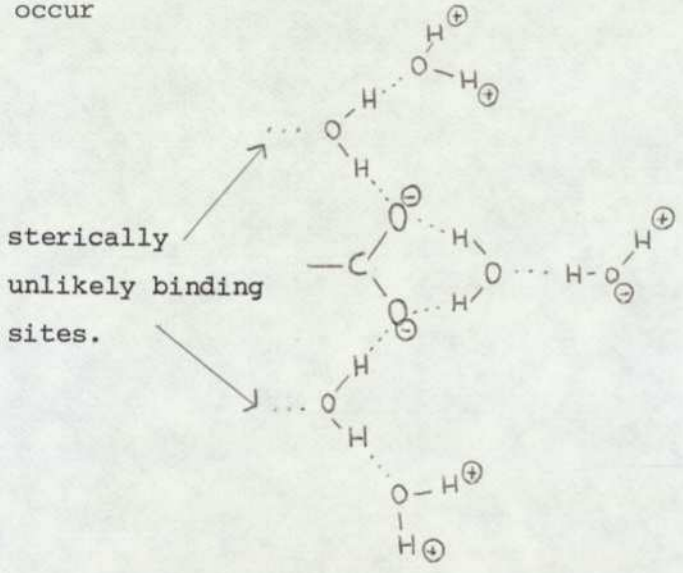

It is noted from the above diagram that a second hydration shell produces positive sites in the ratio of 5:1 over negative sites. Each positive site then produces only positive sites (two of them) in the next hydration shell, whereas each negative site produces one positive and one negative site. Hence, the overall trend is increasingly towards a positive scenario

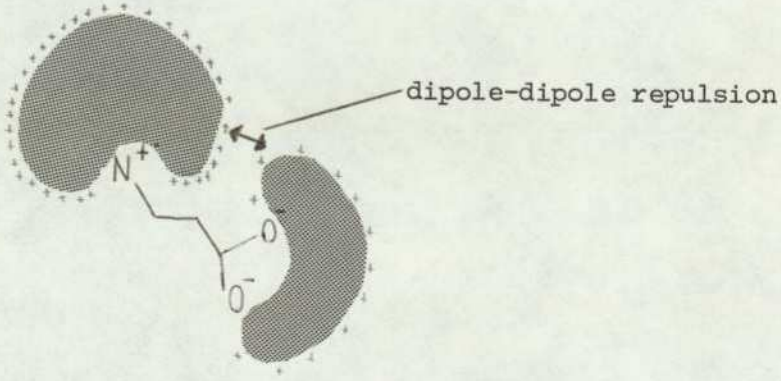

If the above situation does occur then the indicated dipole-dipole repulsion could be a factor in the observed trend for more extended conformations to occur in water.

4.6 Summary and direction of future work in the study of solvent effects

4.6.1 Summary

A study of the two basic methods of including solvent effects (viz supermolecule and continuum) in theoretical calculations of conformation has been made. In order to produce CARs in the GABA system it has been found essential to incorporate the solvent effect into the conservative molecule calculation. The most suitable method was found to be the continuum method as modified for GABA-type molecules by Clarke (1976) based on work by Buckingham (1953). The utility of the supermolecule method in describing the conformational modes of βA is doubtful.

However, the supermolecule may be a useful construction for studying the electronic mechanisms associated with hydration (ie when used in a single-conformation calculation). The hydrogen bonds formed by hydration and their effects on the electron distribution have been looked at in some detail.

It should be realised that both continuum and supermolecule approaches are to be regarded as steps along the way towards an understanding of the solvation process, neither method in its present form represents a satisfactory final theory. It is probably safest to assume that the present methods show the trend that occurs with the solvent effect rather than the fine detail.

4.6.2 Direction of future work

Apart from the methods of accounting for a solvent medium studied in this chapter, several other approaches have been put forward. Among these are techniques for the optimisation of the hydration shell with respect to the number and position of solvation sites, and one such method (Weintraub & Hopfinger, 1974) has been used to determine the conformational modes of acetylcholine in solution. Another idea (Abraham & Birch, 1975) is the use of a 'counter-ion' to (artificially) simulate the electronic buffering effect of the solvent. Used with CNDO/2 it was shown that results paralleling those of a PCILO-supermolecule study could be obtained for the case of the histamine mono- and di- cations. However, we have seen (4.5.2 and 4.5.4) that the supermolecule (1st) hydration shell does not have a buffering effect on the $-NH_3^+$ charges, and

the conformational scenario predicted by the supermolecule seems highly dependent on the mutual steric interactions of the solvent molecule - an effect the counter-ion cannot be expected to reproduce. The latter points place doubts on the validity of the 'counter-ion' method. A full assessment must, however, wait until further results are available.

The possibility of hybrid supermolecule-continuum schemes is also under consideration (Pullman & Pullman, 1975; Beveridge et al, 1974). This idea is an obvious one, to use a supermolecule model for the 1st hydration shell and then to treat subsequent shells as a continuum. However, this method still retains most of the shortcomings inherent in the supermolecule approach (viz optimisation of number and position of solvation sites). Until the supermolecule approach itself is made generally viable there seems little to be gained in building other methods on this shaky foundation.

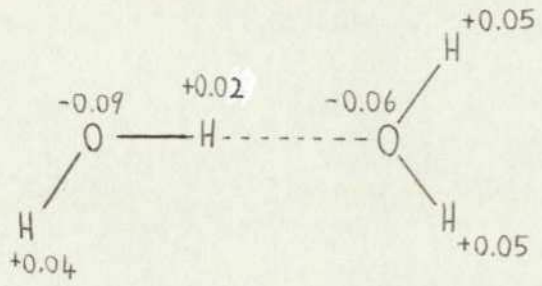

net change: -0.04 +0.04

net charge flow: → +ve

← -ve

Fig. 4.10 Change in charges which occur on dimerisation of water molecules. All charges expressed in terms of unit electron charge (e).

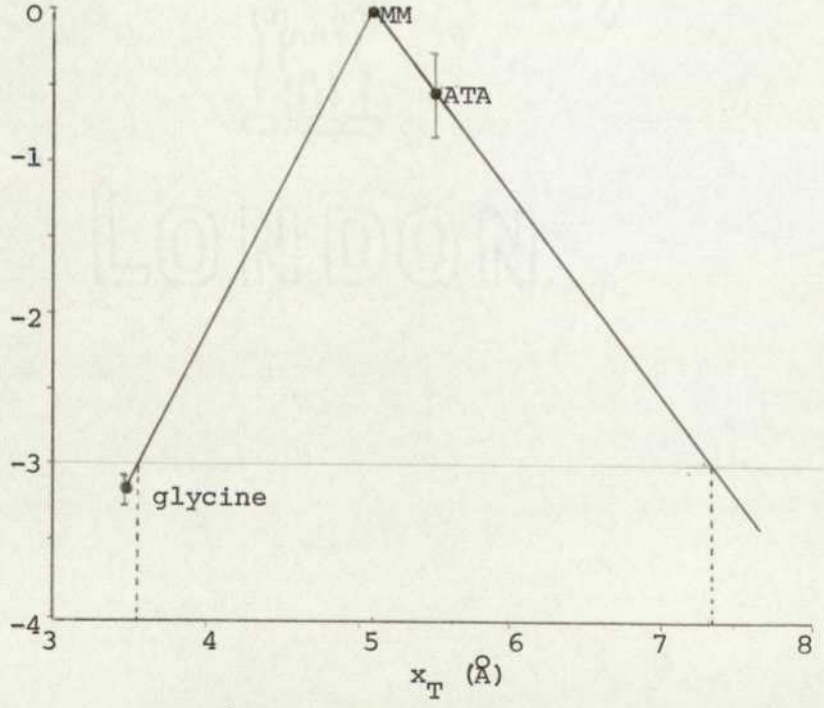

Fig. 5.0 Log(rel. potency) .v. x_T plane for the rigid GABA agonists glycine, MM and ATA. Assuming a potency of 0.001 relative to GABA is ≈inactivity, a required x_T range for GABA agonism is suggested.

5.1 Introduction

5.1.1 Preamble

GABA is generally accepted to be a naturally occurring inhibitory transmitter in the mammalian central nervous system. A number of agonists are now known, exhibiting a range of potencies relative to the canonical molecule (GABA). All are zwitterions at physiological pH and it is apparent that a schematic GABA agonist is essentially characterised by a region of negative charge ($\mathfrak{R}^-$) separated from a region of positive charge ($\mathfrak{R}^+$) by a distance (x_T). The GABA receptor logically would be expected to include two charged regions, at a separation x_R, able to interact with the charged moieties of the transmitter. The nature of the transmitter-receptor interaction is not known, although it is likely that hydrogen bonding, electrostatic and dipole-dipole type forces will be involved, and the interaction will occur for x_T such that $x_T \simeq x_R$.

5.1.2 Aims

We provisionally assume that the differing of the potencies of GABA agonists can be explained in terms of differences in their $\mathfrak{R}^+$, $\mathfrak{R}^-$, x_T or the interaction between $\mathfrak{R}^+$ and $\mathfrak{R}^-$ (which is a function of x_T), ie

$$\log(\mathfrak{P}) = c_1[\mathfrak{R}^+] + c_2[\mathfrak{R}^-] + c_3[x_T] + c_4[\mathfrak{R}^+\mathfrak{R}^-]_{x_T} + c_5 \qquad (1)$$

where [p] is the contribution to the potency ($\mathfrak{P}$) from pharmacophore≠ parameter p. (Note similarity of this equation to that of Free & Wilson (1.2.3).) Equation (1) may be simplified further, since if $x_T >$ ca 3.2Å the $-NH_3^+$ (ie $\mathfrak{R}^+$) and $-COO^-$ (ie $\mathfrak{R}^-$) groups are found to be independent of each other (3.8.4). However, for GABA agonism x_T cannot be less than ca 3.2Å because glycine is inactive at the GABA receptor. This implies as long as we are considering agonists

$$c_4 \simeq 0 \qquad (2)$$

and equation (1) becomes

$$\log(\mathfrak{P}) \simeq c_1[\mathfrak{R}^+] + c_2[\mathfrak{R}^-] + c_3[x_T] + c_5 \qquad (1)^1$$

The aim of this chapter is (i) to give a specification for the $[p_i]$ and then, (ii) to indicate how equation $(1)^1$ can be used to determine relative potencies of GABA agonists.

≠ For definition of pharmacophore and other concepts relevant to this discussion see section 1.1.

Finally, it is stressed that in many of the calculations that follow more sophisticated methods than those employed exist which may yield more accurate absolute data. The use of these more sophisticated methods was not considered necessary since (i) at each stage prior to this point we have justified the method we have chosen as being satisfactory for our needs, and (ii) whenever possible we are only concerned with relative and not absolute values. It is hoped that if any of our results are in error, because of the similarities of the molecules considered, they are all in error by about the same amount and the deductions based on differential changes are therefore valid. These latter features of the type of comparative study which follows should be kept in mind throughout.

5.2 Specifications for the GABA pharmacophore parameters $\mathfrak{R}^-$, $\mathfrak{R}^+$ and x_T

5.2.1 The $\mathfrak{R}^-$ parameter

In all the GABA agonists so far reported the negative terminal-group representing $\mathfrak{R}^-$ is either,

(i) the carboxylate group ($-COO^-$)

(ii) the $-CON^-$-moiety of the isoxazolidone ring

or (iii) the sulphonate group ($-SO_3^-$).

The NAP distributions of these groups are restated below

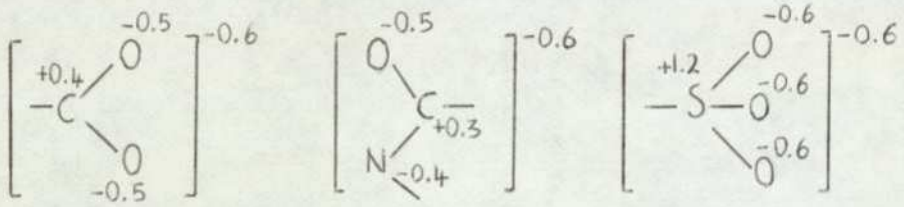

It is noted that the total charge (Σ) associated with each group is -0.6e. It is proposed that Σ is used as a criterion for specifying a necessary (but not sufficient) condition for agonism with respect to the $\mathfrak{R}^-$ pharmacophore parameter.

Working hypothesis I

The $\mathfrak{R}^-$ pharmacophore parameter for a GABA agonist is a functional group (f) such that Σ_f is ca. -0.6e.

5.2.2 The $\mathfrak{R}^+$ parameter

In all GABA agonists so far reported the positive terminal-group representing $\mathfrak{R}^+$ is either,

(i) the onium group ($-NH_3^+$)

(ii) the guanidino group ($-NH.C.(NH_2)_2^+$)

or (iii) the imidazole group

The NAP distributions of these groups are restated below

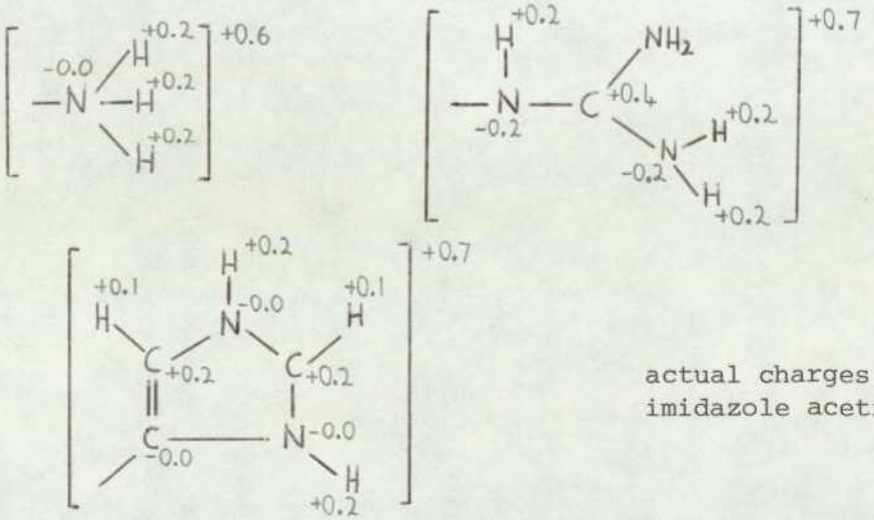

actual charges for imidazole acetic acid.

Again it is proposed that Σ can be used as a possible criterion for specifying a necessary (but not sufficient) condition for GABA agonism with respect to the $\mathfrak{R}^+$ pharmacophore parameter.

Working hypothesis II

The $\mathfrak{R}^+$ pharmacophore parameter for a GABA agonist is a functional group (f) such that Σ_f is ca. +0.6e.

5.2.3 The x_T parameter

The criteria used for specifying this parameter are x_T values taken from the rigid GABA agonists gly, MM and 4-ATA. A x_T.v. log(rel. potency) plane has been constructed in the manner of Fig. 4.6 . (The log(rel. potency) value for 4-ATA has been taken from Steward and Clarke (1975). The estimated value of x_T (=5.8Å) used by them does not agree, however, with the value of 5.55Å calculated from the more recently published crystal structure (Jones & Pauling, 1976) and which is used here.) The assumption has then been made that a potency less than 1 part in a 1000 of GABAs is synonymous with inactivity at GABA synapses. The x_T.v. log(rel. potency) plane is shown in Fig.5.0. The simple linear extrapolation from MM through 4-ATA predicts inactivity at ca. 7.3Å, in broad agreement with the datum used by Steward & Clarke (1975) that imidazoleacrylic acid (x_T = 7.0Å) is inactive. From Fig.5.0 it is possible to formulate

Working hypothesis III

The x_T pharmacophore parameter for a GABA agonist is the distance between the effective charge centres of $\mathfrak{R}^+$ and $\mathfrak{R}^-$, and for agonist activity it must lie in the range, ca. 3.5Å $\leq x_T \leq$ ca. 7.3Å.

5.2.4 Summary

It is stressed that the conditions differentiate only between agonism or non-agonism, they do not imply anything about degrees of agonism. It should also be stressed that Fig. 5.0 is only intended to represent the trend and approximate x_T limits of the x_T -log(rel. potency) relationship. Discussion of rel. potency (ie degree of agonism with respect to GABA) can only validly be made via equation (1)[1] of Section 5.1.2, which will be looked at in more detail forthwith.

5.3 The pharmacophore equation

5.3.1 Discussion

From 5.1.2 we have equation $(1)^1$ for GABA agonists

$$\log \mathcal{P} = c_1 [\mathcal{R}^+] + c_2 [\mathcal{R}^-] + c_3 [x_T] + c_5 \qquad (1)^1$$

Using this equation it is possible to write for the potency of any agonist (a) relative to GABA,

$$\log \frac{\mathcal{P}_a}{\mathcal{P}_{GABA}} = c_1([\mathcal{R}^+]_a - [\mathcal{R}^+]_{GABA}) + c_2([\mathcal{R}^-]_a - [\mathcal{R}^-]_{GABA}) + c_3([x_T]_a - [x_T]_{GABA})$$

usually $\mathcal{P}_{GABA} = 1$ and

$$\log \mathcal{P}_a = c_1 \Delta[\mathcal{R}^+]_{a\text{-}GABA} + c_2 \Delta[\mathcal{R}^-]_{a\text{-}GABA} + c_3 \Delta[x_T]_{a\text{-}GABA} \qquad (3)$$

A complete study of GABA agonism would then involve a multiple linear-regression analysis of equation (3).

Steward and Clarke in their study (1975) of conformation at GABA inhibitory synapses, have used an approach which corresponds to the assumption that $c_3 \gg$ (c_1 and c_2) and thus (3) becomes

$$\log \mathcal{P}_a \simeq c_3 \Delta[x_T]_{a\text{-}GABA} \qquad (4)$$

Equation (4) then simply states that the relative potency of an agonist is explicable in terms of its x_T. More exactly, if $[x_T]$ is identified with the log (interaction probability) parameter then (4) states that a graph of log(rel. potency) v log(rel. interaction probability) should be approximately a straight line though the origin of slope c_3 - which it is (approximately).

In a refinement of the original work Clarke (1976) has produced a self-consistent regression line for log $\mathcal{P}_a$ .v.log(rel. interaction probability). This initial line is based on gly, βA, 4-ATA and MM, hence

(i) all 4 molecules have $-NH_3^+$ groups, and $\Delta[\mathcal{R}^+]$ is rigorously zero in every case.

(ii) 3 molecules have $-COO^-$, and the 4th (muscimol) a $-CON^-$-moiety. The isoxazolidone CON^--moiety is so close a structural and electronic analogue of the carboxylate group (3.7) that $\Delta[\mathcal{R}^-] \equiv 0$.

Thus for this set of molecules, equation (3) leads to

$$\log \mathcal{P}_a = c_3 \Delta[x_T] \quad (\text{if } \mathcal{R}^+ = -NH_3^+ \text{ and } \mathcal{R}^- = -COO^-) \qquad (4)^1$$

It is not therefore surprising that compounds with $\mathcal{R}^+$ other than the $-NH_3^+$ (eg imidazole (Im)) do not fit the regression line satisfactorily. It was also found that deviations from the line occurred for branched α - w acids (eg α FG, β HG and (β-Me)- β A). The reason for the bad fit of the latter substances will become evident from the results of 5.4.(See also fig.5.4.).

The assumption leading to equation (4) and the conditions applying to equation (4)[1] (which are of course two ways of saying the same thing) permit the theoretical prediction of potencies to be made for a restricted subset of GABA agonists. It is clearly necessary, in general, not to forget the presence of c_1 and c_2 in equation (3). The importance of c_2 will become evident from the study of αFG, βHG and GABA, which follows in 5.4.

5.4 A theoretical comparative study of GABA, βHG and αFG

5.4.1 Introduction

In this section is presented an example of how all the preceding methods may be brought together to investigate the agonist properties of molecules. GABA, βHG and αFG in their physiological zwitterionic form are shown in Fig.5.1, and calculations have been made on GABA and the R-forms of βHG and αFG (see Appendix C for definition of R and S convention). The main reasons for studying these 3 molecules are that they (i) represent the canonical transmitter together with a more potent and a less potent agonist, and (ii) in the empirical energy calculations of Clarke (1976) the branched-chain analogues of GABA did not fit the scheme satisfactorily.

The comparative study takes the form of gas-phase calculations (5.4.2), which are necessary for the continuum solvent effect calculations (5.4.4), also a discussion of the EP fields of the molecules (5.4.5) is given.

5.4.2 Theoretical gas-phase study of conformation: introduction

In this study energy maxima and minima have been sought solely with respect to rotations about single bonds. Geometry optimisation of bond-lengths and angles (1.5.4) has not been attempted.

For αFG the torsion angles considered were $T_1 = \{C2.C1\text{-}N7.H16\}$, $T_2 = \{N7.C1\text{-}C2.C3\}$, $T_3 = \{C1.C2\text{-}C3.C4\}$, $T_4 = \{C2.C3\text{-}O4.O5\}$, and additionally $T_5 = \{C1.C2\text{-}O8.H17\}$ for βHG. Torsion angle and numbering schemes (2.3.2) are thus, as far as possible, compatible with the GABA study (see 2.3.3 for CNDO GABA study). To make the conformational problem practicable a number of approximations have been made as before. Thus when the calculations were made for GABA the $(T_2 - T_3)$-surface was calculated for $T_1 = 180^\circ$, $T_4 = 0^\circ$, since T_2, T_3 largely determine the shape of the molecule and thence the intercharge x_T distance. The variation of T_1 and T_4 were then calculated independently at each minima of the (T_2, T_3)-surface. However, we have noted (3.5.1) that for highly folded conformations of flexible GABA-like molecules there is an interaction between the $-NH_3^+$ and $-COO^-$ groups which invalidates the treatment of T_1 and T_4 as totally independent. The above simplification is valid when more extended conformations are considered (3.8.4), and it is these conformations which are found to be of significance when

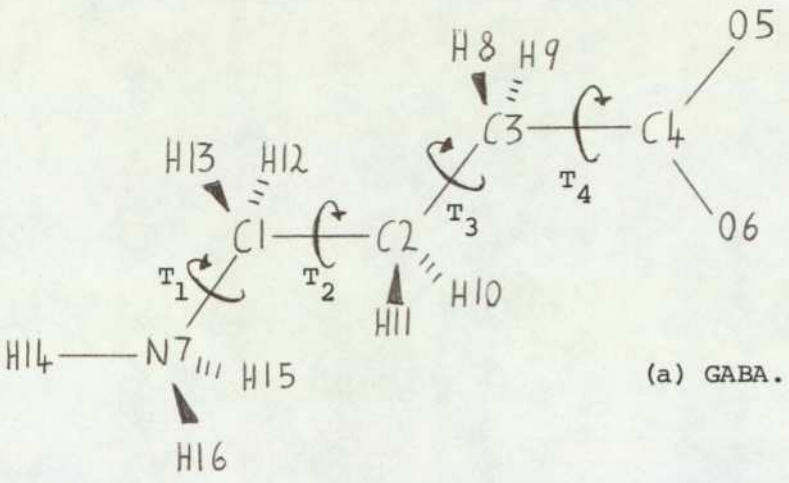

(a) GABA.

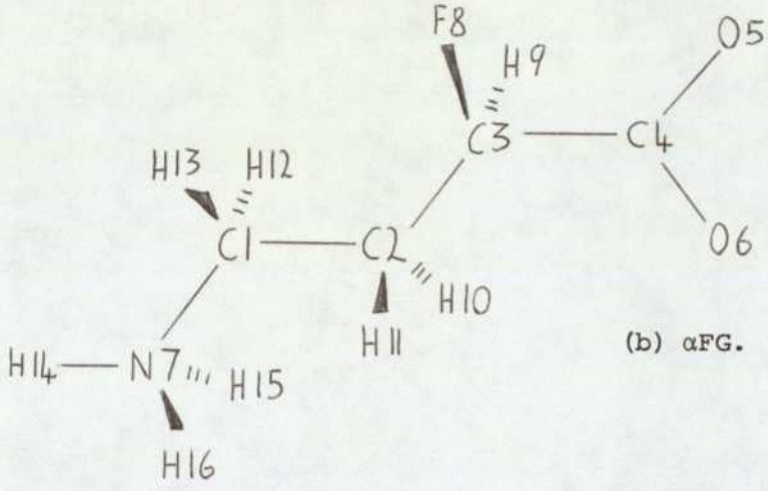

(b) αFG.

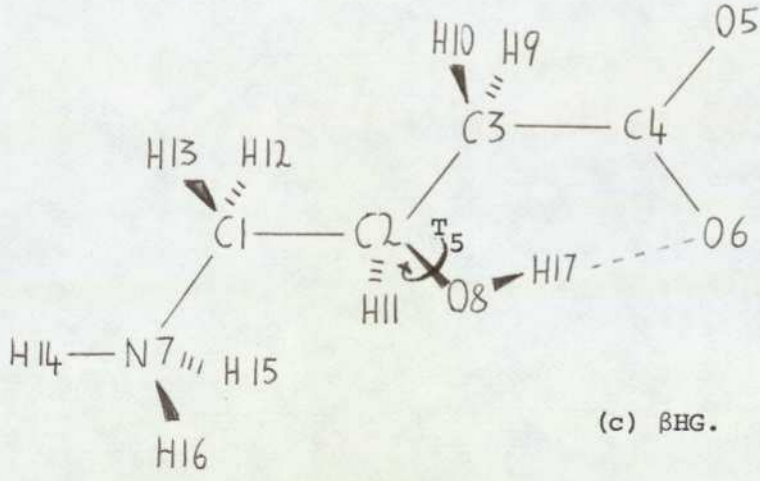

(c) βHG.

Fig. 5.1. The molecules GABA, αFG and βHG, showing the torsion angles considered. (Exact definition of torsion angles is given in the text.)

allowance is made for an aqueous environment (4.4.1). Thus for αFG, as with the original GABA study, the (T_2,T_3)-surface was calculated on a 20° grid with $T_1 = 180^\circ$ and $T_4 = 0^\circ$. The independent variation of T_1 and T_4 was then made for extended conformations only.

With βHG the problem was complicated by the presence of the OH on C2 (Fig.5.1). However, there is evidence (both expermental and theoretical (Catalan & Fernandez-Alonso, 1975 (and refs. contained therein); Tomita, Harada & Fujiwara, 1973)) for an intramolecular OH...O hydrogen bond to form as indicated in Fig.5.1. T_3, T_4 and T_5 were therefore first optimized to investigate the formation of a hydrogen-bonded pseudo-ring. The subsequent form of the study would then be dictated by the existence or otherwise, of the pseudo-ring.

5.4.3 Theoretical gas-phase study of conformation: results and discussion

(i) (R) α-fluoro- γ -aminobutyric acid (αFG) results

The atomic coordinates were obtained using data from the GABA crystal structure and a C-F bond-length was assigned the standard value of 1.36Å (Pople & Beveridge, 1970).

The (T_2, T_3)-surface is shown in Fig.5.2(i), the global minimum occurs at $T_2 = 80^\circ$, $T_3 = -60^\circ$, with 5 other local minima in the region (ℑ) bounded by $(-90^\circ < T_2 < 90^\circ, -60^\circ < T_3 < 60^\circ)$. The energy-range exhibited by all these minima is 6.3 kcal mol^{-1}, the dipole-moment range is 9.6 - 12.3D with 11.2D at the global minimum. Unlike GABA there are no minima associated with extended conformations, probably this is due to the fluorine atom increasing the electrostatic attraction between the ends of the molecule.

The T_1 and T_4 rotations were studied for some extended conformations, and a preference found for $T_1 = 180^\circ$ ('staggered') and $T_4 = 120^\circ$ (carboxylate C-O bond eclipsing the C-F bond), with barriers to rotation of ca. 3.5 and ca. 2.5 kcal mol^{-1}, respectively. Fig.5.2(i) shows that a stabilisation of ca. 60 kcal mol^{-1} exists for some folded rotamers on the (T_2, T_3)-surface.

(ii) (R) β-hydroxy- γ -aminobutyric acid (βHG) results

Atomic coordinates used were taken from the crystal structure data (Tomita, Harada & Fujiwara, 1973). For reasons given earlier (5.4.2) a study of the pseudo-ring involving the OH...O intramolecular bond was first made. A minimum-energy was found for $T_3 = -120^\circ$,

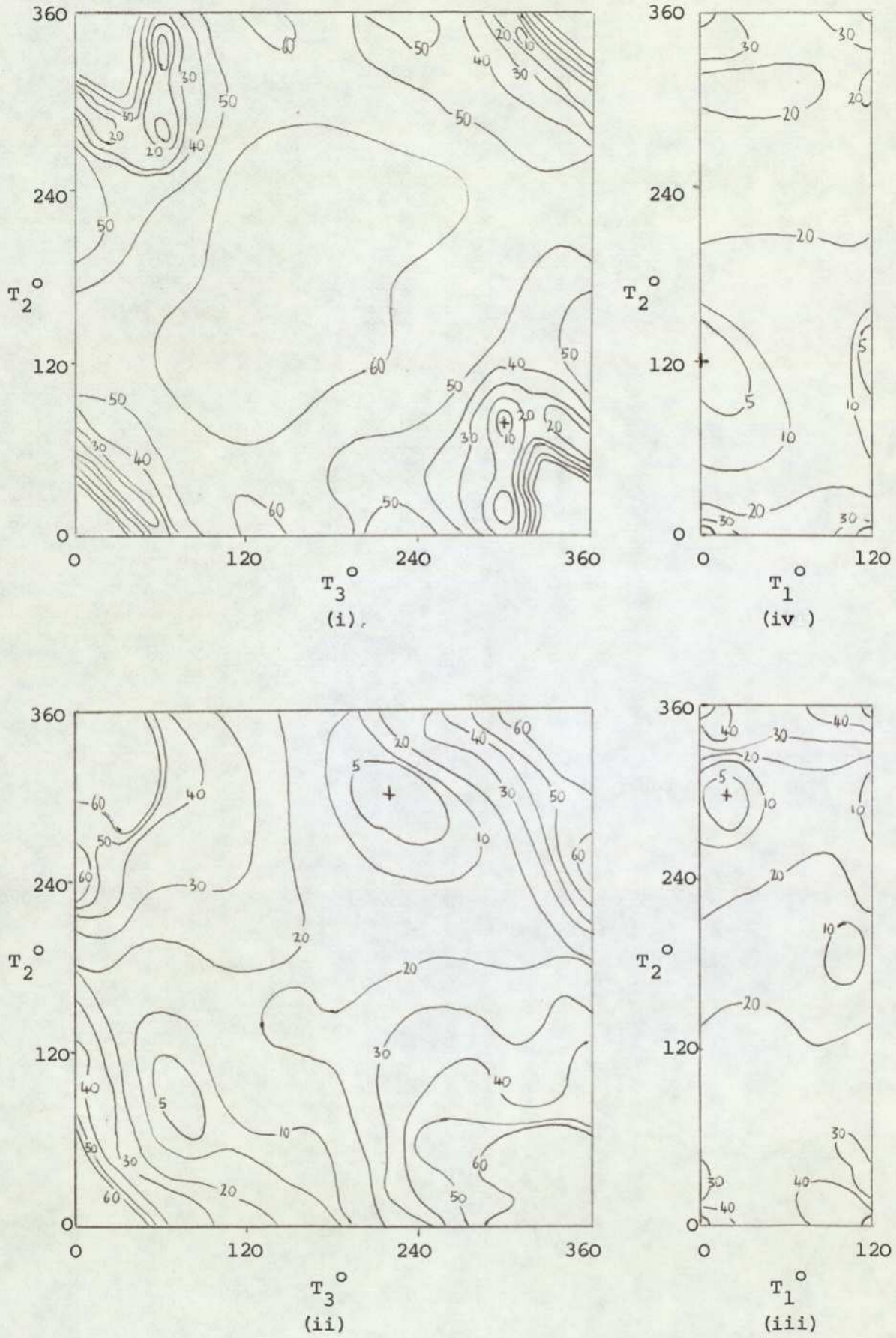

Fig. 5.2. Energy contour maps for (i) αFG in gas-phase, (ii) αFG with solvent effect, (iii) βHG with solvent effect, (iv) β HG in gas-phase. Contours in kcal mol^{-1}.

$T_4 = 20^\circ$ and $T_5 = 120^\circ$, a configuration in which the heavy atoms are quasi-planar. A similar pseudo-ring occurs in salicylic acid, for example, and is observed not only in the solid state but also in a wide range of solvents, implying that it is a very stable bond (Catalan & Fernandez-Alonso, 1975 (and refs. contained therein)).

Assuming the stability of the pseudo-ring the (T_1, T_2)-surface (Fig.5.2(iv)) was calculated, and found to give a global minima at $T_1 = 0^\circ$ ('eclipsed') and $T_2 = 120^\circ$, with a secondary minimum at $T_1 = 40^\circ$, $T_2 = 300^\circ$. These minima are shown below, together with likely reasons for stabilisations. The relative importance of hydrogen bonding and methylene staggering forces in molecules of

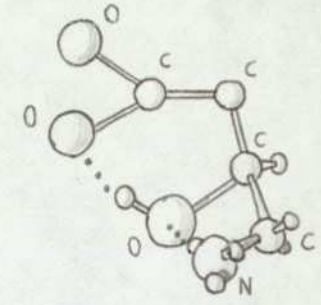

αFG

structure stabilised by N^+-H...O hydrogen bond.

structure stabilised by methylene staggering forces.

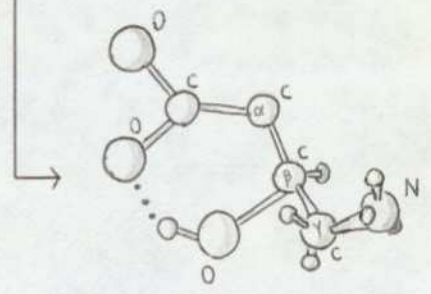

this kind is clearly indicated.

Finally, it was verified that in common with GABA and αFG there are minimum-energy conformations in the folded-region ⅁. These minima (global for full [5] -conformation space) are ca. 30kcal mol^{-1} more stable than the (T_1, T_2)-surface global minimum.

(iii) Discussion

GABA, α-F-GABA and β-OH-GABA all exhibit global minima (in their full conformation spaces) in the region ⅁, of folded conformations, due to the attraction between the zwitterionic end-groups. For αFG the fluorine on C_α increases this end-to-end attraction and no other local minimum is observed outside ⅁. In the case of GABA, however, there are local minima with energies of ca. 50 kcal mol^{-1} above the global minimum occurring in region ⅁. With βHG there are local minima due to intramolecular bonding involving the hydroxyl group, which are only ca. 30 kcal mol^{-1} above those in region .

Thus, in the gas-phase, increased folding of the molecules is predicted in the order βHG → GABA → αFG

5.4.4 Theoretical continuum solvent-effect study: results and discussion

(i) GABA

For GABA the folded conformations of region 5 were found to be no longer preferred- instead the global minimum occurs at $T_2 = -60^\circ$, $T_3 = -140^\circ$.

(ii) αFG

The (T_2, T_3)-surface is shown in Fig.5.2(ii), as with GABA the global minimum now occurs at $T_2 = -60^\circ$, $T_3 = -140^\circ$.

(iii) βHG

Only the (T_1, T_2)-surface (Fig.5.2(iii)) has been considered because of the stability of the ring - the intramolecular hydrogen-bond has previously been discussed in 5.4.3. The global minimum is now at $T_1 = 20^\circ$, $T_2 = -60^\circ$: the methylene staggering dominated minimum of the gas-phase study.

(iv) Discussion of results

All three molecules show a trend towards more extended conformations when some allowance is made for the solvent. The solution modes of the molecules are shown in Fig.5.2. The x_T values at the solvent minima of GABA, αFG and βHG have been computed and are within 0.1Å of each other. Hence, it is concluded that in aqueous solution these molecules display x_T values (ca. 5.2Å) which are indistinguishable to within the accuracy of our models, and on arrival at a distance at which the onset of transmitter-receptor interaction occurs we have

$$[x_T]_{\alpha FG} = [x_T]_{\beta HG} = [x_T]_{GABA} \qquad (5)$$

At an x_T of ca. 5.2Å, the interaction of the $-NH_3^+$ group with the $-COO^-$ is negligible, and there is no longer any apparent interaction between the $-NH_3^+$ group and the OH. Hence we conclude that the $-NH_3^+$ group is an independent and invariant feature of the 3 molecules under consideration, ie

$$[\mathcal{R}^+]_{\alpha FG} = [\mathcal{R}^+]_{\beta HG} = [\mathcal{R}^+]_{GABA} \qquad (6)$$

Substitution of equations (5) and (6) into (3) give

$$\log \mathcal{P}_{\alpha FG} = c_2 \Delta [\mathfrak{R}^-]_{(\alpha FG - GABA)} \qquad (7)$$

$$\log \mathcal{P}_{\beta HG} = c_2 \Delta [\mathfrak{R}^-]_{(\beta HG - GABA)}$$

Equation (7) states that in order to determine the relative potencies of GABA, αFG, and βHG, it is sufficient to study differences in the $\mathfrak{R}^-$ region of the pharmacophore. We have an ideal tool for this purpose in the electrostatic potential map.

5.4.5 Theoretical electrostatic-potential study: Results and discussion

The EP in the region of the $-COO^-$ group has been calculated for GABA, αFG and βHG. For these calculations the molecule has been kept in its solvent conformation. However, the EP maps are valid for a range of T_2, T_3 about their solvent values, since the crucial parameter required for the calculation of EPs are the NAPs. The latter's conformational invariance is especially guaranteed over a reasonable range by the relatively extended conformation of the solvent minima. On the EP maps (Fig.5.3), it is convenient to define two features of the distribution (i) the value of the absolute minimum - this is anticipated as being important in the eventual transmitter interaction at the receptor site; (ii) the extent of the outer -25 kcal mol^{-1} contour - this arbitrary reference contour is likely to be an indication of the transmitter's ability to be recognised by the receptor, and so would be important in the approach to the receptor.

EP for GABA

The general shape of the EP for GABA (unmodified carboxylate group) is nephroid in the Z = 0 plane (Fig.5.3(i)) and it is in this plane that the maximum of the EP occurs, its value is ca. -125 kcal mol^{-1}. In YZ-planes at points whose X-coordinates lie to the left of the $-COO^-$ group the EP exhibits a high degree of isotropy. The absolute minimum of the potential occurs in an area associated with a lone-pair direction of an O^- atom. The position of the minimum as one moves below or above the Z = 0 plane also moves, until at Z = $\pm$ 1Å it lies such that its Y-coordinate is equal to that of the adjacent oxygens. This may be an effect due to the oxygen lone-pair distribution as follows:

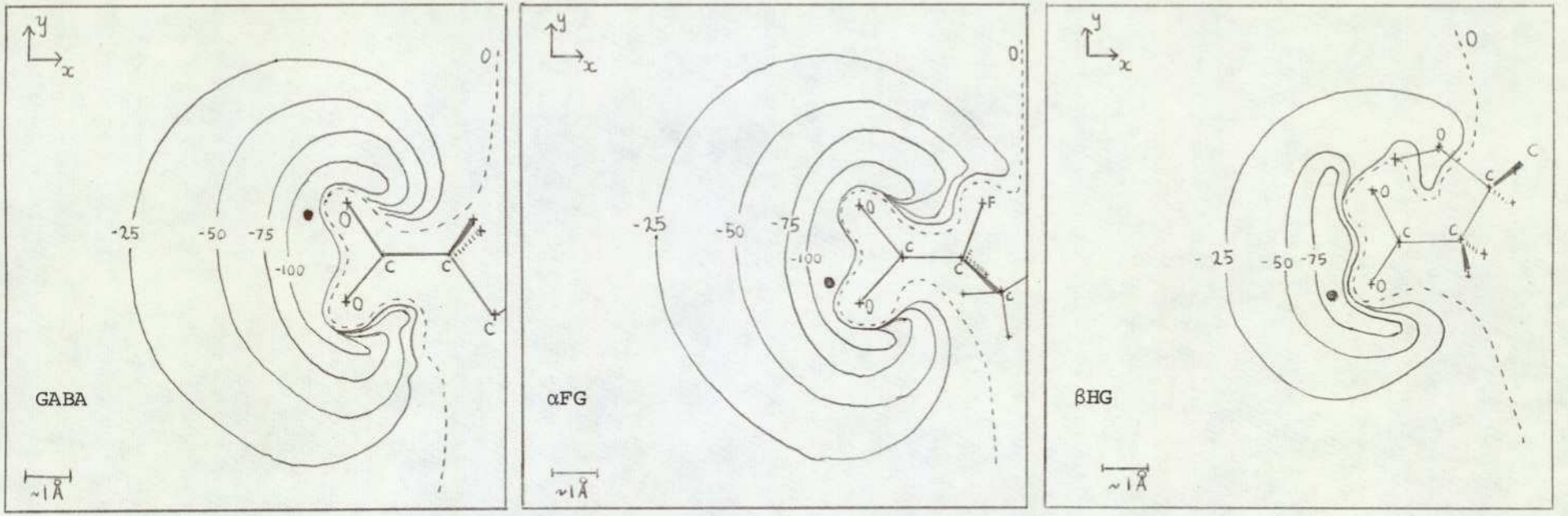

Fig. 5.3. Electrostatic-potential maps for (i) GABA, (ii) αFG, and (iii) βHG. Contours are labeled in kcal mol^{-1}, the global minimum is marked • , and the maps are drawn in the Z=0 plane.

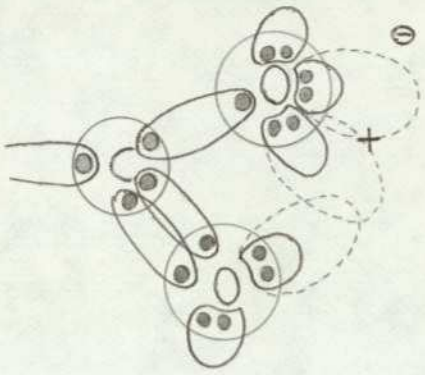

electron distribution in $-\overset{\overset{O}{\|}}{C}-O^-$

electrons (●)
minimum +

If the resonance is shifted slightly towards one of the localised forms as above, the maximum negative charge will be expected at (+), for obvious reasons. A section at right-angles to the plane of the $-COO^-$ group and the C $-COO^-$ bond serves to explain the movement of the minimum.

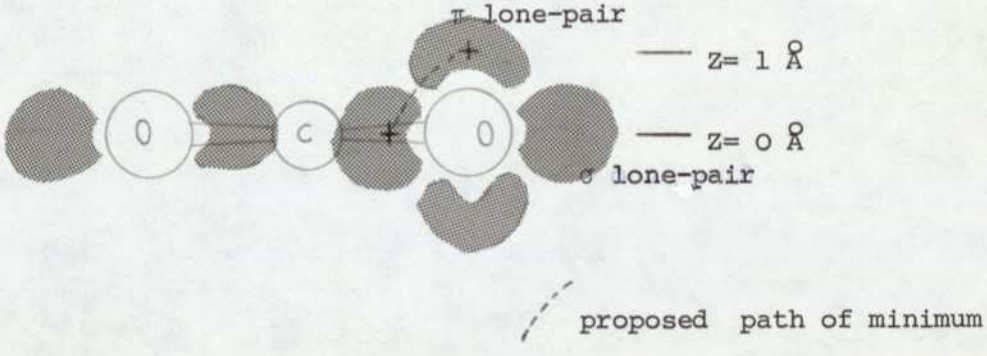

The trend in the migration of the EP minimum can thus be explained in terms of the relative importance of σ and π lone-pairs for differing values of Z.

EP for α FG

For αFG the shape and magnitude of the potential is similar to that of GABA. The presence of the α-fluorine atom, however, can be seen to enhance the EP. The absolute minimum of the EP is in the Z = O plane and again occurs in the lone-pair direction. The 'out-of-plane' behaviour of the minimum is more complex in this case, due to the effect of fluorine lone pairs. The trajectory of the minimum is

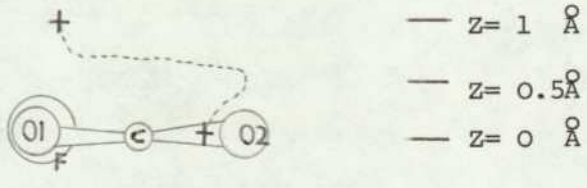

That the 'in-plane' minimum occurs at O2 rather than O1 is explicable in terms of electron induction and the tendency for fluorine to encourage 'back-donation' when it lies in the nodal plane of oxygen lone-pairs (Pople, 1974), ie

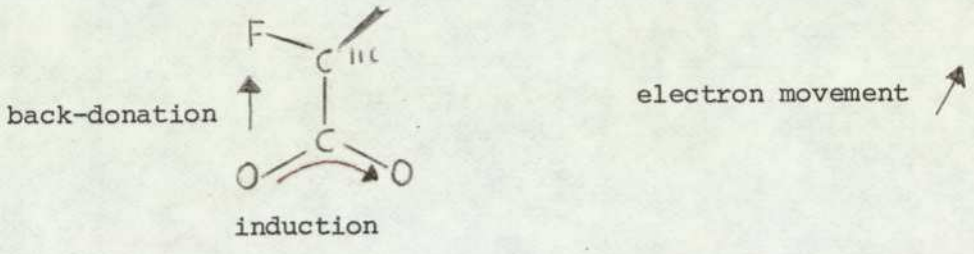

resulting in

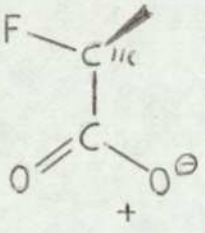

A section perpendicular to the plane of the $-COO^-$ group along the C $-COO^-$ bond shows the expected orientation of lone-pairs,

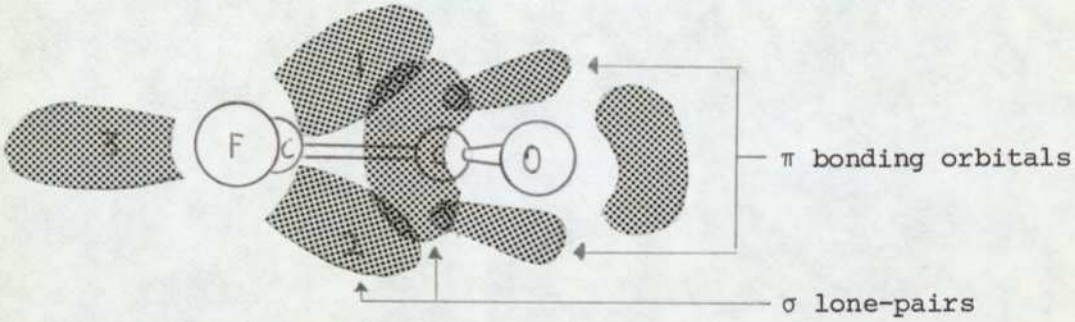

this assumes that the F orbitals approximate to sp^3 hybridisation (so as to be compatible with the hybridisation of the C_α carbon) and that the oxygen orbitals are sp^2 hybridised (compatible with hybridisation of $-C\overset{//}{\backslash}$). It is therefore suggested that the 'out-of-plane' effect of the fluorine lone-pairs (1 and 2) is instrumental in the migration of the EP minimum from O2 to O1 which occurs at some point between 0.5Å and 1Å.

EP for βHG

βHG shows a significantly weaker EP than GABA, due to the involvement of a carboxylate oxygen in the intramolecular hydrogen bond, the minimum of the EP is reduced to ca. -100 kcal mol^{-1}.

Discussion

Finally, the EP was studied in a YZ-plane through the mid-point of the COO^--C bond. Again αFG shows a slightly greater

EP than GABA. The EP in the case of βHG has a local minimum corresponding to an O8 lone pair position, ie

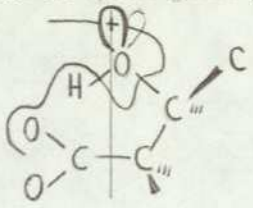

however the overall EP in this YZ-plane is still much diminished with respect to GABA.

As in section 3.7 it is seen that the EP is a convenient medium through which complex quantum chemical effects can be interpreted. With reference to the present problem, there is a clear distinction between the EP maps of GABA and βHG in that the latter has both a reduced absolute value of the EP and a reduced extent of the -25 kcal mol^{-1} contour. Between GABA and αFG the differences are not so marked, however, an enhancement of the potential field does occur for αFG with respect to that of GABA. In conclusion it can be stated there is an order of increasing enhancement of the electrostatic potential field

$$\beta HG \longrightarrow GABA \simeq\!\!\rightarrow \alpha FG \qquad (8)$$

5.4.6 Conclusions of the comparative study of GABA, αFG and βHG

The stronger the EP field the more efficacious will be the $\mathcal{R}^-$ region in interacting with a receptor in electrostatic, hydrogen-bonding and dipole-dipole modes. Thus, combining equation (7) with the trend expressed in (8), it is concluded that (8) is also the order of increasing potency at GABA inhibitory synapses. This ordering is consistent with available results (Curtis & Watkins, 1960; Curtis, Duggan, Felix, Johnson, Tebicis & Watkins, 1972), although on the basis of this study we believe that αFG is unlikely to be much more potent than GABA.

The gross features of the EP field necessary for transmitter activity at GABA receptors are also becoming apparent. These requirements may be refined by consideration of other molecules. For example, methyl-ester-GABA (MEG) has a $\mathcal{R}^-$ region comprising

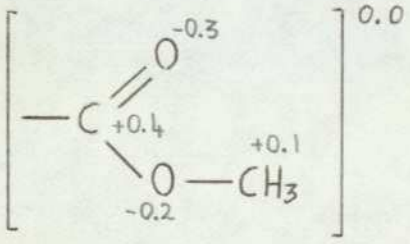

the Σ index of 0.0 does not fulfill the condition of working hypothesis I for agonism (5.2.1) and it is concluded that the molecule is inactive (as is known experimentally (Curtis & Watkins, 1960)). If an EP study were to be made on MEG a lower limit of the EP field values necessary for agonism could be found, resulting in a much refined version of working hypothesis I, ie phased in terms of EP rather than NAP requirements. This latter calculation will form a part of the subsequent studies (5.5.4).

More detailed reasons for the bad fit of αFG and βHG in the CAR study made by Clarke (1976) are therefore now evident. The self-consistent regression line from that earlier work is reproduced in Fig.5.4. The points using experimental potencies and interaction probabilities (T_i) calculated on x_T considerations only are plotted as ○ . If instead of using the experimental potencies the previous T_is and the regression line are used to predict the potencies, βHG is predicted as more potent than either GABA or αFG - in conflict with the experimental evidence (Curtis et al, 1972). However, the results of this section suggest that the interaction probability of αFG is underestimated and βHG is overestimated. This results in movement of points representing αFG and βHG in direction of arrows shown in Fig.5.4. It is evident that the results of this section provide the correct trend in the movement of the points ○ relative to each other to produce the correct ordering of potency in Fig.5.4.

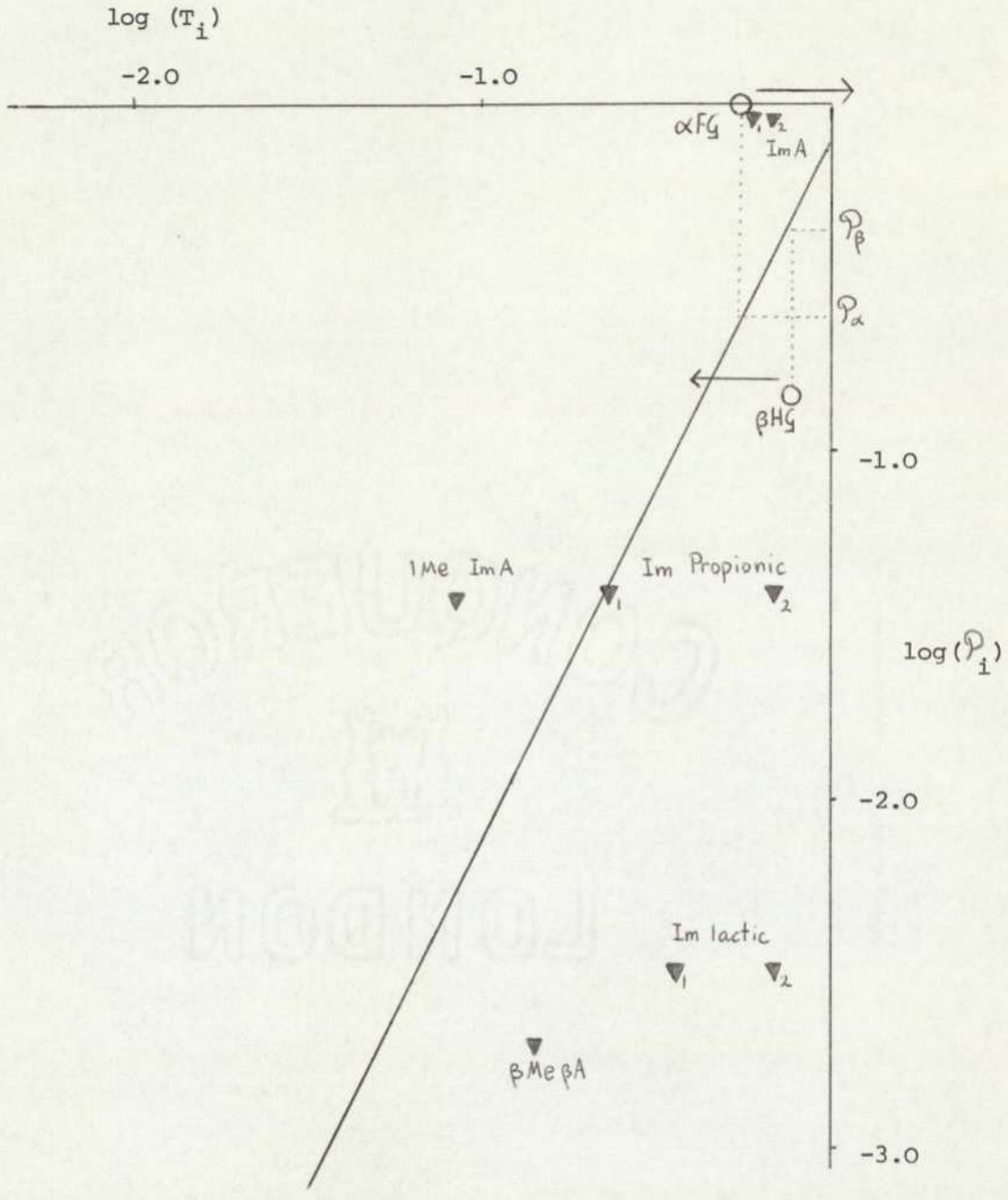

Fig. 5.4 Self-consistent regression line based on unbranched α-ω amino acid GABA-agonists. The branched agonists βHG and αFG when added (o) do not fit into the scheme well (their $\mathcal{R}^-$ regions are modified with respect to those molecules on which the regression line is based). The predicted potencies based on the calculated interaction probabilities are shown (P_α and P_β), and it is noted αFG is predicted as less potent than βHG. ▼ Imidazoles.

5.5 A theoretical study of MM, methyl-ester-GABA (MEG) and α-amino-GABA (αAG)

5.5.1 Introduction

In 5.4 a comparison of αFG and βHG were made with the canonical transmitter (GABA). Throughout, the comparative nature of the study was stressed, and the present chapter is written in the same spirit.

Curtis & Watkins (1960) give GABA a potency of (---) and βHG a potency of (--), in 5.4 it was found that GABA and βHG have absolute EP minima of -125 and -100 kcal mol^{-1}, respectively. If a roughly linear fall-off in potency is hypothesised, then by extrapolation EPs of >ca. 150 kcal mol^{-1} should correspond to (^{o}) (ie, inactivity - at least on mammalian spinal neurons). It is now proposed, in order to test this hypothesis and for other reasons given in 5.2, to investigate the EP field of the inactive GABA derivative MEG.

The EP of MM was fully studied in 3.7.5, in 5.5.2 the relation of that EP to potency is discussed. In 5.5.3 αAG is discussed as a case where an additional consideration regarding potency exists.

5.5.2 The potency of MM

MM is a substituted izoxazolidone, structurally similar to ITA, the potent glutamate agonist. The diagram below shows its similarity to GABA.

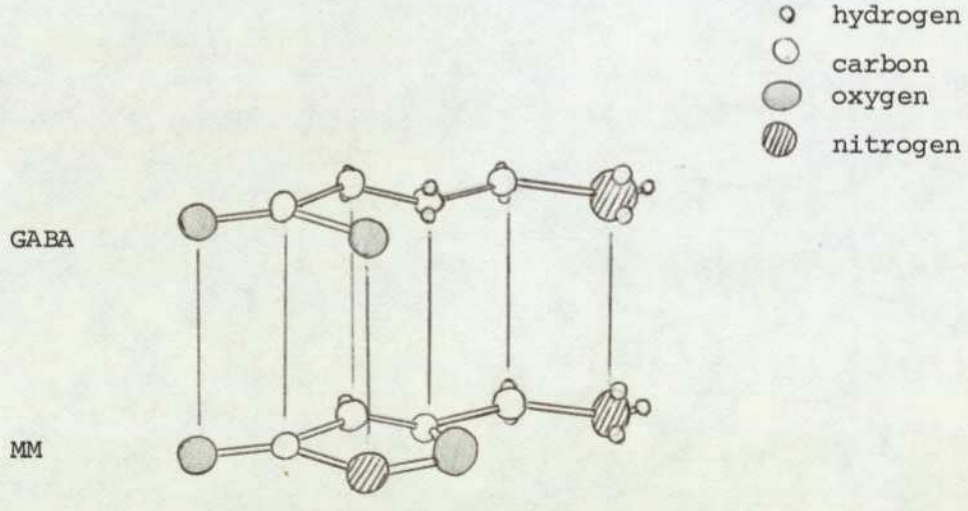

The $\mathcal{R}^{+}$ region of MM is represented by an onium group and, owing to a fortuitous alignment of the axis of rotation for θ and the charge-centre of the $-CON^{-}$ group, the x_T of MM is ca. 5.1Å for all conformers. Hence, equations of the form (7) given in 5.4.4 can again be used in

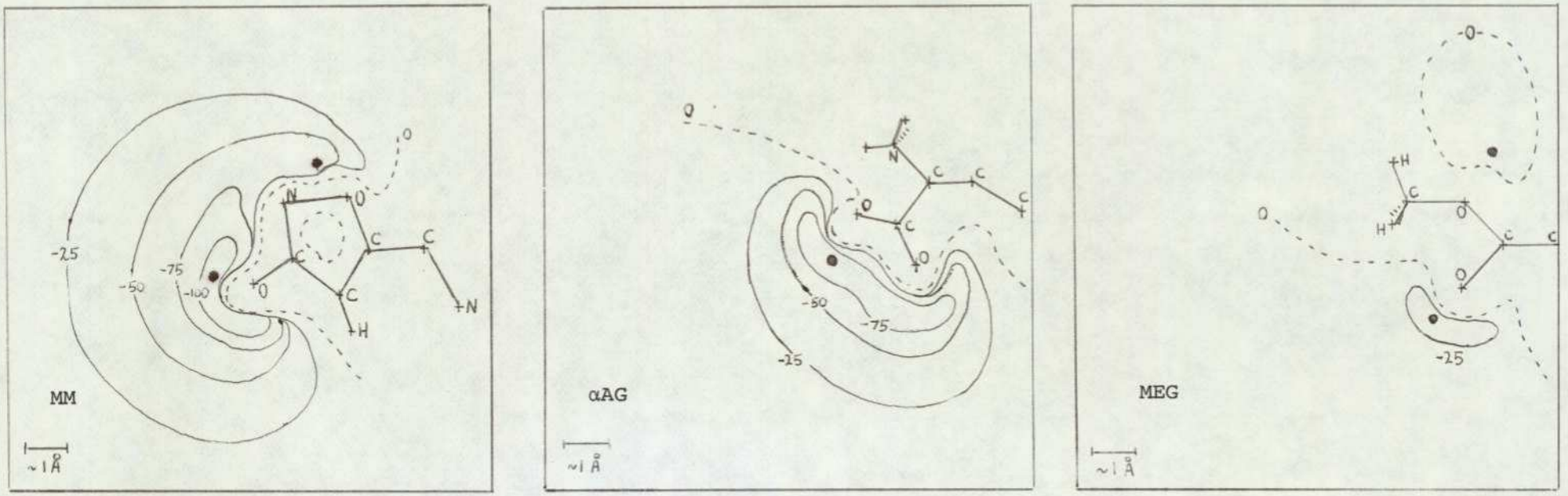

Fig. 5.5 Electrostatic-potential maps for (i) MM, (ii) αAG and (iii) MEG. Contours labeled in kcal mol^{-1}, the minima are marked ● .

order to ascribe the potency to MM relative to GABA as being due to $\mathfrak{R}^-$.

The EP field of MM has already been discussed in some detail in 3.7, where its close similarity to that of the $-COO^-$ group was evident. The EP field is shown in Fig.5.5(i). The extent of the -25 kcal mol^{-1} contour is slightly diminished with respect to GABA (Fig.5.3(ii)), however the absolute minimum value of ca. -125 kcal mol^{-1} is in good agreement with the value found for GABA.

Summing up, a potency for MM 'similar to GABA' is indicated by the EP calculations. This phrase is used by Johnson et al. (1968) to describe the experimentally determined potency of MM.

5.5.3 A discussion of αAG

In order to discuss αAG a full gas-phase/solvent-effect/EP study is required to calculate x_T and the character of its $\mathfrak{R}^-$ region. The αAG molecule exists in the crystalline phase (Hinazumi & Mitsui, 1971) as the mono-cation ($NH_3^+.(CH_2)_2.CH(NH_3^+)COO^-$) and this form is also expected to be predominate in the aqueous phase at physiological pH (pK values from Richards & Thomas, 1974).

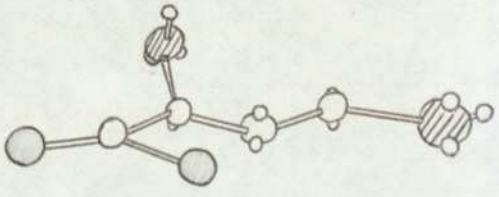

αAG

Although the full gas-phase study is given in Appendix D together with the solvent-effect calculations, the results are briefly summarised here. The gas-phase energy-map shows the global minimum in a folded conformation (within region $\mathfrak{H}$), in common with results for GABA-like zwitterions (5.4.3). However, an allowance for the solvent effect also indicates a folded-molecule as the most stable solution mode, which is contrary to the conformational behaviour of GABA-like zwitterions in solution (5.4.4). At the solvent minimum, since the x_T = ca. 2.4Å, by Working Hypothesis III (5.2.3) the αAG mono-cation cannot display GABA agonism.

However, the mono-cation is not the only species existing in solution and it is expected that there is also a population of the zwitterion. A gas-phase and solvent-effect study was therefore also made on the zwitterion (Appendix D). Briefly, the gas-phase results show the most populated conformations are in the region $\mathfrak{H}$ and the

solvent effect leads to more extended conformations with an x_T = ca. 5.2Å at the minimum.

The EP for the mono-cation is shown in Fig.5.5(ii) and has an extent less than βHG, although the absolute minimum is comparable at ca. -100 kcal mol^{-1}. The EP for the αAG zwitterion is similar to that of GABA itself with a minimum value of ca. -125 kcal mol^{-1}.

The situation then, is that the predominant mono-cation species of αAG has its most populated conformational modes at x_Ts which are not compatible with GABA agonism (by Working Hypothesis III). It is, however, possible that αAG may show some activity due to the action of the relatively small population of the zwitterionic form of the molecule. Experimental results show αAG to have a very low potency, while one study (McGeer et al, 1961) suggests it is inactive. Hence, again our theoretical conclusions are compatible with the available experimental evidence.

5.5.4 MEG

The structure of MEG ($NH_3^+.(CH_2)_3.COOCH_3$) was based on the GABA crystal structure (Steward et al, 1973), with standard bond-lengths and angles for the atoms of the methyl-ester group.

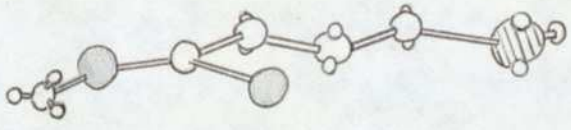

MEG

The EP (Fig.5.5(iii)) is qualitatively similar in form to that found for the methyl-ester moiety in other studies (eg Loew et al, 1974), the absolute minima is ca. -40 kcal mol^{-1}. In 5.5.1 it was suggested that an $\mathcal{R}^-$ EP field minimum of -50 kcal mol^{-1} should be insufficient for GABA agonism, hence on this criterion and the fact that $\Sigma = 0.0$ for the methyl-ester group it is expected that MEG is inactive - this is as found (Curtis & Watkins, 1960). It is noted that an alternate phrasing of Working Hypothesis I is now possible in terms of EP rather than NAP (viz a minimum value of the EP field less than about -50 kcal mol^{-1} is required for agonist activity).

5.5.5 Summary

On the results of 5.4 and 5.5 the theoretically predicted order of decreasing potency of the agonists studied is (using $\simeq\!\!\rightarrow$ to donote approximate equivalency):-

$$\alpha FG \simeq\!\!\rightarrow GABA \simeq\!\!\rightarrow MM \longrightarrow \beta HG \longrightarrow \alpha AG \simeq\!\!\rightarrow MEG$$

This predicted ordering is in accord with the potencies as experimentally determined.

5.6 Antagonism at the GABA receptor

5.6.1 Introduction

Understanding of the GABA receptor has been severely hindered due to the lack of any good specific antagonists. Unlike the acetylcholine neurotransmitter system in which many antagonists are known, in the GABA system (+)bicuculline (BIC) is the only well supported candidate.≠ The speculative nature of this section is a reflection of the lack of reliable pharmacological data concerning GABA antagonism.

The crystal structure of BIC (Gorinsky & Moss, 1973) has been determined (Fig.5.6), sharing a 1S,9R configuration (S & R defined in Appendix C) with the N-methyl group pseudoaxial to the pyridine ring.

The first remarks on BIC's possible actions as a competitive antagonist were made by Curtis, Duggan, Felix & Johnson (1970), who suggested the following isosteric match between GABA and BIC.

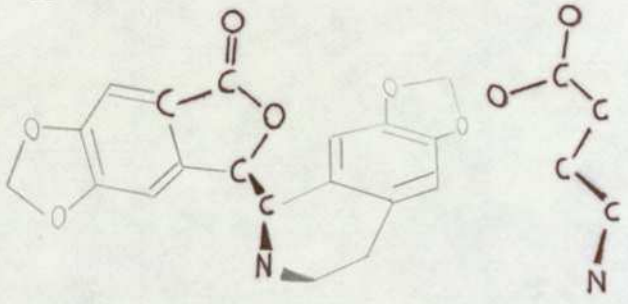

A better match was then suggested by Steward, Player, Quilliam, Brown & Pringle (1971) which preserved the congruence of atoms of the same atomic species more exactly than the Curtis matching:-

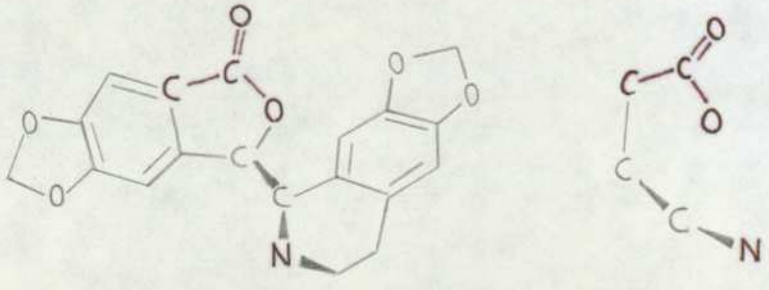

On the basis of these similarities between BIC and GABA it was suggested that BIC could be recognised by the GABA receptor, thereby perhaps providing a starting point for explaining its competitive antagonism.

≠ A good review of the pharmacological data can be found in Chapter 6 (Convulsant Aklaloids by D R Curtis and G A R Johnston) of Neuropoisons, Vol.2, edited by L. L. Simpson and D. R. Curtis, Plenum Publishing Corp, New York (1974).

и

и

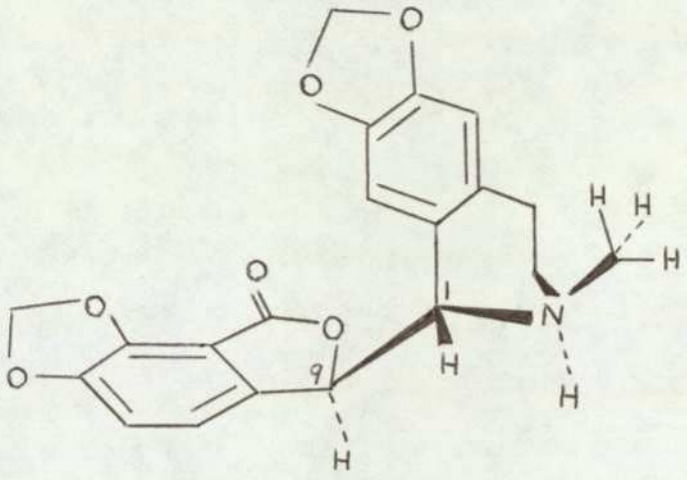

Fig. 5.6 The GABA antagonist BIC (bicuculline). Diagram shows the protonated species (N^+).

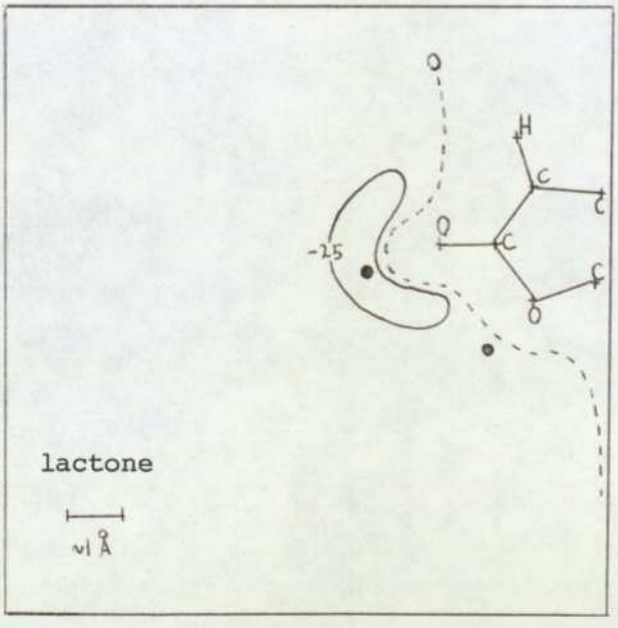

Fig. 5.7 Electrostatic-potential map showing the EP vicinal to a lactone moiety. Contours in kcal mol^{-1}, and the minima are denoted • .

However, the subsequent availability of the BIC crystal structure showed that the above matchings had been made on the wrong diastereomer ie IS.9R (adlumidine). At about the same time as the determination of crystal structure theoretical calculations and NMR results (Andrews & Johnson, 1973) became available for BIC which showed that there is appreciable torsional freedom about the C1-C9 bond (Fig.5.6). Within the allowed angular range it was again possible to attain the isosteric match suggested by Curtis et al (1970) for the wrong BIC configuration. Steward et al pointed out that the match they had suggested was not now so easily obtained, although it was still attainable by the GABA agonist δ-aminovaleric acid, of almost equivalent potency, as follows

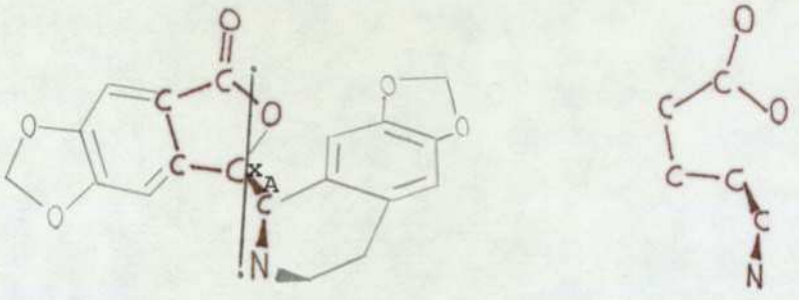

It is therefore possible for BIC to show a charge separation x_A such that $x_A \simeq x_R$, and so be recognised by the GABA receptor. The action of BIC as a competitive antagonist (rather than an agonist - for which it has a suitable intercharge separation) is thus suggested as being due to a feature other than its intercharge distance.

5.6.2 Electronic structure of BIC and GABA

The suggestion that BIC acts at the GABA postsynaptic receptor was based on similarities between their spatial structures. The reason for the antagonism of BIC and the agonism of GABA must be based on inherent differences between the two molecules. We will assume that the lactone ring and pyridine-ring nitrogen of BIC provide the $\mathfrak{R}^-$ and $\mathfrak{R}^+$ regions of the GABA pharmacophore, respectively. It is probably safe to look at the same pharmacophore for BIC and GABA, since it has been shown (Collins, 1977) that BIC inhibits GABA binding to GABA receptors. A comparison of the $\mathfrak{R}^-$ and $\mathfrak{R}^+$ regions of BIC and GABA will be made with the aim of establishing differences which may explain their respective antagonism and agonism.

(i) The $\mathfrak{R}^-$ region

The CNDO charges for the lactone moiety are

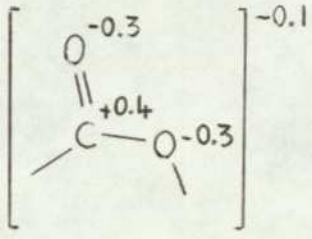

Immediately from Working Hypothesis I BIC is precluded from being an agonist. (It would be unwise, however, to suggest that the BIC $\Sigma = -0.1$ is significantly different from zero (c.p MEG) to be a criterion for antagonism as distinct from inactivity.)

From the BIC NAP data it is suggested that a possible mechanism for competitive antagonism is a charge pattern sufficiently similar to that of an agonist to be 'recognised' and attracted to a receptor, but with charges too weak to mediate a response.

It is expected that the conclusions formed in the previous paragraph should also be consistent with EP field calculations. The EP map for the lactone ring (Fig.5.7) shows a weak field with an absolute minimum of ca. -40 kcal mol^{-1}. This minimum value is similar to the value of the EP field minimum of MEG (inactive), and again BIC is precluded from being an agonist on considerations of EP. Since the BIC EP minimum is the same as that found for MEG, a quantitative EP explanation of agonism, antagonism and inactivity is again not possible (c.p NAP and Σ values). There is, however, an aspect which may differentiate between the MEG (inactive) and BIC (antagonist) EPs, viz the connectivity of the minima associated with the heteroatoms. For BIC (and GABA-like EPs) the minima are connected in the sense that it is possible to pass from one to the other without leaving negative potential field

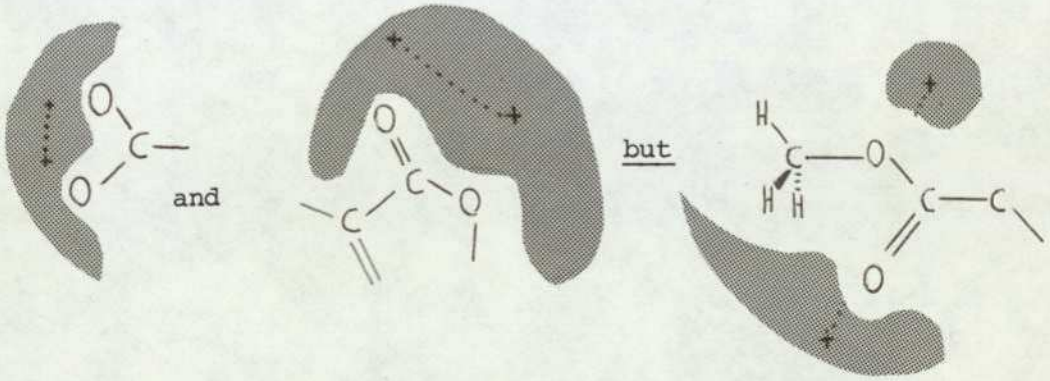

$-COO^-$ (as in GABA) lactone (as in BIC) $-COOCH_3$ (as in MEG)

This intrinsic difference between groups which appear to have action at the receptor and those which do not, may be related to the necessity of the agonist/competitive antagonist to provide a particular hydrogen-bond pattern at the receptor, eg

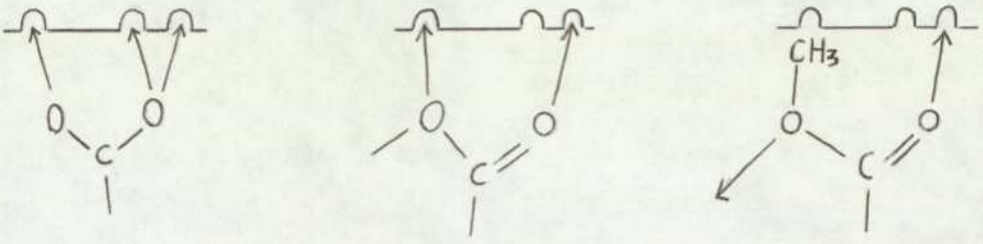

$-COO^-$ lactone methyl-ester

(It has been assumed $\overset{O}{\overset{\|}{}}$ can participate in 1 hydrogen bond , the $-COO^-$ group 3 (see 3.7) and $\diagup O \diagdown$ 1). Suppose that in MEG the methyl group could be rotated to be trans to the esteric oxygen, then the minima would be connected and a hydrogen-bond pattern similar to the lactone moiety would result. The barrier against such a rotation is probably ca. 6 kcal mol^{-1}, this may be compared with the value of 5-6 kcal mol^{-1} which Lambrecht & Mutschler (1974) 'categorically' stated cannot be overcome by receptor-agonist interaction (presumably this statement was intended only to be valid for acetylcholine receptors on which they were working, although this point was not explicitly made in their summing up). If energies of the order of 6 kcal mol^{-1} are, however, characteristic of receptor-agonist systems in general, then under certain conditions the $-COOCH_3$ group can function as an antagonist $\mathfrak{R}^-$-region. This is a possible type of explanation for the antagonist action of diethyl-ester-glutamate at the GLU receptor (which has $\mathfrak{R}^+$ and $\mathfrak{R}^-$ requirements similar to GABA (5.8)).

Translating the preceding ideas on connectivity of minima into charge rather than EP terminology, it is noted that for 'trans' $-COOCH_3$ groups we have $\left[-\overset{+0.4}{C}(=O_{-0.3})-O_{-0.2} \right]^{-0.1}$ (see 5.4.6) - the Me is not included in the summation since it does not sterically affect the heteroatomic pattern. The Σ of -0.1 is now as for the lactone ring implying that -0.1 may indeed be significant with respect to O.O. EP and charge approaches for differentation between agonism, antagonism and inactivity, are now consistent in their predictions (Table 5.1 in 5.6.3).

(ii) The $\mathcal{R}^+$ region

In aqueous solution BIC protonates to HBIC, the charges for the pyridine ring nitrogen and substituents are then

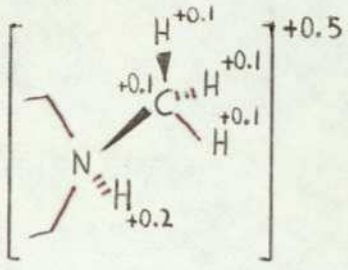

The Σ index is very close to that required for agonism. A difference in the $\mathcal{R}^+$ required for agonism and that required for antagonism can, however, be found.

The methylation of the onium group in GABA results in a dramatic loss in potency (Bowery & Brown, 1974), however, N-Me BIC is a more potent antagonist than HBIC (Pong & Graham, 1972). An implication is that the $\mathcal{R}^+$ region of the receptor is vicinal to a lipophilic moiety, N-Me HBIC can then bind lipophilically to the receptor, making its removal difficult and its antagonism therefore more effective.≠

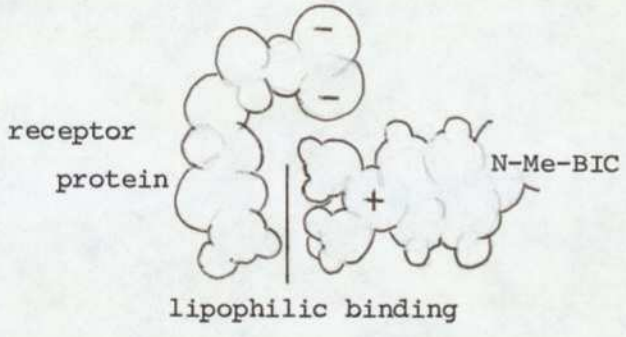

In the case of N-methyl-GABA any lipophilic bonding to tbe receptor may inhibit the removal of the agonist resulting in an eventual occupation of the receptor population (both postsynaptic and uptake) and a static situation within the synaptic process. In this context it is noted that 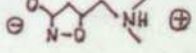 also has a low potency relative to GABA, and β-Me- β-alanine has a potency lower than β-alanine at GABA receptors. The lower potency of methylated agonists may of course be due to factors other than lipophilic binding at the receptor, eg their x_T values.

≠ It has been suggested that the higher potency of N-Me HBIC is due to its pK_a relative to HBIC (Andrews & Johnson, 1973). However, it seems unlikely that this can explain in full the potency difference.

5.6.3 Summary

By considering the GABA antagonist BIC a possible mechanism for competitive antagonism has been suggested viz an EP field (charge pattern) similar enough to that of an agonist to be recognised and attracted to the receptor, too weak to mediate a response, and held by lipophilic binding in the R^+ region to prevent fast removal of the antagonist molecule.

A set of conditions applicable at the R^- region differentiating between agonism, antagonism and inactivity have been proposed, these are summarised in Table 5.1. (It should be remembered that these conditions are only to be regarded as working hypotheses.)

Some observations have also been made concerning methylation of the R^+ regions of BIC and agonists. These can be summarised

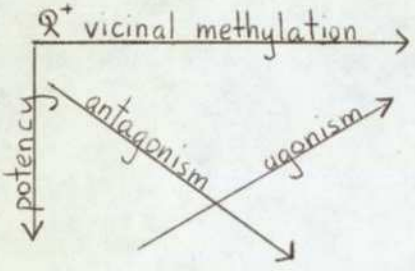

A similar R^+ methylation trend is observed in the histaminergic system, and also for the cholinergics (see, eg, p.178 in Ariens & Simonis, 1973).

The speculative nature of much of this section is a reflection of the lack of reliable data on antagonism. Characterisation of the GABA receptor will be greatly aided by the discovery of other genuinely specific competitive GABA antagonists.

action	EP condition	charge condition
Agonism	absolute minimum <-50 kcal mol^{-1} ,more likely ca -100 kcal mol^{-1}*. Two minima which are connected.*	Σ =ca -0.6
Antagonism	absolute minimum >-50 kcal mol^{-1} Two minima which are connected.*	Σ =ca -0.1 **
Inactivity	absolute minimum >-50 kcal mol^{-1} One minimum,or two if they are unconnected*.	Σ =ca 0.0 **

Table 5.1

Working hypotheses distinguishing between agonism, antagonism, and inactivity at the GABA receptor.* The sense in which the minima are connected or otherwise is defined in 5.6.2.** The extent of the summation is also discussed in 5.6.2.

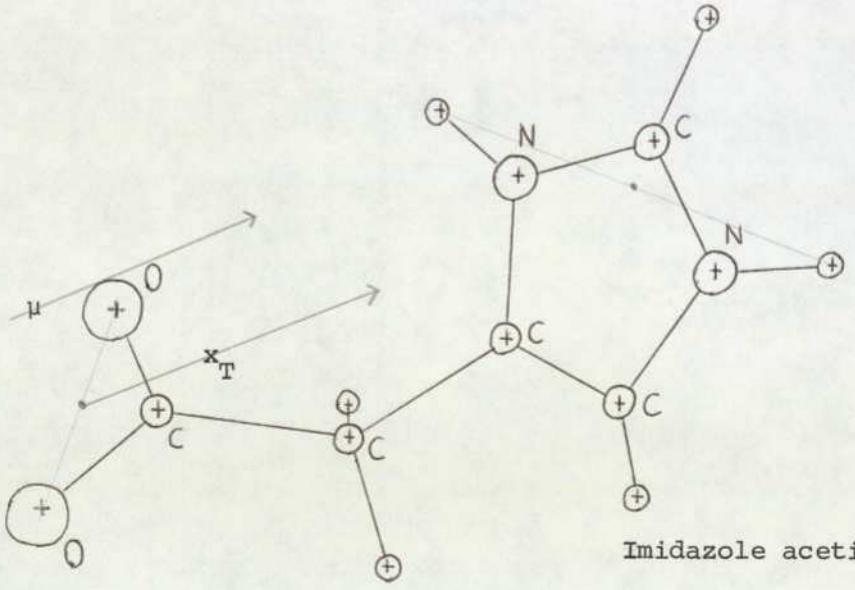

Imidazole acetic acid.

Fig. 5.8 Comparison of CNDO/2 dipole-moment direction with the x_T direction based on the charge centres suggested in the text.

5.7 Some concluding remarks on the GABA system

5.7.1 Other GABA agonists: β-guanidino propionic acid and imidazole acetic acid

In all our calculations on GABA agonists $\mathfrak{R}^+$ has been represented by $-NH_3^+$. There are, however, two important series of agonists where $\mathfrak{R}^+$ is either a guanidino or imidazole group. Typical of these molecules are β-guanidino propionic acid (βGP) and imidazole acetic acid (ImA).

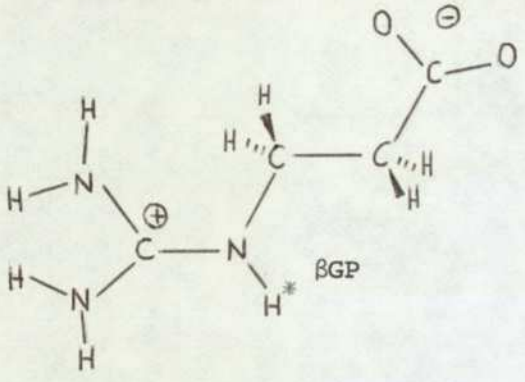

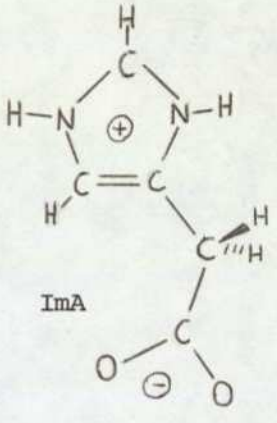

For βGP, CNDO/2 calculations have been made (Warner, 1975) and continuum solvent effects added (Clarke, 1976). A charge centre for the guanidino group has been determined (§5.8.2) based on the direction of the dipole moment of βGP. (It should be pointed out that Steward and Clarke (1975), in their study of GABA agonists in a flexible-receptor model, used a two charge centre model of βGP. They tentatively assumed that the H* proton (see above diagram) is not likely to be involved in the transmitter-receptor interaction. This may, however, be an invalid assumption in view of the relative inactivity (ca. 0.001 as potent as GABA) of creatine 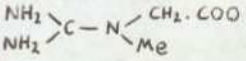 with respect to α-guanidino acetic acid (αGA) 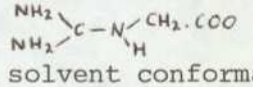 (ca. 0.5 as potent as GABA).) In the preferred solvent conformation the x_T (dipole defined') is ca. 4.5Å, a value which would give βGP a potency slightly below that of βA (x_T = 4.6Å) if the differences in $\mathfrak{R}^+$ were ignored. Values of 33 and 500 are given for βA and βGP respectively (rel. to GABA = 1000) by Dudel (1965), indicating that the differences in $\mathfrak{R}^+$ are very important.

βGP is unusual in that it is reported to be a partial agonist. This behaviour is also noticed for αGA implicating the guanidino group as possibly responsible. One aspect of the guanidino group which differentiates it from the imidazole ring and onium groups is its tendency to form weaker hydrogen bonds than the latter groups

(3.7.3). A difference in hydrogen bonding potential is implied by the charge distribution (5.2.2) viz

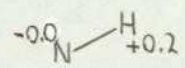

in $-NH_3^+$ and imidazole ring.

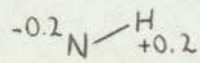

in guanidino group.

This difference in electronic structure may be relevant to the action of guanidino acids as partial agonists.

ImA has been studied by Kier et al (1974) using the EHT MO method. However, there are good reasons (due to failings of EHT, see 2.3.2) for believing that his results are erroneous. The preferred solvent conformation of ImA in the CNDO-continuum scheme has not, at this time, been calculated. A suggested effective charge centre for the Im^+ group is the mid-point of the two protons bonded to the nitrogen atoms. The correlation of $\vec{x}_T$, using this definition of charge centre, with the theoretical $\vec{\mu}$ is shown in Fig.5.8. (This correlation is typical of the other planar projections which are not depicted.)

In view of the high potency of ImA (ca. 1.5 times GABA on one preparation), it is hoped that CNDO/2 calculations can be made on this molecule in the future.

5.7.2 Other GABA agonists: cis, trans-aminocrotonic acids

CNDO calculations have been made on cis and trans aminocrotonic acids (ACA) (Livingstone, Borthwick and Steward, unpublished work) and continuum solvent effects have also been determined (Clarke, 1976).

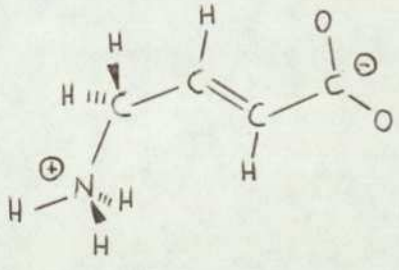

trans- ACA

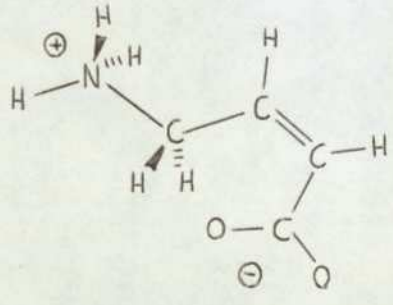

cis- ACA

The x_T values lie on opposite slopes of our log(rel. potency) .v. x_T - plane (Fig.5.0), which is only an indicator of trend in the variation of these parameters. However, using the more refined approach based on receptor flexibility, Clarke (1976) has obtained values of log(interaction probability) for (c)ACA and (t)ACA of -0.103

and -0.092, respectively. Using the pharmacophore equation (1)' and equation (4) (5.3.1)

$$\log \frac{\mathcal{P}_{(t)ACA}}{\mathcal{P}_{(c)ACA}} = \log \frac{\mathcal{P}_{(t)ACA}}{\mathcal{P}_{GABA}} - \log \frac{\mathcal{P}_{(c)ACA}}{\mathcal{P}_{GABA}} = \log T_{(t)ACA} - \log T_{(c)ACA}$$

where T_i is total interaction probability. Hence,

$$\log \frac{\mathcal{P}_{(t)ACA}}{\mathcal{P}_{(c)ACA}} = 0.011 \quad \therefore \quad \frac{\mathcal{P}_{(t)ACA}}{\mathcal{P}_{(c)ACA}} = 1.03$$

a value which does not agree well with the experimental value of ca. 4. It is unlikely this error can be totally explained by an investigation of the effect of the double bond on the $\mathcal{R}^-$ EP field, although the calculation may prove of interest.

5.7.3 Future work: theoretical

Using the theoretical techniques already investigated in this thesis a study of ImA is perhaps called for. The high potency reported for this molecule is explicable only in terms of its $\mathcal{R}^+$ region, since $\mathcal{R}^-$ is a $-COO^-$ group and its x_T cannot better 5.2Å, hence (by equation (3)(5.3.1))

$$\log \frac{\mathcal{P}_{ImA}}{\mathcal{P}_{GABA}} = c_1 \Delta[\mathcal{R}^+]_{(ImA-GABA)}$$

The problem is that the EP can only be calculated for the electrophobic field, calculations at the $\mathcal{R}^+$ electrophilic field are not tractable. A possible solution to the question of electrophilic attack will now be outlined.

For a system of 2n electrons the Hartree-Fock formalism gives rise to more than the required n MOs, hence virtual orbitals exist characterised by being empty and having +ve energy values. For example, 4-ATA (38 electrons, 33 AOs) has an orbital energy spectrum.

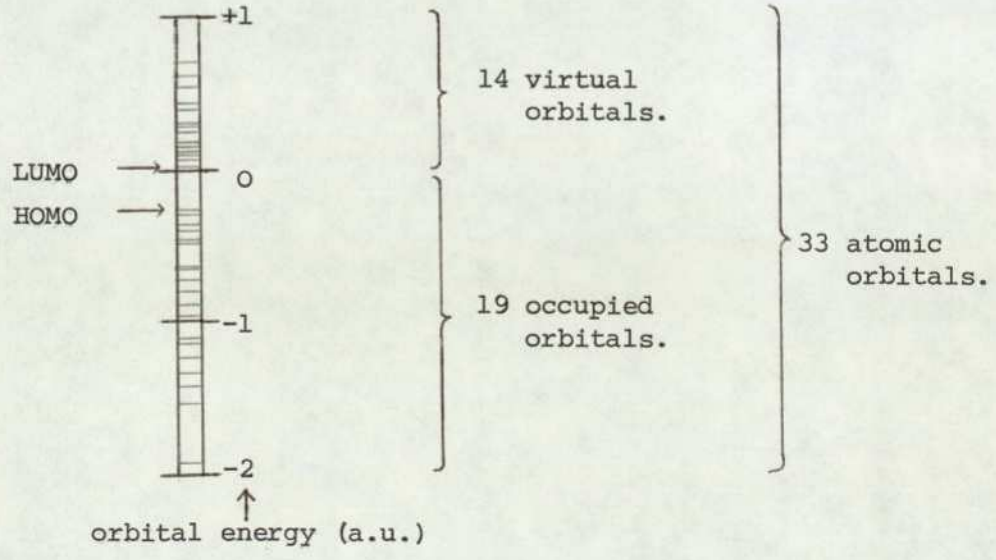

There are two important orbitals in this spectrum, the highest occupied molecular orbital (HOMO) and the lowest unoccupied molecular orbital (LUMO). The HOMO represents the orbital whose electrons are least strongly bound to the molecule, and therefore those most prone to electrophilic attack. Analysis of the wavefunction unambiguously associates the HOMO of ATA with the π lone-pairs of the carboxylate oxygens. The LUMO represents the orbital which is most capable of accepting an electron, and so this orbital is important for electrophobic attack. Again analysis of the ATA wavefunction associates this orbital with the 2s nitrogen and 1s onium proton orbitals. By compiling an electron density map of the LUMO comparisons of $\mathcal{R}^+$ are possible. It is felt such calculations represent the most important direction to which the theoretical techniques can be applied, with respect to the GABA system.

Another problem suited to a theoretical approach is that concerning the amino benzoic acids. These compounds (see diagram below), although possessing all the apparent requirements for GABA agonism, have been reported as inactive.

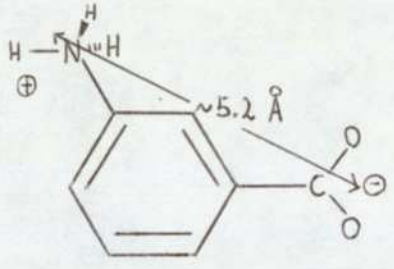

It is particularly vexing that they should be inactive, as they are potentially a set of <u>rigid</u> agonists. Since electronic effects due to the properties of the benzene ring is the most probable reason for their inactivity, a detailed study of the electron distribution may prove fruitful (ie EP maps, LUMO analysis, etc).

The schematic of the GABA pharmacophore

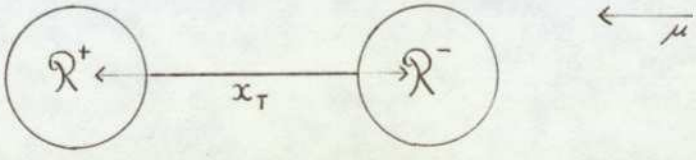

immediately suggests the representation of the molecule as a dipole. The study of intermolecular variation of CNDO/2 dipole moments may, therefore, provide some interesting correlations. It should be noted that $\mu \equiv \mu([\mathcal{R}^+],[\mathcal{R}^-],[x_T])$, and so in theory offers a term describing the contributions of $\mathcal{R}^+$ and $\mathcal{R}^-$, since at a given x_T $[\mu]_{x_T} \equiv f([\mathcal{R}^+],[\mathcal{R}^-])$. This suggests that an SAR based on

$$\log \mathcal{P}_a = c_6 \Delta[\mu]_{x_T} + c_3 \Delta[x_T]$$

might be an improvement over equation (4)[1] (5.3.1), as the heterogeneity of terminal groups can be accounted for by the c_6 term.

Apart from future work which can be carried out using the theoretical methods, there are a great deal of experimental studies which need to be carried out and these are discussed next.

5.7.4 Future work: experimental

The pharmacological reports on the potency of agonists cover a wide range of biological preparations. A comprehensive study of GABA agonists is required on one preparation and using the same measuring techniques throughout. The present experimental situation parallels the theoretical one, where the prediction of conformation and electronic structure are made using a variety of MO methods. This thesis, using one MO method consistently, is the theoretical version of what is required experimentally with regard to potency measurements.

The discovery of a good proven competitive antagonist would greatly aid the elucidation of the nature of GABA receptor-mechanism.

Studying agonists and antagonists is of course an indirect way of investigating the receptor structure. At present it is the only practicable approach to the problem. It is hoped that in the future the isolation of the receptor will be possible, allowing a direct approach to be made towards determining its structure. Consideration of the possibility of elucidating the structure of the GABA-transaminase enzyme, either complexed with GABA or otherwise, is also called for. In view of the remarks made in this paragraph, it appears that the results of X-ray crystal structure determinations, which played a key role in the early studies of the GABA system (and are still of great value), are the means by which the final steps towards an understanding of the transmitter-receptor interaction may be made.

5.8 The Glutamate Neurotransmitter System

5.8.1 Introduction

Although in the preceeding chapters little mention has been made of GLU and its agonists, clearly much of the material is relevant. The important functional groups of the GABA system (ie $-NH_3^+$, $-COO^-$ and isoxazolidone) are also the important ones of the GLU system. Part of the argument for using CNDO/2 was based on a study of the potent GLU agonist ITA, implying the suitability of that method for the mono-anions of the GLU system. The observations of Chapter 3 are therefore immediately applicable to the GLU system. In this section a brief study will be made of ideas subsequent to Chapter 3, this time with direct bearing on the GLU system.

5.8.2 A solvent study of a GLU agonist: ITA

The results of this are most conveniently discussed in terms of alterations to the configuration of the conservative molecule. The stability of the conformation predicted for the conservative molecule appears to be due to the formation of three fused rings, two of which are formed by the interaction between two of the onium protons and nearby O^- atoms (Fig.5.9). Since there is no appreciable bond-index between the H^+ and O^- atoms the interaction is presumably electrostatic. Although the H^+-O^- distances in the pseudo-rings are both ca. 2Å, the product of the NAPs is largest for the interaction O2-H17 in ring 3, and therefore the barrier to rotation about C3.C4 should be greater than that about the C4.C6 (on purely electrostatic considerations): CNDO/2 energy barriers are in accord with this, the barriers being 10.1 and 8.8 kcal mol^{-1}, respectively. Also we note that the conformation of ring 3 is analogous to the CNDO/2 minimum-energy conformation of glycine. The configuration of the quasi planar 5-ring:

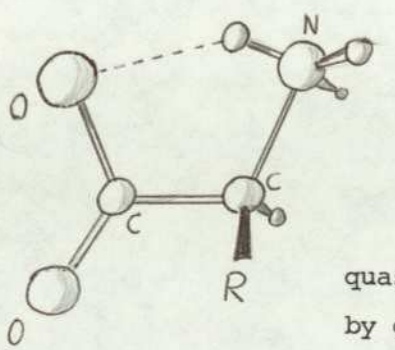

quasi-planar 5-ring formed by glycine moiety.

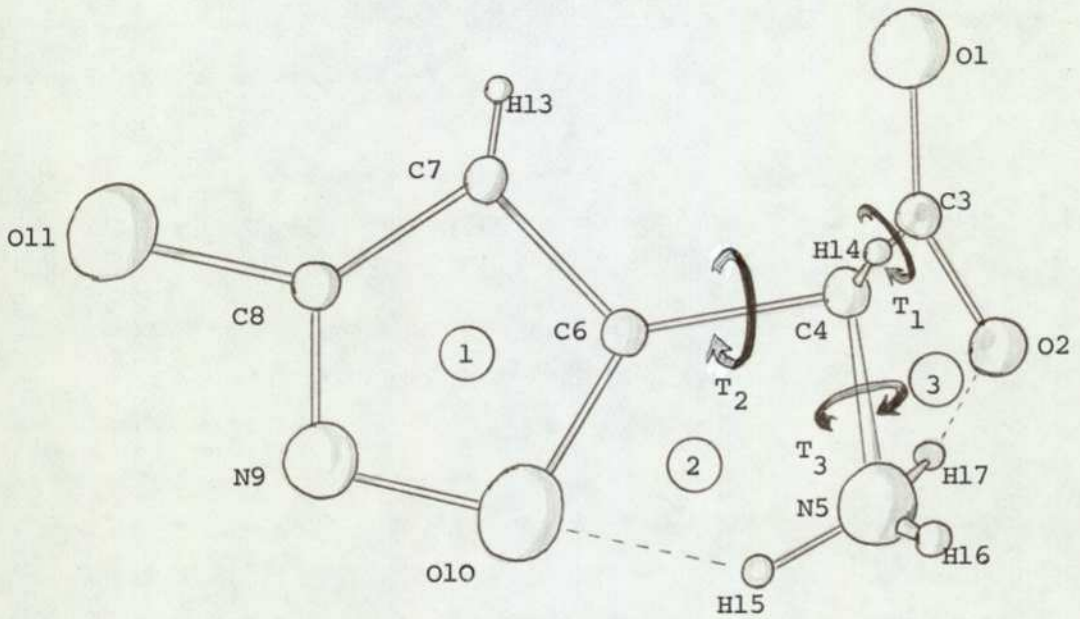

Fig. 5.9 The ibotenic acid mono-anion in its CNDO/2 predicted gas-phase conformation. The torsion angles have been previously defined in 3.6.

is common in crystal structures (eg glycine (Marsh, 1958), amino-malonic acid (Kanters, Kroon, Beurskens & Vliegenthart, 1966), D,L-aspartic acid (Thyagaraja Rao, Srinivasan & Valambal, 1968), D,L-homocysteic acid (Steward & Clarke, in preparation).

The continuum solvent methods described in Chapter 4 have been used, (T_1, T_2) energy maps for the molecule in the gas phase and in the solvent phase are shown in Fig.5.10. Contours are drawn at 1 kcal mol^{-1} intervals around the global minimum: on a classical Boltzmann distribution only those states within 5 kcal mol^{-1} of the global minimum are effectively populated (3.6.3) and this is the highest contour marked.

Neither continuum method shows a change in conservative-molecule minimum-energy conformation about C3.C4 (T_1). In contrast, both methods predict the same change in preferred conformation about the C4.C6 (T_2) bond, viz a further rotation of 200° in T_2 in the sense of Fig.5.9. Calculations on a supermolecule model are not tractable, apart from the larger parent molecules of the glutamate system there are also more solvation sites due to the mono-anionic nature of the drugs.

Unlike the GABA system where the molecules are zwitterions with a single charge-separation parameter (x_T), and where a preliminary PE study has revealed a promising SAR, in the GLU system the presence of three charge-separations

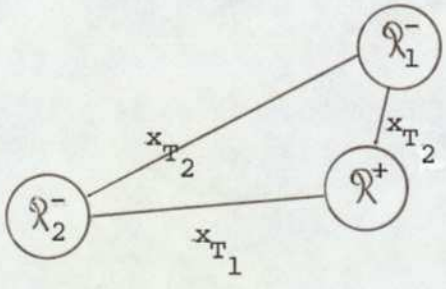

increases the complexity of the problem. However, the present results suggest that the configuration of the glycine-like part of the molecule (which is a feature common to most GLU agonists) is likely to be very stable due to the cyclising tendency, retaining its form even in aqueous solution. This implies that the conformation of this part of the molecule may be regarded as a constant feature of GLU agonists, thereby reducing the problem to two intercharge distance variables x_{T_1} and x_{T_2} (with x_{T_3} constant at ca.3.2Å). The implication of these latter comments to the GLU pharmacophore are now discussed.

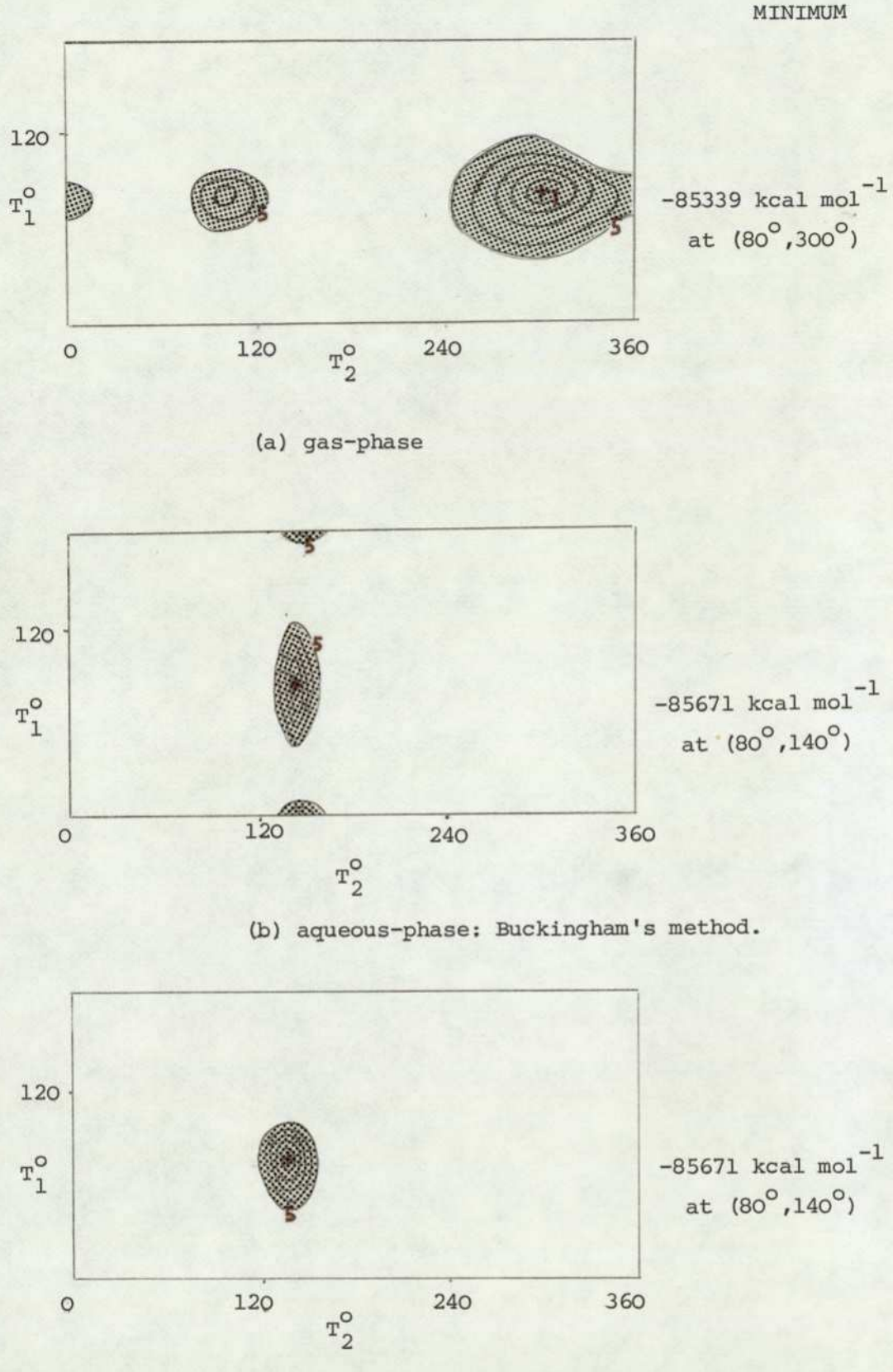

Fig. 5.10 Energy contour maps for the ITA mono-anion (a) in the gas, and (b)&(c) in the aqueous , phases. T_3 has been kept in the conformation shown in Fig. 5.9.

5.8.3 The GLU pharmacophore

The pharmacophore of the GLU system is naturally of much greater complexity than the corresponding GABA one. It is best discussed in terms of a SAR study using empirical calculations similar to that made by Steward and Clarke (1975) for the GABA system.

The GLU agonists considered for this study are

		potency rel. to GLU≠
(i) Ibotenic acid	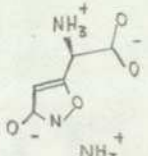	3.5
(ii) amino malonate	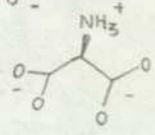	0.24
(iii) aspartate	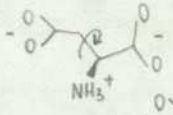	1.0
(iv) glutamate	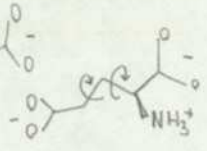	1.0
(v) aminoadipate	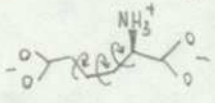	0.24
(vi) aminopimelate	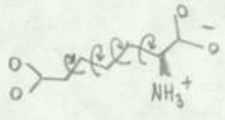	0.24

All possess an asymmetric α-carbon and are thus enantiomorphic. The potencies given above relate to racemic mixtures, and although there is a general tendency for the L-forms to be more potent, the effect of enantiomorphom is neglected in this simplistic study.

In the GABA empirical study the existence of rigid agonists allowed a receptor flexibility curve to be deduced. This approach is not possible here due to the lack of structurally rigid GLU agonists. The best that is possible is to note that owing to a fortuitous alignment of the C4.C6 bond in ITA this molecule is essentially a rigid analogue of GLU (c.p. MM and GABA system). Since ITA exhibits a high potency (4 times the canonical molecule (GLU)) it is deduced that its (constant) values of x_{T_1} = 5.1Å and x_{T_2} = 5.4Å must be close to the optimum charge-separations required by the receptor. Aminomalonic acid (Am) also possesses a unique set of x_Ts. Hence, it is possible to plot the position of these two molecules on an x_{T_1} - x_{T_2} plane, and subsequently to define a linear potency-scale

≠ All potencies from studies on spinal interneurones (Curtis & Watkins, 1960, 1963)

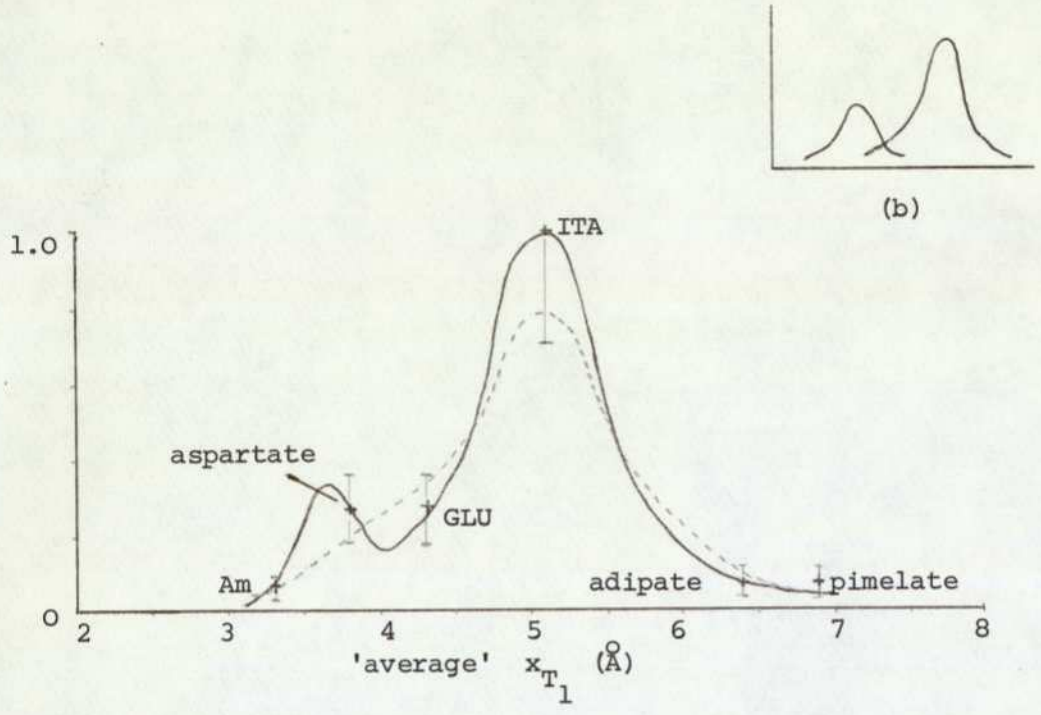

Fig. 5.11 Plot of rel. potency .v. 'average' x_T for GLU agonists. Two possible curves are shown in (a), and an analysis of one of the curves into two receptor populations is suggested in (b).

agonist	T	rel. potency (ITA=1)
Aminomalonate (Am)	0.07	0.07
Aspartate (asp.)	0.23	0.28
GLU	0.43	0.28
Aminoadipate	0.44	0.07
Aminopimelate	0.12	0.07
ITA	1.00	1.00

Table 5.2

Table of relative potency (ITA=1) and total interaction probabilities (T) for some GLU agonists.

based on them (relative to ITA = 1.0)

all measurements in Å

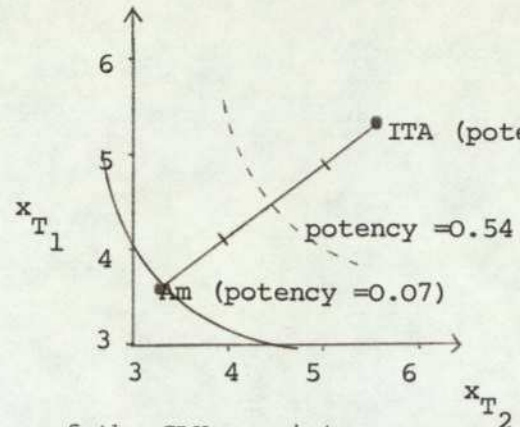

The x_Ts of the GLU agonists are now calculated using the empirical energy method due to Gill (1959, 1965) and used by Steward and Clarke (1975) in their study of GABA agonists. This gives for each agonist a x_{T_1} - x_{T_2} plane (see Appendix E) eg aspartate (asp)

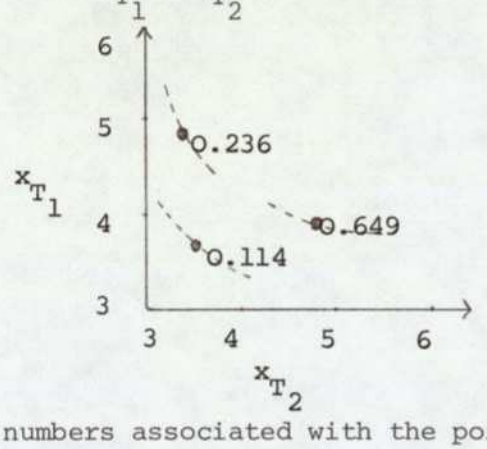

the numbers associated with the points are the relative populations (Pi) having those x_Ts. A total interaction probability (T_n) may now be calculated using the linear potency-scale

$$T_n = \sum_i \text{Pi x (potency of molecule n rel. to ITA)}$$

where i is number of points on x_{T_1} - x_{T_2} plane for molecule (eg 3 for asp). The results are shown in Table 5.2. It is clear that, unlike the GABA study, a linear relationship will not occur for a log (T).v. log(rel. potency) plot. However, using the linear potency-scale it is possible to associate with each T a unique x_{T_1} and x_{T_2}. (This 'average' x_T is thus weighted with respect to the population distribution of the particular molecule (n) under consideration, and represents the x_T of a rigid molecule having a total interaction probability of T_n. A plot of ('average' x_T).v. (rel. potency) is given in Fig.5.11(a)≠, together with a possible

≠ x_{T_1} has been used to illustrate the following analysis, however using x_{T_2} qualitatively similar results are obtained.

curve through the points and in Fig.5.11(b) a subsequent analysis of that curve into 2 components. Within the error limits of the pharmacological data it is just possible to draw a Poissonian curve through the points in 5.11(a) (dotted line). (It is difficult to evaluate the error limits which must exist for x_Ts, but it is probable that these are such as to make the Gaussian-type distribution totally consistent with the points on 5.11(a).)

It is tentatively concluded from this study that the simple empirical calculations are consistent with

(i) a population of receptors with x_R peaking at 5.1Å; or

(ii) a population of receptors of 2 types, one (asp) with x_Rs peaking in the 3-4Å range, and a second (GLU) with x_Rs peaking in the 5-6Å range.

The second possibility is of interest since two distinct populations of GLU receptors have been identified in the insect neuromuscular junction (Lea & Usherwood, 1973), subsequent work by McLennan (1974) and Johnson et al (1974) covering a number of preparations have supported this observation.

5.8.4 Conclusions

The GLU system presents problems of greater complexity than the GABA system. This is true from both a theoretical and experimental viewpoint. The theoretical methods used for the GABA system are all equally applicable for GLU. (CNDO and the continuum solvent-methods have been applied satisfactorily to ITA). As for future work a study of the potent GLU agonist quisqualic acid,

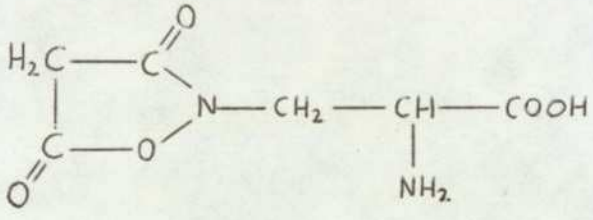

would be relevant for both the GLU and GABA systems. The experimental evidence, and the theoretical possibility noted here - that two types of receptor for GLU may exist - suggests that a conformational MO study of asp and GLU would be of interest.

The Steward and Clarke (1975) study of GABA agonists used an approach which was an extension of that described by Gill (1959, 1965) who related conformational population with activity in two series of acetylcholine antagonists but did not develop a model for receptor flexibility; this was not possible due to lack of rigid acetylcholine antagonists. In the GABA work, however, it was

possible to construct a model of receptor flexibility based on the x_Ts of rigid agonists. In 5.8.3 we have compromised, the lack of an adequate number of rigid agonists has prevented us from constructing a model of receptor flexibility in the way of the GABA study, but on the basis of two rigid agonists a simplistic treatment of flexibility has been made, viz that the receptor response is linear rather than Gaussian.

6.1 Introduction

6.1.1 Preamble

Just as the transition from the GABA to GLU system involved a step up in size and complexity, both with respect to the molecules and their pharmacophores, so too the transition from GLU to the prostaglandins (PGs). Less was known about the GLU receptor population than that of GABA, and even less is known about PG receptors. Because of the lack of pharmacological data on the PGs, this chapter will be by way of a feasibility study on the possible future use of theoretical techniques in PG SAR studies.

6.1.2 Available data

Despite the great amount of effort being directed into PG research, very little pharmacological data has appeared in press. This is due to the fact that activity in PG research, at the present time, is largely the result of the interest shown by multi-national drug companies.

Fortunately the results of X-ray crystal structure determinations are available for PGs A_1, E_2, $F_{1\beta}$, E_1 and B_1 (see Appendix A for nomenclature of PGs). This is important for the construction of the coordinates required for our MO calculations. The crystal structures will be considered in more detail in 6.2.1. Some work has also been carried out using circular dichroism (CD), the implication of this will also be looked at later.

Theoretical calculations on the PGs are, at present, limited to an EHT study of PGE_1 (Hoyland & Kier, 1972) and an '*ab initio* by fragments' study of PGF_1 (Ryan & Christoffersen, 1974). These theoretical studies are briefly reviewed in 6.2.2.

6.2 Discussion of some published results

6.2.1 The experimental methods

Firstly, the conformations obtained from the crystal structures will be discussed; these are shown in Fig.6.1. This Fig. clearly shows the 'hairpin' structure of the PGs. The 'hairpin' has been noted in all PG crystal structures except PGB_1 (De Titta, 1976) where the tendency for two carbon double-bonds to adopt a 'trans' configuration results in

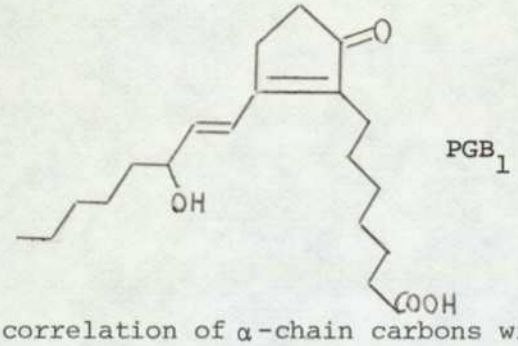

PGB_1

The correlation of α-chain carbons with their vicinal β chain carbon (shown on PGE_1 in Fig.6.1) is reminiscent of lipophilic bonding. An interaction between α and β chains, when in a hairpin configuration, is further suggested from considerations of PGE_1 and PGE_2. In PGE_2 the 5,6 double-bond brings the α-chain closer to the β-chain, apparently resulting in a reorientation of the β-chain about the bond indicated in Fig.6.1. Similarly in $PGF_{1\beta}$ the chains are in closer proximity than with PGE_1 and again there is a re-orientation, this time of the α-chain. In general, the intra-chain orientations remain remarkably constant in all the structures, methylene staggering forces appearing dominant. The CD study of Leovey & Andersen (1975) has been interpreted as implying the close spatial proximity of the chains in polar protic media.

We conclude that (i) an interchain interaction does occur in the crystal phase, and (ii) this interaction is present and may be enhanced (by lipophilic forces) in a solvent phase.

6.2.2 The theoretical methods

Hoyland & Kier (1972) have attempted a conformational study of PGE_1. The study has been carried out in the gas-phase, without any mention of the relevance of this phase to the actual environment in which the molecule acts. The calculation was made prior to the availability of X-ray crystal data, and no details of the geometry used was mentioned. Explicit chain-chain interactions have been added to the usual conformational energies, the electronic data for these interactions having been calculated by IEHT (Iterative

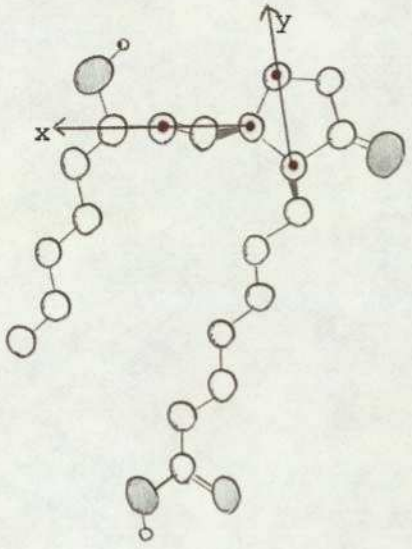

PGA_1 (monoclinic polymorph)

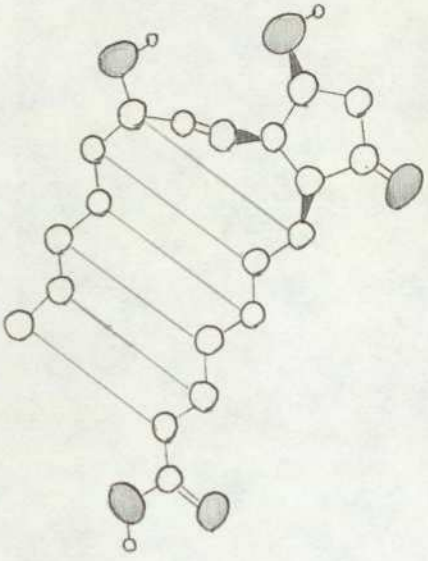

PGE_1

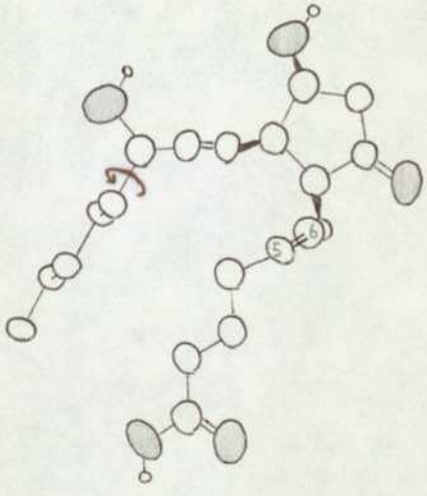

PGE_2

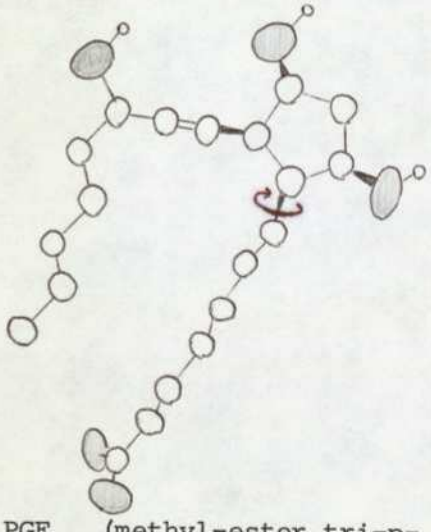

$PGF_{1\beta}$ (methyl-ester,tri-p-bromobenzoate)

Fig. 6.1 Crystal conformation of PGE_1 , PGE_2 , PGA_1 and $PGF_{1\beta}$. Projections are on an x-y plane (defined on PGA_1 diagram) which shows the 'hairpin' configuration of the side chains.

Extended Huckel Theory). The study concludes that the two chains will tend to align themselves due to dispersion forces. It must, however, be mentioned that the study contains several assumptions (re. ring puckering and torsion angles of bonds adjacent to ring) which are open to criticism.

The 'ab initio by fragments' study (Ryan & Christoffersen, 1974) is less ambitious than the previous EHT study, only electron distribution being discussed. The study is of $PGF_{1\beta}$ using the X-ray structure data (Abrahamsson, 1963) to construct the coordinates, again the calculations are for the gas-phase. The orbital energies have been used to identify the reactive regions of the molecule.

These studies represent two very different approaches by two very different MO methods. The $PGF_{1\beta}$ study represents a sophisticated MO method being used to answer some important questions on PG reaction modes. In acknowledgement of the complexity of the PGs the study attempted only to answer questions which were within the scope of the method. In contrast, the comparatively unreliable EHT method has been used on a problem of immense complexity viz the conformational modes of PGE_1. This has necessitated several assumptions, and the validity of the conclusions must be regarded as questionable. For example, in PGE_1 there are 9 Methylene-Methylene bonds, assuming only torsions of $\pm 60^{\circ}$, 180° (staggered configurations) are allowed, this requires 3^9 (ie ca. 10^4) calculations - the study comprised of 400 unspecified calculations including -OH rotations, etc!

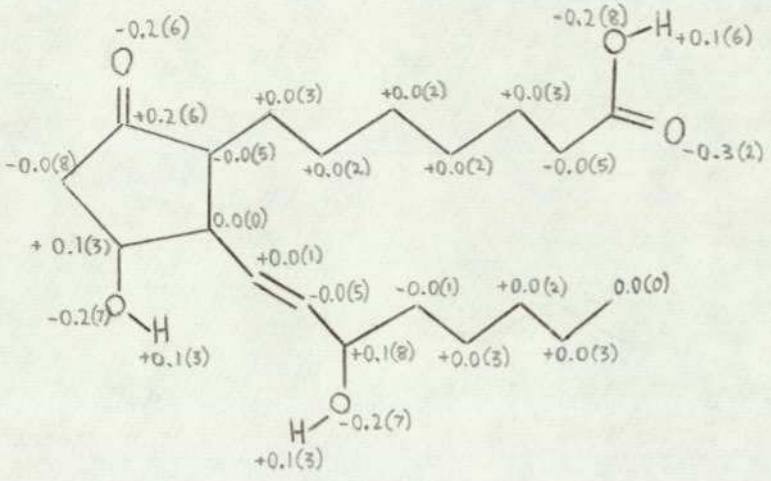

Fig. 6.2 CNDO/2 charges for the PGE_1 molecule. Charges (q) for hydrogens not shown are such that 0.95e<q <1.05e.

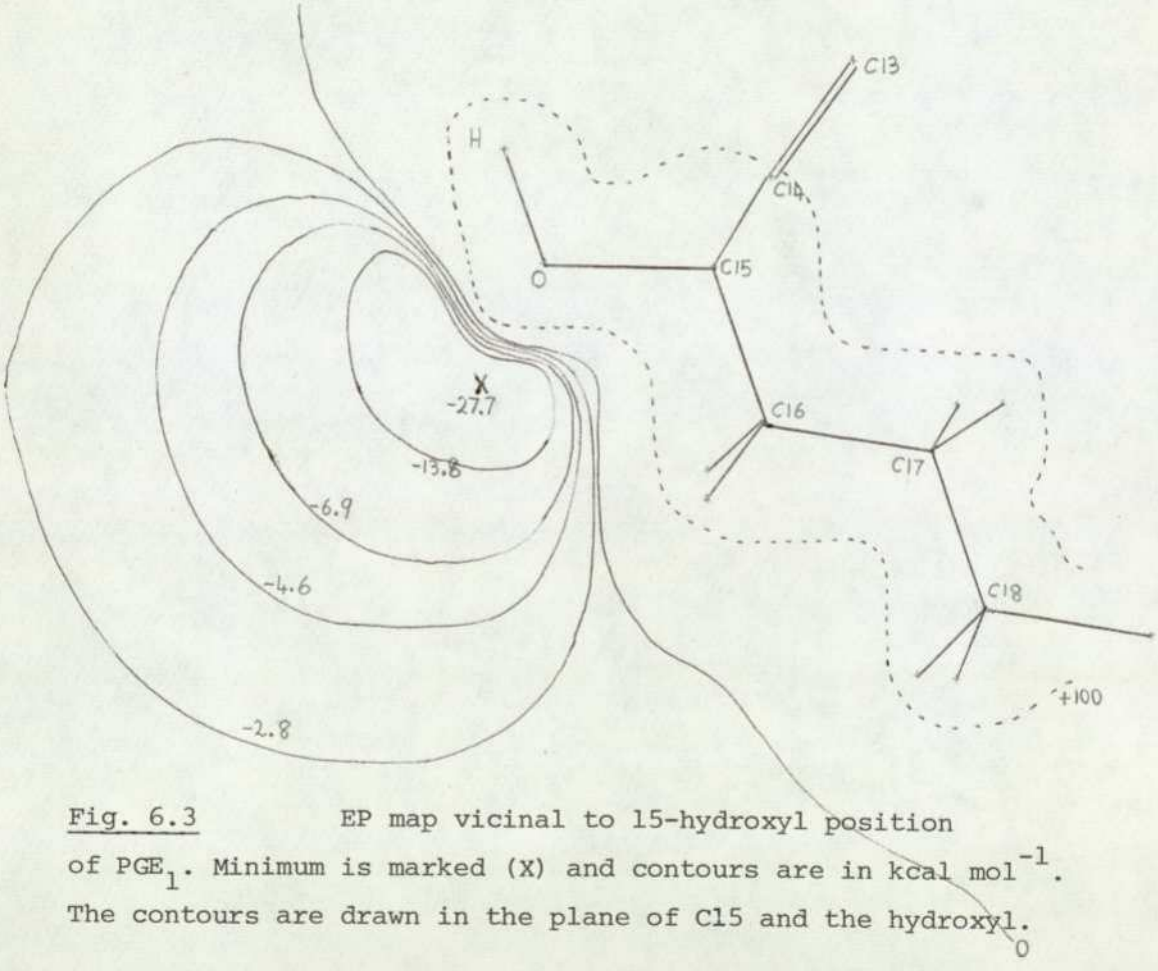

Fig. 6.3 EP map vicinal to 15-hydroxyl position of PGE_1. Minimum is marked (X) and contours are in kcal mol^{-1}. The contours are drawn in the plane of C15 and the hydroxyl.

6.3 A feasibility study on the use of CNDO/2 for the PGs

6.3.1 The initial CNDO/2 calculation

It was decided to perform calculations on PGE_1 in its observed crystal conformation. The bond lengths and angles for the non-hydrogen atoms were taken from the crystal structure determination (Spek, 1974), hydrogen atoms being added at classical positions. The electronic energy converged normally in 757 sec. (CDC 7600 time), which is to be compared with GLUs 35 seconds, and the 9 seconds needed for a GABA calculation. Clearly, conformational studies using CNDO on the full PGE_1 structure are not tractible.

The electronic structure of PGE_1 is shown in Fig.6.2; the charges are unremarkable.

6.3.2 The 'study by fragments' approach: PGE_1^t

Because of the practical problems associated with CNDO computations on a full PG molecule, a study has been made into the possibility that calculations made on isolated fragments of the molecule are relevant to the same fragment as it appears as part of the complete structure. The specific question for which this approach was designed concerned the effect on the 15-hydroxy group of β-chain substitutions at Cn ($n \geqslant 16$) atoms.

Firstly, the EP field vicinal to the 15-hydroxy group was calculated, the absolute minimum of the potential being -27.7 kcal mol^{-1}. The shape of the potential field is typical of the hydroxyl group (see Fig.6.3). The EP field is a superposition of electrostatic contributions from all the atomic cores and associated electron distributions in the molecule. In order to study the through space contributions of the α-chain to the resultant EP at the 15-hydroxy position, the α-chain contributions were suppressed. An EP minimum of -26.3 kcal mol^{-1} was obtained, without any discernible change in the shape of the field. A further suppression of contributions from the ring resulted in a minimum of -31.0 kcal mol^{-1}. It is concluded from this study involving suppression of EP field contributions that the ring and α-chain contributions will not significantly affect deductions, of an electrostatic nature, made in the region of 15-hydroxy and Cn ($n \geqslant 16$) positions.

Since the 'through space' EP contributions of ring and α-chain are of low order significance, it remains to assess the 'through molecule' importance of these moieties (ie internal electronic charges). In order to determine the effect of α-chain and ring on

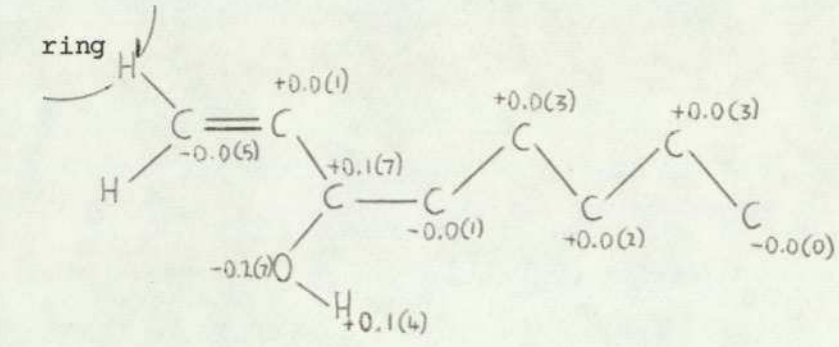

(a)

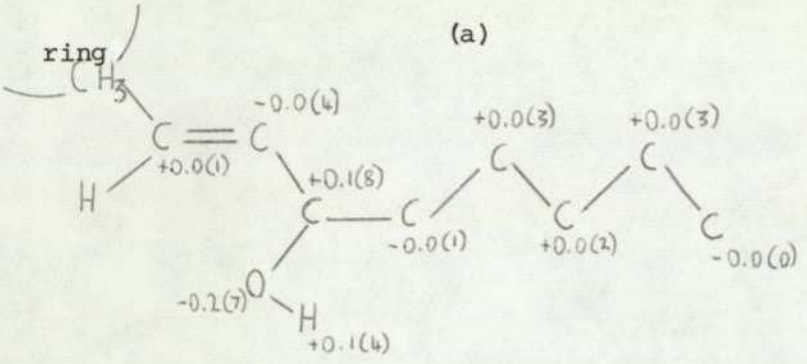

(b)

Fig. 6.4 CNDO/2 calculated charges for PGE_1 β-chain fragments. The fragments differ in their terminations at the 'ring-end', (a) is terminated by a hydrogen atom whereas (b) is terminated by a methyl group.

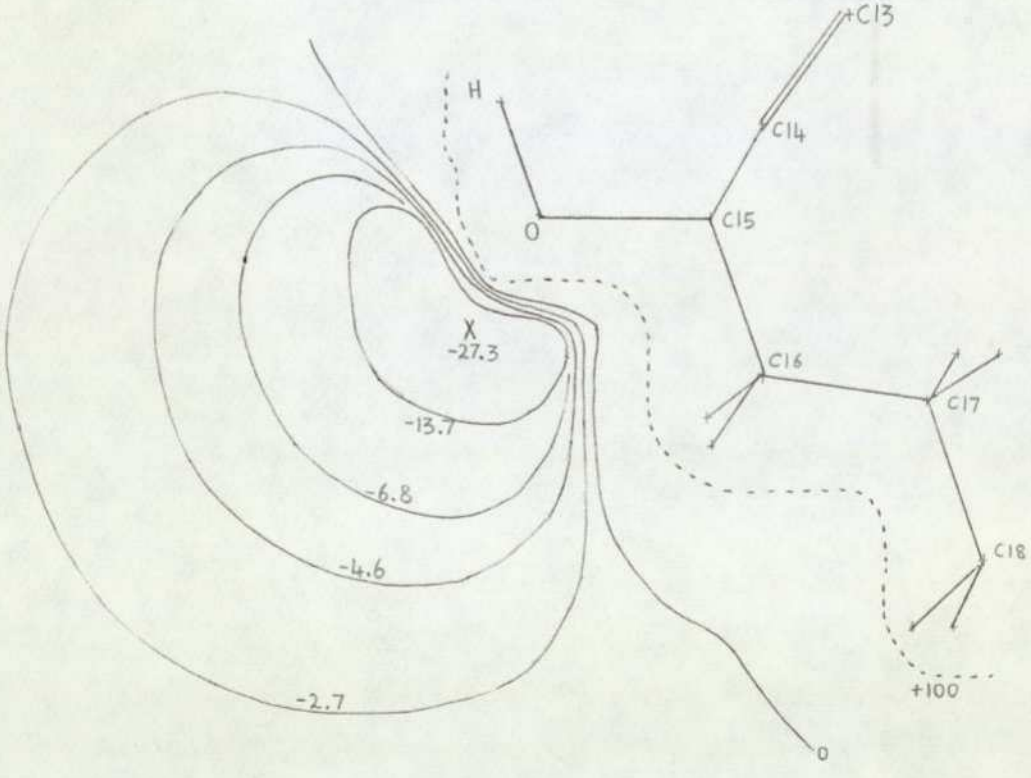

Fig. 6.5 EP map vicinal to 15-hydroxyl position of PGE_1^t. The minimum is marked (X) and contours are in kcal mol^{-1}. Contours are drawn in the plane of C15 and the hydroxyl group.

the internal atomic structure of the β-chain, a study of the NAPs of just the β-chain was made. CNDO/2 calculations were made on the fragment shown in Fig.6.4(a), the resulting NAP values are shown. Comparison of these charges with those of the complete PGE_1 molecule (Fig.6.2) show that the charges around the ethylenic linkage are poorly reproduced. In order to improve the charges a methyl[≠] group was used instead of the hydrogen atom marked H^1. The resulting NAP distribution is shown in Fig.6.4(b). This Me-terminated fragment (hereafter designated PGE_1^t) has the advantages over the previous one in that it (i) preserved the polarity of the ethylenic linkage and (ii) provides (via the methyl protons) a compensatory effect for the steric presence of the ring.

An analysis of the difference in NAPs between PGE_1 and PGE_1^t shows only 3 atoms with a difference of 0.0(1), in all other cases the difference is 0.0(0). The EP field vicinal to the 15-hydroxy has been calculated for PGE_1^t (Fig.6.5). The topography of the field is unchanged from PGE_1, and the absolute minimum of the potential is -27.5 kcal mol^{-1} (c.p. -27.7 kcal mol^{-1} for PGE_1). The CNDO/2 computing-time for one calculation on PGE_1^t is 22 sec (c.p. 757 sec. for PGE_1). It is concluded that for NAP and EP studies concerning the β-chain, PGE_1^t represents a valid model system.

6.3.3 A brief summary of a study* made using PGE_1^t

The PGE_1^t molecule has been used to study the effects of changes in the EP field at the 15-hydroxy position due to Cn ($n \geq 16$) substituents. It was found that the substitutions made at C16 and C17 did not significantly alter the EP field at the 15-hydroxy position. It was concluded that the changes in pharmacological action and potency caused by substituents of the type considered were not due to modification of the 15-hydroxy site, and neither presumably due to modification of the more distal reactive sites, eg O8, -COOH, etc. It therefore appears likely that the substituents produce their effect via conformational rather than electronic modification of the molecule.

≠ The methyl group was chosen to replace H^1 because the properties of this group observed in propene by Pople and Beveridge (1970) seemed appropriate to the present situation.

* This study was suggested as a part of other work taking place in the Department.

6.4 Conclusions

It has been shown that a 'molecular fragments' approach may be employed to study the electronic effects of various substitutions in a particular region of the molecule.

The conformational problems posed by the PGs are too complex for study by a SCF quantum MO method with the theoretical sophistication of CNDO/2. It is doubtful whether a conformational study of any real significance can be made by any MO method. The problem is possibly within the scope of empirical calculations; however the analysis of the data still presents a formidable task. It is fortunate that the PGs are primarily composed of saturated hydrocarbon linages, the conformational description of which the empirical methods are best suited to.

Applied to specific problems the theoretical methods will undoubtedly play a part in the future of PG research. However, the problems to which they are applied must be carefully chosen, with due regard for the limitations of the methods.

7.1 Overview

To fully understand how drugs act, and thereby to have the prospect of being able to design them with reliable prediction of properties, requires knowledge of how they function at the atomic level. Unfortunately, there is no technique offering hope, in the foreseeable future, of direct observation of molecular processes. The methods at present employed by medicinal chemists in developing new drugs are not likely to provide the information required since they largely use macroscopic physico-chemical data. However, the theoretical methods are capable of making an important contribution to the understanding of drug-receptor interactions at a fundemental level.

In this thesis it is hoped that the examples of the GABA, and to a lesser extent, the GLU systems have shown how an understanding of the drug-receptor interaction is possible at the molecular level. The ideas and techniques described here are of quite general applicability and, with care, should be capable of giving some insight into the operation of most drug systems.

The size of molecules to which theoretical methods can be applied is limited by the computational resources available and computer technology in general. The PGs are a case in point, only by the development of a 'fragment' approach could CNDO be applied (to any significant extent) to these molecules. However, it has recently proved possible to extend the population analysis using classical energy (PACE) scheme of Gill (1959, 1964) in order to deal with double bonds and heteroatoms (Borthwick, 1977). This extended-PACE (EPACE) scheme, although empirical, is proving a useful tool in the prediction of molecular conformation. Initial studies indicate that EPACE is well suited to the problem of the conformational modes of the PGs. The use of computationally rapid schemes like EPACE to identify a small set of preferred conformers and the subsequent study of this small set by sophisticated quantum methods may provide the means by which to consider the conformations of large molecules normally not amenable to those quantum methods. [I would therefore like to say, in the light of the work on EPACE, that previous criticisms on the use of classical methods may have been rather harsh].

A particular effort has been made to demonstrate how much information a single theoretical quantum mechanical calculation can

yield. For example; NAPs, BIs, EP maps, orbital energies, dipole-moments and the conformational energy. Perhaps sometimes it is too easily forgotten that the SCF wavefunction is the molecule and as such an identity with that collection of nuclei and electrons we call 'the drug'.

Appendix A - The nomenclature of the prostaglandins

The prostaglandins have a numbering scheme derived from prostane:

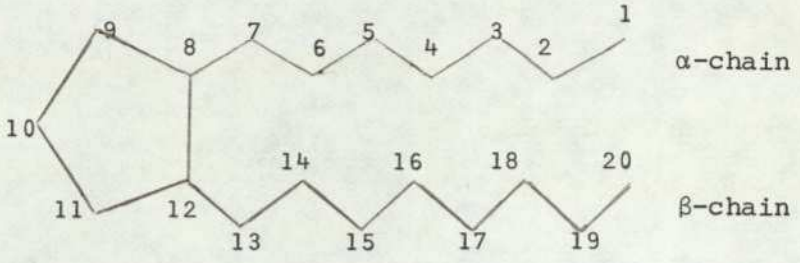

They have a general classification PGX_n, where X defines the form of the ring and n defines the double bonds in the side chains.

The X-parameter

X	ring type
A	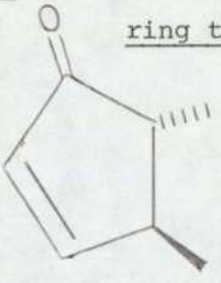
B	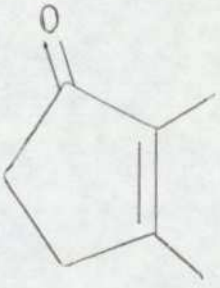
C	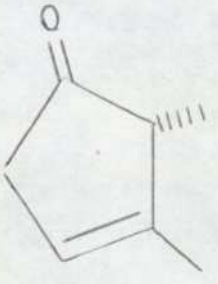
D	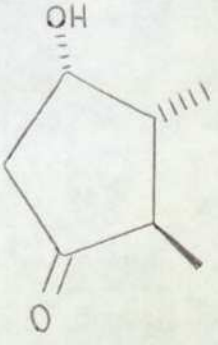
E	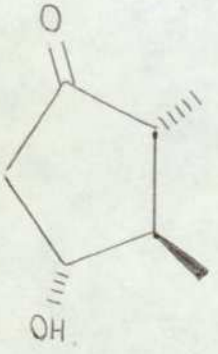

F_α

F_β

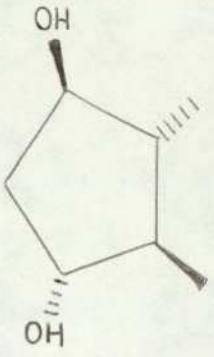

G and H

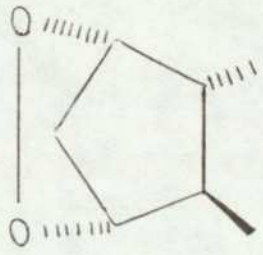

The n-parameter

n	chain type
1	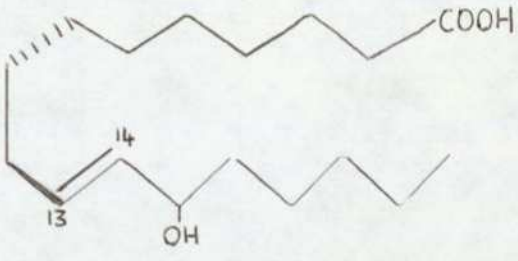
2	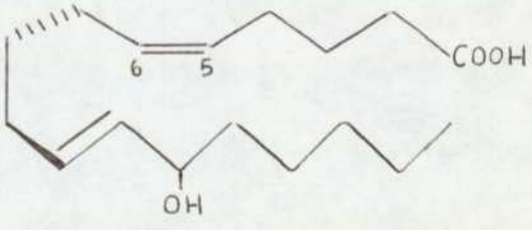
3	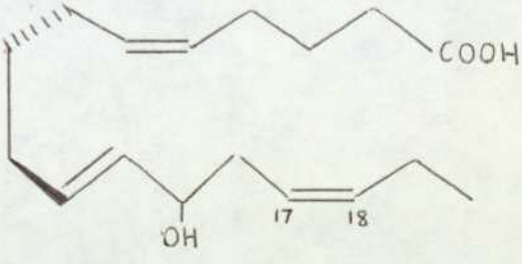

This n-parameter system is valid for all x-parameters from A - F, and for H. However, PGG_n has the form

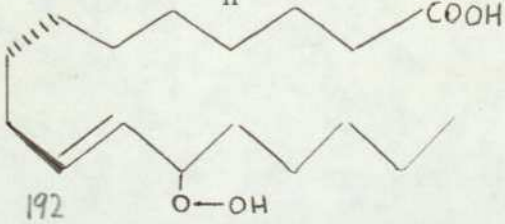

Appendix B - The methods of theoretical conformational analysis

B1 The classical methods

B1.1 Calculation of the total energy

In the direct methods the total internal energy E is minimised with respect to all or certain structural parameters. The two problems which must be solved are (i) how does E depend on the structural parameters, and (ii) how can one minimize E? In the classical method it is usually assumed that $E = V + W$, where W is the energy due to non-bonded interactions and V is the remaining energy contribution. Since V and W are found within different theoretical frameworks, the method is 'non-uniform'.

W is usually estimated as $W = \sum W_j(r_j)$, j indexing pairs of non-bonded atoms and r_j being the distance between the pair. This is the central field model. Common to nearly all classical methods W_j is evaluated by either:

(i) $W_j = -a_j r_j^{-6} + b_j r_j^{-12}$, the Lennard-Jones or '6-12' potential.

(ii) $W_j = -a_j r_j^{-6} + b_j e^{-c_j r_j}$, the Buckingham potential.

(iii) $W_j = 0$, if $r_j \geq$ sum of Van der Waal's radii for atomic pairs, or

$W_j = \infty$ otherwise, this is the hard sphere model. In (i) and (ii) r_j^{-6} terms are London or dispersion terms, they are long range, attractive, and are intended to account for dipole-dipole interactions. The remaining term is short range, repulsive and attempts to account mainly for mutual interpenetration of closed shell electrons. The various non-uniform methods differ mainly in the way they estimate V and minimise the total energy E. Firstly, the calculation of V is considered.

If $\underline{Q}$ is the vector of all bond lengths and angles, then there exists a $\underline{Q}_o$ for which E is minimum, and $\Delta\underline{Q} = \underline{Q} - \underline{Q}_o$. Now we have

$$E(\underline{Q}) = V(\underline{Q}) + \sum_j W_j(r_j(\underline{Q})) \qquad (1)$$

from this a convenient quantity D - the strain energy is defined as

$$D(\underline{Q}) = V(\underline{Q}) - V(\underline{Q}_o) + \sum_j W_j(r_j(\underline{Q})) \qquad (2)$$

The last term in (2) has been discussed, $\Delta V = V(\underline{Q}) - V(\underline{Q}_o)$ is called the deformation energy. For small steric hinderance and nonconjugated systems, V can be approximated by the harmonic model,

$$\Delta V = \tfrac{1}{2}(\Delta\underline{Q})\underline{K}(\Delta\underline{Q})^T \qquad (3)$$

where $\underline{K}$ is the square matrix of force constants. It is usual to neglect off-diagonal terms, so (3) becomes

$$\Delta V = \tfrac{1}{2} \sum_i K_{ii} (\Delta Q_i)^2 \qquad (4)$$

Changes in energy due to the barriers of rotation about single bonds are evaluated by

$$\Delta V_{rot} = V_n(1 + \cos n\theta) \qquad (5)$$

where n is the multiplicity of rotation axis and V_n is the barrier to rotation (obtained empirically). Hence, (4) and (5) give ΔV for equation (2), and (1) becomes

$$E(Q) = D(Q) + V(Q_o) \qquad (6)$$

B1.2 Minimisation of the total energy

In general, the ΔQ_i are not all independent. If q_i are the independent ΔQ_i then the strain energy can be minimised with respect to either all ΔQ_i or just the q_i. In some methods the Q_i are transformed into Cartesian coordinates x_i. This has led to three main methods:

(i) $E(\underline{Q}) \longrightarrow E(\underline{x})$, minimised by steepest descent methods. (Wiberg, 1965).

(ii) D(q), a Taylor expansion of the strain energy leads to a set of equations which are solved iteratively by the Gauss-Newton method (Jacob, Thompson & Bartell, 1967).

(iii) $D(\underline{Q}) \longrightarrow D(\underline{x})$, then as (ii). This leads to analogous equations to (ii) in which q_i are replaced with x_i (Boyd, 1968).

B1.3 Improvements and extensions

The methods that the above approaches lead to are, in principle, applicable to systems which are not conjugated and which exhibit no large steric hindrance, otherwise a delocalisation of any local distortion must be considered. For small distortions the methods described above seem to be adequate (Kitaygorodsky & Dashevsky, 1967), for larger distortions several approaches have been suggested (Coulson & Senent, 1955; Coulson & Haigh, 1963). Other refinements are the inclusion of electrostatic interactions due to charges localised on atoms and the effect of hydrogen bonding (Lugovsky & Dashevsky, 1972). A further extension has been the

the inclusion of solvent effects (Lipkind, Arkhipava & Popov, 1970).

B1.4 Discussion

The use of an r^{-6} potential is only valid for spherical charge distributions (ie atoms in s-states). For interactions between two atoms one in a p-state and one in an s-state the dispersion forces have an r^{-3} form and are repulsive. There are internal difficulties when heteroatoms are considered, and classical analysis is not justified when large distortions are involved (eg π-electron systems with conjugated double-bonds). Owing to many oversimplifications (eg hard-sphere model) the results of classical analysis are often uncertain, although successes are by no means rare.

It is not possible of course to calculate any electronic parameters from the classical analysis since no explicit account is made of the electron. Their position with respect to calculating conformational energies may, therefore, be likened to a rather superior form of space-filling model.

A rather different empirical approach was suggested by Gill (1959, 1964) which is based on population analysis. The method can be used with an electrostatic correction term which allows for consideration of the solvent. Although originally applicable only to saturated hydrocarbons, the method has been extended to successfully predict the preferred conformers of molecules containing unsaturated linkages and heteroatoms (Borthwick, 1977).

B2 The Quantum mechanical formalism

B2.1 The Hamiltonian operator

The starting point for any quantum mechanical approach is the non-relativistic electronic Schrodinger equation for a molecule with n electrons

$$\tilde{H}|\Psi\rangle = E|\Psi\rangle \qquad \text{(i)}$$

where $|\Psi\rangle$ is the molecular wavefunction which is dependent on the spatial and spin coordinates x_i of the electronic distribution, $\tilde{H}$ is the Hamiltonian (the tilde is used to stress its operator nature) and E is the total electronic energy. By 'non-relativistic' it is implied that $\tilde{H}$ does not contain spin-spin, spin-orbit coupling terms, etc. However, it should be noted that spin does enter the problem in an essential way via our insistance that Ψ should be an eigenvector of

$$\tilde{P}\,|\Psi\rangle = (-1)^P\,|\Psi\rangle \qquad \text{(ii)}$$

where $\tilde{P}$ is the permutation operator ((ii) is a mathematical expression of the Pauli exclusion principle (Pauli, 1925)).

The 'electronic' part of (i) emerges from the Born-Oppenheimer approximation, this is the assumption that the electrons adjust instantaneously to the motion of the nuclei. Equivalently, the Born-Oppenheimer approximation may be stated as being the assumption that the nuclei are static. This means their kinetic energy is zero, and their potential energy of interaction,

$$V_{NN} = \sum_{\alpha}^{N} \sum_{\beta>\alpha}^{N} Z_\alpha Z_\beta / R_{\alpha\beta} \qquad \text{(iii)}$$

where α,β label the N nuclei of the system, is decoupled from the problem and may be independently accounted for at the end of the calculation.

The 'electronic' Hamiltonian operator $\tilde{H}$ can now be written,

$$\tilde{H} = \sum_{i=1}^{n} -\tfrac{1}{2}\nabla_i^2 - \sum_{i=1}^{n}\sum_{\alpha}^{n} Z_i/R_{\alpha i} + \sum_{i=1}^{n}\sum_{j=i+1}^{n} 1/r_{ij} \qquad \text{(iv)}$$

The major difficulty in solving (iv) is the presence of the r_{ij}^{-1} terms. The model of independent electrons allows a simpliciation by introducing for each electron the mean potential V_i produced by all the other electrons and the nuclei. This is the Hartree-Fock model (Hartree, 1928; Fock, 1930) and it allows (iv) to be written as

$$\tilde{H} = \sum_{i=1}^{n}(-\tfrac{1}{2}\nabla_i^2 - \sum_{\alpha} Z_i/R_{\alpha i} + V_i) = \sum_{i=1}^{n} \tilde{h}_i^{eff} \qquad (v)$$

where $\tilde{h}_i^{eff}$ is the effective one-electron Hamiltonian operator. It is evident that V_i depends on the spatial distribution of all the other electrons. In other words it is necessary to know the solutions of (i) with Hamiltonian (v) in order to construct V_i: if solutions of (i) using (v) are identical to those used in construction V_i then they are said to be self-consistent, ie consistent with their own potential field. This concept of a self-consistent field (SCF) is crucial to the development of the following theory.

B2.2 Wavefunctions and orbitals

The solution of the Hartree-Fock problem is usually expressed in terms of spin orbitals. An orbital is strictly defined as an eigenvector of the one-electron Hamiltonian (v), although it has become common to use the term rather more loosely. The spin orbitals are conveniently written as $|ij\uparrow\rangle$ or $|ij\downarrow\rangle$, i being the spatial orbital the j^{th} electron occupies and $\uparrow,\downarrow$ indicate the spin state of the electron. (Note it has become customary to write the two spin orbitals $|ij\uparrow\rangle$ and $|ij\downarrow\rangle$ as $|ij\rangle$ and $|\bar{ij}\rangle$, respectively). The spin orbitals are then used to construct an approximate molecular wavefunction which satisfies the antisymmetry requirements of the Pauli exclusion principle, these requirements are met by the Slater determanent (Slater, 1930[a], 1959),

$$|\Psi\rangle = A \begin{vmatrix} |\underline{1}1\rangle & |\underline{1}2\rangle \ldots\ldots |\underline{1}n\rangle \\ |\bar{1}1\rangle & |\bar{1}2\rangle \ldots\ldots |\bar{1}n\rangle \\ \ldots\ldots\ldots\ldots\ldots\ldots \\ |\tfrac{1}{2}n1\rangle & |\tfrac{1}{2}n2\rangle \ldots\ldots |\tfrac{1}{2}nn\rangle \\ |\tfrac{\overline{1}}{2}n1\rangle & |\tfrac{\overline{1}}{2}n2\rangle \ldots\ldots |\tfrac{\overline{1}}{2}nn\rangle \end{vmatrix} = A\,|\,|1\rangle\,|\bar{1}\rangle \ldots |\tfrac{1}{2}n\rangle|\tfrac{\overline{1}}{2}n\rangle\,| \qquad (vi)$$

where A is a normalisation factor as determined by the condition

$$\langle\Psi|\Psi\rangle = 1 \qquad (vii)$$

B2.3 The Roothaan-Hartree-Fock equations

In order to further facilitate solution of the Hartree-Fock equations Roothaan (1951) suggested that the spin orbitals $|i\rangle$ of (vi) should be approximated as a Linear Combination of Atomic Orbitals (LCAO),≠

≠ Throughout this and subsequent chapters Latin indices will label spin orbitals and Greek indices the AOs.

$$|i\rangle = \sum_{\nu} c_{i\nu} |\nu\rangle \qquad \text{(viii)}$$

The atomic orbitals (AO) employed are usually either Slater type orbitals (STO) (Slater, 1930[b]) or Gaussian type orbitals (Boys, 1950) (GTO). The type of AO used will be discussed in more detail later.

Equation (i) may be written as, (using (vii))

$$E = \langle \Psi | \tilde{H} | \Psi \rangle \qquad \text{(ix)}$$

if now a δ-variation of E is made with respect to the SOs then

$$\delta E = 0 \qquad \text{(x)}$$

gives the condition for a minimum of the energy. This variation is carried out by the method of undetermined multiplyers and leads to the equations of Roothaan,

$$\sum_{\nu} F_{\mu\nu}^{(i)} c_{i\nu} = E_i \sum_{\nu} S_{\mu\nu}^{(i)} c_{i\nu} \qquad \text{(xi)}$$

where the E_i are the orbital energies (eigenvalues of the i^{th} MO),

$$S_{\mu\nu}^{(i)} = \langle \mu | \nu \rangle \quad , \text{ the overlap integrals} \qquad \text{(xii)}$$

and $F_{\mu\nu}^{(i)}$ is called the Fock matrix.

B2.4 The atomic integrals

The Fock matrix of equation (xi) is explicitly

$$F_{\mu\nu}^{(i)} = \left[\langle \mu i \left| -\tfrac{1}{2}\nabla_i^2 - \sum_{\alpha} V_{\alpha}(r) \right| i\nu \rangle\right] + \left[\sum_{\lambda\sigma} P_{\lambda\sigma} \{\langle \mu i | \nu i \rangle r_{ij}^{-1} \langle \lambda j | \sigma j \rangle - \tfrac{1}{2}\langle \mu i | \sigma i \rangle r_{ij}^{-1} \langle \nu j | \lambda j \rangle\}\right] = H_{\mu\nu}^{(i)} + G_{\mu\nu}^{(i)} \qquad \text{(xiii)}$$

The core Hamiltonian matrix ($H_{\mu\nu}$) contains terms due to the kinetic energy of the electrons and the potential energy of the effective electrostatic field produced by the nuclei and the other electrons (see equation (v)). The total electron-interaction matrix ($G_{\mu\nu}$) is notationally written as

$$G_{\mu\nu} = \sum_{\lambda\sigma} P_{\lambda\sigma} \{(\mu\nu|\lambda\sigma) - \tfrac{1}{2}(\mu\sigma|\nu\lambda)\} = J_{\mu\nu} - \tfrac{1}{2}K_{\mu\nu} \qquad \text{(xiv)}$$

where $P_{\lambda\sigma} = 2\sum c_{i\lambda} c_{i\sigma}$ (i summed over all occupied orbitals) is the density matrix. The matrix $J_{\mu\nu}$ is the matrix of the Coulombic repulsion integrals, ie the integrals describing the total electron-electron repulsion assuming that all electrons move independently in the orbital assigned to them. The matrix $K_{\mu\nu}$ is the matrix of the exchange integrals and these are a correction for the stabilisation due to correlation of parallel spinning electrons.

We have, therefore, the following integrals which must be evaluated,

$$\text{overlap integrals } S_{\mu\nu} = \int \phi_\mu(i)\phi_\nu(i)\, d\underline{x}_i \qquad (<\mu i| = \phi_\mu(i))$$

$$\text{core integrals } H_{\mu\nu} = \int \phi_\mu(i)\, h_i^{\text{eff}}\, \phi_\nu(i)\, d\underline{x}_i$$

$$\text{Coulomb integrals } J_{\mu\nu} = \iint \phi_\mu(i)\phi_\nu(i)\, r_{ij}^{-1}\, \phi_\lambda(j)\phi_\sigma(j)\, d\underline{x}_i d\underline{x}_j \qquad \text{(xv)}$$

$$\text{exchange integrals } K_{\mu\nu} = \iint \phi_\mu(i)\phi_\nu(j)\, r_{ij}^{-1}\, \phi_\lambda(j)\phi_\sigma(i)\, d\underline{x}_i d\underline{x}_j$$

The integrals are of the one-electron (3-dimensional) and two-electron (6-dimensional) type over spatial coordinates (spin coordinate integrals have at this stage been explicitly evaluated).

B2.5 Solution of the Roothaan-Hartree-Fock (RHF) equations

The RHF-equations (xi) are evaluated as a self-consistent eigenvalue problem in the following manner:

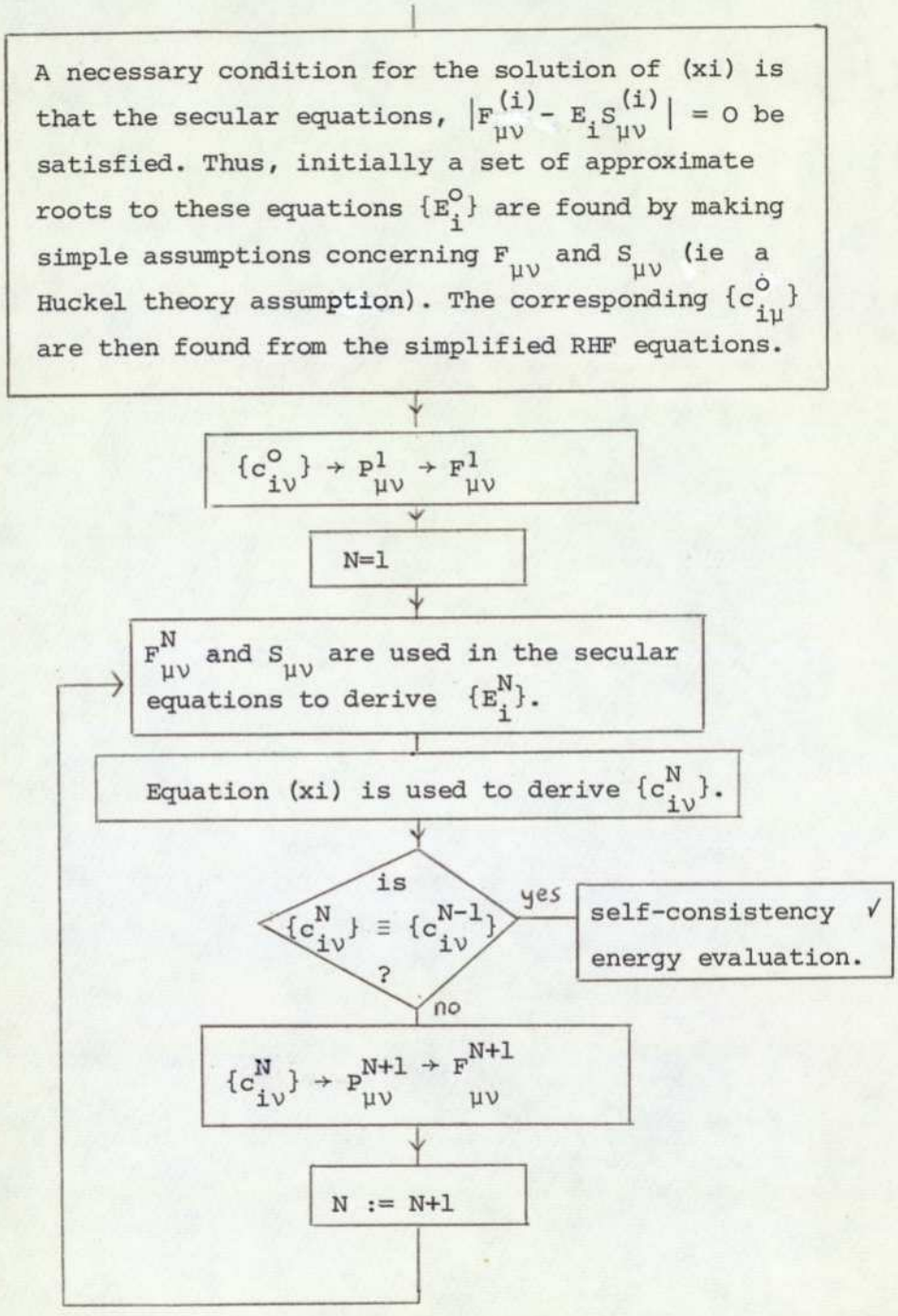

The set of self-consistent LCAO coefficients are then used to construct the total electronic energy ($\mathcal{E}_{el}$),

$$\mathcal{E}_{el} = \tfrac{1}{2} \sum_{\mu\nu} P_{\mu\nu}(H_{\mu\nu} + F_{\mu\nu}) \qquad \text{(xvi)}$$

and the total internal energy follows from (xvi) and (iii)

$$\mathcal{E}_{tot} = \mathcal{E}_{el} + V_{NN} \qquad \text{(xvii)}$$

B2.6 Improvements and extensions

In the ground state of an n electron system a given spatial orbital may contain electrons of opposite spin, the orbital energy of those electrons being degenerate. In such a system n/2 spatial orbitals will be (doubly) occupied, the electronic configuration being written as $\langle 1|^2\langle 2|^2 \ldots \langle \tfrac{1}{2}n|^2$. A configuration in which all occupied spatial orbitals contain their maximum allowed two electrons is called a closed-shell configuration. If the number of electrons is odd, the ground-state electronic configuration is represented as $\langle 1|^2\langle 2|^2 \ldots \langle \tfrac{1}{2}n|^2\langle \tfrac{1}{2}n+1|$, such a configuration is called open-shell, these configurations mainly arise in the description of excited states. The discussion of the quantum mechanical method described in B2.2 has been restricted to closed-shell systems, however, the theory is extendable to open-shell systems (Slater, 1930; Pople & Nesbet, 1954). In this thesis we have been exclusively concerned with closed-shell problems.

The SCF MO method is based on the independent-particle model (B2.1), this neglects the tendency for a given electron to adopt a position of maximum separation from all other electrons (subject to orbital constraints). This electron-correlation problem can, in theory, be resolved within the SCF MO formalism by configuration interaction (CI). CI can be explained by writing $\langle 1|^2\langle 2|^2 \ldots \langle \tfrac{1}{2}n|^2$ for the ground-state configuration and then assigning one of the electrons (say in the i^{th} orbital) to a previously unoccupied (virtual) orbital, to give the singly excited configuration $\langle 1|^2\langle 2|^2 \ldots \langle i|^1 \ldots \langle \eta_\rho|\langle \eta_{i+1}|$. In an analogous way it is possible to build doubly, triply and higher order excited configurations, the correct total wavefunction is then assumed to be the superposition of wavefunctions (Slater determinants) of all possible configurations. CI is computationally a time consuming procedure and we will assume that, in general, for ground-state conformational

studies SCF MO theory is satisfactory. This is equivalent to the assumption that the correlation energy is not dependent on the detailed structure of the molecule.

In early computations it was customary to use Slater type orbital (STO) as the AOs of the LCAO expansion. Later in order to facilitate rapid evaluation of the atomic integrals it was suggested that a linear combination of n Gaussian functions be used in place of the STOs (eg STO-3G) (Hehre, Stewart & Pople, 1969). A further development has been the use of extended basis sets. These extended bases offer a more flexible description of the atoms in the valence regions. A commonly used basis is one in which the orbitals are split into inner and outer parts, since there are now two orbital exponents (ζ) instead of the usual one, they are known as 'double-zeta' bases (Ditchfield, Hehre & Pople, 1971). If the inner shell is represented by 4 Gaussians and the valence shell orbitals by a 3 Gaussian inner part and a 1 gaussian outer part, then the basis is denoted 4-31G. The 4-31G double-zeta basis has been applied to a number of organic molecules and generally offers a considerable improvement over STO-3G ab initio results. An even more sophisticated basis results if extra orbitals of higher angular symmetry (ie d orbitals on carbon, nitrogen, etc) are included (Cade & Huo, 1967). Two bases of this kind which have been used is a 6-31G with d-orbitals on heavy atoms (designated 6-31G*), and a 6-31G* with additional p-orbitals added to hydrogen atoms (designated 6-31G**).

B2.7 Discussion

The method outlined in B2 constitutes the ab initio approach to MO theory. Clearly it is a non-empirical method of high theoretical validity. The major problem is the fact that computation times are very high even for a single conformation. Recently an efficient and rapid ab initio program has been written, and limited conformational studies on organic molecules in small basis sets (STO-3G) are now possible (Hehre, Lathan, Ditchfield, Newton & Pople, 1973).

It should be stressed that although the ab initio method is of high theoretical validity, this feature is not necessarily reflected in the results. Absolute energies are in error by c. 100 kcal mol^{-1} per atom, ΔH_a can be in error by up to $\pm$100% (even with CI) and heats of reaction are inaccurate if small basis sets are used (Dewar, 1975). In general, however, the ab initio methods represent the most reliable and widely applicable of the theoretical methods.

B3 The semi-empirical methods

B3.1 Introduction

The classical non-uniform empirical methods and the quantum uniform non-empirical *ab initio* methods form the 'computationally-fast/theoretically-weak' and the 'computationally-slow/theoretically-strong' poles of a spectrum of semi-empirical (SE) methods. Such SE methods are clearly required to allow conformational studies of reasonable theoretical validity to be made using a practicable amount of computer time. The empiricism of the SE methods manifests itself in the evaluation of the atomic integrals defined in B2.4. The SE methods will now be discussed as approximations within the Hartree-Fock formalism (with the exception of PCILO (B3.6), which is theoretically beyond the scope of the Hartree-Fock method).

B3.2 The Huckel Molecular Orbital (HMO) method

The HMO method (Huckel, 1931) is based on the π-electron approximation in which the electronic structure of unsaturated systems may be studied. The π-electron approximation makes the assumption that the σ-π electron systems are decoupled ($\Delta E = \Delta E_{\pi} + \Delta E_{\sigma} + \Delta W$) and explicit account is then made only of the π-electrons, the σ-electrons being included in the atomic cores. The elements of the Fock Hamiltonian are regarded as constants to be chosen empirically,

$$F_{\mu\mu} = \alpha_{\mu} \quad ; \quad F_{\mu\nu} = \beta_{\mu\nu} \qquad \text{(i)}$$

The further approximations that (a) $\beta_{\mu\nu} = 0$ for non-bonded atoms and (b) $S_{\mu\nu} = \delta_{\mu\nu}$, are made. Case (b) states that the approximation of zero differential overlap (ZDO) (Parr, 1952) is assumed for the $S_{\mu\nu}$ integrals. ZDO is an important concept in SE theory as we shall see. Solving the problem is thus reduced to finding the roots of the secular equations and the coefficients of the π-orbitals in the molecular wavefunction. In HMO analysis the π -electron energy is just the sum of the orbital energies of all the π-electrons. Huckel theory in its most basic form is not applicable to conformational problems; the inclusion of non-bonded interactions by means of a classical approximation allows conformational predictions to be made. However, the use of classical non-bonded interaction terms then makes the method non-uniform and indeed not strictly a quantum method at all!

B3.3 The Pariser-Parr-Pople (PPP) method

PPP (Pariser & Parr, 1953; Pople, 1953) is similar to the HMO method, the π-electron approximation and ZDO are again the main underlying assumptions. Again as with the HMO method a variety of approximations are used for the estimation of E_σ and W. In PPP theory for closed-shell systems, the π-electron energy follows from the formula

$$E_\pi = 2\sum_i E_i - \tfrac{1}{2}\sum_{\mu\nu}(P_{\mu\mu}P_{\nu\nu} - \tfrac{1}{2}P_{\mu\nu}^2)\gamma_{\mu\nu} \qquad \text{(ii)}$$

where the first term is the sum of orbital energies of all π-electrons (if HMO method), and $\gamma_{\mu\nu}$ is the Coulomb interaction energy of two π-electrons. (The connection between the second term of equation (ii) above and the definition of $\bar{\epsilon}_{el}$ from equation (xvi) of B2.5 is evident from the condition of ZDO ($\phi_\mu\phi_\nu\, d\tau = \delta_{\mu\nu}$) and equations (xiv), (xv) of B2.4.) The $\gamma_{\mu\nu}$ integrals are treated in an empirical way; the PPP method contains more empirical parameters than the HMO method.

B3.4 The Extended-Huckel Theory (EHT) method

The EHT method lies beyond the π-electron approximation and is the only SE method discussed so far that, since it is uniform, can be called truly quantum. In EHT both π and σ-valency electrons are considered explicitly, the Fock Hamiltonian is given by

$$F_{\mu\nu} = H_{\mu\nu}^{eff} \qquad \text{(iii)}$$

comparison of this with Eqn. (xiii) of B2.4 shows that EHT neglects electron interaction (ie $G_{\mu\nu}$ matrix). The $H_{\mu\mu}$ terms in (iii) are approximated by the valence orbital ionisation potential, and the off-diagonal terms are then usually evaluated by the Wolfsberg-Helmholz (1952) formula

$$H_{\mu\nu} = \tfrac{1}{2}K.S_{\mu\nu}(H_{\mu\mu} + H_{\nu\nu}) \qquad \text{(iv)}$$

where K is an empirical parameter. It should be noted that the ZDO assumption $S_{\mu\nu} = \delta_{\mu\nu}$ is not applied in EHT, but that the overlap integrals are explicitly found from the STOs.

Calculations in the EHT method are quite simple consisting of

(a) Evaluating $S_{\mu\nu}$ integrals

(b) Evaluating $H_{\mu\nu}$ matrix from (iv)

(c) Solving secular equations $\left|F_{\mu\nu}^{(i)} - E^{(i)} S_{\mu\nu}\right| = 0$

(d) Evaluating energy as $E_{total} = 2\sum_i E_{(i)}$

Since the Fock Hamiltonian is independent of the LCAO

coefficients, there is no self-consistency procedure of the type described in B2.5 and hence EHT is computationally rapid.

Finally it is of note that the kinetic energy of the electrons and their effect on the electrostatic field of the cores (ie terms in $H_{\mu\nu}$ of Eqn. (xiii) Section B2.4) and the core-core repulsion are all to be accounted for by the empirical constant K.

B3.5 The uniform SCF semi-empirical methods

The Huckel type semi-empirical methods described have all been such that Fock Hamiltonian is independent of the LCAO coefficients, this has meant that the SCF procedure described in B2.5 is unnecessary in the determination of the wavefunction. The methods described in this section lie closer to ab initio than the non-SCF methods so far mentioned.

The first of the SCF LCAO MO methods to be described in this section is based on the ZDO approximation and is called the Complete Neglect of Differential Overlap method (CNDO)(Pople & Beveridge, 1970). In accordance with ZDO the integral approximation

$$(\mu\nu|\lambda\sigma) = \delta_{\mu\nu}\delta_{\lambda\sigma}\,\gamma_{\mu\lambda} \qquad \text{(v)}$$

is made; unfortunately this approximation destroys the invariance of the RHF equations and further approximations are needed to restore it. Hence, the assumption that $\gamma_{\mu\nu}$ depends only on the type of atoms $\langle\mu|$ and $\langle\nu|$ are associated with (ie $\gamma_{\mu\nu} = \gamma_{AB}$, if $\langle\mu|$ centred on atom A and $\langle\nu|$ centred on atom B). Evidently Eqn. (xiii) Section B2.4 then becomes

$$F_{\mu\nu} = H_{\mu\nu} - \tfrac{1}{2}P_{\mu\nu}\,\gamma_{\mu\nu} \qquad \mu \neq \nu$$

$$F_{\mu\mu} = H_{\mu\mu} + \sum_{B\neq A}\Big(\sum_{\nu}^{B} P_{\nu\nu}\Big)\gamma_{AB} + \Big(\sum_{\nu}^{A} P_{\nu\nu}\Big)\gamma_{AA} - \tfrac{1}{2}P_{\mu\mu}\gamma_{AA} \qquad \mu=\nu \qquad \text{(vi)}$$

The core Hamiltonian matrix ($H_{\mu\nu}$) can be written from Eqn. (xiii) Section B2.4 as

$$H_{\mu\mu} = \langle\mu|-\tfrac{1}{2}\nabla^2 - V_A|\mu\rangle - \sum_{B\neq A}\langle\mu|V_B|\mu\rangle \qquad |\mu\rangle \text{ centred on A}$$

$$= \text{(by definition)}\ U_{\mu\mu} - \sum V_{AB} \qquad \text{(vii)}$$

$U_{\mu\mu}$ is now evaluated as an empirical parameter. Hence, if I_μ and A_μ are the ionisation potential and the electron affinity respectively and if Z_A is the core charge of atom A, then

$$U_{\mu\mu} = -\tfrac{1}{2}(I_\mu + A_\mu) - (Z_A - \tfrac{1}{2})\,\gamma_{AA} \qquad \text{(viii)}$$

The non-diagonal core Hamiltonian elements are given by

$$H_{\mu\nu} = (\beta^{o}_{A} + \beta^{o}_{B})\tfrac{1}{2}S_{\mu\nu} = \beta^{o}_{AB}\, S_{\mu\nu} \qquad \begin{matrix} <\mu| \text{on A}, <\nu| \text{ on B} \\ \mu \neq \nu \end{matrix} \qquad \text{(ix)}$$

$$= 0 \qquad <\mu| \text{and} <\nu| \text{ on A}$$

where β^{o}_{A} is an empirical parameter depending only on the type of atom A. Note (a) ZDO is not applied in the case of all overlap integrals (eg Eqn. (ix)) and (b) in contrast to the Wolfsberg-Helmholtz formula (Eqn. (iv) B3.4), Eqn. (ix) above does not upset the invariance of the equation with respect to basis-set transformations.

Returning to Eqn. (vi) we now have after assuming $V_{AB} = Z_B\, \gamma_{AB}$,

$$F_{\mu\nu} = \beta^{o}_{AB}\, S_{\mu\nu} - \tfrac{1}{2}P_{\mu\nu}\, \gamma_{AB} \qquad \text{(x)}$$

$$F_{\mu\mu} = -\tfrac{1}{2}(I_{\mu} + A_{\mu}) + \gamma_{AA}((P_{AA} - Z_A) - \tfrac{1}{2}(P_{\mu\mu} - 1)\gamma_{AA} + \sum (P_{BB} - Z_B)\gamma_{AB}$$

(having used equations (vi), (vii), (viii) and writing $P_{AA} = \sum^{A} P_{\mu\mu}$). Equations (ix) and (x) illustrate that in order to evaluate the total electronic energy as defined in B2.5 Eqn. (xvi), it is only necessary to explicitly calculate integrals of the type γ_{AB} and $S_{\mu\nu}$.

The SE scheme which has been outlined is, as stated earlier, known as the CNDO method. There are many ways in which the empirical parameters may be chosen leading to CNDO/1 (Pople & Segal, 1965), CNDO/2 (Pople & Segal, 1966), CNDO/BW (Boyd & Whitehead, 1972) etc methods. The variant described here is the one which has gained the most widespread acceptance - that is the CNDO/2 parameterisation.

The CNDO method is the archetype of a family of similar semi-empirical methods. Thus the INDO (Intermediate Neglect of Differential Overlap) method offers increased sophistication to CNDO by retaining one-centre monoatomic overlap integrals,

$(\mu\nu|\lambda\sigma)$ all orbitals centred on atom A

The next level of sophistication is the NDDO (Neglect of Diatomic Differential Overlap) method, here monoatomic overlap is retained on both one and two centre integrals. The following diagram clarifies the situation,

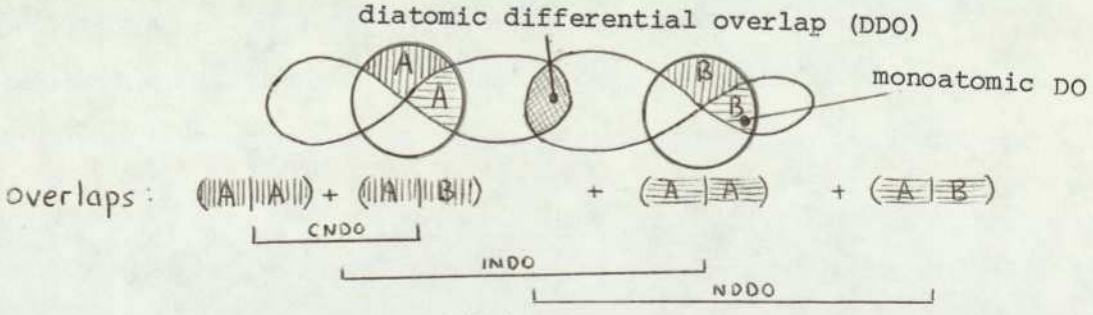

Finally, a recent development in SCF semi-empirical formalism is the MINDO/3 (eg Dewar, 1975) method (Modified-INDO). This method differs from the usual INDO approach in a fundamental way. In the INDO approach the empirical parameters were chosen in order that the method should reproduce ab initio results on small molecules. In contrast MINDO aims to reproduce experimental results, and the parameters are accordingly fitted to atomic spectroscopic data.

B3.6 The Perturbation of Configuration Interaction using Localised Orbitals (PCILO) method

In a Huckel theory study of ethylene, it is found that two MOs exist, these can be represented as

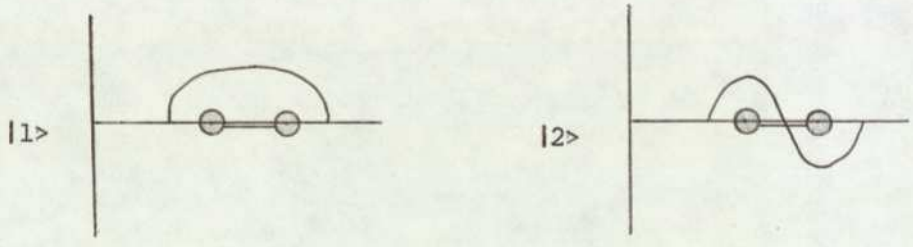

The MO $|1\rangle$ is of a bonding type, since the contour tends to suggest that the carbons are to be considered together. MO $|2\rangle$ however, because the contour suggests the carbons to be separated is called an anti-bonding MO. The MOs of ethylene are clearly delocalised over the entire molecule, and it is from delocalised MOs that the Slater determinant is formed (B2.2 Eqn. (vi). An alternative approach is possible in which the Slater determinant is constructed with localised MOs, in particular those of the valency bonds.

In the PCILO (Diner, Malrieu & Claverie, 1969; Malrieu, Claverie & Diner, 1969; Diner, Malrieu, Jordan & Gilbert, 1969)

method, the Slater determinant is constructed from localised bonding-MOs, this is then regarded as a zeroth order wavefunction ($|\Psi_o\rangle$). Anti-bonding orbitals (since they have higher energies associated with them) are then used to construct wavefunctions for singly- and doubly- excited configurations (see B2.6). The methods of perturbation theory are then used to derive a perturbation expansion for the approximate ground-state energy and wavefunction.

The PCILO method lies beyond those of the Hartree-Fock formalism in the sense that CI (see B2.6) is implicit in the method. The calculation of the energy is achieved by the evaluation of a perturbation series and hence no self-consistency procedure is required. This means PCILO is computationally rapid. A convenient simplification to further reduce the time taken in evaluating the integrals of the perturbation expansion is the assumption of ZDO by the use of CNDO/2 parameterisation.

Because $|\Psi_o\rangle$ is constructed by localised MOs on the valency bonds, it is often stated that PCILO is based on the assumption that 'the chemical formula is a good approximation to the molecular wavefunction'. Unfortunately when resonance is involved it is not possible to write down a single chemical structure and in this situation PCILO also fails. It is necessary to localise the resonance structures in order to make PCILO calculations: this is an inconvenience not encountered with the Hartree-Fock delocalised MO approach. A final problem with PCILO is that the density matrix is not exactly n-representable, ie orbitals can, in theory, contain electron density outside the interval 0-2 (eg Daudey, 1972).

Appendix C - Conventions for describing molecular structures

(i) Torsion angle convention

If a, b, c and d are four atoms, such that a, b, c and b, c, d are non-collinear, then the torsion angle {a. b - c.d} is defined by:- {a.b - c.d} is the angle through which the bond ab must be revolved to eclipse the bond cd, the clockwise direction being taken as positive. For example

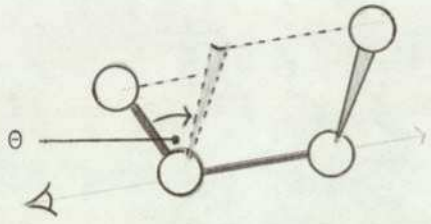

{a.b - c.d}= +Θ°

Note {d.c - b.a} = +Θ°.

(ii) The R and S system of nomenclature

For an asymmetric carbon the following situation can occur

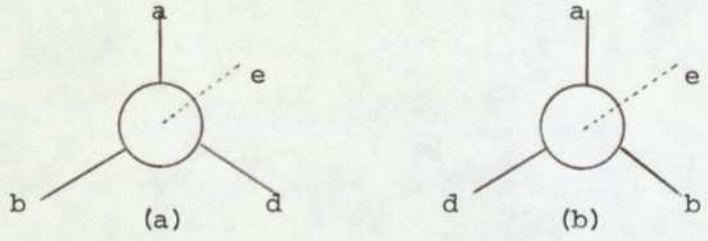

A priority sequence is now established by a set of rules which will be given later, assume that this sequence is b> a> d> e. Now, draw the three-dimensional figure so that, looking down upon it, it is seen with the lowest priority group pointing away from the observer, ie

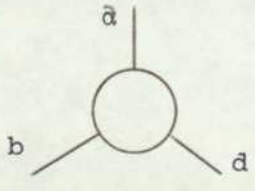

An arrow is now drawn in the direction of decreasing priority

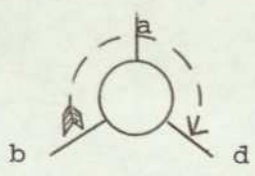

If the direction of the arrow is clockwise configuration is R, if it is anti-clockwise configuration is S. All that remains is to establish the rules for assigning priorities, these are

(a) Groups attached to the asymmetric carbon atom are arranged in the order of decreasing atomic number of the atom bound to the carbon.

(b) If two or more of the atoms attached to the asymmetric carbon have the same atomic number, the priority is determined by the atoms attached to these (again in order of decreasing atomic number).

(c) If the second set of atoms are the same in the two groups, the number of such atoms determines priority.

(d) Rule c is extended to the third, fourth, and other positions if necessary.

(e) If the atom attached to the asymmetric carbon atom is bound to other atoms by a double or triple bond, the atom at the end of the multiple bond is counted twice (for a double bond) or three times (for a triple bond).

An example of this system is given below

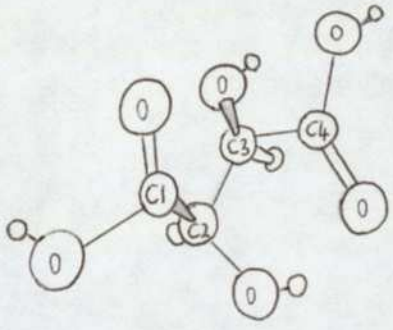

L-(+)-tartaric acid

carbon 2

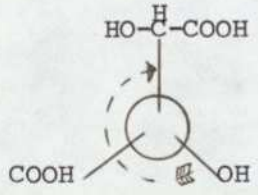

(3 oxygens bonded to carbon)

R

(1 oxygen bonded to carbon)

carbon 3

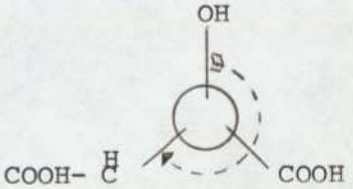

R

Thus L-(+)- tartaric acid is (2R:3R)-2,3-dihydroxy butanedioic acid.

(iii) Approximate description of conformation

If, as often happens, only an approximate description of a torsion angle is required, the Klyne-Prelog convention is useful (W. Klyne & V. Prelog, 1960). This is summarised in the following table

sector	designation	abbreviation	
$0^\circ \pm 30^\circ$	± syn-periplanar	± sp	sp = 0° = cis
$+60^\circ \pm 30^\circ$	+ syn-clinal	+ sc	
$+120^\circ \pm 30^\circ$	+ anti-clinal	+ ac	
$180^\circ \pm 30^\circ$	± anti-periplanar	± ap	ap = 180° = trans
$-120^\circ \pm 30^\circ$	- anti-clinal	- ac	
$-60^\circ \pm 30^\circ$	- syn-clinal	- sc	

Thus the minimum-energy conformation of the GABA zwitterion ($T_1 = 180^\circ$, $T_2 = 80^\circ$, $T_3 = 305^\circ$, $T_4 = 180^\circ$) is expressed as (ap, +sc, -sc, ap).

(iv) Description of five-membered rings

In the study of prostaglandins it is convenient to have a method of describing the puckering of the five-membered ring. It is possible to discuss the puckering of the ring in terms of the 3 ideal forms

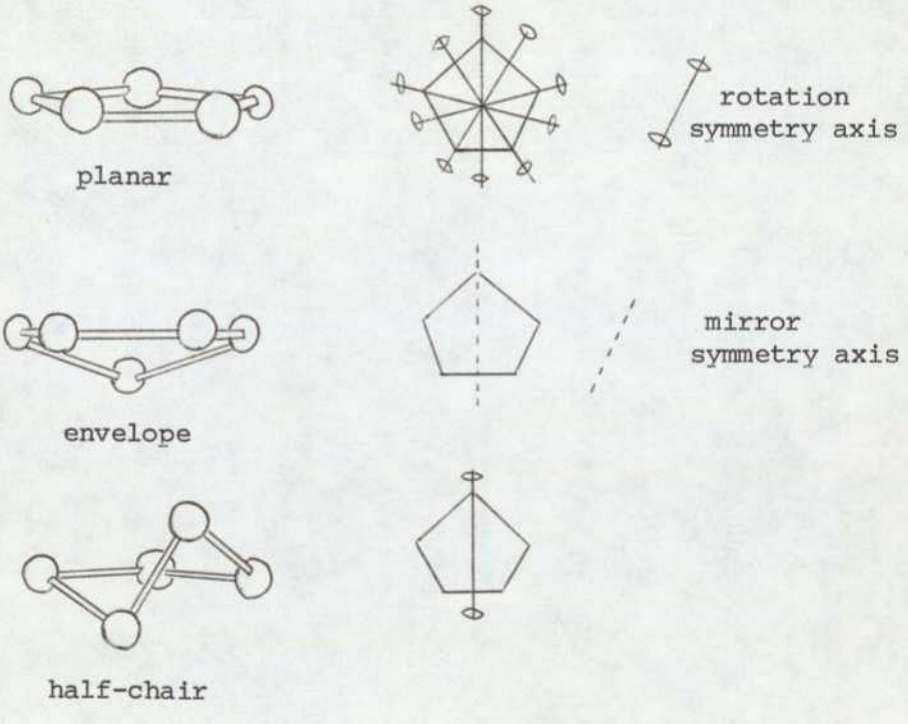

Now, the torsion angles i ± 1 and i ± 2 are defined as

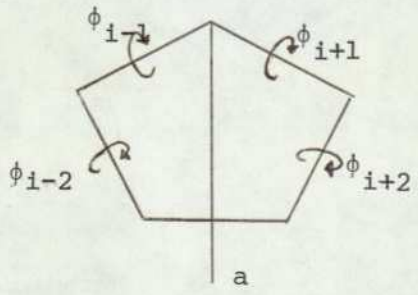

with respect to the atom i. The quantities (ΔC_s) and (ΔC_2), which describe the deviations from perfect mirror and rotation symmetry about the axis a, are now defined as

$$(\Delta C_s)_i = \{((\phi_{i+1} + \phi_{i-1})^2 + (\phi_{i+2} + \phi_{i-2})^2)/2\}^{\frac{1}{2}}$$

$$(\Delta C_s)_i = \{((\phi_{i+1} + \phi_{i-1})^2 + (\phi_{i+2} + \phi_{i-2})^2)/2\}^{\frac{1}{2}}$$

As an example the ring structure of PGE_1 is considered

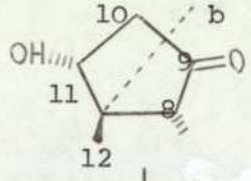

	$(\Delta C_s)_i$					$(\Delta C_2)_i$				
i =	8	9	10	11	12	8	9	10	11	12
	33.2	49.3	46.2	24.9	5.1	48.3	13.7	26.2	56.1	64.5

From the above results, it is evident that the ring in PGE_1 is best described as an envelope about the axis b.

Appendix D - A brief CNDO/2 study with solvent effects of α,γ-aminobutyric acid (αAG).

Introduction

Using CNDO/2 a conformational gas-phase and aqueous phase study of α,γ-aminobutyric acid (αAG) has been made. The zwitterionic ($NH_3^+.(CH_2)_2.CH(NH_2).COO^-$) and mono-cationic ($NH_3^+.(CH_2)_2.CH(NH_3^+)\ COO^-$) species of the R-enantiomer have been considered. The torsion angles are shown in Fig.D1 and are defined as T_1:= {H11.N4-C8.C7} , T_2:= {N4.C8 - C7.C6} , T_3:= {C8.C7 - C6.C5} , T_4:= {N3.C6 - C5.O1} and T_5:= {C5.C6 - N3.H10}. The labelling of the torsion angles is consistent with that used in the study of GABA. Structural parameters for the coordinates have been taken from the X-ray crystal structure determination (Hinazumi & Mitsui, 1971) and a grid of 30° has been used for the conformational energy surface.

Results and discussion

(i) Gas-phase

(a) Zwitterion

Firstly, a simultaneous optimisation of T_4 and T_5 was made, the result of which is summarised in Fig.D2. Briefly, the optimum conformation is with $T_4 = T_5 = 0^\circ$, ie O1, O2, C5, C6, N3 and H10 planar. Fixing T_4 and T_5 at these optimised values and assuming $T_1 = 60^\circ$ ('staggered'), a T_2- T_3 energy-surface was computed (Fig.D3). In common with other GABA-type zwitterions the global minimum occurs for a highly-folded conformation (within region 5 (see 5.4.3)).

There is also a local minimum at $T_2 = 60^\circ$, $T_3 = 210^\circ$ which can be identified with the configuration

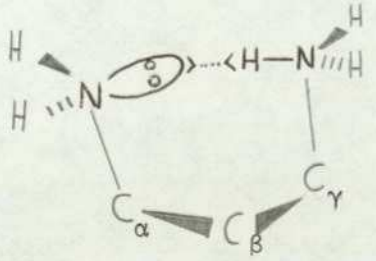

The extended conformations are seen to be energetically unfavourable with a region of particularly high energy centred on $T_2 = 0^\circ$, $T_3 = 240^\circ$. This can be identified with the following unfavourable configuration (destabilisation ca. 70 kcal mol^{-1}).

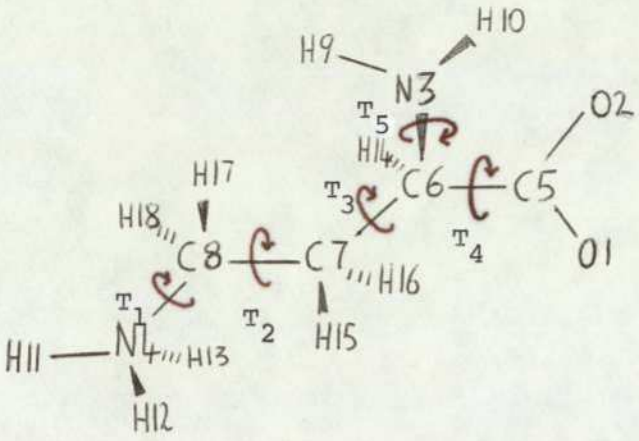

Fig. D1. The αAG zwitterion, showing the numbering scheme and the torsion angles.

minimum	T_2 °	T_3 °	rel. energy (kcal/mol)	dipole D
zwitterion-global	-30	-30	282	8.6
zwitterion-local	60	210	311	17.3
mono-cation-global	-60	60	0	38.9

Table D1

Minimum conformation statistics for αAG molecules.

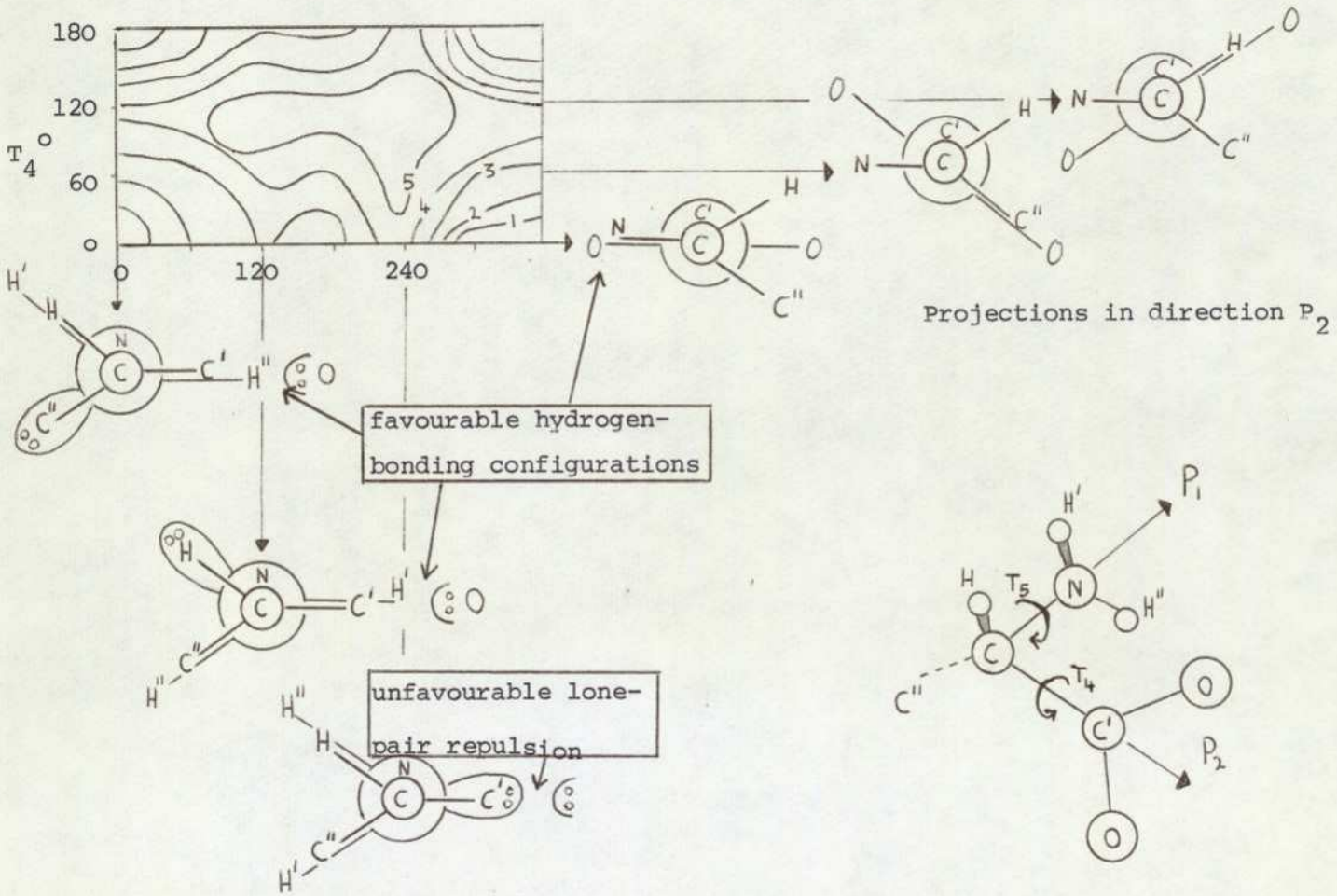

Fig. D2 The T_4-T_5 energy surface for αAG zwitterion. Conformations are explained by Newman projections in directions P_1 and P_2. Energies in kcal mol^{-1}

All energies in kcal mol^{-1} relative to the global minimum (+).

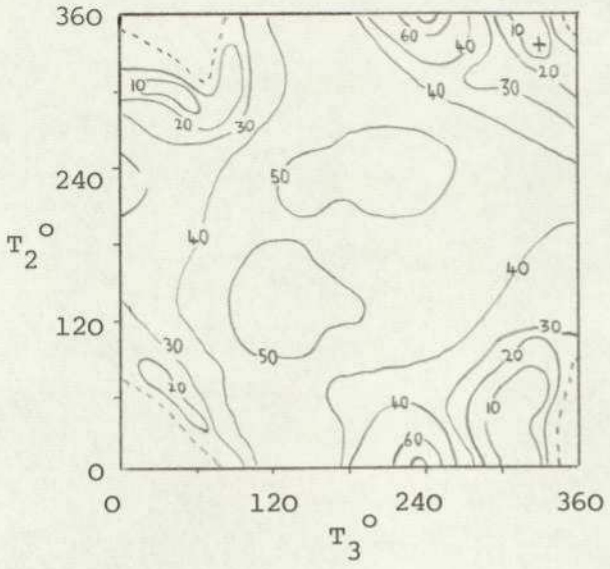

Fig. D3. T_2-T_3 energy surface for αAG zwitterion in the gas-phase.

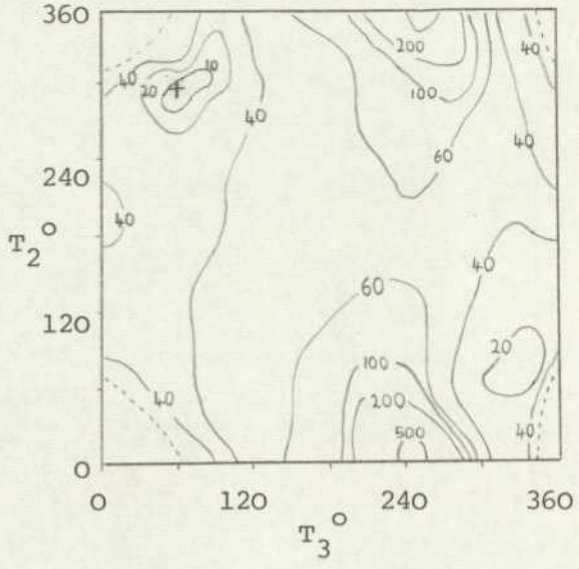

Fig. D4. T_2-T_3 energy surface for αAG mono-cation in the gas-phase.

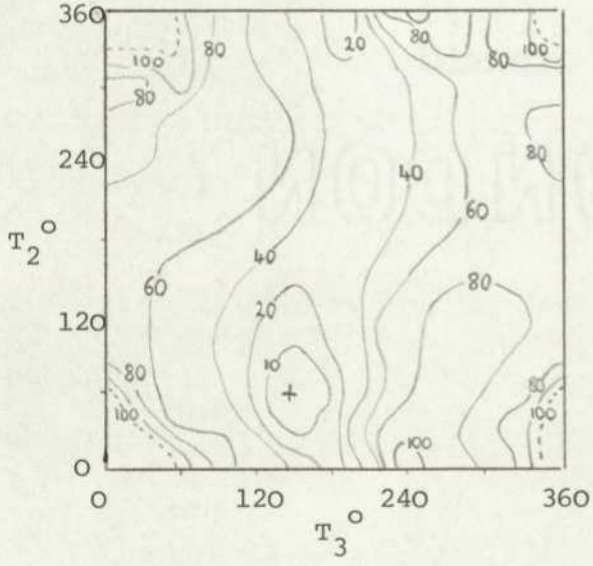

Fig. D5. T_2-T_3 energy surface for αAG zwitterion in the aqueous phase.

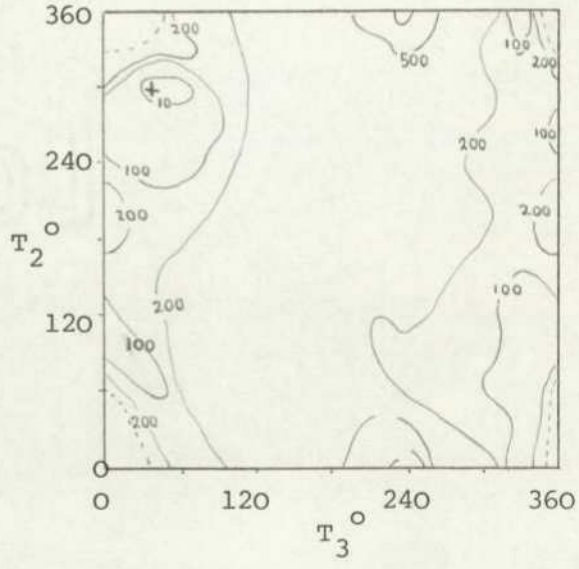

Fig. D6. T_2-T_3 energy surface for αAG mono-cation in the aqueous phase.

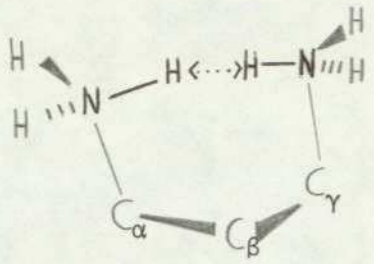

The energy and dipole moment at the global minimum are given in Table D1.

(b) Mono-cation

Calculation of a T_4 - T_5 surface was not made in this case. Instead the conformation

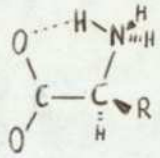

was assumed. There is a great deal of evidence that this conformation has exceptional stability in gas, crystal and aqueous phases. Assuming then that $T_4 = T_5 = 0^\circ$ and $T_1 = 60^\circ$, a T_2 - T_3 energy-surface was computed (Fig.D4). There is an overall similarity to the zwitterionic energy-surface, however the range of the global minimum is much reduced for the mono-cation. The global minimum again occurs for a folded conformation (within $\frac{1}{3}$), there are no local minima in the more extended conformations, and again when the onium groups are close the resulting energies are high (destabilisation ca. 500 kcal mol^{-1}). Energy and dipole moment at the minimum are given in Table D1.

(ii) Solvent-phase

(a) Zwitterion

The continuum method has been used to calculate the solvent effect, the resulting energy map is shown in Fig.D5. The global minimum occurs at $T_2 = 60^\circ$ and $T_3 = 150^\circ$, corresponding to an $x_T = 5.2\text{Å}$. In the aqueous phase (as with other GABA-type zwitterions) the very folded conformations are no longer favoured, and in this case the close approach of $-NH_3^+$ and $-NH_2$ groups is still not allowed (destabilisation ca. 110 kcal mol^{-1}).

(b) Mono-cation

The resulting energy map showing the solvent effect is to be found in Fig.D6. There is but little change in the position of the minimum of the gas-phase results - the solvent minimum occurs at $T_2 = -60^\circ$, $T_3 = 30^\circ$ (cp $T_2 = -60^\circ$, $T_3 = 60^\circ$ for gas phase). The minimum-energy conformation corresponds to an $x_T = 2.4\text{Å}$: this is considerably more folded than the solution conformations of GABA-

type zwitterions. The close approach of onium groups is still highly unfavourable (destabilisation ca. 700 kcal mol^{-1}). It is interesting that the destabilisation due to the approach of the α and γ substituents is greater in solution than in the gas phase. This is not an unreasonable prediction since in solution the groups have a greater steric volume, both possessing several hydration sites which will be occupied thereby increasing their effective size in solution.

Appendix E - PACE results for GLU agonists

GLU homologues studied by the PACE method were treated as branched chains as described by Gill (1959). The molecules considered were the L forms of the first five homologues of the GLU series. The values of x_{T_1} and x_{T_2} were measured from models for each sterically permitted conformation (x_{T_3} remains constant). The probabilities for each possible combination of x_{T_1} and x_{T_2} are given in Table E1.

TABLE E1

x_T PROBABILITIES FOR GLUTAMATE AGONISTS

SUBSTANCE	x_{T_1} (Å)	x_{T_2} (Å)	PROBABILITY (scaled to 1.0)
Amino malonate	3.3	3.2	1.000
Aspartate	4.8	3.4	0.236
	3.5	3.5	0.114
	3.6	4.7	0.649
Glutamate	5.1	4.1	0.047
	2.7	4.2	0.043
	2.4	5.0	0.277
	5.1	5.0	0.063
	5.8	5.0	0.198
	4.1	5.1	0.090
	5.0	5.7	0.281
Amino Adipate	4.6	3.2	0.009
	5.2	4.9	0.016
	5.7	4.9	0.052
	6.0	4.9	0.014
	6.6	4.9	0.044
	5.4	5.4	0.074
	4.9	5.5	0.074
	5.8	5.5	0.059
	5.8	5.7	0.062
	7.1	5.7	0.185
	4.9	5.8	0.021
	5.6	5.8	0.066
	5.1	6.5	0.084
	5.6	7.0	0.296

SUBSTANCE	x_{T_1} (Å)	x_{T_2} (Å)	PROBABILITY (scaled to 1.0)
Amino pimelate	6.9	4.5	0.007
	6.3	4.6	0.008
	6.4	4.7	0.002
	7.3	5.1	0.029
	6.2	5.2	0.009
	5.9	5.8	0.011
	7.2	5.8	0.034
	7.3	6.0	0.045
	6.0	6.1	0.012
	6.2	6.1	0.011
	4.5	6.2	0.022
	5.3	6.2	0.014
	6.3	6.2	0.011
	6.4	6.2	0.003
	6.3	6.3	0.003
	4.3	6.7	0.020
	7.1	6.7	0.040
	7.3	6.8	0.011
	5.7	7.0	0.053
	6.8	7.1	0.045
	5.2	7.2	0.061
	7.2	7.2	0.043
	7.3	7.2	0.084
	8.2	7.2	0.141
	6.2	7.3	0.064
	6.8	7.3	0.012
	7.2	8.1	0.175

References

Abraham, R J & Birch, D, Molec. Pharmacol, 11 (1975) 663

Abrahamsson, S, Acta Cryst, 16 (1963) 409

Akimoto, T & Iikata, Y, Acta Cryst, B28 (1972) 3106

Allen, L C, Sigma Molecular Orbital Theory (Yale University Press, Newhaven, 1970)

Allen, L C & Russell, J D, J. Chem Phys, 46 (1967) 1029

Almenningen, A & Bastiansen, O, Acta Chem Scand, 12 (1958) 1221

Andersen, N H & Ramwell, P W, Arch Intern Med, 133 (1974) 30

Andrews, P R & Johnson, G A R, Nature new Biol, 243 (1973) 29

Ariens, E J & Simonis, A M

Avignon, M, Garrigou-Lagrange, C & Bothorel, P, Biopolymers, 12 (1973) 1651

Barker, R, in Organic Chemistry of Biological Compounds (Prentice-Hall, 1971)

Beart, P M, Johnson, G A R, Curtis, D R, Game, C J A, McCulloch, R M & Twitchin, P, J. Neurochem, 24 (1975) 157

Benghait, V, Kanfman, H W, Leiserowitz, L & Schmidt, G M J, J C S Perkin II (1972) 1758

Benghait, V & Leiserowitz, L, J C S Perkin II (1972) 1763

Berges, J & Peradejordi, F, in Molecular and Quantum Pharmacology (Reidel, 1974)

Beveridge, D L, Radna, R J, Schnuelle, G W & Kelly, M K, in Molecular and Quantum Pharmacology (Reidel, 1974)

Blyholder, C & Coulson, C A, Theor Chim Acta, 10 (1968) 316

Bonaccorsi, R, Pullman, A, Scrocco, E & Tomasi, J, Theor Chim Acta, 24 (1972) 51

Bonner, W A & Castro, A J, Essentials of Modern Organic Chemistry (Reinhold, 1965)

Born, M & Oppenheimer, Ann Physik, 84 (1927) 457

Borthwick, P W & Steward, E G, J Mol Struct, 31 (1976) 143

Borthwick, P W & Steward, E G, ibid, 33 (1976) 141

Borthwick, P W, appendix A, May & Baker report no 5 (1977)

Bowery, N G & Brown, D A, Brit J Pharmacol, 50 (1974) 205

Boyd, R H, J Chem Phys, 49 (1968) 2574

Boyd, R J & Whitehead, M A, J Chem Soc, (1972) 82

Boys, S F, Proc Roy Soc, A200 (1950) 542

Brehm, L, Acta Chem Scand, 26 (1972) 1298

Brehm, L, Krogsgaard-Larsen, P & Hjeds, H, ibid, B28 (1974) 308

Buckingham, A D, Aust J Chem, 6 (1953) 93, 324

Burdon, J & Parsons, I W, Tetrahedron, 32 (1976) 103

Butcher, S S & Wilson, E B, J Chem Phys, 40 (1964) 1671

Bye, E, Mostad, A & Romming, C, Acta Chem Scand, 27 (1973) 471

Cade, P E & Hud, W M, H Chem Phys, 47 (1967) 614

Catalan, J & Fernandez-Alonso, J I, J Mol Struct, 27 (1975) 59

Clarke, G R, PhD thesis (City University, London, 1976)

Christoffersen, R E, Advan Quantum Chem, 6 (1972) 333

Collins, J F, Neurochemistry:Receptors for Drugs and Neuro-transmitters, to be published

Coulson, C A & Haigh, C W, Tetrahedron, 19 (1963) 527

Coulson, C A & Senent, S, J Chem Soc (1955) 1819

Csizmadia, I G, Theor Chim Acta, 34 (1974) 93

Cung, M T, Marraud, M & Neel, J, in Conformation of Biological Molecules and Polymers (Academic, N Y, 1973)

Curtis, D R, Duggan, A W, Felix, D & Johnson, G A R, Nature, 226 (1970) 1222

Curtis, D R, Duggan, A W, Felix, D, Tebicis, A K & Watkins, J C, Braim Res, 41 (1972) 283

Curtis, D R & Watkins, J C, Pharmacol Rev, 17 (1965) 347

Curtis, D R & Watkins, J C, J Neurochem, 6 (1960) 97

Cuthbert, M F, Brit Med J, 4 (1969) 723

Dashevsky, V G, Russ Chem Rev, 42 (1973) 969

Dandey, J P, QCPE 220 (1973)

Davidson, R B, Jorgensen, W L & Allen, L C, J Am Chem Soc, 92 (1970) 749

Dean, S M & Richards, W G, Nature, 256 (1975) 473

Derissen, J L, Endeman, H J & Peerdeman, A F, Acta Cryst, B24 (1968) 1349

DeTitta, G T, Nature, 191 (1976) 1271

Dewar, M J S, Chem in Britain, 11 (1975) 97

Dewar, M J S, in The Molecular Orbital Tehory of Organic Chemistry (McGraw-Hill, N Y, 1969)

Diner, S, Malrieu, J P, Jordan, F & Gilbert, M, Theor Chim Acta, 15 (1969) 100

Diner, S, Malrieu, J P & Claverie, P, ibid, 13 (1969) 1

Ditchfield, R, Hehre, W J & Pople, J A, J Chem Phys, 54 (1971) 724

Dressler, K & Ramsay, D A, Phil Trans Roy Soc London, A251 (1959) 553

Donohue, J, in Structural Chemistry and Molecular Biology (Freeman, 1968)

Dudel, J, Pflugers Arch, 284 (1965) 81, 104

Edwards, J T, Farrell, P G & Job, J L, J Am Chem Soc, 96 (1974) 902

Edwards, J T, Farrell, P G & Job, J L, J Phys Chem, 77 (1973) 2191

Edwards, C & Kuffler, S W, J Neurochem, 4 (1959) 19

Farnell, L, Richards, W G & Ganellin, C R, J theor Biol, 43 (1974) 389

Feynman, R P, Phys Rev, 56 (1939) 340

Fock, V, Z Phys, 61 (1930) 126

Fraenkel, G & Kim, J P, J Am Chem Soc, 88 (1966) 4203

Free, S M & Wilson, J W, J Med Chem, 7 (1964) 395

Giessner-Prettre, C & Pullman, A, Theor Chim Acta, 37 (1975) 335

Giessner-Prettre, C & Pullman, A, ibid, 25 (1972) 83

Gill, E W, Proc Roy Soc, B150 (1959) 381

Gill, E W, Prog Med Chem, 4 (1964) 39

Golebiewski, A & Parcezewski, A, Chem Rev, 74 (1974) 519

Gordon, M S & Neubauer, L, J Am Chem Soc, 96 (1974) 5690

Gorinsky, C & Moss, D S, J Cryst Mol Struct, 3 (1973) 299

Gray, G, Proc Roy Soc, B190 (1975) 369

Gropen, O & Seip, H M, Chem Phys Lett, 11 (1971) 445

Ham, N S, in Molecular and Quantum Pharmacology (Reidel, 1974)

Hammett, L P, Physical Organic Chemistry (McGraw-Hill, N Y 1940)

Hansch, C, in International Encyclopedia of Pharmacology and Therapeutics (Pergamon, 1973)

Hansch, C & Fujita, T, J Am Chem Soc, 92 (1970) 2191

Hartree, D R, Proc Cambridge Phil Soc, 24 (1928) 89, 111, 426

Hehre, W J, Lathan, W A, Ditchfield, R, Newton, M D & Pople, J A, QCPE 236 (1973)

Hehre, W J, Stewart, R F & Pople, J A, J Chem Phys, 51 (1969) 2657

Hehre, W J & Pople, J A, J Am Chem Soc, 92 (1970) 2191

Heitler, W & London, F, Z Physil, 44 (1927) 455

Hellmann, H, in Einfuhrung in die Quantenchimie (Franz Deuticke, Leipzig, 1937)

Hendrickson, W A & Karle, J, Acta Cryst, B27 (1971) 427

Hensby, C N, Biochim Biophys Acta, 348 (1974) 145

Herndon, W C & Fever, J, Tetrahedron Lett, 22 (1968) 2625

Hinazumi, H & Mitsui, T, Acta Cryst, B27 (1971) 2152

Hirokawa, S, ibid, 8 (1955) 637

Hoffman, R & Olofsen, R A, J Am Chem Soc, 88 (1966) 943

Hoffman, R, Bissell, R & Farnum, D J, J Phys Chem, 73 (1969) 1789

Hopfinger, A J, in Conformational Properties of Macromolecules (Academic, N Y, 1973)

Horton, Brit Med Bull, 29 (1973) 148

Howland, J C & Flurry, R L, Theor Chim Acta, 26 (1972) 157

Howland, J C & Flurry, R L, Theor Chim Acta, 26 (1972) 157

Hoyland, J R & Kier, L B, ibid, 15 (1969) 1

Hoyland, J R & Kier, L B, J Med Chem, 15 (1972) 84

Huckel, E, Z Physik, 70 (1931) 204

Hund, F, Z Physik, 40 (1927) 742; 42 (1927) 93

Jacob, E J, Thompson, H B & Bartell, L S, J Chem Phys, 47 (1967) 3736

Johnson, G A R, Curtis, D R, Davis, J & McCulloch, R M, Nature, 248 (1974 804

Johnson, G A R, Curtis, D R, De Groat, W C & Duggan, A W, Biochem Pharmacol, 17 (1968) 2488

Jones, G P & Pauling, P J, J C S Perkin II, (1976) 32, 34

Jose, P & Pant, L M, Acta Cryst, 18 (1965) 806

Jug, K, Theor Chim Acta, 31 (1973) 63

Kanters, J A, Kroon, J, Beurskens, P T & Vliegenthart, J A, Acta Cryst, 21 (1966) 990

Karabatsos, G J & Hsi, N, J Am Chem Soc, 87 (1965) 2864

Karim, S M M, Carter, D C, Bhana, D & Genesan, Prostaglandins, 4 (1973) 71

Karim, S M M & Filshie, G M, Lancet, 1 (1970) 157

Karim, S M M, Trussell, R R, Patch, R C & Hillier, K, Brit Med J, 4 (1968) 621

Kier, L B, Molecular Orbital Theory in Drug Research (Academic, N Y, 1971)

Kier, L B & George, J M, Eperientia, 29 (1973) 501

Kier, L B & Truitt, E B, ibid, 26 (1970) 988

Kier, L B, George, J M & Holtje, H-D, J Pharmaceut Sci, 63 (1974) 1435

Kirkwood, J G, J Chem Phys, 2 (1934) 351

Kitaygorodsky, A I & Dashevsky, V G, Teor Eksp Khim, 3 (1967) 35

Klyne, W & Prelog, V, Experientia, 16 (1960) 521

Kroon, J, Kanters, J A, Van Duikneveldt-Van de Rijdt, J G C M, Van Duikneveldt, F B & Vliegenthart, J A, J Mol Struct 24 (1975) 109

Kloeze, J, in Nobel Symposium 2: Prostaglandins (Almgvist and Wiksell, Stockholm, 1967)

Kohler, H-J, Z Chem, 11 (1971(467

Kohler, H-J, Weller, Th & Klopper, D, ibid, 15 (1975) 224

Lambrecht, G & Mutschler, E, in Quantum and Molecular Pharmacology (Reidel, 1974)

Lea, T J & Usherwood, P N R, Comp Gen Pharmacol, 4 (1973) 333

Leovey, E M K & Andersen, N H, J Am Chem Soc, 97 (1975) 4148

Lipkind, G M, Arkhipova, C F & Popov, E M, Strukt Khim, 11 (1970) 121

Loew, G H, Berkowitz, D, Weinstein, H & Srebrenik, S, in Quantum and Molecular Pharmacology (Reidel, 1974)

Lugovsky, A A & Dashevsky, V G, Zh Strukt Khim 13 (1972) 122

Madden, J J, McGandy, E L, Seeman, N C, Harding, M M & Hoy, A, Acta Cryst, B28 (1972) 2377

Maeda, T, Fujiwara, T & Tomita, K, Bull Chem Soc Jap, 45 (1972) 3628

Malrieu, J P, Claverie, P & Diner, S, Theor Chim Acta, 13 (1969) 18

Marsh, R E, Acta Cryst, 11 (1958) 654

McGeer, E G, McGeer, PC & McLennan, H, J Neurochem, 8 (1961) 36

McIlwain, H & Bachelard, in Biochemistry and the CNS (Churchill & Livingstone, 1971)

McLennan, H, Neuropharmacol, 13 (1974) 449

Morita, H & Nagakura, S, Theor Chim Acta, 27 (1972) 325

Mostad, A & Romming, C, Acta Chem. Scand., 27(1973)401.

Mostad, A, Romming, C & Rosenquist, E, Acta Chem Scand, 27 (1963) 164

Muller, N & Pritchard, D E, J Chem Phys, 31 (1959) 1471

Mulliken, R S, Phys Rev, 32 (1928) 186, 761

Mulliken, R S, ibid, 33 (1929) 720

Mulliken, R S, J Chem Phys, 23 (1955) 1833, 1841

Mulliken, R S, ibid, 36 (1962) 3428

Neidle, S & Rogers, D, J Chem Soc (B), (1970) 694

Oegerle, W R & Sabin, J R, J Mol Struct, 15 (1973) 131

Offenhartz, P O'D, in Atomic and Molecular Orbital Theory (McGraw-Hill) N Y, 1970)

Onsager, L, J Am Chem Soc, 58 (1936) 1486

Pariser, R & Parr, R G, J Chem Phys, 21 (1953) 466, 767

Parr, R G, ibid, 20 (1952) 239

Parry-Jones, G, Roberts, R T & Ahmed, A I, Mol Phys, 22 (1971) 547

Pauli, W, Z Physik, 31 (1925) 765

Pharriss, B B & Wyngarden, L, Proc Soc Exp Biol Med, 130 (1969) 92

Perahia, D & Pullman, A, Chem Phys Lett, 19 (1973) 73

Pong, S F & Graham, L T, Brain Res, 42 (1972) 486

Port, G N & Pullman, A, Theor Chim Acta, 31 (1973) 231

Port, G N & Pullman, A, Intern J Quantum Chem, 1974 (1974) 21

Pople, J A, Trans Faraday Soc, 49 (1953) 1375

Pople, J A, Tetrahedron, 30 (1974) 1605

Pople, J A & Beveridge, D L, Approximate Molecular Orbital Theory, (McGraw-Hill, N Y, 1970)

Pople, J A & Gordon, M, J Am Chem Soc, 89 (1967) 4253

Pople, J A & Nesbet, R K, J Chem Phys, 22 (1954) 571

Pople, J A & Segal, G A, ibid, 43 (1965) 5136

Pople, J A & Segal, G A, ibid, 44 (1966) 3289

Pullman, A, Int J Quantum Chem, 25 (1968) 187

Pullman, B & Berthod, H, C r hebd Seanc Acad Sci, Paris, 278 (1974) 1433

Pullman, B & Berthod, H Theor Chim Acta, 36 (1975) 317

Pullman, B & Berthod, H, ibid, 10 (1968) 461

Pullman, A & Pullman, B, Quarterly Rev of Biophys, 4 (1975) 505

Radom, L, Latham, W A, Hehre, W J & Pople, J A, J Am Chem Soc, 95 (1973) 693

Richards, R E & Thomas, N A, J C S Perkin II, (1974) 368

Robert, A, in Prostaglandin Symposium of the Worcester Foundation for Experimental Biology (Interscience, N Y, 1968)

Roby, K R, Mol Phys, 27 (1974) 81

Roothaan, C C J, Rev Mod Phys, 23 (1951) 69

Roy, P N, Majumbar, S K & Saha, N N, Indian J Phys, 41 (1967) 771

Ryan, J A & Christoffersen, R E, in Quantum and Molecular Pharmacology (Reidel, 1974)

Ryan, J A & Whitten, J L, J Am Chem Soc, 94 (1972) 2396

Schroder, M A, Makino, R C & Tolles, W M, Tetrahedron, 29 (1973) 3463

Segal, G A, QCPE 91 (1966)

Shoemaker, D P, Barieau, R E, Donohue, J & Le, C S, Acta Cryst, 6 (1953) 241

Shoemaker, D P, Donohue, J, Schomaker, V & Corey, R B, J Am Chem Soc 72 (1950) 2328

Singh, R D & Ferro, D R, J Phys Chem, 78 (1974) 970

Slater, J C, Phys Rev, 35 (1930) 509

Slater, J C, ibid, 34 (1929) 1293

Slater, J C, ibid, 36 (1930) 57

Slater, J C, ibid, 35 (1930) 210

Spek, A L, in Molecular Conformation of the Prostaglandins (ed G De Titta) unpublished communication

Steward, E G, Borthwick, P W, Clarke, G R & Warner, D, Nature, 256 (1975) 600

Steward, E G & Clarke, G R, J Theor Biol, 52 (1975) 493

Steward, E G, Warner, D & Clarke, G R, Acta Cryst, B30 (1974) 813

Steward, E G, Player, R, Quilliam, J P, Brown, D A & Pringle, M J, Nature new Biol, 233 (1971) 87

[a]Steward, E G, Player, R & Warner, D, Acta Cryst, B29 (1973) 2038

[b]Steward, E G, Player, R & Warner, D, ibid, B29 (1973) 2825

Swagel, M W, Ikeda, K & Roberts, E, Nature new Biol, 246 (1973) 91

Taft, R W, in Steric Effects in Organic Chemistry (Wiley, N Y, 1956)

Thyagaraja Rao, S, Srinivasan, R & Valambal, V, Indian J Pure Appl Phys, 6 (1968) 523

Tomita, K, Harada, M & Fujiwara, T, Bull Chem Soc Jap, 46 (1973) 2854

Tomita, K, I Tetrahedron lett, 1971 (1971) 2587

Upjohn Veterinary Symposium (Proceedings of -, 1975)

Veillard, A, Chem Phys Lett, 33 (1975) 15

Warner, D, PhD thesis (City University, London, 1975)

Warner, D, Borthwick, P W & Steward, E G, J Mol Struct, 25 (1975) 397

Warner, D & Steward, E G ibid, 25 (1975) 403

Watase, H, Tomiie, Y & Nitta, I, Bull Chem Soc Jap, 31 (1958) 714

Weintraub, H J R & Hopfinger, A J, in Quantum and Molecular Pharmacology (Reidel, 1974)

Weller, Th, Klopper, D & Kohler, H-J, Chem Phys Lett, 36 (1975) 475

Wiberg, K B, J Am Chem Soc, 87 (1965) 1070

Wiberg, K B, Tetrahedron, 24 (1968) 1083

Willcott, M R & Davis, R E, Science, 190 (1975) 850

Wolfsberg, M & Helmholtz, L, J Chem Phys, 20 (1952) 837

Wyman, J, Chem Rev, 19 (1936) 213